Technology Innovation Institute

IAPS International Association of Protective Structures

12th - 15th May, 2025

Abu Dhabi, United Arab Emirates

THE 7TH INTERNATIONAL CONFERENCE ON PROTECTIVE STRUCTURES

CONFERENCE PROGRAMME & BOOK OF ABSTRACTS

tii.ae

CONFERENCE PROGRAMME

Organized by
Technology Innovation Institute (TII) and
International Association of Protective Structures (IAPS)

Edited by
Rafael Santiago, Omar Ba Nabila, Alia Ruzanna Aziz
and, Naresh Kakur

Design
Nancy AlGhazo and Andrew Chopra

Authors
Multiple

Title
Conference Programme for the 7th International
Conference of Protective Structures.

TABLE OF CONTENTS

SPONSORS & EXHIBITORS

Gold Sponsors

ANSYS “Founded in 1970, Ansys is a world leader in numerical simulation, specializing in the development of advanced software solutions that enable engineers to virtually design, test and validate products before they go into production. Its tools cover various fields such as fluid mechanics, electromagnetism and structural dynamics.

Through a unique expertise and more than 30 years of experience, THIOT INGENIERIE is a world leader for studying the behavior of materials in fast dynamics conditions. With more than 30 experts we develop and supply fast dynamics equipment for research centers and manufacturers all over the world.

THIOT INGENIERIE also boasts the first private Shock Physics laboratory, with cutting-edge test equipment and metrology solutions. Its combination with our know-how in numerical calculation aims to study the behavior of materials and structures under shock stress (crashes, ballistic impacts, blasts, etc.) in the minutest detail to enable our customers to develop the most reliable products capable of handling the threats they face

Exhibitors & Publishing Partner

Publisher in Materials Science & Engineering

FOREWORD

Dr. Rafael Santiago
Senior Director
Technology Innovation Institute (TII)
Conference Chair

It is an honour and a privilege to welcome you to the 7th International Conference of Protective Structures (ICPS7). As the Conference Chair, I am delighted to introduce this book, a collective testament to the exceptional research, ingenuity, and collaboration that define our field.

ICPS7 brings together a vibrant community of engineers, scientists, and innovators dedicated to advancing the science and application of protective structures. This book reflects the dynamic exchange of ideas, the depth of exploration, and the global relevance of the work being presented. It offers a snapshot of where we stand today and, more importantly, where we are headed.

In an era defined by complex challenges and rapidly evolving threats, the role of protective structures has never been more critical. This conference provides a vital platform for sharing new findings, methodologies, and technologies to help shape safer and more resilient societies. The work represented in these abstracts highlights our community's commitment to advancing the frontiers of knowledge and delivering real-world impact.

I would like to extend my deepest appreciation to all the authors, organisers, reviewers, keynote speakers, sponsors, participants and staff for their dedication and support. Your efforts make ICPS7 a truly international and inspiring event.

I invite you to explore the pages ahead with curiosity and enthusiasm. May they spark new ideas, foster meaningful collaborations, and inspire continued excellence in our shared pursuit of innovation and safety.

Welcome to Abu Dhabi and enjoy the conference!

Warm regards,
Dr. Rafael Santiago

About ICPS7

It is with great pleasure that we present the book for ICPS7 – The 7th International Conference of Protective Structures - that will be held from 12 to 15 May 2025 in Abu Dhabi. Abu Dhabi is an emerging global hub for innovation and education with cutting-edge research facilities, prestigious academic institutions, and a vibrant cityscape, offering a perfect setting for the ICPS7 conference. Embark on a groundbreaking experience as we host the first ICPS in this dynamic region, offering a unique chance to engage and exchange insights with peers and researchers from around the globe at the leading international conference dedicated to protective structures.

ICPS originated in 2010 in Manchester, UK (1st ICPS). This global event has since traversed the globe, making impactful stops in Potsdam, Germany in 2013 (2nd ICPS/ISIEMS), Newcastle, Australia in 2015 (3rd ICPS), Beijing, China in 2016 (4th ICPS), Poznan, Poland in 2018 (5th ICPS) and Auburn, USA in 2023 (6th ICPS). The organizing committee is pleased to present the conference program with four reputable keynote speakers in the field of material engineering. In addition, more than 150 presentations covered most domains in the field of material and impact loadings. Also, four sponsors and exhibitors from leading instrument-providing and cutting-edge technology companies in the field participated in the event.

This conference is organised by the Technology Innovation Institute (TII), a global research centre dedicated to pushing the frontiers of knowledge. Our teams of scientists, researchers, and engineers work in an open, flexible, and agile environment to deliver discovery science and transformative technologies. Our work means we will not only prepare for the future; we will create it. Working together, we are committed to inspiring innovation for a better tomorrow. TII is part of the Abu Dhabi Government's Advanced Technology Research Council (ATRC), which oversees technology research in the emirate.

We hope this book will be a valuable resource and inspiration for researchers. We can work together to build a safer and more secure future by enhancing our knowledge of advanced materials and their applications.

We wish you a pleasant stay in our nice city, Abu Dhabi, and an incredible conference experience.

Yours Sincerely
The Organizing Committee

LOCAL COMMITTEE MEMBERS

Dr. Rafael Santiago
Conference Chair
Senior Director in Material Research Centre
Technology Innovation Institute, UAE

Dr. Alia Ruzanna Aziz
Program Chair
Senior Researcher,
Technology Innovation Institute, UAE

Omar Ba Nabila
Co-Program Chair
Senior Engineer
Technology Innovation Institute, UAE

Andrew Chopra
ICPS7 Event Manager
Senior Manager – Events
Technology Innovation Institute, UAE

IAPS Steering Committee

Prof. Mark Stewart, University of Technology Sydney, Australia
Prof. James S. Davidson, Auburn University, United States of America
Prof. Piotr Sielicki, Poznan University of Technology, Poland
Prof. Qin Fang, Army Engineering University of PLA, China
Prof. Norbert Gebbeken, University of the Bundeswehr Munich, Germany
Prof. Hong Hao, Guangzhou University, China / Curtin University, Australia
Prof. Qingming Li, University of Manchester, England, United Kingdom
Prof. Zhong-Xian Li, Tianjin University, China
Prof. Jeffrey Packer, University of Toronto, Canada
Prof. Masuhiro Beppu, National Defense Academy, Japan
Prof. David Yankelevsky, Technion-Israel Institute of Technology, Israel
Dr. Rafael Santiago, Technology Innovation Institute, United Arab Emirates

Scientific Committee

Prof. Wesley Cantwell, Khalifa University, United Arab Emirates
Prof. Guoxing Lu, Swinburne University of Technology, Australia
Prof. Dora Karagiozova, Bulgarian Academy of Sciences, Bulgaria
Prof. Xiaowei Chen, China Academy of Engineering Physics, China
Prof. Dong Ruan, Swinburne University of Technology, Australia
Prof. Marcílio Alves, University of São Paulo, Brazil
Prof. Steeve Chung Kim Yuen, University of Cape Town, South Africa
Prof. Jin Zhou, Xian Jiaotong University, China
Prof. Magnus Langseth, Norwegian University of Science and Technology, Norway
Prof. Sandro Amico, Federal University of Rio Grande do Sul, Brazil
Prof. Victor Shim, National University of Singapore (NUS), Singapore
Prof. Avraham Dancygier, Technion - Israel Institute of Technology, Israel
Prof. Flavio Silva, Pontificia Universidade Católica do Rio de Janeiro, Brazil
Prof. Jian Xiong, Harbin Institute of Technology, China
Prof. Guangyong Sun, Hunan University, China
Prof. Tore Borvik, Norwegian University of Science and Technology, Norway
Prof. Francois Boussu, GEMTEX ROUBAIX, France

Prof. Michael Seica, University of Toronto, Canada
Prof. Yanchao Shi, Tianjin University, China
Prof. Yang Ding, Tianjin University, China
Prof. Jiabao Yan, Tianjin University, China
Prof. Licheng Guo, Harbin Institute of Technology, China
Prof. Yanhong Chen, Harbin Institute of Technology, China
Prof. Xianfeng Zhang, Nanjing University of Science and Technology, China
Prof. Daniel Ambrosini, University of Cuyo, Mendoza, Argentina
Prof. Yong Lu, University of Edinburgh, Scotland, United Kingdom
Prof. Ser Tong Quek, National University of Singapore
Prof. Zhongwei Guan, University of Liverpool, United Kingdom
Assoc. Prof. Vegard Aune, Norwegian University of Science and Technology, Norway
Assoc. Prof. Jian Cui, Tianjin University, China
Dr. Waleed Ahmed, United Arab Emirates University, UAE
Dr. Teresa Fras, French-German Research Institute of Saint-Louis (ISL), France
Dr. Ehsan Noroozinejad, University of British Columbia (UBC), Canada
Dr. Leopold Kruszka, Military University of Technology, Poland
Dr. Ziwen Xu, Harbin Institute of Technology, China
Dr. Hasan Al Rifaie, Poznan University of Technology, Poland
Dr. Mohd Zuhri Mohamed Yusoff, University Putra Malaysia, Malaysia
Dr. S Kanna Subramaniyan, Universiti Tun Hussein Onn, Malaysia
Dr. Lei Yang, Johns Hopkins University, United States of America
Dr. Tomas Gajewski, Poznan University of Technology, Poland
Alexander Stolz, Fraunhofer EMI, Germany

Acknowledgment

We would like to extend our deepest gratitude to H.E. Faisal Al Bannai, Dr. Najwa Aaraj and Prof. Vincenzo Giannini for their generous and unwavering support for ICPS7. We sincerely appreciate the International Association of Protective Structures (IAPS) for endorsing this conference in Abu Dhabi and the Advanced Technology Research Council (ATRC). Special acknowledgement to Prof. Zhongwei Guan and Geeta Gidwani for their invaluable support throughout the planning and organisation of the event. Finally, we would like to recognise and thank everyone who contributed to the success of the conference, including our dedicated conference members, authors, and scientific committee, for their commitment and hard work.

Conference Venue

Venue: W Hotel Abu Dhabi – Yas Island
Address: Yas Island, Abu Dhabi, United Arab Emirates
Hotel Website: https://www.marriott.com/

Conference Dates & Hours

Mon, 12th May	17:30 – 21:00	Registration & Welcome Reception
Tues, 13th May	08:00 – 23:00	Registration, Keynotes, Parallel sessions, Desert Safari Tour
Wed, 14th May	08:20 – 22:30	Keynotes, Parallel sessions, Workshops, Gala Dinner
Thu, 15th May	08:20 – 15:00	Keynote, Parallel sessions, Closing Ceremony & Awards

Registration Desk

Location:
W Hotel Abu Dhabi – Yas Island
Opening Hours:

- **12th May:** 17:30 – 21:00 (Rush Bar, W Hotel)
- **13th-15th May:** 08:00 – 17:00

On-site Support: Our staff will be available to assist with name badges, programs, and general questions. Badges will be printed on-site. (Hallway of Concrete Ballroom)

Gen
Guide

Conference Sessions

- Sessions will be held in five designated rooms. Please refer to the conference floor plan and program schedule for room assignments.

Exhibitor & Sponsor Booths

- Located in the Exhibition Area in the Conference corridors.
- Open daily from 09:00 to 17:00.
- Visit our sponsors to learn more about cutting-edge technologies in the field.

Presentation guidelines

- The presentation should not exceed 15 minutes, followed by 3-5 minutes Q&A (20-minute slot each). Kindly adhere to the allocated time slots.
- Each conference room will have a laptop. Speakers must bring a USB drive and upload their presentation to the designated folder either a day before or at least 10 minutes before the session starts.
- The presentation should be in pdf or ppt format only.
- Please ensure that **mobile phones** are set to **silent** mode during all sessions.

eral
elines

Meals & Activities

- **Welcome Reception**
  12th May, 17:30 – 21:00 (Rush Bar, W Hotel)
- **Daily Coffee Breaks**
  10:30 & 15:30 PM (Hallway of Concrete Ballroom)
- **Daily Lunch**
  12:30 PM - 14:30 (Garage Restaurant, W Hotel)
- **Desert Safari**
  13th May, 14:30 – 23:00 (BBQ Dinner)
- **Gala Dinner:** 14th May, 19:00 – 22:30 (Concrete Ballroom)

Emergency & Contact Information

Police / Ambulance / Fire
999
Dial from any phone in UAE

W Hotel Front Desk
+971 2 656 0000
Available 24/7 for assistance

Nearest Hospital
Burjeel Medical City
+971 800 55
Located ~10 minutes from the venue

Conference Local Commitee Contacts

Rafael Santiago
+971 58 944 6966

Omar Ba Nabila
+971 52 616 6010

Alia Aziz
+971 55 105 0512

On-site conference staff for urgent needs

Floor Plan

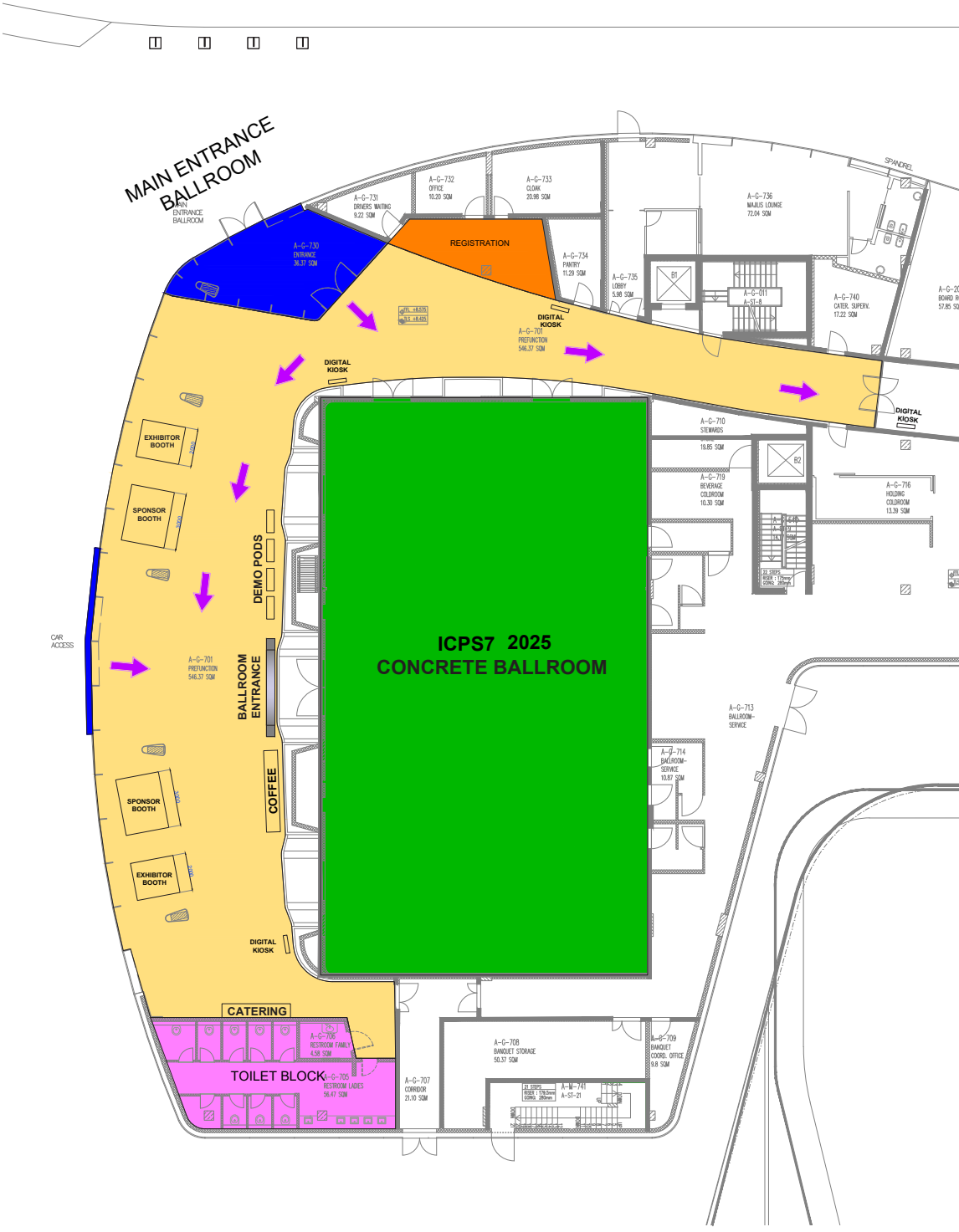
MAIN ENTRANCE BALLROOM
REGISTRATION
DIGITAL KIOSK
DIGITAL KIOSK
DIGITAL KIOSK
DIGITAL KIOSK
EXHIBITOR BOOTH
SPONSOR BOOTH
DEMO PODS
BALLROOM ENTRANCE
SPONSOR BOOTH
EXHIBITOR BOOTH
COFFEE
CAR ACCESS
ICPS7 2025
CONCRETE BALLROOM
CATERING
TOILET BLOCK
A-G-730 ENTRANCE 36.37 SQM
A-G-731 DRIVERS WAITING 9.22 SQM
A-G-732 OFFICE 10.20 SQM
A-G-733 CLOAK 20.96 SQM
A-G-734 PANTRY 11.29 SQM
A-G-735 LOBBY 5.98 SQM
A-G-736 MAJLIS LOUNGE 72.04 SQM
A-G-740 CATER. SUPERV. 17.22 SQM
A-G-701 PREFUNCTION 546.37 SQM
A-G-710 STEWARDS 19.85 SQM
A-G-719 BEVERAGE COLDROOM 10.30 SQM
A-G-716 HOLDING COLDROOM 13.39 SQM
A-G-713 BALLROOM-SERVICE
A-G-714 BACKROOM-SERVICE 10.87 SQM
A-G-709 BANQUET COORD. OFFICE 9.8 SQM
A-G-708 BANQUET STORAGE 50.37 SQM
A-G-707 CORRIDOR 21.10 SQM
A-G-705 RESTROOM FAMILY 4.58 SQM
A-G-705 RESTROOM LADIES 56.47 SQM
A-ST-21
A-ST-11
B1
B2
SPANDREL

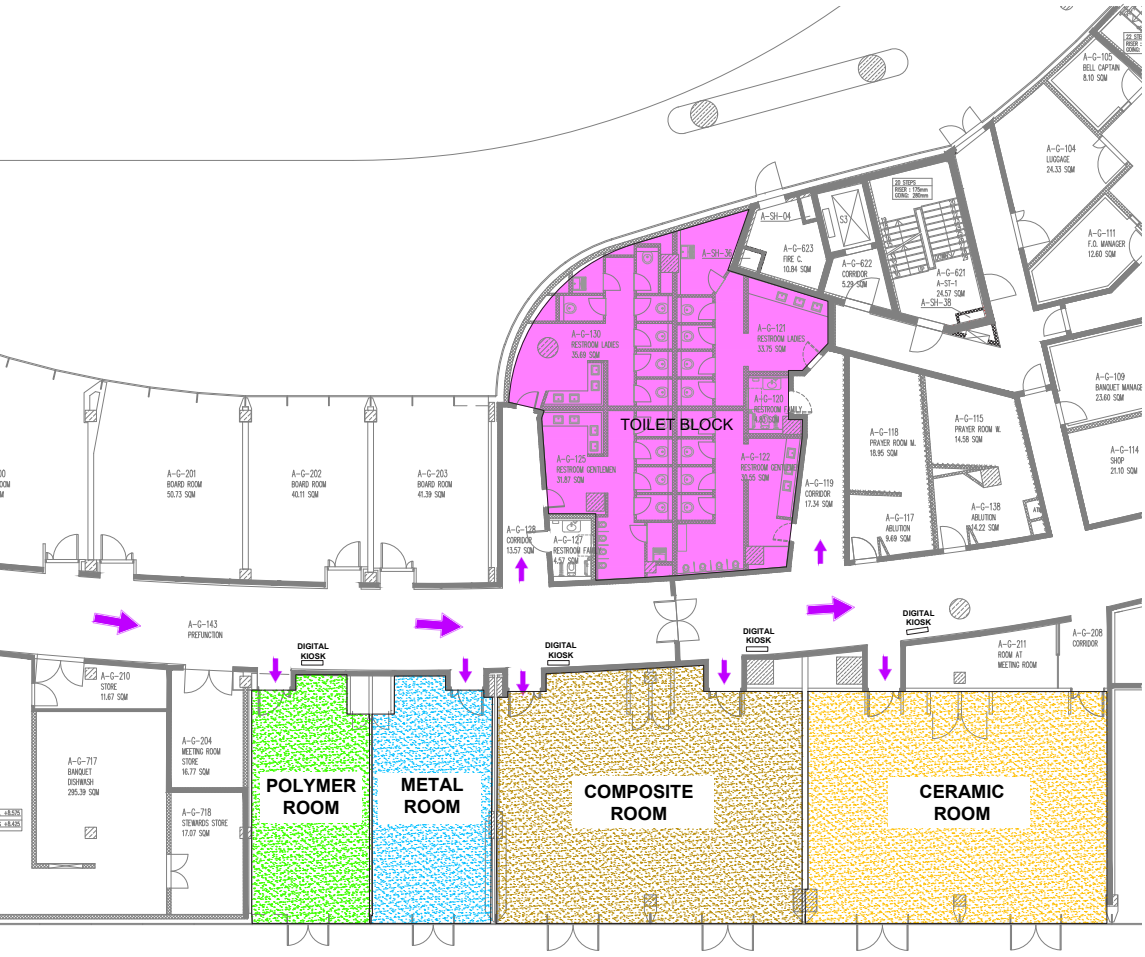

OVERALL FLOOR PLAN

LEGEND:

- CONCRETE BALLROOM
- ENTRANCES
- REGISTRATION
- PRE FUNCTION AREA
- TOILET (MALE / FEMALE)
- POLYMER ROOM
- METAL ROOM
- COMPOSITE ROOM
- CERAMIC ROOM

Norman Jones Award

Prof. Dr.-Ing. Werner Riedel
Chief Scientist Defense of Fraunhofer EMI, Germany
Winner of Norman Jones Award

Norman Jones Lecture Title

25 Years of concrete modeling: Some key lessons learned for predictive simulations in hydrocodes

We are honored to welcome Prof. Werner Riedel, a distinguished scientist and academic, as the presenter of the Norman Jones lecture and winner of the Norman Jones Prize for Outstanding Scientific Achievement at ICPS7. This distinguished award is named after Professor Norman Jones and is a testament to the significance of this award and the values it represents—innovation, dedication, and scientific excellence in the field of protective structures.

Prof. Dr. Werner Riedel is the Chief Scientist of the Division for Defense Science and Technology of Fraunhofer EMI. He received degrees in Mechanical Engineering from the Technical University of Munich (1994) and the École Nationale Supérieure des Mines de Compiègne, France (1996). At EMI, he specialized in numerical modelling of materials and components under dynamic loads. In 2000, he received a doctoral degree from the University der Bundeswehr in München. Selected projects include the ADAMMO (European Space Agency, material models for orbital debris impact on ISS, principal investigator), VITRUV (European Commission FP-7, urban security, consortium coordinator), as well as numerous projects for the German automotive, nuclear-electric and defense industry. Dr. Riedel was invited as a visiting professor to Tokyo Institute of Technology in 2006/09 and has served at Nanyang Technological University, Singapore, Protective Technology Research Center since 2017. He was continuously appointed as an honorary professor by Furtwangen University in 2012 in Security & Safety Engineering. He has written and contributed to 149 scientific publications, with a current h-index of 21 according to Scopus. Standford University ranked him for 2022 among the 2% best scientist worldwide, regarding impact and citations of publications.

We are privileged to have Prof. Riedel not only as a guest of honor but also as a keynote speaker at ICPS7. His address promises to be a highlight of the conference, offering insights from decades of research, leadership, and innovation.

Dr. Abdulla Al-Dhaheri

Engineer & Innovation Consultant, UAE

Lecture Title

An overview of protective construction and an experimental design of bunker buster slab under projectile impact in UAE

Dr. Abdulla Al-Dhaheri is an accomplished Emirati engineer and innovation consultant with a Ph.D. in Industrial Management and Systems Engineering from Montana State University, USA. His academic and professional journey spans civil engineering, project management, and innovation systems, with expertise in TRIZ methodology and idea generation metrics.

He has held roles in solving real case problems in public and private sectors in the UAE using TRIZ problem solving and measuring their innovation performance, such as companies like Al Ain Municipality, Abu Dhabi Airports, GDRFA Dubai, and others. He has led numerous workshops to enhance creativity, process improvement, and strategic thinking within organizations.

Dr. Abdulla has authored and presented research at international conferences, with published work on green supply chains and leadership's impact on innovation. In addition to these researches, he helped planning and developing many types of experimental designs such as concrete protection against penetation and blast attacks and measured their results numerically using design of experiment.

He is skilled in MATLAB and SPSS, which helped him in planning and analyzing experiments. Moreover, he is also skillful in AutoCAD and Primavera and is fluent in Arabic and English. Passionate about technology, leadership, and organizational growth, he continues to contribute to the UAE's innovation landscape.

Prof. Zhong-Xian Li

Chair Professor of Civil Engineering,
Tianjin University, China

Board member of the IAPS

Lecture Title

Research Progress on Performance-based Design Theory and Methods of Building Structures against Blast Loading

Prof. Zhong-Xian Li is a Chair Professor of civil engineering at Tianjin University of China and the Dean of Key Laboratory of Coast Civil Structure Safety of the Ministry of Education, China. He was jointly trained by Tianjin University and University of Basilicata in Italy and obtained his PhD in 1990 from Tianjin University. He once visited University of Cambridge in UK for one year in 1995 and served as the President of Tianjin Chengjian University from 2010 to 2022. His current research interests are seismic and blast resistant analysis and design of buildings and bridges, and most recently focused on performance-based blast resistant design of building structures and multi-disaster resilience of large sea-crossing bridges.

He developed the world's first Underwater Shaking Table Array System and edited in chief the first Standard for Blast Protection Design of Civil Buildings in China. He has published more than 300 journal papers and has won two National Awards on Science and Technology Advancement of China and one National Award on Technological Invention of China. He is a board member and elected Fellow of the International Association of Protective Structures (IAPS) and serves on the editorial board of the International Journal of Protective Structures (ICPS).

Prof. Dr.-Ing. François Boussu

Full professor, ENSAIT University of Lille, France

Lecture Title

Textile materials as an effective protective solution against multi-velocity and multi-threat impacts

Prof. François Boussu is a full professor at ENSAIT (École Nationale Supérieure des Arts et Industries Textiles) University of Lille, where he has been a faculty member since 1998. His teaching activities centre on weaving technology, the modelling of woven structures, and the theory of fundamental and derivative weave diagrams, with a particular emphasis on 3D warp interlock structures.

His research is structured around two main themes. The first focuses on the dynamic behaviour of fibrous materials under impact, with applications ranging from soft body armour to rigid vehicle protection. The second addresses the design, manufacturing and characterisation of multilayer woven fabrics used as reinforcements in composite materials, with a strong emphasis on structural lightweighting for aerospace, automotive, and rail sectors.

He has supervised 24 PhD theses (including 3 ongoing) and 78 Master's dissertations. His scientific output includes over 90 publications, comprising 62 peer-reviewed journal articles indexed in international databases, 16 chapters in scientific books, and 10 patents (4 international, 2 European, and 4 national). His work has been presented in over 200 conference proceedings, including 16 invited keynote lectures.

He served as scientific co-director of several dedicated international conferences (TEXCOMP, LWAG, 3D Fabrics), and is an active member of the scientific committees of several major international conferences in textile and composite research.

Programme

Sessions Overview

Date	Session	Time	Title	Location
Mon. 12 May		17:30-21:00	Registration and welcome reception	Rush Bar (W Hotel)
Tue. 13 May	1	08:00-08:40	Registration	Hallway
	2A	08:40-08:50	Conference opening by Dr. Rafael Santiago (ICPS7 Chair)	Concrete Ballroom
	2B	08:50-09:05	Prof. Mark Stewart (IAPS President)	Concrete Ballroom
	2C	09:05-09:20	Dr. Najwa Aaraj (TII CEO)	Concrete Ballroom
	3	09:20-09:50	“Norman Jones” Lecture: Prof. Werner Riedel	Concrete Ballroom
	4	09:50-10:20	Keynote 1: Dr Abdulla Al-Dhaheri	Concrete Ballroom
		10:20-10:30	Group photo: Faces of ICPS7	Concrete Ballroom
		10:30-10:50	Coffee Break	Hallway
	5A	10:50-12:50	Response of structures and structural elements to explosion and impact loads	Concrete Ballroom
	5B		Blast and impact resistant design of structures	Ceramic Room
	5C		Innovative materials for protection applications	Composite Room
	5D		Techniques for mitigating blast load and penetration effects	Metal Room
	5E		Projectile penetration and perforation mechanics	Polymer Room
		12:50-14:30	Lunch Break	Garage Restaurant (W Hotel)
		14:30-23:00	Tour to Desert Safari (BBQ Dinner)	Concrete Ballroom
Wed. 14 May	6	08:20-08:30	Organizational Remarks	Concrete Ballroom
	7	08:30-09:00	Keynote 2: Prof. Francois Boussu	Concrete Ballroom
	8	09:00-09:30	Thiot: Equipment/expertise for protective structures	Concrete Ballroom
	9A	09:30-10:30	Response of structures and structural elements to explosion and impact loads	Concrete Ballroom
	9B		Blast and impact resistant design of structures	Ceramic Room
	9C		Innovative materials for protection applications	Composite Room
	9D		Techniques for mitigating blast load and penetration effects	Metal Room
	9E		Projectile penetration and perforation mechanics	Polymer Room
		10:30-10:50	Coffee Break	Hallway
	10A	10:50-12:50	Response of structures and structural elements to explosion and impact loads	Concrete Ballroom

Wed. 14 May	10B	10:50-12:50	Blast and impact resistant design of structures	Ceramic Room
	10C		Innovative materials for protection applications	Composite Room
	10D		Techniques for mitigating blast load and penetration effects	Metal Room
	10E		Projectile penetration and perforation mechanics	Polymer Room
		12:50-14:00	Lunch Break	Garage Restaurant (W Hotel)
	11	14:00-14:30	Keynote 3: Prof. Zhong Xian Li	Concrete Ballroom
	12	14:30-15:30	Ansys: Simulation for blast/impact	Concrete Ballroom
		15:30-15:50	Coffee Break	Hallway
	13A	15:50-17:30	Response of structures and structural elements to explosion and impact loads	Concrete Ballroom
	13B		Blast and impact resistant design of structures	Ceramic Room
	13C		Material behavior at high strain rates	Composite Room
	13D		Post-event evaluation and performance assessment	Metal Room
	13E		Experimental techniques	Polymer Room
	14	16:00-18:00	IAPS Board Meeting (members only)	Meeting Room
		19:00-22:30	Gala Dinner	Concrete Ballroom
Thu. 15 May	15	08:20-08:50	Keynote 4: TBC	Concrete Ballroom
	16A	08:50-10:30	Response of structures and structural elements to explosion and impact loads	Concrete Ballroom
	16B		Blast and impact resistant design of structures	Ceramic Room
	16C		Material behavior at high strain rates	Composite Room
	16D		Post-event evaluation and performance assessment	Metal Room
	16E		Experimental techniques	Polymer Room
		10:30-10:50	Coffee Break	Hallway
	17A	10:50-12:10	Response of structures and structural elements to explosion and impact loads	Concrete Ballroom
	17B		Blast and impact resistant design of structures	Ceramic Room
	17C		Material behavior at high strain rates	Composite Room
	17D		Post-event evaluation and performance assessment	Metal Room
	17E		Experimental techniques	Polymer Room
		12:10-13:10	IAPS General Assembly, Award and Conference Closure	Concrete Ballroom
		13:10-15:00	Lunch Break	Garage Restaurant (W Hotel)

Detailed Sessions

Monday 12 May 2025

17:30 – 21:00	Registration and Welcome reception	**Rush Bar**

Tuesday 13 May 2025

General Sessions		**Concrete Ballroom**
08:00-08:40	Registration	
08:40-08:50	Conference opening by Dr. Rafael Santiago (ICPS7 Chair)	
08:50-09:05	Prof. Mark Stewart (IAPS President)	
09:05-09:20	Dr. Najwa Aaraj (TII CEO)	
"Norman Jones" Lecture: Prof. Werner Riedel		**Concrete Ballroom**
09:20-09:50	**25 Years of concrete modeling: Some key lessons learned for predictive simulations in hydrocodes** *Werner Riedel, Christoph Grunwald* Submission ID: 5120	
Keynote 1: Dr Abdulla Al-Dhaheri		**Concrete Ballroom**
09:50-10:20	**An overview of protective construction and an experimental design of bunker buster slab under projectile impact in UAE** *Abdulla Al-Dhaheri* Submission ID: 9941	
10:20-10:30	**Group photo: Faces of ICPS7**	
10:30-10:50	Coffee Break	
Session 5A: Response of structures and structural elements to explosion and impact loads **Session chair: Toshiyuki Horiguchi, Tomasz Gajewski**		**Concrete Ballroom**
10:50-11:10	**Design and optimization of ballistic panels for light armored vehicles** *Rafael Santiago, Alia Ruzanna Aziz, Fengbo Han, Rafael Savioli, Naresh Kakur, Rubayea Alameri, Nikolaos Nikos and Henrique Ramos* Submission ID: 4543	
11:10-11:30	**Study of a protective structure made of soil-cement using weight dropping device for an impact resistance** *Toshiyuki Horiguchi and Ichiro Kuroda* Submission ID: 3202	
11:30-11:50	**Experimental and numerical investigation on the attenuation of blast stress waves in concrete induced by dynamic explosion** *Xin Zhou, Bin Feng and Li Chen* Submission ID: 8025	
11:50-12:10	**Explosive Field Trial to Measure Spatial Variability of Fragmentation Safety Hazards from VBIEDs** *Mark Stewart, Michael Netherton and Hao Qin* Submission ID: 0814	

12:10-12:30	**Experimental Study on Short-Term Flexural Behaviour of One-Way Seawater-Sea Sand Concrete Slabs Reinforced with GFRP under Impact Loading** *Hai La-Hong, Long Nguyen-Minh and Thong Pham* Submission ID: 2363
12:30-12:50	**Impact Response of Steel Tubular Columns: Role of Axial Load, Connecting member Stiffness, Projectile Mass, and Span Length** *Prithvi Sangani and Anil Agarwal* Submission ID: 5961
Session 5B: Blast and impact resistant design of structures **Session chair: Steeve Chung Yuen, Zoran Ren**	**Ceramic Room**
10:50-11:10	**Experimental study on the effect of front wall width on blast characteristics surrounding box-type structures** *Chien Trinh Minh, Masuhiro Beppu, Hiroyoshi Ichino and Ryo Matsuzawa* Submission ID: 0801
11:10-11:30	**Development of the BLADE tool for blast load assessment and damage evaluation** *Vasilis Karlos, Orestis Ioannou, Ralf Schumacher and Martin Larcher* Submission ID: 4926
11:30-11:50	**Combined blast and fragments loading of explosively welded plates** *Ye Yuan, Yufeng Zhang, Qibo Zhang, Yan Liu, Guangyan Huang and Mengqi Yuan* Submission ID: 0499
11:50-12:10	**Numerical Evaluations on the Blast Response Behavior of Cross-Laminated Timber Panels** *Erkan Mutlu, James Davidson, David Roueche and Kadir Sener* Submission ID: 5166
12:10-12:30	**Fast Prediction Model for Explosion Loads in Complex Scenarios** *Suwen Chen, Yang Huang and Dingkun Luo* Submission ID: 3480
12:30-12:50	**Comparison of ALE, LBE, and the idealized triangular loading method for evaluating an EDST blast loading on a laboratory-scale RC column** *Walid Ben Kraiem, Mohamed Ben Rhouma, Bachir Belkassem and David Lecompte* Submission ID: 3546
Session 5C: Innovative materials for protection applications **Session chair: Yanhong Chen, Hasan Al-Rifaie**	**Composite Room**
10:50-11:10	**Enhanced Anchorage Techniques for Smooth Surfaced Nitinol-SMA Rebars** *Moustafa Basha, Anas Issa and Ahmed Bediwy* Submission ID: 4699
11:10-11:30	**Hybrid metallic and composite armouring solution for blast protected vehicles** *Ilyass Benmessaoud, Hugo Vanmaele, Paul Paul Guillou-Keredanguillou-Keredan, Sebastien Lemercier and Francois Boussu* Submission ID: 8044

11:30-11:50	**Development of gyroid lattice structures for enhancing the energy absorption of motorcycle helmets at realistic impact conditions** *Henrique Ramos, Rafael Santiago and Marcilio Alves* Submission ID: 9483
11:50-12:10	**Ballistic impact performance of gradient structured AZ31 Mg alloy with enhanced strength and plasticity** *Jianguo Li, Qinghui Zhang and Tao Suo* Submission ID: 1677
12:10-12:30	**Blast Resilience of Polycarbonate Panels** *Gauthier Stiegler, Giovanni Milan and Tung Tran* Submission ID: 0646
12:30-12:50	**Impact Loading of Isotropic Shell-Based Stochastic Cellular Metamaterials Fabricated via Additive-Enabled Casting** *Oraib Al-Ketan, Nejc Novak, Matej Vesenjak, Valentina Ortiz, Anja Mauko, Lovre Krstulović-Opara, Shigeru Tanaka, Kazuyuki Hokamoto, Reza Rowshan, Rashid Abu Al-Rub and Zoran Ren* Submission ID: 6030
Session 5D: Techniques for mitigating blast load and penetration effects **Session chair: Teresa Fras, Yanchao Shi**	**Metal Room**
10:50-11:10	**Modelling of the Retrofitting of Existing Structural Shielding in Radiology Facilities** *Mustafa Majali, Ali Al Remeithi, Buthaina Al Ameri and Kaltham Al Hosani* Submission ID: 9624
11:10-11:30	**Numerical Investigation of Hydrogen Leakage Dispersion and Explosion Consequences under Coupled Factors at Refueling Stations** *Yanchao Shi, Ziyu Zhong, Zhong-Xian Li and Jian Cui* Submission ID: 5527
11:30-11:50	**Finite Element Analysis of Gusset Plate and Joint Sections for Buckling Restrained Braced Frames under Seismic Loading** *Brwa Bebani and Mieczysław Kuczma* Submission ID: 6368
11:50-12:10	**A dimensionless metric for quantifying fluid-structure interaction in blast-loaded plates** *Giovanni Marchesi, Luca Lomazzi, Vegard Aune, Andrea Manes and Trevor John Cloete* Submission ID: 6709
12:10-12:30	**Impact of Reinforcement ratio and CFRP on the Blast Performance of Reinforced Concrete slabs: A Numerical Approach** *Sai G R K O, Arumugam D, Tamilselvan K and Dhanasekaran B* Submission ID: 7390
12:30-12:50	**Key considerations and methodologies for analyzing LVBIED blast events on long-spanning roof diagrid structures** *Gabriel Martin, Simone Volpe and Laura Cannon* Submission ID: 6269

Session 5E: Projectile penetration and perforation mechanics Session chair: Licheng Guo, Lina M. Lopez		Polymer Room
10:50-11:10	**Enhanced Penetration Through Two-Stage Double-Blunt Projectile** *Shaima Alhosani, Sanan Khan and Afsar Husain* Submission ID: 7043	
11:10-11:30	**Detonation chamber for end of life warheads disposal in fully confined conditions: from design to proof tests** *Jérôme Mespoulet, Maëlle Peyratout, Sébastien Boussac and Paul Deconinck* Submission ID: 7452	
11:30-11:50	**Parameter calibration of Kong-Fang constitutive model for geopolymer based ultra-high performance concrete (G-UHPC)** *Fangming Tian and Li Chen* Submission ID: 0824	
11:50-12:10	**Numerical Analysis of Energy Dissipation and Temperature during Impact Tests on S235 Steel Specimens at Various Impact Angles** *Maciej Klosak, Michal Grazka and Leopold Kruszka* Submission ID: 6591	
12:10-12:30	**Micro-CT scan analysis for ballistic cement-based composites** *Omar Ba Nabila, Felipe Rodrigues and Ana Jimenez* Submission ID: 6034	
12:30-12:50	**Experimental and Numerical Investigation of Aluminum/Polyethylene Sandwich Structures under Varied Loading Rates and Temperatures for Protective Applications** *Amine Bendarma, Tomasz Jankowiak, Alexis Rusinek, Christophe Czarnota, Richard Bernier and Tomasz Jankowiak* Submission ID: 9311	
12:50-14:30	**Lunch Break**	Garage Restaurant (W Hotel)
14:30-23:00	**Tour to Desert Safari (BBQ Dinner)**	Concrete Ballroom

Wednesday 14 May 2025

General Sessions		Concrete Ballroom
08:20-08:30	Organizational Remarks	
Keynote 2: Prof. Francois Boussu		**Concrete Ballroom**
08:30-09:00	**Textile materials as an effective protective solution against multi-velocity and multi-threat impacts** *Francois Boussu* Submission ID: 0501	
09:00-09:30	**THIOT: Equipment/expertise for protective structures**	**Concrete Ballroom**

Session 9A: Response of structures and structural elements to explosion and impact loads Session chair: Mark Stewart, Piotr Sielicki	Concrete Ballroom
09:30-09:50	**Application of 2D to 3D ALE Mapping in Designing Column Structures under a Close-in Detonation** *Tin Do, Rajendra Bohara and Asher Gehl* Submission ID: 0562
09:50-10:10	**High-velocity impact behaviour of Carbon epoxy composite with PAN nanofiber reinforcement** *Vishnu Vijay Kumar, Khaled Shahin, Suresh Rajendran, Anupoju Rajeev, Prince Jeya Lal Lazar, Sharan Chandran and Seeram Ramakrishna* Submission ID: 2357
10:10-10:30	**The blast mitigation performance of curtain-type blast wall** *Xingjun Fan, Zhejian Li, Hong Hao and Wensu Chen* Submission ID: 1429
Session 9B: Blast and impact resistant design of structures **Session chair: Nikoloz Chikhradze, Jun Yu**	**Ceramic Room**
09:30-09:50	**Field tests and numerical analysis of the blast-absorbing composite structure** *Robert Studziński, Hasan Al-Rifaie, Michał Malendowski, Wojciech Sumelka, Tomasz Gajewski and Piotr Sielicki* Submission ID: 2325
09:50-10:10	**Equivalency method for evaluating the high-velocity impact performance of composite panels** *Chao Zhang and Chunlin Du* Submission ID: 2929
10:10-10:30	**Blast protection of steel- aluminum foam sandwich structures using polyurea and stiffeners** *Harshada Sharma, Kusum Saini, Satinder Paul Singh and Vasant Matsagar* Submission ID: 2480
Session 9C: Innovative materials for protection applications **Session chair: Francois Boussu, Victor P.W. Shim**	**Composite Room**
09:30-09:50	**Experimental Analysis and Numerical Modeling of Energy Absorption Capability and High Deformation Response in 3D-Printed Multilayer Panels** *Hour Alhefeiti, Amged Elhassan, Khalifa Harib, Waleed Ahmed, Farook Al-Jahwari and Kubilay Aslantas* Submission ID: 7761
09:50-10:10	**Characterization of a Modified Multi-material Auxetic Re-entrant Honeycomb for Protective Applications** *Alexander Engel, Oraib Al-Ketan and Anne Jung* Submission ID: 2815
10:10-10:30	**An experimental investigation on the low velocity impact response of novel thermoplastic and thermoset sandwich composite** *Laila Alhadary, Mahmoud Mohamed, Haibin Ning and Selvum Pillay* Submission ID: 5624

Session 9D: Techniques for mitigating blast load and penetration effects Session Chair: Ziwen Xu, Fabio Brantschen	Metal Room
09:30-09:50	**Period-based anti-explosion protective wall. Design procedure and application manual** *Alejandro Perez Caldentey, Maria Chiquito, Anastasio Santos, Lina López and Ricardo Castedo* Submission ID: 8286
09:50-10:10	**Blast Response of Masonry Wall Under Contact Explosion Using CFRP as Externally Bonded Reinforcement: Experimental and Numerical Analysis** *Azer Maazoun, Oussama Atoui, Mohamed Ben Rhouma, Ahmed Siala, Bachir Belkassem, Stijn Matthys and David Lecompte* Submission ID: 3879
10:10-10:30	**Experimental and numerical investigation on the protective performance of polymeric pre-layered steel targets under high-velocity ballistic loadings** *Fras Teresa* Submission ID: 4196
Session 9E: Projectile penetration and perforation mechanics Session Chair: Anupoju Rajeev, Leopold Kruszka	**Polymer Room**
09:30-09:50	**Behavior of structures fabricated of ice and thin steel plates impacted by high-speed striker** *Maxim Orlov, Victor Glayrin and Talgat Fazylov* Submission ID: 8087
09:50-10:10	**Automated finite element modeling of multi-layer composite structures against projectile impact: from Abaqus plug-in to large language model-based applications** *Fengbo Han, Kapil Krishnan, Jide Oyebanji, Changze Sun, Rafael Savioli, Naresh Kakur, Alia Ruzanna Aziz, Henrique Ramos, Nikolaos Nikos and Rafael Santiago* Submission ID: 8032
10:10-10:30	**Dynamic properties of materials subjected to perforation tests in a wide range of temperatures - a review of experimental studies** *Leopold Kruszka, Maciej Klosak and Kamil Sobczyk* Submission ID: 0632
10:30-10:50	Coffee Break
Session 10A: Response of structures and structural elements to explosion and impact loads Session Chair: Piotr Sielicki, Mark Stewart	**Concrete Ballroom**
10:50-11:10	**Performance Evaluation of a 4-m-High Conventional Rockfall Protection Fence** *Masato Komuro, Tomoki Kawarai, Takuro Nakamura and Norimitsu Kishi* Submission ID: 1699

11:10-11:30	**Subterranean Pipe Response to Above-Ground Blast: Part 1 - Experimental Testing** *Chris Taggart, Alex Rogers and Steve Fay* Submission ID: 6019
11:30-11:50	**Ballistic Penetration Resistance of Reinforced and Non-Reinforced Concrete Formulations under High-Velocity Gas-Gun Impact** *Henrique Ramos, Felipe Rodrigues de Souza, Nikolaos Nikos, Omar Ba Nabila, Rafael Savioli, Flavio de Andrade Silva and Rafael Santiago* Submission ID: 3334
11:50-12:10	**Modelling vehicular impact for threat-dependent progressive collapse assessments** *Gioele Montalbetti, Alex Sixie Cao and Andrea Frangi* Submission ID: 4058
12:10-12:30	**Blast Characterisation and Structural Response in Large-Scale Unconfined Hydrogen Explosions: An Australian Field Study** *Zhenying Huang, Edward Gan, Alex Remennikov, Damith Mohotti and Kasun Wijesooriya* Submission ID: 0856
12:30-12:50	**Development and Validation of an Advanced CFD Model for Predicting Hydrogen Explosion Dynamics** *Wimukthi Senarathna, Damith Mohotti, Kasun Wijesooriya, Chi-King Lee, Edward Gan and Alex Remennikov* Submission ID: 2274
Session 10B: Blast and impact resistant design of structures. Session Chair: Jun Yu, Nikoloz Chikhradze	**Ceramic Room**
10:50-11:10	**Numerical Investigation of Close-in Blast Loads in Partially Confined Spaces** *Hwee Kiat Yeo and Swee Hong Tan* Submission ID: 5017
11:10-11:30	**Effect of Partial Composite Action on Performance of Precast Concrete Sandwich Wall Panels under Blast Load** *Lekhani Gaur, Bhavin Zaveri and Jagriti Mandal* Submission ID: 7661
11:30-11:50	**Effects of resin coating on the blast resistant performance of concrete plates under contact explosion** *Hiroyoshi Ichino, Yuto Nomura, Masuhiro Beppu and Toshiya Yamauchi* Submission ID: 8476
11:50-12:10	**Numerical investigations on the effects of detonation products on blast load** *Pu Huo, Jun Yu and Banruo Li* Submission ID: 8981
12:10-12:30	**Influence of Layering on the Blast Performance of Laminated Glass** *Sa-Aadat Parker, Steeve Chung Kim Yuen and Gerald Nurick* Submission ID: 8882
12:30-12:50	**Dynamic response and failure mechanism of Double-Double laminate under high-speed ballistic impact** *Lijun Xiao, Hong Zhen and Weidong Song* Submission ID: 6379

Session 10C: Innovative materials for protection applications. Session Chair: Victor P.W. Shim, Francois Boussu	Composite Room
10:50-11:10	**Crashworthiness of cellular protective structures: from positive to negative to zero Poisson's Ratio** *Hasan Al-Rifaie, Nima Movahedi and Teik-Cheng Lim* Submission ID: 8041
11:10-11:30	**Experimental study on the anisotropic response of additively-manufactured polymeric lattices subjected to compression in different directions** *Zhengping Sun, Yuanyuan Ding and Victor P.W. Shim* Submission ID: 2797
11:30-11:50	**Underexcitation prevents crystallization of granular assemblies subjected to high-frequency vibration** *Sara Almahri* Submission ID: 6332
11:50-12:10	**The ballistic performance of composite walls made of 3D printed concrete** *Richard Dekker, Dieter van der Pol, Erik Carton, Elfi van Zeijl and Hugo Dijkers* Submission ID: 5249
12:10-12:30	**Advanced blast containment technologies for passenger aircraft: Description of blast testing, and recommendations for application in other domains** *Donato Zangani, Alessandro Bozzolo and Andrew Tyas* Submission ID: 0423
12:30-12:50	**Dynamic analysis of lattice-based metamaterials for impact protection** *Salvatore Annunziata, Edison Shehu, Luca Lomazzi and Andrea Manes* Submission ID: 6792
Session 10D: Techniques for mitigating blast load and penetration effects Session Chair: Fabio Brantschen, Ziwen Xu	**Metal Room**
10:50-11:10	**The role of metamaterials in protecting ship equipment from underwater explosion shock** *Jacopo Bardiani, Giada Kyaw Oo D'Amore, Giovanni Marchesi, Marco Biot, Claudio Sbarufatti and Andrea Manes* Submission ID: 9313
11:10-11:30	**Evaluating High-Rise Building Vulnerability to Blast and Progressive Collapse Using the Applied Element Method** *Ayman Elfouly* Submission ID: 2559
11:30-11:50	**Blast protective system for concrete walls: experimental tests and numerical simulation** *María Chiquito, Anastasio P. Santos, Lina M. López, Ricardo Castedo, Alejandro Pérez-Caldentey, Luis Iglesias and Iván Gil* Submission ID: 2421

11:50-12:10	**Ultra-high performance curved concrete slabs against blast loading** *Manish Kumar, Alok Dua and Shreya Korde* Submission ID: 2974	
12:10-12:30	**Exploring the role of detailing in earth-covered magazines: review of current design solutions** *Fabio Brantschen, Andrea Peruzzi, Duarte Miguel Viula Faria and Miguel Fernández Ruiz* Submission ID: 9825	
12:30-12:50	**Effects of Triggering Event Characteristics on the Progressive Collapse Response of Reinforced Concrete Moment-Resisting Frames** *Foad Kiakojouri, Elahe Zeinali and Valerio De Biagi* Submission ID: 2713	
Session 10E: Projectile penetration and perforation mechanics **Session Chair: Leopold Kruszka, Anupoju Rajeev**		**Polymer Room**
10:50-11:10	**Review of modern design methods for blast loaded floor slabs** *Franciszek Woloch, Piotr Nowak, Artur Szlachta, Tomasz Gajewski and Piotr W. Sielicki* Submission ID: 9578	
11:10-11:30	**Multiple Impact Behaviour of Nanoparticle Strengthened UHMWPE Composite Ballistic Helmet** *Madhav Umbharatwala, Manmohan Dass Goel, Marcus Maeder and Steffen Marburg* Submission ID: 2444	
11:30-11:50	**Penetration Resistance of Green Concrete and a Predictive Model Based on Macroscopic Effective Hardness** *Jie Zhang and Leong Hien Poh* Submission ID: 9595	
11:50-12:10	**Experimental Investigation of Smart Composite Structural Insulated Panels with Integrated Piezoelectric Sensors for Damage Localization in Extreme Conditions** *Anupoju Rajeev, Vishnu Vijay Kumar, Amit Shelke, Khaled Shahin and Prince Jeya Lal Lazar* Submission ID: 8359	
12:10-12:30	**A novel hydro-elastoplastic model for concrete-like materials under impact and explosion loadings considering modulus damage** *Junfeng Wang and Li Chen* Submission ID: 6676	
12:30-12:50	**Enhancing Ballistic Resistance of High-Performance Fiber-Reinforced Concrete Panels Using Polyurethane Coatings and Epoxy Composites** *Petr Hála, Přemysl Kheml, Alexandre Perrot, Jiří Mašek and Radoslav Sovják* Submission ID: 5037	
12:50-14:00	**Lunch Break**	Garage Restaurant (W Hotel)

Keynote 3: Prof. Zhong Xian Li		Concrete Ballroom
14:00-14:30	**Research Progress on Performance-based Design Theory and Methods of Building Structures against Blast Loading** *Zhong-Xian Li, Yang Ding, Yanchao Shi and Jian Cui* Submission ID: 1400	
14:30-15:30	**Ansys: Simulation for blast/impact**	**Concrete Ballroom**
15:30-15:50	Coffee Break	
Session 13A: Response of structures and structural elements to explosion and impact loads **Session Chair: Tomasz Gajewski, Toshiyuki Horiguchi**		**Concrete Ballroom**
15:50-16:10	**High Strain Rate Properties of Fibrous Cement-based Composites using the Split-Hopkinson Pressure Bar** *Felipe Rodrigues de Souza, Henrique Ramos, Alia Ruzanna Aziz, Omar Ba Nabila, Rafael Savioli, Nikolaos Nikos, Flavio de Andrade Silva and Rafael Santiago* Submission ID: 1888	
16:10-16:30	**Field Tests of Square RC Column under Vehicle Impact Loads** *Sanghee Kim* Submission ID: 6533	
16:30-16:50	**Subterranean pipe response to above-ground blast: Part 2 – Numerical Analysis** *Christopher Taggart, Alex Rogers and Sam Chacksfield* Submission ID: 3893	
Session 13B: Blast and impact resistant design of structures **Session Chair: Zoran Ren, Steeve Chung Yuen**		**Ceramic Room**
15:50-16:10	**Assessment of precast prestressed concrete beams subjected to blast loading** *Anqi Chen, Jin Zhang and Gauthier Stiegler* Submission ID: 5416	
16:10-16:30	**Restraining Effect for Scabbing Fragments of RC Slab Subjected to Projectile Impact by Polyurea Resin and Aramid Fiber Sheet** *Koki Mori, Masuhiro Beppu, Hiroyoshi Ichino and Shuhei Fukui* Submission ID: 5320	
16:30-16:50	**Experimental study on structural behavior of GFRP-concrete-steel double-skin tubular column under near-field blast load** *Jun Yu, Yun-Hao Geng and Xiao-Wei Feng* Submission ID: 7542	
16:50-17:10	**RC beams: full-scale tests and numerical modelling** *Ricardo Castedo, Ángel Prado, Alejandro Alañón, Anastasio P. Santos, Lina M. López and María Chiquito* Submission ID: 8951	
17:10-17:30	**Temperature Distribution in Underground Structure Subjected to Blast and Subsequent Fire Loads** *Abhishek Mohapatra, Sunita Mishra and Wensu Chen* Submission ID: 5003	

Session 13C: Material behavior at high strain rates Session Chair: Hasan Al-Rifaie, Yanhong Chen	Composite Room
15:50-16:10	**High-Strain Rate Characterization of Loblolly Pine Mechanical Properties under Extreme Temperature and Moisture Conditions** *Ryan Holtzscher, James Davidson, David Roueche and Kadir Sener* Submission ID: 8838
16:10-16:30	**Multiscale modelling of the structural response of plain-woven composites** *Ziwen Xu, Yanhong Chen, Zhongwei Guan and Wesley Cantwell* Submission ID: 2842
16:30-16:50	**Contact Explosion Resistance of a Steel Sandwich Panel Containing an Aluminum Honeycomb Layer** *Nikoloz Chikhradze, Edgar Mataradze and Irakli Akhvlediani* Submission ID: 7387
16:50-17:10	**A self-consistent modelling methodology for predicting the mechanical behavior of interleaved composites** *Yanhong Chen, Ziwen Xu and Licheng Guo* Submission ID: 7482
17:10-17:30	**Experimental study of the behaviour of SLA sandwich panels with different lattice structures under repeated loading** *Gizem Köse, Kubilay Aslantas and Waleed Ahmed* Submission ID: 1933
Session 13D: Post-event evaluation and performance assessment Session Chair: Yanchao Shi, Teresa Fras	**Metal Room**
15:50-16:10	**Large-caliber Compressive Air Gun in Tongji University, China** *Liangliang Ma, De Chen, Hao Wu and Yuehua Cheng* Submission ID: 8614
16:10-16:30	**Accidental Explosions in Urban Environments: A Case Study of a 2024 Blast in Poznań** *Peter McDonald, Andrew Nicholson, Christopher Stirling and Piotr Sielicki* Submission ID: 8666
16:30-16:50	**Effects of eccentric impacts and corrosion on the structural behaviour of retaining wire ring nets** *Francesco Pimpinella, Maddalena Marchelli and Valerio De Biagi* Submission ID: 6212
16:50-17:10	**Response of Mortar-less Interlocking Brick Walls under Impulsive Loading** *Xihong Zhang, Guochao Wang and Hong Hao* Submission ID: 0414
17:10-17:30	**Impact Response of Glass Façade to Wind Borne Debris: A Numerical Study** *Deenay Ambade, Manmohan Dass Goel and L M Gupta* Submission ID: 1484

Session 13E: Experimental techniques Session Chair: Lina M. Lopez, Licheng Guo		Polymer Room
15:50-16:10	**Fragmentation Analysis of Unexploded Underwater Ordnance** *Piotr Nowak, Ross Waddoups, Dain Farrimond, Tomasz Gajewski, Tommy Lodge, Genevieve Langdon, Andy Tyas, Piotr Sielicki, Elliot Tam and Mark Whittaker* Submission ID: 8673	
16:10-16:30	**Mesoscale in-situ methods for characterizing the interfacial properties of the 3DWC** *Licheng Guo, Qingsong Zong, Jinzhao Huang and Yunpeng Gao* Submission ID: 6366	
16:30-16:50	**Investigation into the Effects of Blockage and Frangible Tunnel Sections on Blast Pressure Profiles** *Aljo Jose, Chris Taggart and John Adams* Submission ID: 5468	
16:50-17:10	**Engineering model to determine the residual static load-bearing capacity of reinforced concrete and steel fibre reinforced concrete structures after contact detonation** *Vahan Zohrabyan and Thomas Braml* Submission ID: 3888	
16:00-18:00	**IAPS Board Meeting (members only)**	**Meeting Room**
19:00-22:30	Gala Dinner	

Thursday 15 May 2025

Keynote 4: TBC		Concrete Ballroom
08:20-08:50	**Keynote**	
Session 16A: Response of structures and structural elements to explosion and impact loads Session Chair: Waleed Ahmed, Vishnu Vijay Kumar		**Concrete Ballroom**
08:50-09:10	**Study of the uncertainty in the experimental evaluation of the TNT equivalent of a plastic explosive and numerical validation** *Lina M. Lopez, María Chiquito, Anastasio P. Santos, Ricardo Castedo, Ana López, Andrew Nicholson, Peter McDonald and Chris Stirling* Submission ID: 6657	
09:10-09:30	**Blast Resistance and Fragility Analysis of RC Columns with Chloride-induced Corrosion** *Yu Liu, Hong Hao and Yifei Hao* Submission ID: 3326	
09:30-09:50	**Design and development of an interchangeable clamp for tensile testing of UHMWPE composites with 3D-DIC** *Alia Ruzanna Aziz, Naresh Kakur, Henrique Ramos and Rafael Santiago* Submission ID: 2949	

09:50-10:10	**A Comparative Study for Evaluating Secondary Debris Throw of Building Components from an Internal Explosion** *Xiao Ding Bu and Anay Raibagkar* Submission ID: 6767
10:10-10:30	**Experimental Investigation of Energy Absorption in 3D-Printed Polymeric Axial Members Under High and Low-Speed Impact Using Various Infill Patterns** *Raed Shwaish, Hind Abdulridha, Adil Jaber and Waleed Ahmed* Submission ID: 8328
Session 16B: Blast and impact resistant design of structures **Session Chair: Werner Riedel, Nejc Novak**	**Ceramic Room**
08:50-09:10	**Derivation of P-I diagram for UHPC protective wall against gaseous explosion based on calibrated K&C model and machine learning** *Di Chen, Chengqing Wu and Jun Li* Submission ID: 3511
09:10-09:30	**Investigating the effects of delaying the removal of frangible elements in CFD blast simulations.** *Gabriel Martin, Simone Volpe and Laura Cannon* Submission ID: 2820
09:30-09:50	**Response of Gradient Hexachiral Auxetics Under Impact Loadings: Experimental Study** *Li Xin and Chen Chuanqing* Submission ID: 7372
09:50-10:10	**Modeling of confined explosions: an uncoupled eulerian-lagrangian approach for blast wave propagation and structural assessment** *Edison Shehu, Luca Lomazzi and Andrea Manes* Submission ID: 6425
10:10-10:30	**Computational simulations of blast loading of auxetic and TPMS-filled sandwich panels** *Nejc Novak, Oraib Al-Ketan, Matej Vesenjak and Zoran Ren* Submission ID: 8035
Session 16C: Material behavior at high strain rates **Session Chair: Felipe Souza, Jian Cui**	**Composite Room**
08:50-09:10	**Deformation Behavior of Additively Manufactured Cellular Metamaterials at Different Strain Rates** *Zoran Ren, Anja Mauko, Oraib Al-Ketan and Nejc Novak* Submission ID: 6539
09:10-09:30	**Dynamic response of BFRP bars subjected to impact loading at high strain rates** *Zeinah Elnassar, Maen Alkhader and Farid Abed* Submission ID: 5813
09:30-09:50	**A constitutive model considering hydrostatic damage for high dynamic properties of concrete** *Jian Cui, Xianglong Guan, Yanchao Shi and Zhong-Xian Li* Submission ID: 8082

09:50-10:10	**Shock Tube Tests and Modeling of Buildings Materials and Structural Components Exposed to Critical Blast Loads** *Mohsen Sanai, Waylon Weber, Joe Crepeau Crepeau and Sean Cooper* Submission ID: 3908
10:10-10:30	**Numerical Study on Ballistic Impact Behavior of Laminated Glass Systems** *Nexia Murali, Roouf Un Nabi Dar, Kaviarasu K and Alagappan P* Submission ID: 4380
Session 16D: Post-event evaluation and performance assessment **Session Chair: Wensu Chen, Maddalena Marchelli**	**Metal Room**
08:50-09:10	**Novel approaches to modeling debris loading after building structural collapse** *Marcin Nowak, Piotr Nowak, Artur Szlachta, Franciszek Woloch, Tomasz Gajewski and Piotr Sielicki* Submission ID: 8071
09:10-09:30	**Post-fire Impact Resistance of Ultra-high Performance Concrete Beams** *Junjie Huang, Jun Li and Chengqing Wu* Submission ID: 2465
09:30-09:50	**Estimation of the probability distribution of rockfall barriers energy absorption capacity through a global analytical model** *Francesco Pimpinella, Maddalena Marchelli and Valerio De Biagi* Submission ID: 7332
09:50-10:10	**Coupled Effect of Temperature and Impact Loading on the Mechanical Properties of Ultra High Performance Concrete** *Gabriel Erlacher, Flavio Silva and Daniel Cardoso* Submission ID: 4089
10:10-10:30	**Investigating Fragmentation Risk in ARMOX 440T Steel plates Under Localized Blast Loading** *Haleimah Alabdouli, Richard Curry and Genevieve Langdon* Submission ID: 3689
Session 16E: Experimental techniques **Session Chair: Yuanxiang Sun, Selvum Pillay**	**Polymer Room**
08:50-09:10	**Utilizing LiDAR to Effectively Assess Residual Capacity of Damaged Structures** *Samuel Benson, Samuel Keys and Eric Williamson* Submission ID: 3828
09:10-09:30	**The Study on Interaction between Bubble and Double-layer Structure with Hole** *Yuanxiang Sun* Submission ID: 8347
09:30-09:50	**Post-tensioned reinforced concrete column sections under impact loading** *Ghazaleh Taheri, Petr Máca, Thomas Schubert, Nicholas Unger, Silke Scheerer, Birgit Beckmann and Steffen Marx* Submission ID: 2390

09:50-10:10	**Impact performance of RC beam-column joints with seismic-induced damage** *Jixian Li, Hongyu Chen, Huawei Li, Wensu Chen and Hong Hao* Submission ID: 9001
10:10-10:30	**Experimental Analysis of Pre-cracked Sandstone Rock at High Strain-Rate Loading Conditions** *Rabin Kumar Samal and Sunita Mishra* Submission ID: 8086
10:30-10:50	Coffee Break
Session 17A: Response of structures and structural elements to explosion and impact loads **Session Chair: Vishnu Vijay Kumar, Waleed Ahmed**	**Concrete Ballroom**
10:50-11:10	**Structural response and failure modes of armor steel plates under dynamic underwater explosions** *Prince Jeya Lal Lazar, Vishnu Vijay Kumar, Khaled Shahin and Anupoju Rajeev* Submission ID: 8925
11:10-11:30	**Preliminary Study on Design, Manufacture and Finite Element Analysis of The Absorbing Liner for Motorcycle Helmet** *Henry Lim Yi Zong and S. Kanna Al Subramaniyan* Submission ID: 7937
11:30-11:50	**High Velocity Impact Studies of Ceramic/UHMWPE Composite Ballistic Plate Configurations** *Rubayea Alameri, Naresh Kakur, Rafael Savioli, Nikolaos Nikos and Rafael Santiago* Submission ID: 7008
11:50-12:10	**A Scaled Model Correction Technique for Predicting the Impact Response of Curved Beams** *Xinzhe Chang, Fei Xu, Wesley Cantwell and Wei Feng* Submission ID: 0108
Session 17B: Blast and impact resistant design of structures **Session Chair: Nejc Novak, Omar Ba Nabila**	**Ceramic Room**
10:50-11:10	**Energy-Based Monitoring Technique for Progressive Collapse Prevention in Complex Structures** *Lorenza Abbracciavento and Valerio De Biagi* Submission ID: 7056
11:10-11:30	**Projectile impact behaviour of geopolymer-based ultra-high performance concrete (G-UHPC)** *Kefo Qu and Jian Liu* Submission ID: 5256
11:30-11:50	**Deep Learning-based Framework to Predict Spatio-temporal Reflected Pressure on Structural Surfaces** *Chamodi Widanage, Damith Mohotti, Kasun Wijesooriya and Chi-King Lee* Submission ID: 8803

11:50-12:10	**Machine learning prediction of fragment distribution with graph neural networks** *Zhijie Zhang, Qiushi Yan, Yeqing Chen, Mengnan Dai and Longyun Zhou* Submission ID: 6786
Session 17C: Material behavior at high strain rates **Session Chair: Jian Cui, Felipe Souza**	**Composite Room**
10:50-11:10	**A Constitutive Model of Heavyweight Concrete for Blast Simulation** *Chunyuan Liu, Yifei Hao, Xueqiang Li, Siyao Wang and Guowei Ma* Submission ID: 5454
11:10-11:30	**The use of high performance fiber reinforced cement based composites to strength concrete structures under impact loading** *Felipe Souza, Julio Nunes, Victor Lima and Flávio Silva* Submission ID: 5053
11:30-11:50	**Numerical investigations on the dynamic response of near-field blast-loaded steel plates** *Weifang Xiao, Xianzhong Zhao and Jiannan Ye* Submission ID: 8875
11:50-12:10	**Dynamic response of small-scale circular RC columns under localized blast loading** *Mohamed Ben Rhouma, Aldjabar Aminou, Azer Maazoun, Bachir Belkassem, Tine Tysmans and David Lecompte* Submission ID: 7408
Session 17D: Post-event evaluation and performance assessment **Session Chair: Maddalena Marchelli, Wensu Chen**	**Metal Room**
10:50-11:10	**Damage assessment of ultra-high performance concrete column subjected to contact explosion** *Raghav Kumar Mishra and Alagappan Ponnalagu* Submission ID: 0551
11:10-11:30	**Analysis on the effect of crash-induced shock on representative electric vehicle battery modules and packs** *Yuyang Xing and Qingming Li* Submission ID: 9542
11:30-11:50	**Vehicle borne improvised explosive devices – experimental study** *Tomasz Gajewski, Piotr Peksa, Robert Studziński, Michał Malendowski, Piotr Nowak, Artur Szlachta, Krzysztof Szajek, Wojciech Sumelka and Piotr Sielicki* Submission ID: 1143
11:50-12:10	**Impact Response of Ambient-Cured Fibre-Reinforced Geopolymer Concrete Beams with Steel-BFRP Composite Bars** *Zhijie Huang, Wensu Chen and Hong Hao* Submission ID: 0483

17E: Experimental techniques Session Chair: Selvum Pillay, Yuanxiang Sun		Polymer Room
10:50-11:10	**Electromagnetic Hopkinson bar: A powerful tool to study mechanical behavior of materials at high strain rates** *Weibin Wang, Yazhou Guo and Yulong Li* Submission ID: 1733	
11:10-11:30	**Kinetic Energy Penetrator (KEP) impact on confined concrete** *Hakim Abdulhamid, Fabien Plassard, Jérôme Mespoulet and Paul Deconinck* Submission ID: 6131	
11:30-11:50	**The Low Velocity Impact Properties of Multi- Axial Three Dimensional (3D) Woven Composites** *Mehmet Korkmaz, Ahmad Rashed Labanieh, Xavier Legrand and Francois Boussu* Submission ID: 0541	
11:50-12:10	**Experimental study on falling debris impact: a basis for pancake-type progressive collapse assessment** *Elahe Zeinali, Foad Kiakojouri and Valerio De Biagi* Submission ID: 8529	
12:10-13:10	**IAPS General Assembly, Award and Conference Closure**	**Concrete Ballroom**
13:10-15:00	**Lunch Break**	Garage Restaurant (W Hotel)

Abstracts

A Scaled Model Correction Technique for Predicting the Impact Response of Curved Beams

Xinzhe Chang [1,2], Fei Xu [1,*] Wesley Cantwell [2], and Wei Feng [1]

[1]*School of Aeronautics, Northwestern Polytechnical University, Xi'an, Shaanxi, China*

[2]*Department of Aerospace Engineering, Khalifa University of Science and Technology, Abu Dhabi, United Arab Emirates*

[*]Corresponding author: xufei@nwpu.edu.cn

In practical engineering applications, curved beam structures are found in aerospace applications, bridges and marine components, such as submarines, etc. Their dynamic response under high velocity impact conditions has an important influence on their safety and durability. In the field of impact dynamics, designing scaled models, based on similarity theory, to predict the impact response of prototypes has attracted significant attention in recent years [1]. However, due to the effects of both strain-rate and strain-hardening on material properties, especially when different materials are selected for the scaled model and the prototype, there is a potential for discrepancies to occur between the scaled model and the prototype, limiting the accuracy of the scaled model.

In this study, the key dimensionless parameters for curved beams during the impact process, whose structural shape is shown in Fig. 1, are proposed using a dimensional analysis method [2]. On this basis, the similarity scaling relationship of the impact response of the curved beam structure is derived. Then, in order to solve the problem of distortion, due to strain-rate effects, strain-hardening effects and differences between the scaled model material and the prototype material, a velocity correction technique is introduced [3]. More specifically, based on the optimal approximation between the predicted yield stress of the scaled model and the dynamic yield stress of the prototype, the scaling factor for the impact velocity is directly derived, which ensures the similarity of the impact response between the model and the prototype under these dynamic loading conditions. A series of numerical models of curved beams subjected to impact by a mass are established to verify the effectiveness of this correction technique. From the numerical results, as shown in Fig. 2, compared with the traditional scaled model design method, the technique shows a significant improvement in accuracy and reliability, and provides a more effective solution for predicting the dynamic response of curved beam structures.

Keywords: scaled model, strain rate effect, impact response.

[1] Jones N. (2011). Structural impact (2nd ed.). Cambridge University Press. DOI: 10.1017/CBO9780511820625.

[2] Wang S., Xu F., Dai Z. (2020). Suggestion of the DLV dimensionless number system to represent the scaled behavior of structures under impact loads. Archive of Applied Mechanics, 90(5), 707-719. DOI: 10.1007/s00419-019-01635-9.

[3] Wang S., Xu F., Zhang X.Y., et al. (2021). Material similarity of scaled models. International Journal of Impact Engineering, 156, 103951. DOI: 10.1016/j.ijimpeng.2021.103951.

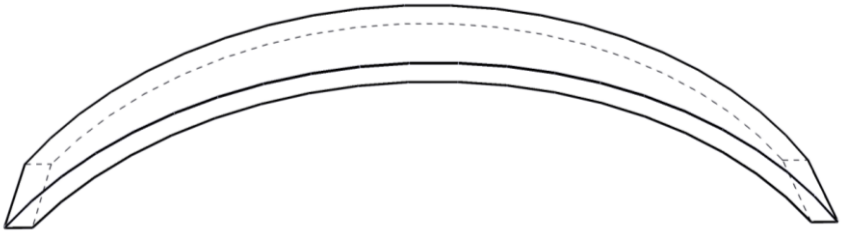

Fig. 1 Schematic diagram of curved beam structure.

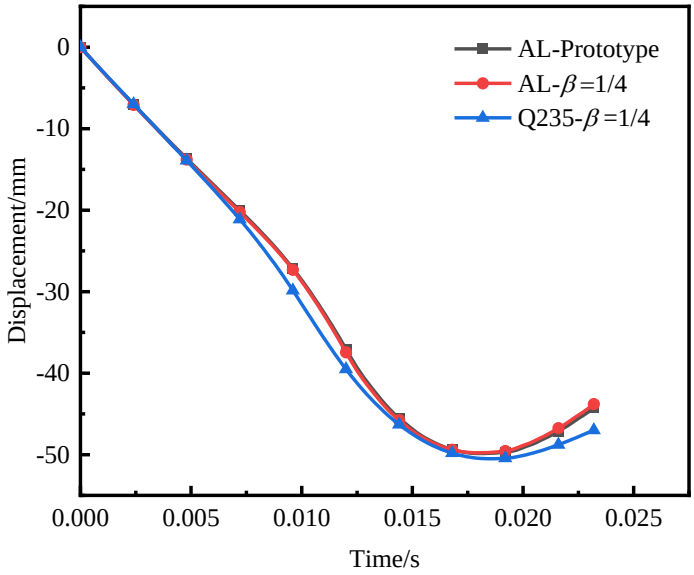

Fig. 2. Displacement time curve of curved beam.

Response of Mortar-less Interlocking Brick Walls under Impulsive Loading

Guochao Wang[1], Xihong Zhang[2], Hong Hao[3]

[1] *Centre for Infrastructure Monitoring and Protection, Curtin University, Bentely, Australia*

[2] *Centre for Infrastructure Monitoring and Protection, Curtin University, Bentely, Australia*

[3] *Centre for Infrastructure Monitoring and Protection, Curtin University, Bentely, Australia; Guangzhou University, Guangzhou, China*

Mortar-less interlocking brick is a novel construction product and technology that offers outstanding structural performance and construction efficiency. Our previous studies have quantified the fundamental mechanical properties, and the responses of interlocking brick walls under in-plane cyclic loading and earthquake loading. This paper presents our recent study on the response of mortar-less interlocking brick walls under impulsive loading generated through an airbag using a pendulum impact testing system. With the assistance of digital-image-correlation technique, a high-speed camera is used to monitor the deformation-to-failure process of the wall. The applied pressure time history applied to the wall, and the deflection time histories of the wall at various points are recorded. The damage and failure mode of interlocking brick wall is investigated in detail. Numerical modeling is also carried out to assist analyze the behavior of interlocking brick wall. Results reveal that comparing to conventional mortar bonded clay brick walls or concrete masonry units, mortar-less interlocking brick walls show much less damaged. Interlocking brick walls exhibit outstanding deformation ability and energy dissipation capability. A homogenized constitutive model using Representative Volume Element (RVE) is established for simulating the responses of interlocking brick walls under impact loading, where the equivalent material properties are determined through numerical simulations under diverse stress states, incorporating nonlinear material behaviors and strain rate effects.

Keywords: mortar-less; interlocking brick; impact; blast

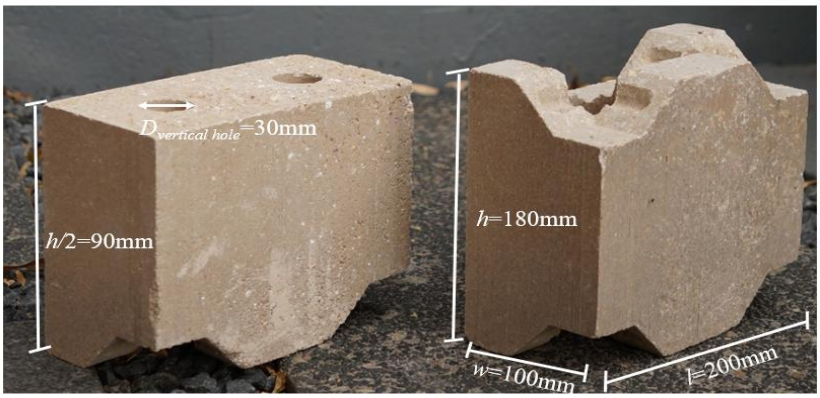
$D_{vertical\ hole}$=30mm
h/2=90mm
h=180mm
w=100mm
l=200mm

ADVANCED BLAST CONTAINMENT TECHNOLOGIES FOR PASSENGER AIRCRAFT: DESCRIPTION OF BLAST TESTING, AND RECOMMENDATIONS FOR APPLICATION IN OTHER DOMAINS

Donato Zangani
R&D Director, RINA SpA, Via Cecchi 6, 16129 Genova, Italy, donato.zangani@rina.org

Alessandro Bozzolo
Industrial Design Manager, RINA Consulting SpA, Via Cecchi 6, 16129 Genova, Italy, alessandro.bozzolo@rina.org

Andrew Tyas
Professor, University of Shieffield, School of Mechanical, Aerospace and Civil Engineering, Sir Frederick Mappin Building (Broad Lane Building), Mappin Street, Sheffield, S1 3JD, a.tyas@sheffield.ac.uk

ABSTRACT
The study reviews advanced blast containment technologies designed to counteract bombs on commercial aircraft. Past catastrophes like the Lockerbie disaster and the Metrojet disaster, both caused by onboard explosives detonated during flight, highlight this threat.
The security procedures in airports have grown tremendously with the introduction of scanners and various security systems, including the use of digital technologies and advanced sensor technologies. However it should be considered that a small amount of an explosive, below the detection threshold of instruments, might go undetected or be smuggled into an aircraft. The solutions outlined herein are engineered to absorb and mitigate the impact of an explosion from explosives concealed in luggage or located within the aircraft cabin. The primary challenges to be addressed include not only the capacity to effectively absorb the blast impact to the greatest extent possible but also ensuring compliance with requirements for lightweighting and usability in the aircraft environment, including operability by the crew.
Two types of blast containment units are described, respectively for Improvised Explosive Devices (IEDs) hidden in the luggage compartment of narrow body aircraft, or found in the cabin environment. Prototypes were subjected to rigorous full-scale blast testing. The results demonstrated significant improvements in blast resistance, validating the feasibility of these technologies for deployment in aviation. Finally the potential application of such containment solution for risk mitigation in the transportation of pressure vessels is considered, highlighting the adaptability and efficacy of such approach in various high-risk scenarios.

Keywords: Technical Textiles, Blast Protection, Blast Containment

Impact Response of Ambient-Cured Fibre-Reinforced Geopolymer Concrete Beams with Steel-BFRP Composite Bars

Zhijie Huang[1], Wensu Chen[1*] and Hong Hao[2,1*]

[1]*Center for Infrastructural Monitoring and Protection, School of Civil and Mechanical Engineering, Curtin University, Australia*

[2]*Earthquake Engineering Research & Test Center, Guangzhou University, China*

Emails: wensu.chen@curtin.edu.au (W. Chen); hong.hao@curtin.edu.au (H. Hao)

In recent years, geopolymer concrete (GPC) structures reinforced with Steel-Fibre reinforced polymer (FRP) Composite Bars (SFCBs) have emerged as the alternatives to conventional steel reinforced concrete (RC) structures, addressing high carbon dioxide emissions associated with cement production and the corrosion of steel. Concrete structures might be subjected to impact loads such as falling rocks and vehicle collisions during their service lives. It is essential to study the shear performance of concrete beams made of sustainable GPC and durable SFCBs subjected to impact loads. Given the low tensile strength and brittle behaviour of concrete, adding fibres is a common approach to improve the mechanical properties of concrete and structural performance. In this study, Basalt Macro Fibres (BMFs) were used as non-corrosive and cost-effective fibres with high strength. Three beams (with 0%, 1%, and 2% BMFs by volume fraction) were prepared and tested to investigate the effect of BMFs on the shear performance of GPC beams reinforced with Steel-Basalt FRP composite bars (SBCBs) subjected to impact loads by using a pendulum impact testing system. Each beam was subjected to two impacts with release angles of 20° (1.6 m/s) and 50° (3.8 m/s). The results revealed that increasing the BMF content could reduce the maximum midspan deflections of the beams by up to 13% at 1.6 m/s and 88% at 3.8 m/s. The findings indicate that the addition of BMFs by up to 2% could effectively reduce the damage and enhance the impact-resistant performance of GPC beams reinforced with SBCBs under impact loads.

Keywords: Geopolymer concrete beams, Steel-BFRP composite bars (SBCBs), Basalt Macro Fibres (BMFs), Shear performance, Impact loads.

Blast and ballistic resistance of explosively welded plates

Ye Yuan [1] , Yufeng Zhang [1] , Mengqi Yuan [1] ， Guangyan Huang [1] , Yan Liu [1], and Qibo Zhang [1]

[1] *School of Mechatronical Engineering, Beijing Institute of Technology, Beijing, China*

In the present study, the blast and ballistic perforation resistance of steel/titanium/aluminum (STA) multilayer protective systems were investigated experimentally, numerically, and analytically. In the ballistic loading, projectiles with different nose shapes, i.e. spherical, ogival, conical, and blunt, were considered. The targets were manufactured via explosive welding technique to achieve a strong interfacial strength. Explosively welded plates displayed superior performance compared to monolithic steel plates of equal weight. An analytical model was developed to elucidate the enhancing mechanism of the explosively welded plates. The projectile nose shape was found to significantly affect the failure modes and ballistic limit velocities of the STA composite plate. Detailed three-dimensional finite element simulations were performed to provide insights into the penetration process and energy absorption characteristics of the STA composite plate. An analytical model was developed to predict the entry and exit penetration phases of a rigid projectile of different nose shapes into the STA target through ductile hole expansion. The model simplified the STA composite plate to be an equivalent monolithic based on the weighting of material resistance and specific cavitation energy in each layer. The analytical and numerical predictions of the residual velocity were in excellent agreement with the experimental data. The predicted evolution of projectile velocity with penetration depth was found to be in satisfactory correlation with those from the numerical simulation. The proposed analytical model shall be useful for designers of multilayer metallic protective structures against fragments from improvised explosive devices.

Keywords: Explosively welded plates, Ballistic tests, Finite element simulation, Ballistic model, Blast resistance, Nose shape

Submission ID: 0501

Textile materials as an effective protective solution against multi-velocity and multi-threat impacts

François Boussu

Univ. Lille, ENSAIT, GEMTEX–Laboratoire de Génie et Matériaux Textiles, F-59000 Lille, France

Corresponding author: francois.boussu@ensait.fr - Tel: +33 (0)3 20256476

Abstract In recent years, numerous studies have highlighted the various advantages of using 3D warp interlock fabrics for a wide range of applications. Both technical and economic benefits, compared to other textile reinforcements, have been demonstrated in different composite material applications [1]–[8]. However, these fabrics also present certain drawbacks due to their specific architecture and manufacturing process [9]–[12]. Based on these research findings, including our own studies [13]–[18], we have identified the strengths and limitations of their production process and structural design. These fabrics offer a high degree of flexibility in warp and weft yarn arrangements, both within the plane and through the thickness of the 3D woven structure [19]. This paper will first introduce and explain the key motivations for using 3D warp interlock fabrics, followed by a general definition of these materials [20]. Various types of 3D warp interlock fabric architectures will be presented to illustrate the design methodology. Finally, we will explore different applications related to the dynamic characterization of these fabrics, ranging from soft protection against needle puncture, stabbing, and low-velocity projectiles to hard armour solutions for countering low-velocity impacts, high-velocity ammunition, improvised explosive devices (IEDs), and blasts.

References

[1] F. Boussu and X. Legrand, "Technical and Economical performances of 3D Warp Interlock Structures," in SAMPE 08, Long Beach, CA, USA, May 18-22, 2008.

[2] X. Chen and D. Yang, "Use of 3D Angle-Interlock Woven Fabric for Seamless Female Body Armor: Part 1: Ballistic Evaluation," Textile Research Journal, vol. 80, no. 15, p. 1581–1588, September 2010.

[3] X. Chen, W. Lo, A. Tayyar and R. Day, "Mouldability of Angle-Interlock Woven Fabrics for Technical Applications," Textile Research Journal, vol. 72, no. 3, pp. 195-200, March 2002.

[4] S. Lomov, A. Bogdanovich, D. Ivanov, D. Mungalov, M. Karathan and I. Verpoest, "A comparative study of tensile properties of non crimp 3D orthogonal weave and multi layer plain weave e-glass composites. Part1: Materials, Methods and Principal Results," Composites Part A: Applied Science and Manufacturing, vol. 40, no. 8, pp. 1134-1143, August 2009.

[5] J. Grogan, S. Tekalur, A. Shukla, A. Bogdanovich and R. Coffelt, "Ballistic Resistance of 2D and 3D Woven Sandwich Composites," Journal of Sandwich Structures and Materials, vol. 9, pp. 283-302, 2007.

[6] M. Mohamed, A. Bogdanovich, L. Dickinson, J. Singletary and R. Lienhart, "A new generation of 3D woven fabric preforms and composites," Sampe Journal, vol. 37, no. 3, May/June 2001.

[7] F. Ko, "3-D textile reinforcements in composite materials," in 3-D Textile Reinforcements In Composite Materials, A. Miravete, Ed., Cambridge, Woodhead Publishing Limited, 1999, pp. 9-40.

[8] A. Mouritz, M. Bannister, P. Falzon and K. Leong, "Review of applications for advanced three-dimensional fibre textile composites," Composites Part A: Applied Science and Manufacturing, vol. 30, pp. 1445-1461, 1999.

[9] F. Boussu, I. Cristian and X. Legrand, "General specification of warp interlock structure: application for carbon fiber multi-layer fabrics," in Avantex techtextil symposium, Frankfurt, Germany, from 16/06/2009 to 17/06/2009.

[10] L. Lee, S. Rudov-Clark, A. Mouritz, M. Bannister and I. Herszberg, "Effect of weaving damage on the tensile properties of three-dimensional woven composites," Composite Structures, vol. 57, pp. 405-413, 2002.

[11] P. Callus, A. Mouritz, M. Bannister and K. Leong, "Tensile properties and failure mechanisms of 3D woven GRP composites," Composites Part A, vol. 30, pp. 1277-1287, 1999.

[12] B. Cox, M. Dadkhah and W. Morris, "On the tensile failure of 3D woven composites," Composite part A Applied Sciences Manufacturing, vol. 27, pp. 447-458, 1996.

[13] S. Nauman, «Modélisation Géométrique de tissu 3D Interlock,» Roubaix, France, 2008.

[14] S. Nauman, "Geometrical modelling and characterization of 3D warp interlock composites and their on-line structural health monitoring using flexible textile sensors," Lille, 24/03/2011.

[15] P. Lapeyronnie, «Mise en œuvre et comportement mécanique de composites organiques renforcés de structures 3D interlocks,» Douai, France, 14/12/2010.

[16] C. Ha-Minh, «Comportement mécanique des matériaux tissés soumis à un impact balistique : approches expérimentale, numérique et analytique,» Lille, France, 17/11/2011.

[17] M. Lefebvre, «Résistance à l'impact balistique de matériaux composites à renforts Interlocks tissés. Application au blindage de véhicules,» Valenciennes, 07/12/2011.

[18] B. Provost, «Étude et Réalisation d'une solution à renfort tissé interlock pour la protection balistique de véhicule,» Valenciennes, 14/01/2013.

[19] H. Yi and X. Ding, "Conventional Approach on Manufacturing 3D Woven Preforms Used for Composites," Journal of Industrial Textiles, pp. 34-39, 2004.

[20] F. Boussu, I. Cristian and S. Nauman, "General definition of 3D warp interlock fabric architecture," Composites Part B, vol. 81, pp. 171-188, 22 07 2015.

The Low Velocity Impact Properties of Multi- Axial Three Dimensional (3D) Woven Composites

Mehmet Korkmaz [1], Ahmad Rashed Labanieh[2], Xavier Legrand[2], Francois Boussu[2]

[1]*Department of Textile Engineering, Dokuz Eylul University, Buca 35397, Izmir, Türkiye.*

[2]*Univ. Lille, ENSAIT, ULR 2461 - GEMTEX - Génie et Matériaux Textiles, Lille, France.*

The integrated structure and remarkable thickness values of 3D woven fabrics confer outstanding properties to their composites, such as high fracture toughness, advance damage tolerance, high impact energy absorption capacity, etc. However, the orientation of the yarn groups through the thickness direction of the fabric degrades the in-plane mechanical properties of 3D woven fabrics/composites. This phenomenon led to the development of multi-axial 3D woven fabrics. Due to the advanced weaving methods, the bias warp yarns can be incorporated into the 3D woven structure. It has already been demonstrated in the previous studies that the bias warp yarns significantly improve the in-plane shear properties of 3D woven fabrics/composites. On the other hand, the impact properties of multi-axial 3D woven composites have not been investigated. This study investigated the low velocity impact properties of multiaxial 3D woven composites. Firstly, the composites were impacted at impact energy levels of 25J, 45J and 55J. The damaged specimens were then tested under the 300J impact energy level to determine the effect of the woven fabric architecture on the impact properties and damage mechanisms of the composites. In addition, the 3D warp interlock woven and traditional laminated composites were fabricated and tested to perform the comparative investigation. The fabrics produced and their composites are shown in Figure 1.

Structures	Surface appearance of woven fabrics	Composites
Multi- Axial 3D Woven Composite		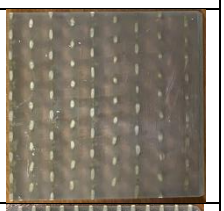
3D Warp Interlock Woven Composite	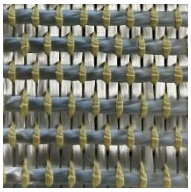	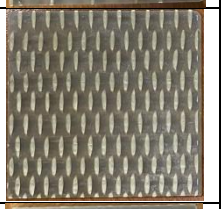
Laminated Composite	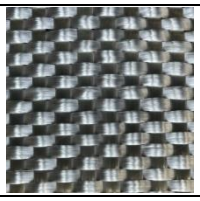	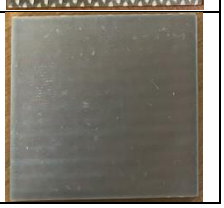

Figure 1. The produced woven fabrics and their composites

The maximum energy absorbed by the composites is shown in Figure 2. It was concluded from the research study that the bias warp yarns distribute the impact energy more homogeneously to the other parts of the composite. Therefore, the multiaxial 3D woven composites can absorb more impact energy than 3D warp interlock woven and laminated composites. The results obtained make the multi-axial 3D woven fabrics and their composites one of the best solutions for impact applications among the current fabric technologies.

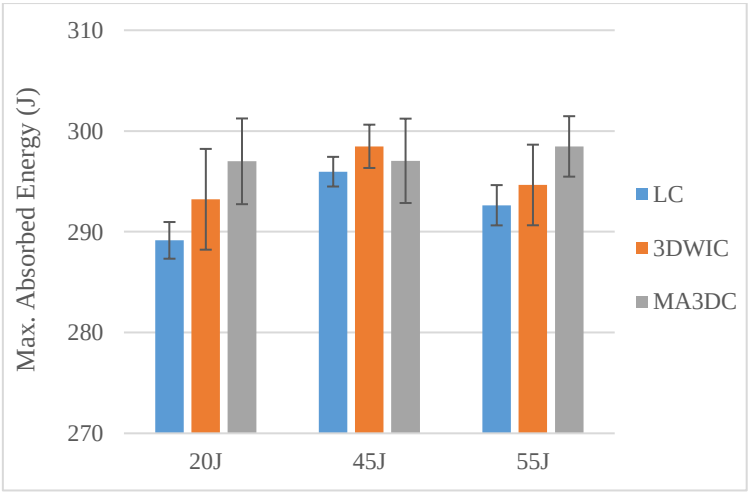

Figure 2. The maximum absorbed energy values of damaged composites under 300J energy level

Keywords: Multi- axial 3D weaving, low velocity impact test, impact energy absorption.

Damage assessment of ultra-high performance concrete column subjected to contact explosion

Raghav Kumar Mishra[1], Alagappan Ponnalagu[2]

[1]*Graduate student, Indian Institute of Technology Madras, Chennai, India*

[2]*Assistant Professor, Indian Institute of Technology Madras, Chennai, India*

Abstract:

A blast is a sudden release of energy that imposes a hazardous shock wave on the structure in its proximity. The consequences of the rising blast incidents result in massive loss of lives and the economy due to the failure of critical structure members may lead to the progressive collapse of the structure. The reinforced concrete columns are a critical structural member highly vulnerable to explosions due to their easy accessibility. Contact explosions have one of the most devastating effects among close-in and far-field explosions, causing significant localized damage to the targeted structural element. It directly transmits high-intensity compression shock waves to impact the face, resulting in crater formation by crushing concrete. Compression shock waves become tensile stress waves at the free surface due to the interaction of waves, causing tensile failure at the side and rear face. The reinforced concrete columns are a critical structural member highly vulnerable to contact explosions due to their easy accessibility. In pursuing structural elements, ultra-high performance concrete (UHPC) is expected to be suitable for contact explosion scenarios due to its high compressive and tensile strength. This study evaluated the local damage of UHPC columns with different reinforcement detailing using high-fidelity finite element (FE) software LS-DYNA. It is validated with the experimental data available in the literature. The detonation and propagation of blast waves are simulated by explicitly modeling the explosive and surrounding air using multi-material Arbitrary Lagrangian-Eulerian (MMALE) formulation. Lagrangian elements are used to model structure and fluid interaction (FSI), which is employed to the coupling between the ALE and Lagrangian elements. Subsequent displacement control quasi-static load is applied to estimate the residual capacity. A damage index based on residual loading capacity is used to quantify local damage. The findings of this study demonstrate that the UHPC and reinforcement detailing notably reduced local damage and preserved strength and ductility. The UHPC and reinforcement detailing reduces local damage due to contact explosions by preventing concrete crushing and minimizing tensile failures. It enhances blast resistance, preserves its strength and ductility capacity, and can be effectively used to mitigate contact explosion effects. This study provides valuable insights and can help design UHPC columns against contact explosions.

Keywords: Contact explosion, Ultra-high performance concrete (UHPC), Residual capacity, Damage index.

Application of 2D to 3D ALE Mapping in Designing Column Structures under a Close-in Detonation

Rajendra Prasad Bohara, Tin Van Do and Asher Gehl

Karagozian & Case (K&C) Australia, Bondi Junction, NSW, Australia, 2022

bohara@kcse.com.au, van@kcse.com.au and gehl@kcse.com.au

ABSTRACT

The Arbitrary Lagrangian-Eulerian (ALE) formulation is an effective approach to model structural performance under a close-in blast load with consideration of fluid-structure interaction. However, this method is highly sensitive to air domain and structural mesh sizes and material input parameters, leading to an increased computation time and resource for an accurate prediction of blast wave magnitude, propagation, and interaction with structure. Therefore, this paper aims to utilise the application of a 2D to 3D ALE mapping technique to design a normal reinforced concrete (RC) and a steel-jacketed RC column against the detonation of a close-in vehicle-borne improvised explosive device (VBIED). The design of the columns included three steps: preloading under gravity load, blast effects analysis of the preloaded column, and determination of the residual capacity of the blast-damaged column. First, a 2D ALE model was developed and validated with the Kingery-Bulmash model calculation. In the validated 2D ALE model, the prescribed VBIED was detonated. The 2D model was terminated before the blast wave propagated the full standoff distance to the structural surface. Then, the blast wave was mapped into a 3D ALE model with the preloaded column structure, where appropriate fluid-structure interaction (FSI), material properties with strain rate effects, equations of states (EOS), boundary conditions, etc. were defined. The results of the 2D to 3D mapping model were also compared with the conventional ALE model. Finally, the residual capacities of the damaged column structure were determined by subjecting them to an incremental displacement-controlled load. Although the structural responses of the columns were observed to be similar in conventional 3D ALE and 2D to 3D mapped ALE models, the computational time was reduced significantly with the same resources. Based on a series of 2D to 3D ALE mapping models, key parameters affecting the blast wave magnitude, propagation, interaction with structural surfaces, and fluid boundaries were identified. Additionally, recommendations for efficient and accurate use of the 2D to 3D ALE mapping method for designing RC structures were made in this paper. The findings of this study are useful for professional engineers and researchers working in the field of structural blast engineering for the effective use of 2D to 3D ALE mapping techniques in the design and analysis of RC structures under blast load.

Keywords: 2D to 3D ALE, Close-in detonation, Modelling, Finite Element Analysis, RC column

Dynamic properties of materials subjected to perforation tests in a wide range of temperatures - a review of experimental studies

Leopold Kruszka[1], Maciej Klosak[2] and Kamil Sobczyk[1]

[1]*Faculty of Civil Engineering and Geodesy, Military University of Technology, Warsaw 00-908, Poland*

[2]*Laboratory for Sustainable Innovation and Applied Research, Technical University of Agadir, Universiapolis, Agadir 80000, Morocco*

Ballistic tests for the purpose of determining the resistance to penetration by projectiles of protective casings are the subject of many analyses, both at the theoretical, experimental and numerical levels. A great deal of research related to the problem of perforation of thin specimens made of various materials have been described in the literature, and the analytical models have been developed to determine the relationship between the residual velocity of a projectile and its initial velocity. The mechanism of destruction of a thin plate subjected to perforation by projectiles of different shapes has been analyzed in many numerical works with a wide spectrum of materials analyzed: starting from metals through multi-layer (composite) materials ending with polymers. The paper presents an overview of the most important experiments and recent publications, presenting previous and current trends in experimental research in recent years around ballistic perforation testing based on pneumatic launcher and target thermal chamber (**Figure 1**) with also the use of high-speed camera recording. Those experiments were done with the help of various shape projectiles. Comparative analyses of tests for a given initial velocity of the projectile, but different temperatures, indicated a significant effect of temperature on the form of destruction. For metals, this is a change in the shape and number of cracks (petals) and the ballistic point curves (curves of the dependence of the residual velocity of the projectile and its initial velocity – see **Figure 2**). For polymers, the phase transition from brittle to plastic behavior can be observed, and the material's melting temperature can be estimated. The need to learn about dynamic properties of materials subjected to perforation tests in a wide range of temperatures for the selection of structural design solutions for the protection elements of critical infrastructure was emphasized.

Keywords: perforation tests, pneumatic launcher, thermal chamber, review.

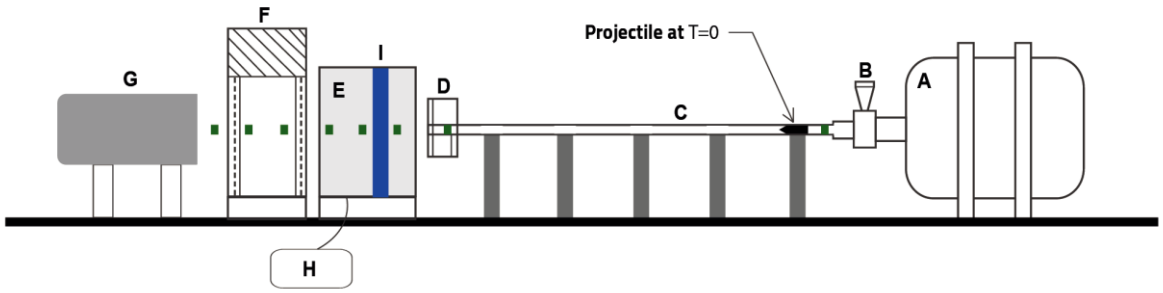

A: pneumatic chamber, **B**: quick valve, **C**: gas gun tube with supports, **D**: sensor to measure initial impact velocity, **E**: thermal chamber and specimen holder, **F**: sensor to measure residual velocity, **G**: projectile catcher, **H**: electronic heat controller, **I**: specimen – plate, ■■■ projectile trajectory.

Figure 1. Schematic of pneumatic gun with thermal chamber used for perforation tests at high impact velocities and high temperatures.

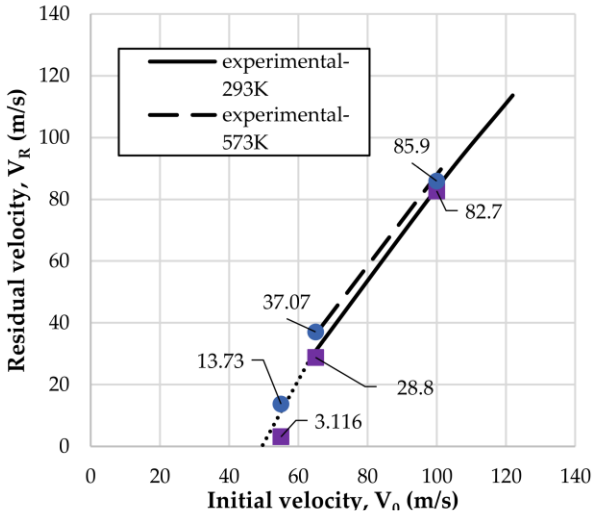

Figure 2. Experimental ballistic curves V_0 vs. V_R with marked experimental results: temperature range 293 K-573 K, tested material: aluminium 2024-T3 [1]

[1] Klosak M., Santiago R., Jankowiak T., Bendarma A., Rusinek A., Bahi S., (2021). The Influence of Temperature in the Al 2024-T3 Aluminum Plates Subjected to Impact: Experimental and Numerical Approaches, Materials, 14(15), p. 4268, DOI: 10.3390/ma14154268.

Blast Resilience of Polycarbonate Panels

Gauthier Stiegler[1], Giovanni Milan[2] and Tung Tran[3]

[1]*Arup, London, United Kingdom*

[2]*Arup, Amsterdam, Netherlands*

[3]*Arup, Perth, Australia*

Polycarbonate sheets are ideal for applications requiring impact resistance, ballistic protection, lightweight and flexible solutions, making them more economical and easier to handle and install compared to laminated glass. However, counter-terrorism security guidance typically advises against their use due to the potential fragmentation under blast loads, which would not show up easily on medical x-ray equipment. When retrofitting buildings not initially designed considering blast, replacing traditional glazing panels with blast-enhanced laminated glass is often unfeasible due to the added weight. Sensitive heritage buildings are often retrofitted with lightweight polycarbonate roofing panels as a result.

For blast resilience, a risk-based approach is proposed to understand and minimize hazards associated with polycarbonate roofing panels. Potential failure modes include (a) fragmentation of the panel, (b) partial failure of the retention system and dislocation of the panel from its framing support, (c) failure of the framing system, or (d) failure of the fixings or supporting structure.

To assess the likelihood of fragmentation, non-linear finite element analysis was carried out on typical polycarbonate sheets using rigid boundary conditions. Results confirm that polycarbonate sheets do not shatter easily and, with a strong retention system and framing, can resist typical levels of blast resilience for counter-terrorism security requirements. However, the resulting in-plane and out-of-plane reactions are very high. Typical polycarbonate sheets are therefore unlikely to result in fragments (a) and the risk of casualties from fragments not showing up on medical x-ray equipment is relatively low.

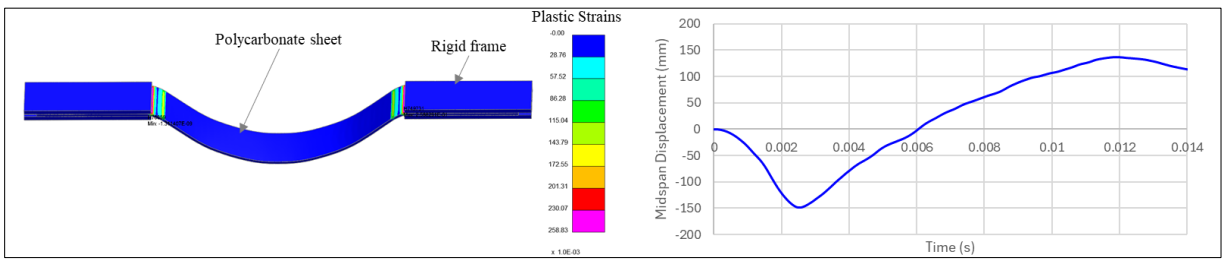

Figure 1 Deformations and plastic strains of polycarbonate sheet under blast loading (in LS-DYNA)

Typical support bar systems have also been numerically modeled and coupled to the polycarbonate sheets to assess other failure modes. This assessment shows that typical polycarbonate systems would be expected to lead to a failure mechanism for typical levels of blast resilience for counter-terrorism security requirements. However, design enhancements can improve blast performance and mitigate hazards.

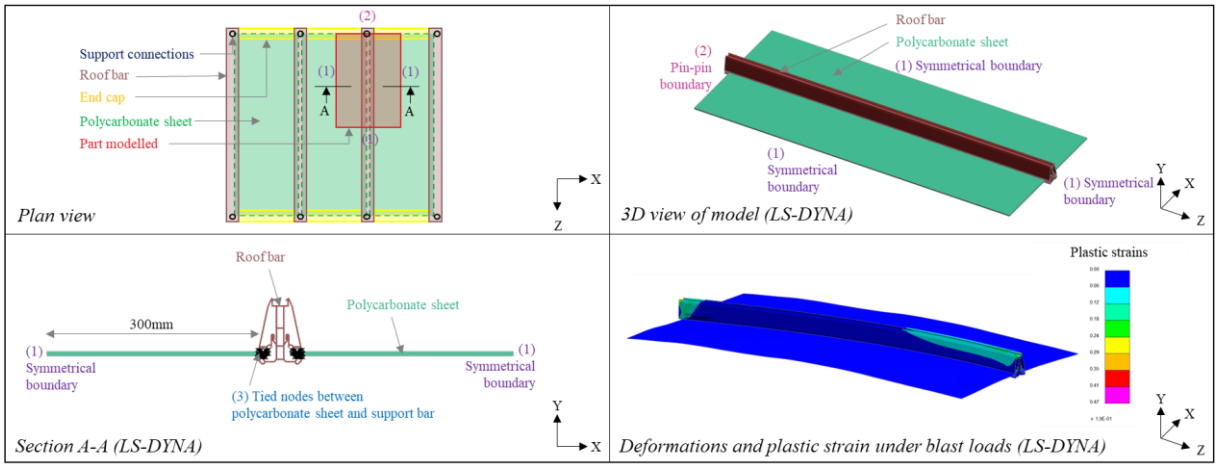

Figure 2 Numerical simulation of polycarbonate roofing system under blast loading (in LS-DYNA)

To reduce the risk of failure at the retention system and dislocation of the panel from its framing support (b), it is possible to oversize the polycarbonate sheet and implement deep rebates. Support bar systems can be hardened where stress concentrations occur, particularly near the supports, to prevent failure of the support bars (c). Fixings can be enhanced to distribute the loads safely into the structural elements (d). A balanced approach to enhance polycarbonate systems can mitigate risk to a tolerable level. This can be achieved by ensuring that loads are effectively distributed back to the structure and that failure mechanisms are limited to the area near the detonation point. The next stage of the project will be to validate and calibrate the numerical analysis models based on experimental testing of typical polycarbonate roofing systems.

Keywords: polycarbonate, numerical simulation and modelling, strengthening and retrofitting techniques, blast resistant design.

Fundamental study on the blast pressure acting on front wall of box-type structures

Chien Trinh Minh [1], Masuhiro Beppu [2], Hiroyoshi Ichino [2] and Ryo Matsuzawa [3]

[1]*Graduate School of Science and Engineering, National Defense Academy of Japan, Kanagawa, Japan*

[2]*Department of Environmental and Civil Engineering, National Defense Academy of Japan, Kanagawa, Japan*

[3]*ITOCHU Techno-Solutions Corporation, Tokyo, Japan*

When a blast wave impinges on a box-type structure, the blast pressure on the front wall instantly rises to a peak reflected pressure and it is immediately reduced by the clearing effect regarding expansion waves generated at free edges. Although the behavior of clearing effect could be affected by the size and shape of the structure, the influence was insufficiently investigated. This study aims to investigate the effect of size and shape of the front wall on blast pressure characteristics surrounding box-type structures by conducting explosion tests and numerical simulation. Prior to the tests, a method for evaluating blast pressure characteristics proposed by the Unified Facilities Criteria was described, and its concept was discussed. Then, explosion tests using C-4 high explosive were conducted to investigate the blast effects on two test specimens with different front wall widths. The test results revealed that there was a significant change in blast impulse acting on front wall and top roof by varying the width of front wall. The test results were reproduced by numerical simulations. While the numerical results underestimated the peak pressure at several locations, it reproduced the blast impulse relatively well. The trend of blast impulse with respect to the front wall width in the numerical results agreed well with the test results. Based on the simulated results, the correlation between size, shape of the front wall and the difference in blast duration as well as blast impulse was discussed. The pressure distributions exhibited that the wider the front wall is, the longer it takes for the reflected pressure to be cleared, which resulted in longer blast duration and higher blast impulse at the front wall. A parametric study using numerical simulations was conducted to evaluate the effect of different size and shape of the front wall on the blast impulse acting on it as shown in (Fig.1).

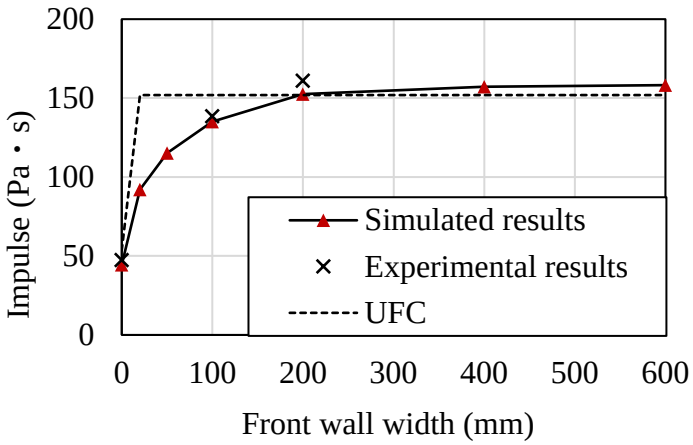

Fig.1 Effects of front wall width on blast impulse acting on front wall

Keywords: blast pressure, blast-resistant design of structures, Unified Facilities Criteria, numerical simulations.

Explosive Field Trial to Measure Spatial Variability of Fragmentation Safety Hazards from VBIEDs

Mark G. Stewart[1], Michael D. Netherton[1,2] and Hao Qin[1]

[1]*University of Technology Sydney, Australia*

[2]*Karagozian & Case, Sydney, Australia*

A Vehicle Borne Improvised Explosive Device (VBIED) explosive field trial was conducted for three identical medium-sized cars, and is described in this paper. Explosive charge shape and location were identical for each vehicle, minimising test set-up variability. The purpose of the trials was replicate tests to help probabilistically characterise the uncertainty and variability of blast pressures and fragment generation, trajectories, and density. The paper describes the spatial variability (directionality) of incident pressure, impulse and time of positive phase duration, and compares these to the hemispherical surface burst Kingery and Bulmash polynomials often used for predicting blast loads from IEDs, such as ConWep. This also allows directional airblast factors to be quantified. The spatial distribution of over 26,000 fragments on the ground is also presented over the 250 m × 300 m test arena. The fragment densities and velocities obtained from the witness panels are also described, and preliminary fatality risks estimated. These data will help develop or validate airblast and fragment hazard numerical or other models. Ultimately, probabilistic approaches will provide decision support for the determination of safety distance and risk reduction measures to prevent fatality and injury from blast pressure and fragmentation hazards.

Keywords: VBIED, explosive field trial, risk, safety

Parameter calibration of Kong-Fang constitutive model for geopolymer based ultra-high performance concrete (G-UHPC)

Fangming Tian [1,2], Li Chen [1,2]

[1] *School of Civil Engineering, Southeast University, Nanjing, 210096, China*

[2] *Engineering Research Center of Safety and Protection of Explosion & Impact of Ministry of Education (ERCSPEIME), Southeast University, 211189, Nanjing, China*

Due to the time-consuming, expensive and uncontrollable factors of physical experiments, numerical simulation has become an effective, economical and safe method. In numerical simulation, the choice of constitutive model and the determination of parameters are the key to ensure the accuracy of prediction results. However, most of the parameters of the constitutive model are automatically generated and calibrated for ordinary concrete (NSC), which cannot be directly applied to G-UHPC. This paper aims to provide a set of calibration parameters to simulate the Kong-Fang constitutive model of G-UHPC material under strong dynamic loads such as projectile impact. The research was carried out mainly through experimental and numerical simulation methods. Firstly, triaxial tests and hydrostatic compression tests were carried out for G-UHPC, and combined with the existing Hopkinson bar (SHPB) and Hugoniot test data, the strength surface, strain rate effect and equation of state parameters of KongFang model were systematically calibrated. Subsequently, the experiment of 50mm projectile penetrating G-UHPC at 350m/s and 700m/s was carried out, and the numerical simulation results were compared to verify the calibrated KongFang constitutive model parameters.Finally, two strength plane parameters a_0,a_1,G-UHPC compression DIF, tensile DIF and 10 groups of state equation parameters are obtained. The results show that the penetration depth (DOP) obtained by numerical calculation is in good agreement with the experimental data. The corrected KongFang model can effectively predict the DOP of G-UHPC targets under projectile impact. Finally, based on the calibrated and verified KongFang model, the effects of G-UHPC uniaxial compressive strength, projectile impact velocity and mass on DOP were studied. Based on the results of parametric study, an empirical equation containing the above variables is proposed to predict the penetration depth. It is found that DOP increases with the increase of projectile impact velocity and mass, and decreases with the increase of G-UHPC uniaxial compressive strength.

Keywords: G-HUPC, calibration, penetration, Kong-Fang constitutive model.

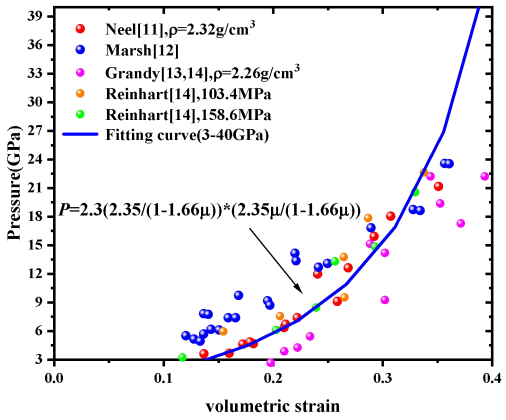

Fig. 1. G-UHPC Equation of State Diagram (3-40GPa)

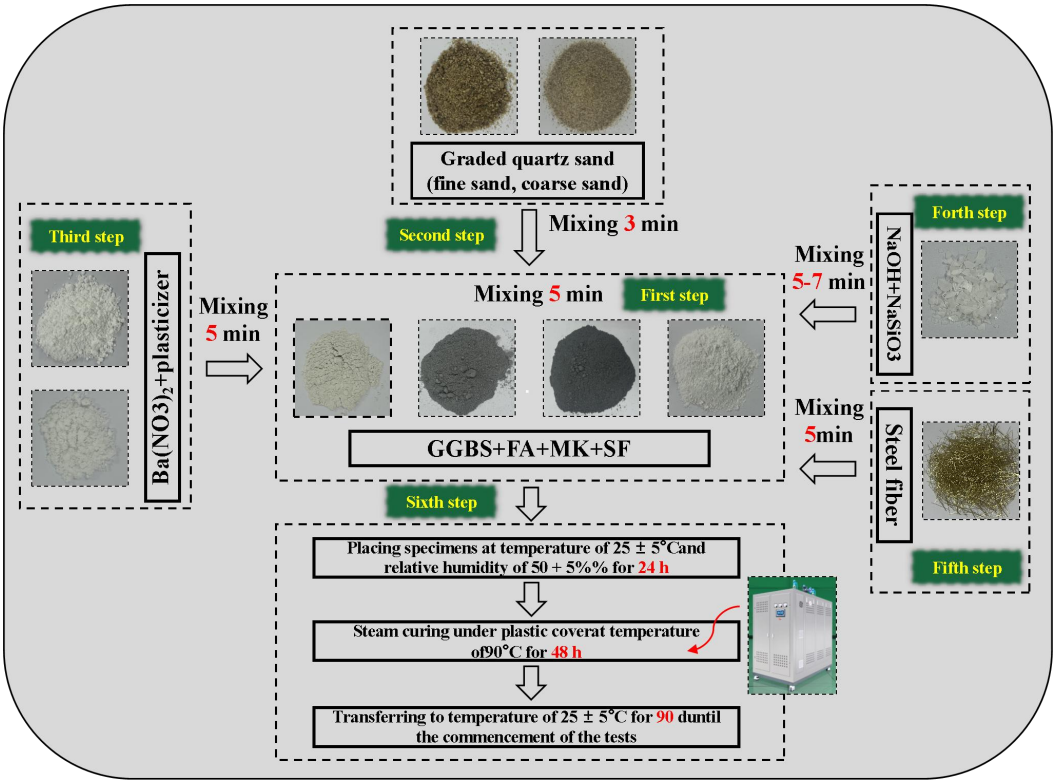

Fig. 2. preparation flow chart of G-UHPC

Blast Characterisation and Structural Response in Large-Scale Unconfined Hydrogen Explosions: An Australian Field Study

Edward Gan[1], Alex Remennikov[1], Zhenying Huang[1], Kasun Wijesooriya[2], Wimukthi Senarathna[2], Damith Mohotti[2]

[1] *School of Civil, Mining Environmental and Architectural Engineering, University of Wollongong, NSW 2522, Australia*

[2] *School of Engineering and Technology, The University of New South Wales, Canberra, ACT, 2600, Australia*

Hydrogen is expected to play a vital role in decarbonisation efforts, which are crucial as the world faces the urgent challenge of mitigating global warming and reducing greenhouse gas emissions. As an alternative to fossil fuels, hydrogen offers a clean and sustainable energy solution. As a fuel, it produces no carbon emissions, with water being the sole by-product. However, hydrogen is classified as highly flammable, posing significant risks related to fire and explosion due to its broad flammability range and low minimum ignition energy. Recently, UOW and UNSW Canberra conducted a large-scale explosion field experiment aimed at characterising the blast environment resulting from both deflagration and detonation of unconfined hydrogen-air clouds. While research teams in other countries have already begun investigating these hazards, this study is among the first of its kind conducted in Australia. In addition to characterising the blast environment, the structural response of various structural elements when subjected to the blast loads was assessed. The data collected from this experiment will contribute towards building a comprehensive database to support the development of empirical relationships for predicting blast effects from hydrogen explosive accidents. This work aims to support the development of structural safety guidelines to mitigate hydrogen explosion hazards.

Keywords: Gas deflagration; gas detonation; explosive field trials

Vehicle borne improvised explosive devices – experimental study

Tomasz Gajewski[1], Piotr Peksa[1], Robert Studziński[2], Michał Malendowski[1],
Piotr Nowak[3], Artur Szlachta[3], Krzysztof Szajek[1],
Wojciech Sumelka[1] and Piotr W. Sielicki[1]

[1] *Institute of Structural Analysis, Poznan University of Technology, Poland*
[2] *Institute of Building Engineering, Poznan University of Technology, Poland*
[3] *Doctoral School of Poznan University of Technology, Poland*

Terrorist attacks pose a significant threat to civilians and infrastructure, often utilizing improvised explosive devices (IEDs) like personal-borne IEDs [1] and vehicle-borne IEDs (VBIEDs) [2]. VBIEDs are particularly dangerous, capable of carrying up to hundred kilograms of explosives and generating over 2,500 lethal fragments from the vehicle's mass, severely impacting public safety and critical infrastructure.

In this study, the detonations of vehicle-borne improvised explosive devices was conducted and analyzed. Six VBIED tests with varied cars were prepared and tested on a military range ground. Military range ground was prepared and cleaned after each test. The approximate vehicle weights ranged from 1000 to 1500 kg. Three different explosive materials of varying masses (up to 50 kg) were used in the experiments, also the placement of explosive material was differentiated (back seat, trunk and under the car). Fragmentation patterns were investigated based on collected debris, the maps of the patterns were created. Blast wave dynamics was registered by pencil gauges. All experiments were registered with high-speed cameras with resolution of 22 000 fps.

The study provided valuable understanding of the fragmentation behavior and shockwave dynamics associated with car bomb detonations. It appeared that VBIEDs eject numerous debris, larger components, such as the mask, the vehicle doors, up to 40 meters, while smaller fragments, like glass, were launched up to 130 meters. The results demonstrate a consistent pattern in the distribution and angles of debris impact in relation to the vehicle's symmetrical components, highlighting the predictable characteristics of these explosions.

This research emphasizes the severe risks VBIEDs pose to public safety, especially in crowded urban spaced and near open air events, such as concerts and festivals. Accurate modeling of explosions due to its nonlinear character is a challenging task, hence the necessity of field tests

arises to evaluate real-world risks. The findings of the study provide valuable data for validating numerical simulations and analytical models of blast waves and fragment trajectories, helping to create a better safety protocols and risk assessment strategies. Additionally, the study highlights the critical need for ongoing research and testing to improve safety standards and mitigate the threats posed by VBIEDs.

Keywords: vehicle borne improvised explosive device, safety zone, fragments.

[1] Sielicki, P. W., Stewart, M. G., Gajewski, T., Malendowski, M., Peksa, P., Al-Rifaie, H., Studziński, R., & Sumelka, W. (2020). Field test and probabilistic analysis of irregular steel debris casualty risks from a person-borne improvised explosive device. *Defence Technology*. https://doi.org/10.1016/j.dt.2020.10.009

[2] Stewart, M. G., Netherton, M. D., Qin, H., & Li, J. (2024). Explosive field trial for repetitive testing of VBIEDs to probabilistically measure blast and fragmentation hazards. *International Journal of Protective Structures*, *0*(0), 1–27. https://doi.org/10.1177/20414196241233757

Performance-based Design Theory and Methods of Building Structures against Blast Loading

Zhong-Xian Li [1], Yang Ding [1], Yanchao Shi [1] and Jian Cui [1]

[1]*School of Civil Engineering, Tianjin University, Tianjin, China*

The contemporary practices adopt limit state design approach for structural protection against blast and lack of guidelines for structural systems and components design under different blast resistance performance levels. Moreover, using the current design method, the safety of the structure might not be guaranteed, especially when unexpected explosions occur. This study establishes a performance-based blast-resistant design method for civil structures by systematic investigations. The series of researches start with the analysis of uncertainties of blast load and derivation of its statistical model. Then the damage mechanisms, the failure modes and the damage criteria of structural and non-structural components were investigated. The performance indices and their limits for corresponding components against blast loads were proposed, and based on which the performance-based blast resistant design method and performance improvement technology were established. A new efficient macro-model of structures considering beam-column joints damage was proposed which could capture the collapse process of the structures precisely. The criterion and the performance indices of structures for progressive collapse resistance were proposed by analyzing the collapse law of different structure systems. To improve the performance of structural collapse resistance, a pre-stressed precast structure system was devised and proven to have a good robustness against progressive collapse. Base on above studies, the design methods for structural components against blast loading and structures against progressive collapse were integrated to form the performance-based design system of structures subjected to explosion effects.

Keywords: performance-based design, blast loading, blast-resistant design, performance improvement, progressive collapse

The blast mitigation performance of curtain-type blast wall

Xingjun Fan[1], Zhejian Li[1,2*], Hong Hao[2,3*], Wensu Chen[3]

[1] *Guangdong Provincial Key Laboratory of Earthquake Engineering and Applied Technology, Earthquake Engineering Research & Test Center, Guangzhou University, China*

[2] *Key Laboratory of Earthquake Resistance, Earthquake Mitigation and Structural Safety, Ministry of Education, Guangzhou University, China*

[3]*Center for Infrastructural Monitoring and Protection, School of Civil and Mechanical Engineering, Curtin University, Australia*

* *Corresponding authors: zhejian.li@gzhu.edu.cn; haohong@gzhu.edu.cn*

Given the increasing frequency of explosions from terrorist attacks and industrial accidents, the importance of blast resistance in urban environments becomes ever more crucial. Blast walls function as barriers that separate explosive sources from protected structures, effectively blocking or attenuating blast waves to safeguard buildings and occupants behind them. Traditionally constructed from materials such as reinforced concrete, masonry, or steel plates, these walls are bulky, heavy, and often visually intrusive [1]. Their primary applications are as permanent blast protection structures in essential sectors, including defense and civil protection, which limits their use in civilian architecture within urban environments. Conventional blast walls rely on their inherent strength to absorb explosive energy, typically sacrificing their structural integrity to shield the objects behind them. Once damaged, they are challenging to be repaired and usually provide only a single-use protective capability. Furthermore, the failure of these walls produces debris, poses a significant risk of secondary injuries to those protected [2]. This highlights the need for innovative solutions that can enhance blast protection while mitigating these drawbacks.

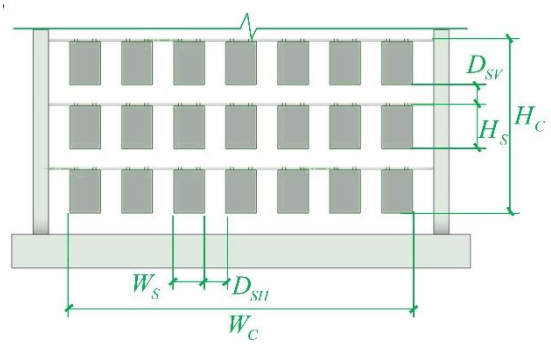

Figure 1. A schematic drawing of curtain-type blast wall

To address the limitations of traditional blast walls—namely their cumbersome design, inability to withstand multiple explosions, and potential for secondary injuries—this study introduces a novel concept inspired by curtains: the partial conversion of explosive energy into kinetic energy to attenuate blast waves. This leads to the development of the "curtain-type blast wall," a lightweight, detachable structure composed of independent, rotatable hanging steel plates that effectively transform a portion of the explosive energy into kinetic energy through rotation, as shown in Figure 1. The curtain-type blast wall exhibits low intrusion and is particularly suitable for urban environments. A numerical model was firstly developed and validated. Utilizing this validated model, the blast attenuation capabilities of the curtain-type blast wall was then investigated, as well as the mechanisms underlying blast wave propagation and attenuation. Comparing with free air blast scenarios, the curtain-type blast wall reduces the peak overpressure behind it by 71.1% and the maximum incident impulse by 69.7% as illustrated in Figure 2, outperforming the existing fence blast walls [3]. These findings highlight the superior blast mitigation efficacy of the curtain-type blast wall.

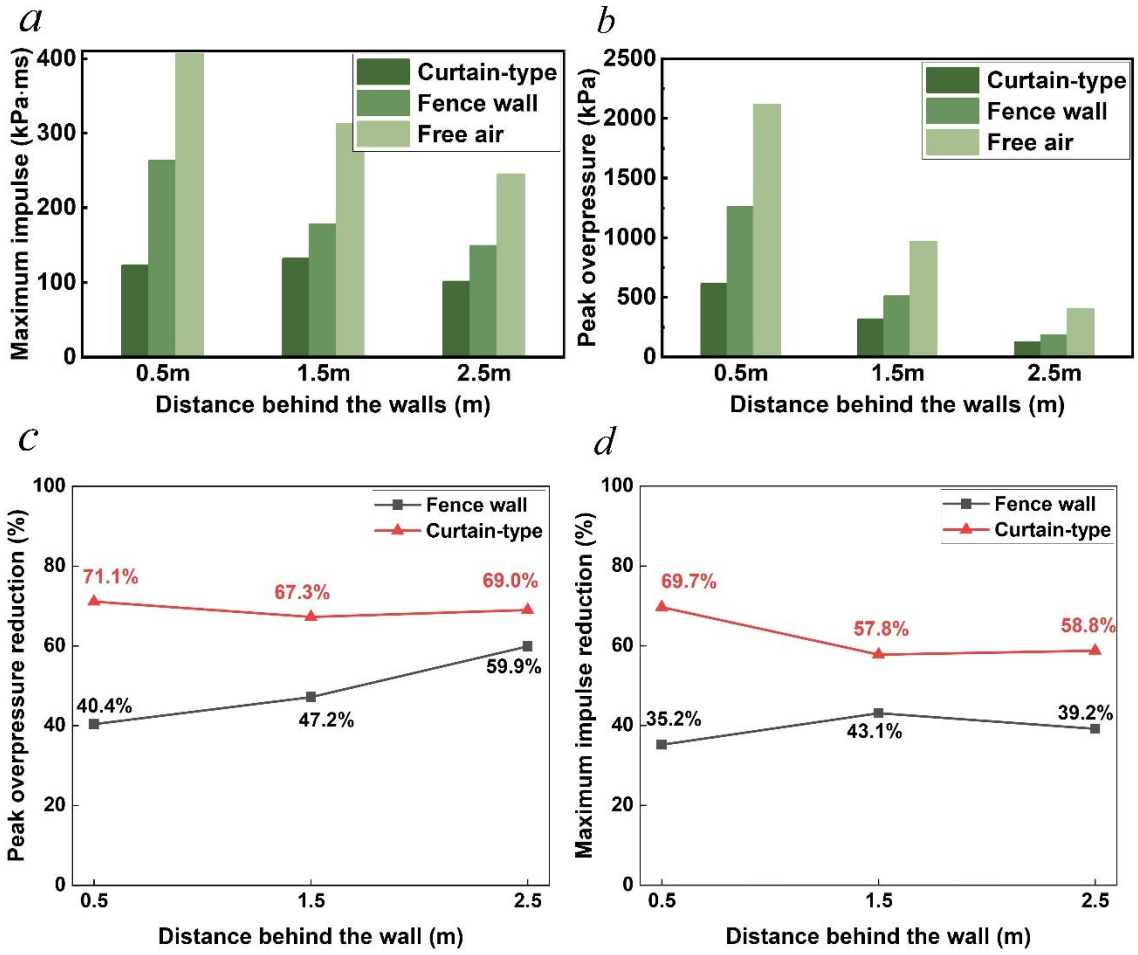

Figure 2. Comparison of blast wave attenuation effect at different gauges for three scenarios under 5 kg TNT explosion at the standoff distance of 0.4 m: (a) peak overpressure, (b) maximum impulse, (c) peak overpressure reduction, (d) maximum impulse reduction.

Keywords: curtain-type blast wall, blast mitigation, blast wave, blast energy.

[1] Hao, Y., Hao, H., Shi, Y., Wang, Z., & Zong, R. (2017). Field testing of fence type blast wall for blast load mitigation. International Journal of Structural Stability and Dynamics, 17(09), 1750099.

[2] Jin, M., Hao, Y., & Hao, H. (2019). Numerical study of fence type blast walls for blast load mitigation. International Journal of Impact Engineering, 131, 238-255.

[3] Xiao, W., Andrae, M., & Gebbeken, N. (2018). Experimental and numerical investigations of shock wave attenuation effects using protective barriers made of steel posts. Journal of Structural Engineering, 144(11), 04018204.

Impact Response of Glass Façade to Wind Borne Debris: A Numerical Study

Deenay Ambade[1], Manmohan Dass Goel [1*] and L. M. Gupta [1]

[1]*Department of Applied Mechanics, Visvesvaraya National Institute of Technology, Nagpur 440 010, Maharashtra, India*

[*]*mdgoel@apm.vnit.ac.in*

Glass façades have become a prominent feature in modern architecture, offering aesthetic appeal and abundant natural light. However, in regions exposed to severe weather conditions, particularly during storms, glass façades are vulnerable to damage from wind-borne debris. The impact of such debris can compromise the structural integrity of the façade, leading to potential safety hazards. Despite the significant threat posed by wind-borne debris to the safety and performance of glass façades, the behavior of these materials under impact is not extensively studied. This study presents a comprehensive numerical analysis of the impact behavior of laminated glass panels subjected to debris typically propelled by strong wind forces, using LS-DYNA®. The simulation models the interaction between wind-borne debris and glass panels of varying debris masses. The mechanical behavior of the glass is incorporated using fracture mechanics to simulate cracking and failure under impact. A range of impact scenarios is considered, including variations in debris mass, impact velocity, and impact locations, to replicate real-world conditions as accurately as possible. The numerical model integrates material properties, layer configurations, and impact conditions to closely reflect actual scenarios. In this study, wooden blocks of different masses are impacted on the laminated glass panels at varying locations and impact velocities. The results reveal the critical factors influencing the glass façade's response, such as the velocity of the incoming debris and the material strength of the glass. This study offers valuable insights for improving the safety and durability of glass façades. Thus, by understanding the complex dynamics of glass response to wind-borne debris, the study contributes to the development of more resilient architectural systems, leading to better risk management strategies for buildings in areas prone to extreme weather events.

Keywords: Impact, Laminated Glass, LS-DYNA®, Numerical Simulation, Wind Borne Debris.

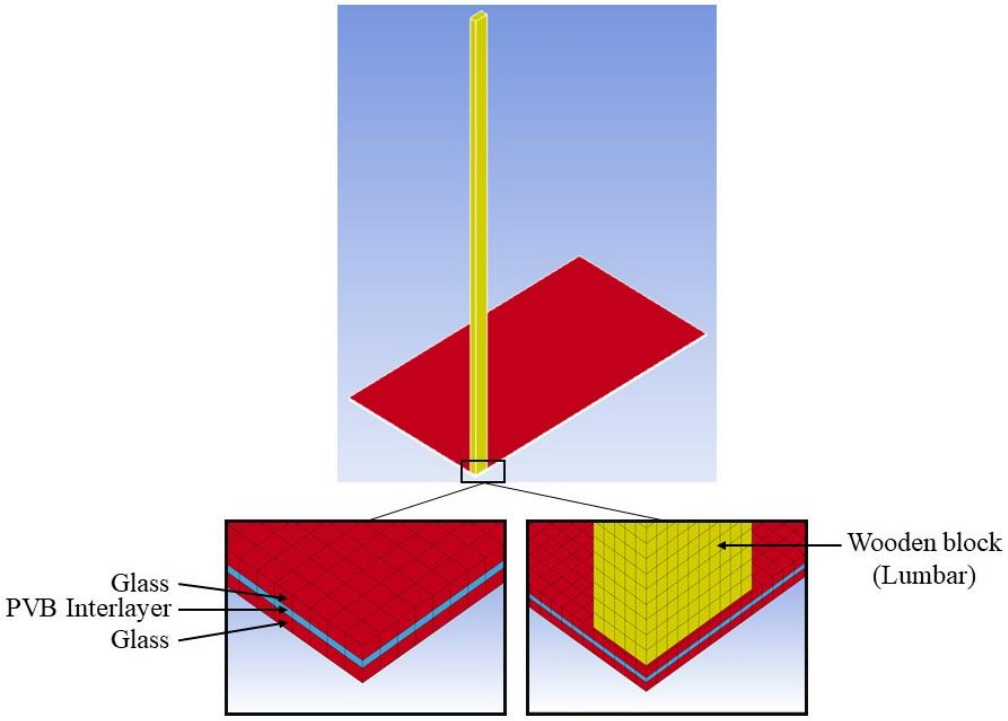

Figure 1. Numerical model of laminated glass

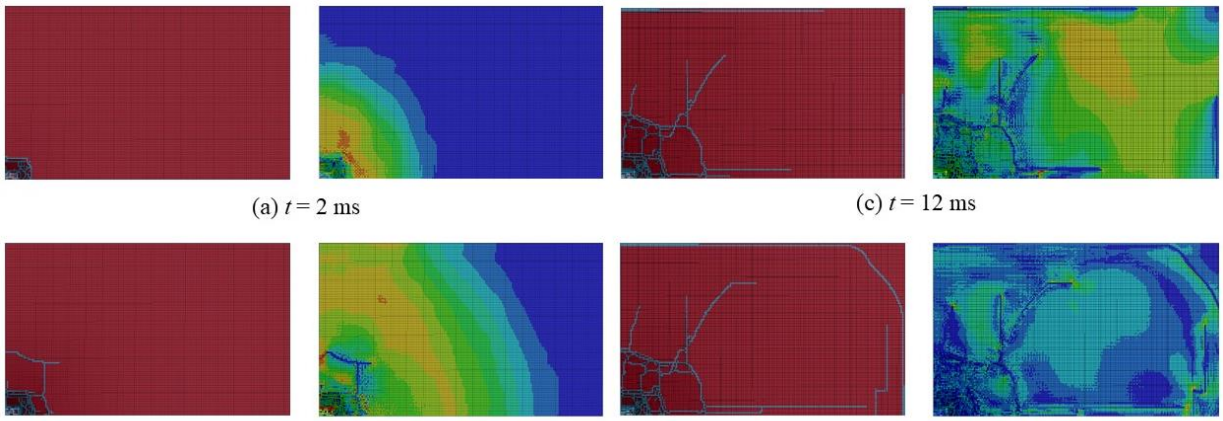

Figure 2. Glass cracking process and stress distribution

Ballistic impact performance of gradient structured AZ31 Mg alloy with enhanced strength and plasticity

Jianguo Li [1,2,3,4] , Qinghui Zhang [1] and Tao Suo [1,2,3,4]

[1] *School of Aeronautics, Northwestern Polytechnical University, Xi'an, PR China*

[2] *Institute of Extreme Mechanics, Northwestern Polytechnical University, Xi'an, PR China*

[3] *Shaanxi Key Laboratory of Impact Dynamics and Its Engineering Application, Xi'an, PR China*

[4] *Joint International Research Laboratory of Impact Dynamics and Its Engineering Application, Xi'an, PR China*

Due to their low density, high specific damping capacity and high shock absorbency, magnesium (Mg) alloys have great potential for development as high-performance lightweight armor materials in industrial applications. However, their applications are still limited owing to low strength, ductility and formability. Gradient structure design has been shown to be a good method for improving the mechanical properties and ballistic resistance of Mg alloy plate. It was demonstrated that the positive effects of twin-twin interactions resulting from the strain gradient made great contributions to a better combination of strength and ductility for the GS Mg alloy. Its strength and elongation rate increased simultaneously and hence it can be seen as an ideal alternative alloy for producing reliable lightweight armor systems. This work aims to thoroughly reveal the root causes of ballistic performance enhancement of gradient structured (GS) Mg alloy armor material through ballistic tests and finite element simulations. Compared with homogeneous Mg alloy plate of the same dimensions, the impact energy absorption of GS plate is increased by about 40%. The enhanced strength and plasticity from the gradient structure design certainly contribute in part to the ballistic resistance. More importantly, the gradient structure results in a transition of failure modes from the typical petal-shaped dehiscence to delamination and shear fracture. Based on detailed finite element analysis, we deeply understand the deformation process and the effect of the gradient structure on the propagation of stress wave during ballistic impacting. The energy absorption by each defeat mechanism is also theoretically calculated to quantitatively interpret their intrinsic effects. Meanwhile, microstructural observations and fracture morphology have demonstrated the appearance of adiabatic shear bands along the boundary of the cylindrical plunger after ballistic perforation of GS plate. Therefore, the failure mode transition caused by gradient structure design must also play a major role in

improving the ballistic resistance. Such a gradient structure design strategy provides a new way to create advanced lightweight armor systems. This method can be extended and applied to some other materials as well. Meanwhile, the ballistic performance of monolithic metal plate has been improved by the internal gradient structure design, in the next step we can further explore the feasibility of multiple lightweight GS Mg alloy plates in the design of multilayer armor plate to optimize the ballistic resistance of protective systems.

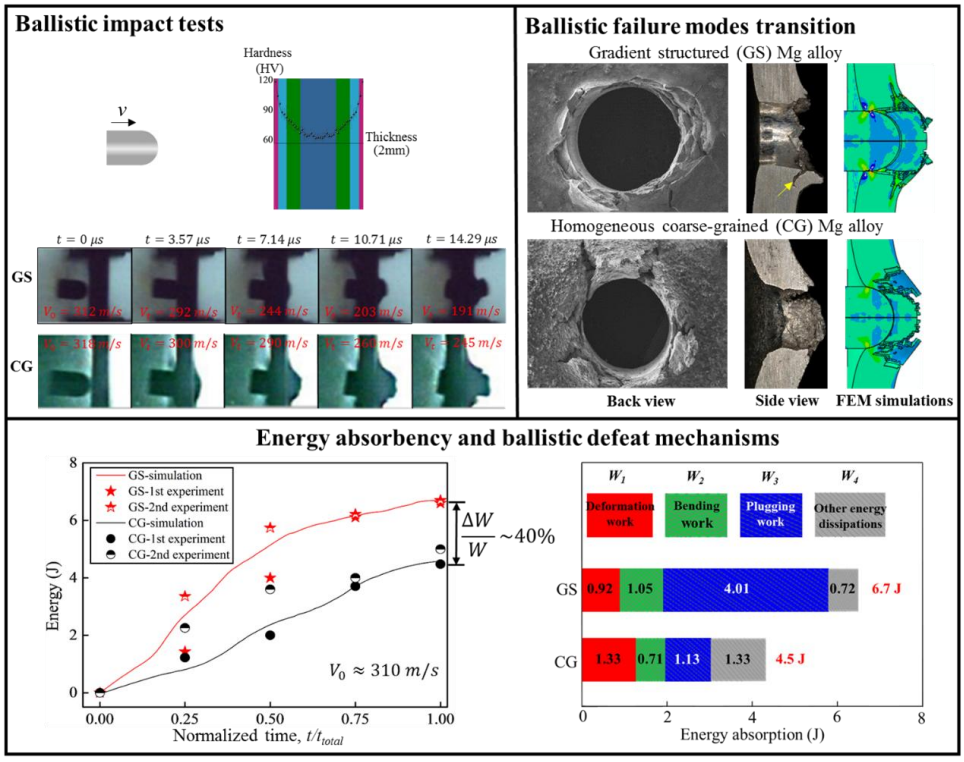

Fig.1 The results of high-speed penetration experiments show an impressive improvement in ballistic performance due to the gradient structure design, and through systematic FEM simulations, the effects of the gradient structure on the modification of the ballistic defeat mechanisms have also been thoroughly understood.

Keywords: Magnesium alloy, Gradient structure, Ballistic impact, Failure mechanism, Adiabatic shear band.

[1] Qinghui Zhang, Jianguo Li, Kun Jiang, Pu Li, Yusheng Li, Yong Zhang, Tao Suo, (2023). Gradient structure induced simultaneous enhancement of strength and ductility in AZ31 Mg alloy with twin-twin interactions, Journal of Magnesium and Alloys, https://doi.org/10.1016/j.jma.2021.10.014.

[2] Qinghui Zhang, Jianguo Li, Tengfei Ren, Bohan Ma, Tao Suo, (2023). Ballistic response and failure mechanisms of gradient structured Mg alloy, Journal of Materials Research and Technology, https://doi.org/10.1016/j.jmrt.2023.08.245.

Performance Evaluation of a 4-m-High Conventional Rockfall Protection Fence

Masato Komuro[1], Tomoki Kawarai[1], Takuro Nakamura[2], and Norimitsu Kishi[1]

[1]*Muroran Institute of Technology, Muroran, Japan*

[2] *Civil Engineering Research Institute for Cold Region, PWRI, Sapporo, Japan*

In Japan, many rockfall protection structures have been constructed in the mountainous regions and along coastlines to protect transportation networks and human lives from falling rocks. One type called as a conventional rockfall protection fence is made combining with H-shaped steel posts, wire ropes, diamond-shaped wire mesh, and clearance-keeping strips. The designed energy absorption is relatively small, approximately 50 to 100 kJ, depending on the height and length of the fence. In previous studies, the authors conducted impact load tests and three-dimensional elasto-plastic impact response analyses on a 2 m high fence to investigate the impact-resistant behavior and protective performance of the fence. On the other hand, depending on the condition of the slope and the type of rockfall risk, fences with a height of 2 m or more may be installed, however the impact-resistant behavior and protective performance of such fences are not yet fully understood.

From this point of view, in order to investigate impact-resistant behavior and protective performance of a full-scale of conventional rockfall protection fence with a height of 4 m, an impact loading test and 3D elasto-plastic impact response analysis were conducted. The impact loading test was conducted by lifting a steel weight (mass: 1,181 kg) suspended by a truck crane to a predetermined height and subsequently releasing it to collide with the center of the fence specimen through pendulum motion. The point of impact on the specimen was located at a height of 2.67 m above ground level (see Figure 1). The measurement items were as follows: 1) the impact force of the weight, 2) the horizontal movement of the weight, 3) the tension force of the wire rope, and 4) the axial strain of the posts.

As a result, 1) it was experimentally confirmed that the steel weight with 90% of the designed absorption energy can be captured by the fence (see, Figure 2). 2) Although it was not possible to simulate in fine detail the phenomenon of the weight passing through the ropes, it was demonstrated that the proposed numerical analysis method can accurately represent the impact behavior of the fence up to the moment just before slipping occurs.

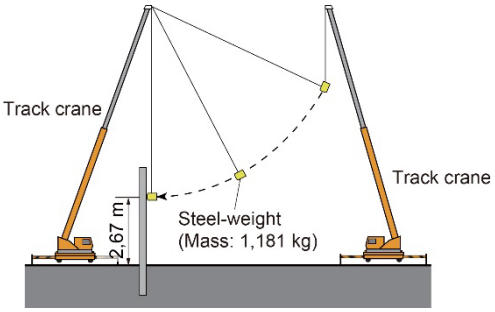

Figure 1 Setup for impact loading test.

Figure 2 Deformation of fence under impact loading

Keywords: rockfall protection fence, impact-resistant behavior, impact loading test, nonlinear FE analysis

Electromagnetic Hopkinson bar: A powerful tool to study mechanical behavior of materials at high strain rates

Weibin Wang[1,3,4], Yazhou Guo[1,3,4] , Yulong Li*[1,2,3,4]

[1]*School of Aeronautics, Northwestern Polytechnical University, Xi'an 710072, China*

[2]*School of Civil Aviation, Northwestern Polytechnical University, Xi'an 710072, China*

[3]*Shaanxi Key Laboratory of Impact Dynamics and Engineering Application, Northwestern Polytechnical University, Xi'an 710072, China*

[4]*Joint International Research Laboratory of Impact Dynamics and Engineering Application, Northwestern Polytechnical University, Xi'an 710072, China*

Abstract: Split Hopkinson bar (SHB) has been widely used for testing the dynamic mechanical behavior of materials. However, it is hard to involve complex stress conditions in traditional SHB due to its intrinsic characteristics. Electromagnetic Hopkinson bar (E-Hopkinson bar) has been recently proposed as a solution. Different from traditional SHB, the stress pulse of E-Hopkinson bar is generated directly by electromagnetic force. Therefore, the stress pulse that loads the specimen can be accurately controlled. With this advantage, some experiments that cannot be done with traditional SHB can be conducted by E-Hopkinson bar technique. In this case, we intbaruced briefly the basic principles of E-Hopkinson bar. Some lasted tests, such as symmetrically dynamic compression/tension of materials, testing technique for brittle materials, dynamic Bauschinger effect of metals, intermediate strain rate tests, trapezoidal stress pulse generation and dynamic multi-axial tests were also intbaruced. This new technique will be helpful for those researchers in the field of solid mechanics, especially when strain rate and complex stress condition are involved.

Keywords: Electromagnetic Hopkinson bar; Dynamic Bauschinger effect of metals; Dynamic multi-axial tests; Constant strain rate

1. Intbaruction

Split Hopkinson pressure bar (SHPB) [1] is a widely used experimental technique to characterize the mechanical properties of materials at high strain rates. In the SHPB system, the loading is an incident stress pulse (compressive, tensile or torsional pulse), which is created by two basic methods. One is to impact the incident bar by a projectile (striker bar or tube in the tensile version [2]). The projectile can be launched by ex- plosive, gas gun, or more recently, by electromagnetic driving tech- nology [3, 4]. Another method is the sudden

release of a pre-stressed section of the incident bar with torsional [5], tensile [6], or even compressive elastic strain energy [7].The aforementioned techniques to generate the incident pulse are basically triggered by mechanical means, which creates a difficulty to control the triggering instant within an accuracy of a millisecond. Compared with the entire pulse length of about hundreds of micro- seconds of a common SHPB system, it is hardly possible to launch simultaneously multiple incident pulses to realize a combined tension-torsion test or a bi-axial impact test. In order to obtain an accurate trigger control, an alternative technique to generate the stress pulse is highly desired.In this paper, the principle of electromagnetic riveting is adapted to create directly an incident pulse in the split Hopkinson compression/ tension bar without mechanical commands.

2. Methodology

The proposed electromagnetic split Hopkinson pressure bar setup is composed of charging and RLC discharge circuits, a stress pulse generator containing active and inductive coils, and a common pressure bar system. A schematic diagram of the setup is shown in Fig. 1.

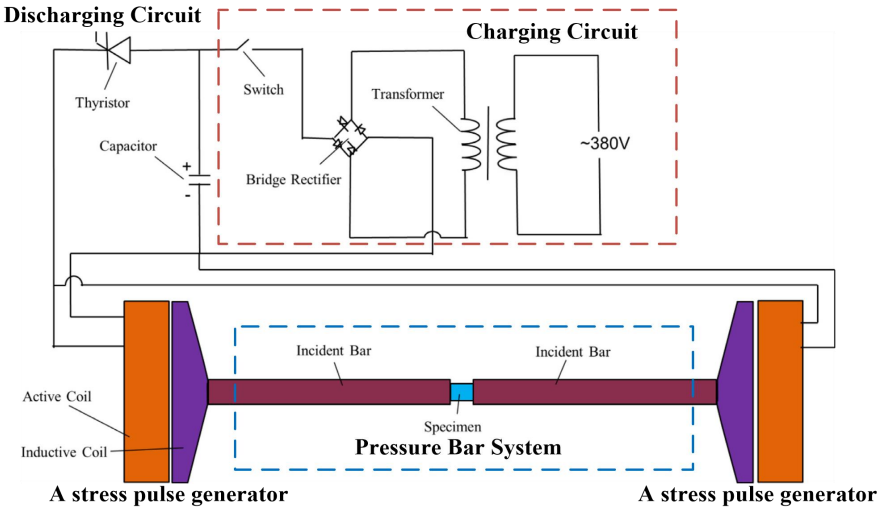

Fig. 1. Schematic diagram of the symmetric split Hopkinson compression bar

In Fig. 1, RLC circuits can be considered equivalent to a typical second-order RLC circuit [8]. The transient analysis of this second-order RLC circuit reveals that the current I_L exhibits a half-sine wave waveform during this period. According to Maxwell-Ampere's law [9], the generation of a magnetic field results from a time-varying electric field. Therefore, when the pulse current passes through the active coil, it generates a pulsed magnetic field A around it. Subsequently, following Faraday's law [10] of electromagnetic induction, this time-varying magnetic field induces an electric field that also varies with time.

Therefore, the inductive coil generates a time-varying electric field when influenced by pulsed magnetic field A. This, in turn, induces a time-varying pulsed magnetic field B. The interaction of magnetic fields A and B results in the generation of electromagnetic forces that repel each other in opposite directions. These electromagnetic forces drive the inductive coil to impact the incident bar, ultimately pbarucing stress waves within the bar [11]. This process can be represented by the following equation:

$$\sigma(t)=\frac{r\mu_0\omega Mn^2}{\alpha\sqrt{R^2+(\omega L_1)^2}\cdot\pi(r_2^{\,2}-r_0^{\,2})}I_m^{\,2}e^{-2\delta t}\sin^2(\omega t) \tag{1}$$

Equation (1), r_0 represents the radius of the coil guide shaft, r_2 denotes the radius of the inductive coil, μ_0 stands for vacuum permeability, and ω indicates the oscillation frequency of the discharge loop. The mutual inductance between the active coil and inductive coil is denoted as M ; n represents the number of turns of the active coil; α refers to the distance between the active coil and inductive coil; R signifies the resistance of the discharge circuit; L denotes the inductance of the discharge loop.

3. Results

FIG. 2 shows the different experimental results of the electromagnetic Hopkinson bar. FIG. 2(a) is the biaxial dynamic tensile equivalent curve, FIG. 2(b) is the biaxial tensile specimen, FIG. 2(c) is the strain rate and stress balance coefficient R(t) -time curve of the brittle material under biaxial compression, and FIG. 2(d) is the compressive tensile waveform consistency curve under dynamic Bauschinger effect of metals. Figure 2(e) is the strain rate tensile curve of 6061 aluminum 15s-1, and Figure 2(f) is the trapezoidal wave generated by E-Hopkinson bar technique.

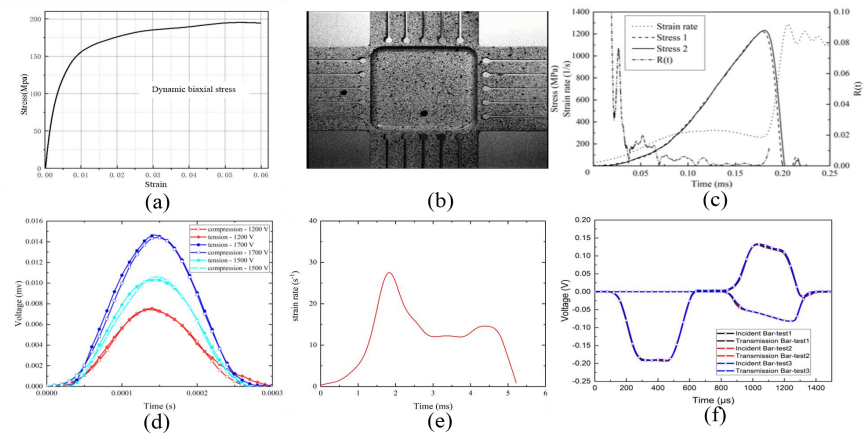

Fig. 2. Experimental results of electromagnetic Hopkinson bar in different research directions

4. Conclusions

The experimental technique proposed in this paper is an innovation of the traditional stress wave loading technique in Hopkinson bar. It uses electric field instead of elastic potential energy to generate stress wave, and realizes the functions of accurate control of stress wave loading time and synchronous loading. At present, the technique has been applied in symmetrically dynamic compression/tension of materials, testing technique for brittle materials, dynamic Bauschinger effect of metals, intermediate strain rate tests, trapezoidal stress pulse generation and dynamic multi-axial tests, and has also been involved in the field of dynamic strain rate experiments in materials and geotechnical disturbance dynamics. With the further study of E-Hopkinson bar experiment technology, it is believed that this technology will be applied to more fields in the future.

Reference

[1] Hopkinson B. A method of measuring the pressure pbaruced in the detonation of high explosives or by the impact of bullets. Philos Trans R Soc London 1914;213(612):437–56.

[2] Harding J, Wood E, Campbell J. Tensile testing of materials at impact rates of strain. J Mech Eng Sci 1960;2(2):88–96.

[3] Silva CMA, Rosa PAR, Martins PAF. An innovative electromagnetic compressive split Hopkinson bar. Int J Mech Mater Des 2009;5(3):281–8.

[4] Liu Z, Chen X, Lv X, Xie H. A mini desktop impact test system using multistage electromagnetic launch. Measurement 2014;49(1):68–76.

[5] Duffy J, Campbell JD, Hawley RH. On the use of a torsional split Hopkinson bar to study rate effects in 1100-0 Aluminum. J Appl Mech 1971;38(1):83–91.

[6] Staab GH, Gilat A. A direct-tension split Hopkinson bar for high strain-rate testing. Exp Mech 1991;31(3):232–5..

[7] Mancini E, Sasso M, Rossi M, Chiappini G, Newaz G, Amodio D. Design of an in- novative system for wave generation in direct tension–compression split Hopkinson bar. J Dyn Behav Mater 2015;1(2):201–13.

[8] Qiu G Y,Luo X J.Circuits (5th Edition).Higher Education Press 2006..

[9] Hill S E .Reanalyzing the Ampère-Maxwell Law.The Physics Teacher, 2011, 49(6):343-345.

[10] Agassiz. Faraday Biography . The Commercial Press,2002..

[11] Fenton G K,Daehn G S. Modeling of electromagnetically formed sheet metal.Journal of Materials Processing Technology 1998.75(1):6-16.

HIGH STRAIN RATE PROPERTIES OF FIBROUS CEMENT-BASED COMPOSITES USING THE SPLIT-HOPKINSON PRESSURE BAR

Felipe Rodrigues de Souza
Department of Civil and Environmental Engineering, Pontificia Universidade Catolica do Rio de Janeiro (PUC-Rio), Brazil
Technology Innovation Institute, Advanced Materials Research Centre, Abu Dhabi, United Arab Emirates, felipe.rodrigues@tii.ae (corresponding author)

Henrique Ramos
Department of Mechatronics and Mechanical Systems Engineering, Group of Solid Mechanics and Structural Impact, University of Sao Paulo, Brazil
Technology Innovation Institute, Advanced Materials Research Centre, Abu Dhabi, United Arab Emirates, henrique.ramos@tii.ae

Alia Ruzanna Aziz
Technology Innovation Institute, Advanced Materials Research Centre, Abu Dhabi, United Arab Emirates, alia.aziz@tii.ae

Omar Ba Nabila
Technology Innovation Institute, Advanced Materials Research Centre, Abu Dhabi, United Arab Emirates, omar.nabila@tii.ae

Rafael Savioli
Technology Innovation Institute, Advanced Materials Research Centre, Abu Dhabi, United Arab Emirates, rafael.savioli@tii.ae

Nikolaos Nikos
Technology Innovation Institute, Advanced Materials Research Centre, Abu Dhabi, United Arab Emirates, nikolaos.nikos@tii.ae

Flavio de Andrade Silva
Department of Civil and Environmental Engineering, Pontificia Universidade Catolica do Rio de Janeiro (PUC-Rio), Rio de Janeiro, Brazil, fsilva@puc-rio.br

Rafael Santiago
Technology Innovation Institute, Advanced Materials Research Centre, Abu Dhabi, United Arab Emirates, rafael.santiago@tii.ae

ABSTRACT

The mechanical properties of concrete and cementitious composites are influenced by strain rate, making assessment and understanding their dynamic behavior essential to ensure proper design under dynamic loading conditions. The Split-Hopkinson Pressure Bar (SHPB) technique is commonly used for characterizing the dynamic stress–strain response of concrete and cementitious composites under high-

strain-rate loading. In this study, the compressive and tensile properties of Ordinary Portland Cement concrete (OPC), Steel Fiber Reinforced Concrete (SFRC), and Ultra-High-Performance Concrete (UHPC) were investigated. Five cylindrical specimens with a diameter of 42 mm and a height of 21 mm were tested using the SHPB setup equipped with an ultra-high-speed camera for each test configuration. Dynamic Increase Factors (DIFs), accounting for strain-rate effects, were determined for each material and compared with quasi-static results obtained using specimens of the same geometry. Additionally, images of the tests were used to assess the failure modes. The experimental findings indicate that specimen geometry significantly influences the stress capacity of concrete. Furthermore, at a strain rate of approximately 600 s^{-1}, the strength increased by up to 1.76 times the compressive strength and up to 4.21 times the tensile strength for a 440 s^{-1} strain rate, underscoring the importance of understanding the behavior of concrete under high-strain-rate conditions.

Keywords: SHPB, dynamic properties, fiber-reinforced concrete, UHPC, high-strain-rate, dynamic increase factor.

Experimental study of the behaviour of SLA sandwich panels with different lattice structures under repeated loading

Gizem Köse[1], Kubilay Aslantas[1], Waleed Ahmed[2]

[1]*Afyon Department of Mechanical Engineering, Faculty of Technology, Afyon Kocatepe University, 03200, Afyonkarahisar, Turkiye*

[2]*Mechanical Engineering Department College of Engineering, UAE University Al Ain, Abu Dhabi, UA*

Sandwich panels are employed extensively in various engineering contexts due to their favorable combination of lightweight and strength properties. However, the long-term strength and performance characteristics of these structures under repeated loads can vary considerably depending on the geometry of the lattice structure. The objective of this study was to experimentally investigate the behaviour of sandwich panels produced using the SLA (Stereolitografi) method under different lattice structures under repeated loading conditions. In the context of this study, a series of sandwich panels with varying lattice geometries were designed and subjected to a specified number of repetitive loads. During the experiments, the mechanical deformations of the panels and the stress relaxation over time were meticulously measured and analyzed. The findings obtained are intended to contribute to the optimization of sandwich panels and the development of long-lasting and durable designs. Furthermore, this study aims to make a valuable contribution to the existing literature by elucidating the effects of different lattice geometries on engineering performance in design processes.

Keywords: Sandwich panel, Lattice structure, SLA

Development and Validation of an Advanced CFD Model for Predicting Hydrogen Explosion Dynamics

W. Senarathna[1], K. Wijesooriya[1], E.C.J. Gan[2], A. Remennikov[2], C.K. Lee[1], D. Mohotti[1*]

[1]*School of Engineering and Technology, The University of New South Wales, Canberra, ACT 2600, Australia*

[2]*School of Civil, Mining Environmental and Architectural Engineering, Faculty of Engineering and Information Sciences, University of Wollongong, Wollongong, NSW 2522, Australia*

Recent research has highlighted the growing importance of developing a robust CFD modelling framework to accurately simulate hydrogen explosions and assess the impact of various parameters, particularly in predicting explosion modes such as deflagration and detonation. However, many existing studies tend to focus on simplified models that overlook detailed chemical kinetics, often compromising computational efficiency. Therefore, this study aims to develop an enhanced numerical model that provides accurate predictions while ensuring computational efficiency. An experimental test of a small volume of hydrogen-oxygen explosion was used for validation purposes. The numerical model consists of two computational zones, namely large eddy simulation (LES) and Reynolds-Averaged Navier-Stokes (RANS), which were used to model explosion scenario efficiently in the polyhedral meshed numerical model. For example, the numerical model predicted the maximum overpressure at the sensor located at 100 mm away from the centre of the domain with an accuracy exceeding 90%. The propagation of flame and its behaviour is presented in this study with dynamics of flame radius and flame speed. In addition, the numerical model solved the computational fluid dynamics problem by utilizing detailed reaction mechanisms. The evolution of reaction species and their behaviour is also presented. This detailed numerical model can provide accurate predictions, regardless of the varying domain and mixture configurations. By enhancing the predictive capabilities of CFD models, this research contributes to more effective safety assessments for hydrogen infrastructure and aids in the design of robust explosion mitigation strategies. The results demonstrate that CFD modelling, when combined with detailed solutions and efficient techniques, plays a crucial role in advancing the understanding of hydrogen explosions, ultimately improving safety in hydrogen-based systems and facilities.

Keywords: Hydrogen Safety, Overpressure, Hydrogen Explosions, CFD Modelling

Field tests and numerical analysis of the blast-absorbing composite structure

Studziński Robert[1], Hasan Al-Rifaie[1], Michał Malendowski[1], Wojciech Sumelka[1], Tomasz Gajewski[1], and Piotr W. Sielicki[1]

[1]*Poznan University of Technology, Faculty of Civil and Transport Engineering, Poznan, Poland*

The article presents research on new components designed for the passive protection of building façades against potential blast wave loads. These components aim to absorb the energy of the explosion, thereby enhancing the safety and reliability of building operation. The analyzed elements belong to the category of sacrificial components. The presented component consists of a layered core enclosed within a steel casing. The core is composed of freely arranged, non-connected, profiled aluminum sheets with a gradient-varying thickness. During the test, the two types of aluminum panels were tested. One panel, called trapezoidal, has a perpendicular arrangement of the free core layers, while another one, called honeycomb, has a parallel arrangement of the free core layers, as illustrated in Figure 1.

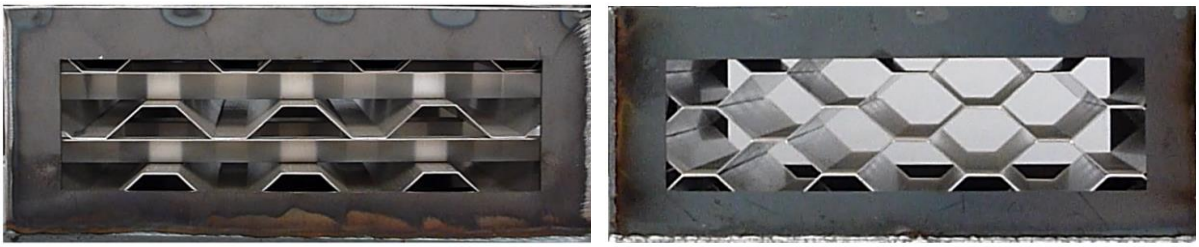

(a) (b)

Figure 1. Blast-absorbing units: a) trapezoidal, b) hexagonal

Numerical and experimental studies were conducted, including both static and blast load tests. All experimental investigations were preceded by numerical analyses, which were performed using the Abaqus software. For the static analysis, the surface load on the freely arranged core layers was modelled as a displacement-driven static force. In the case of blast load simulations, the CONWEP tool was utilized to simulate blast pressure loads. Based on the numerical analyses, a scenario for field tests was developed, involving a constant magnitude of the blast load (0.5 kg of TNT) applied at varying distances from the top layer of the unit H (1.5 m, 1.0 m, and 0.5 m), as shown in Figure 2.

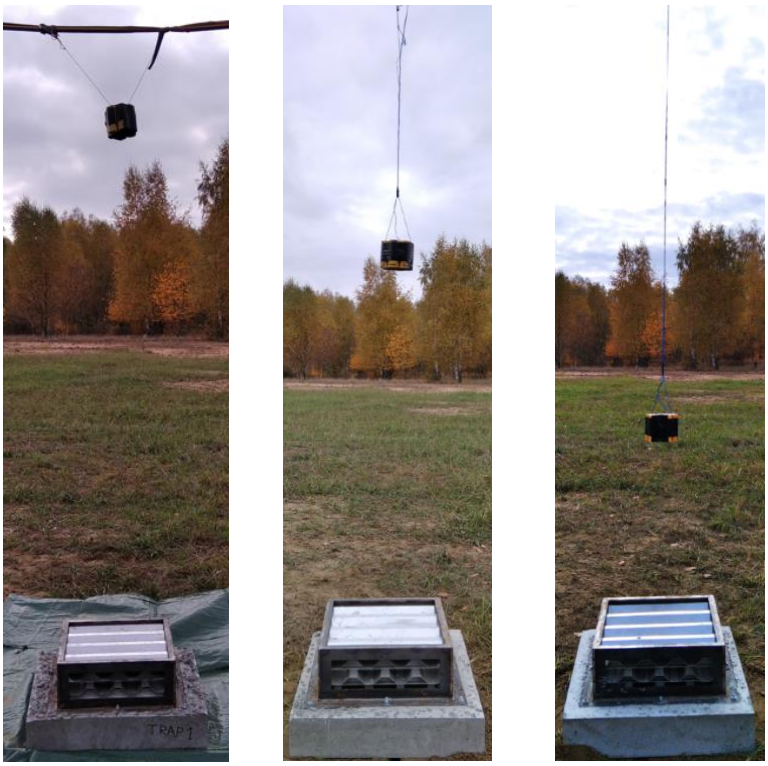

(a) (b) (c)

Figure 2. Distance between top layer of the blast-absorbing unit and the charge:
a) H = 1.5 m, b) H = 1.0 m, c) H = 0.5 m

The static load test was performed in the laboratory using a universal testing machine. The test involved applying uniform compression to the freely arranged, non-connected, profiled aluminum sheets of the core. As a result, equilibrium paths were obtained, illustrating the core's compression behavior under static loading conditions.

The blast load tests were conducted at a testing ground. The ballistics tests included three loading scenarios, with detonation occurring at three different heights relative to the tested element, as proposed based on the results of numerical analyses. The blast load experiments revealed that at a distance of 1.5 m, the first two layers were damaged; at 1.0 m, the first four layers sustained damage; and at 0.5 m, all six layers were destroyed. Finite element simulations accurately predicted the failure of the aluminum panels with trapezoidal and hexagonal layers.

Keywords: blast load, sacrificial elements, sandwich structures, metallic core, unconnected layers, reliability of structures.

High-velocity impact behaviour of Carbon epoxy composite with PAN nanofiber reinforcement

Vishnu Vijay Kumar[1,*], Khaled Shahin[1,*], Suresh Rajendran[2], Anupoju Rajeev[3], Prince Jeya Lal Lazar[4], Sharan Chandran[5], Seeram Ramakrishna[6]

[1] *Structural Engineering, Division of Engineering, New York University Abu Dhabi (NYUAD), Abu Dhabi, United Arab Emirates*

[2] *Department of Ocean Engineering, Indian Institute of Technology, Madras (IITM), India*

[3] *Department of Civil and Environmental Engineering, National University of Singapore (NUS), Singapore*

[4] *Department of Mechanical Engineering, Rajalakshmi Institute of Technology, Chennai, India*

[5] *School of Mechanical Engineering, Vellore Institute of Technology, Vellore, India-632014*

[6] *Department of Mechanical Engineering, National University of Singapore (NUS), Singapore*

[*] Corresponding author: e-mail: vishnu.v@nyu.edu; Khaled.shahin@nyu.edu

This research presents a comprehensive investigation into the high-velocity impact response of Carbon fiber-reinforced polymer (CFRP) composites enhanced with electrospun Polyacrylonitrile (PAN) nanofiber interleaving. The study employs a multi-faceted approach combining experimental high-velocity testing, advanced numerical simulation, and detailed morphological analysis to quantify and characterize the enhancement in impact resistance achieved through nanofiber integration. The experimental methodology utilized vacuum bagging techniques for specimen fabrication, with the modified variant incorporating strategically positioned electrospun PAN nanofibers within the interlaminar regions. Morphological examination revealed that nanofiber integration significantly reduced void ratios and enhanced fiber-matrix interfacial stress transfer mechanisms. Mechanical characterization demonstrated marked improvements across key performance metrics, with the nanofiber-enhanced CFRP exhibiting increases of 8%, 12%, and 11% in ultimate tensile strength, Young's modulus, and strain at break, respectively, compared to the baseline CFRP.

High-velocity impact testing was conducted using a calibrated single-stage gas gun apparatus equipped with high-speed imaging capabilities for event capture and analysis. The results demonstrated a significant enhancement in ballistic limit velocity from 70 m/s in conventional CFRP to 80 m/s in nanofiber-enhanced specimens, corresponding to an 8.7% improvement in ballistic limit per unit areal density. Moreover, the energy absorption capacity per unit areal

density showed a substantial increase of 24% in the nanofiber-enhanced configuration. The computational results exhibited a strong correlation with experimental data, particularly in predicting post-impact residual velocities. Analysis of energy dissipation mechanisms revealed that nanofiber-enhanced specimens primarily absorbed energy through secondary fiber deformation (33%), delamination (26%), and matrix cracking (25%), whereas conventional CFRP specimens predominantly dissipated energy through primary fiber tensile failure (37%). Post-impact specimen characterization using scanning electron microscopy provided detailed insights into damage morphology and progression patterns, validating the beneficial effects of nanofiber integration. The findings demonstrate that incorporating nanofibrous materials, constituting merely 1-2% of the total composite mass can significantly enhance ballistic resistance properties. This research establishes a robust foundation for future investigations into the optimization of nanofiber-enhanced composites and their potential applications in high-performance, impact-resistant structures. The methodology and results presented herein contribute valuable insights to the growing body of knowledge regarding nanofiber-enhanced composite materials and their response to high-velocity impact conditions.

Keywords: High-velocity impact, Carbon fiber, Polyacrylonitrile, Nanofiber, Fiber-reinforced composite, Ballistics, Material testing.

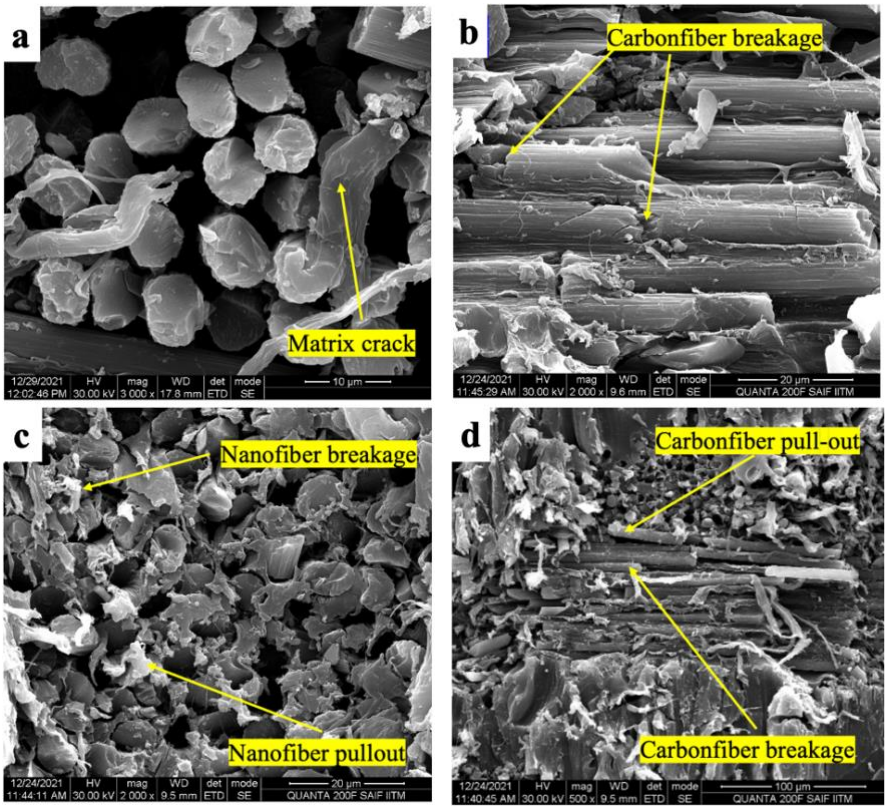

Figure 1. Scanning Electron Microscopy images obtained for the **(a,b)** CFRP and **(c,d)** CFRP-Nano composite

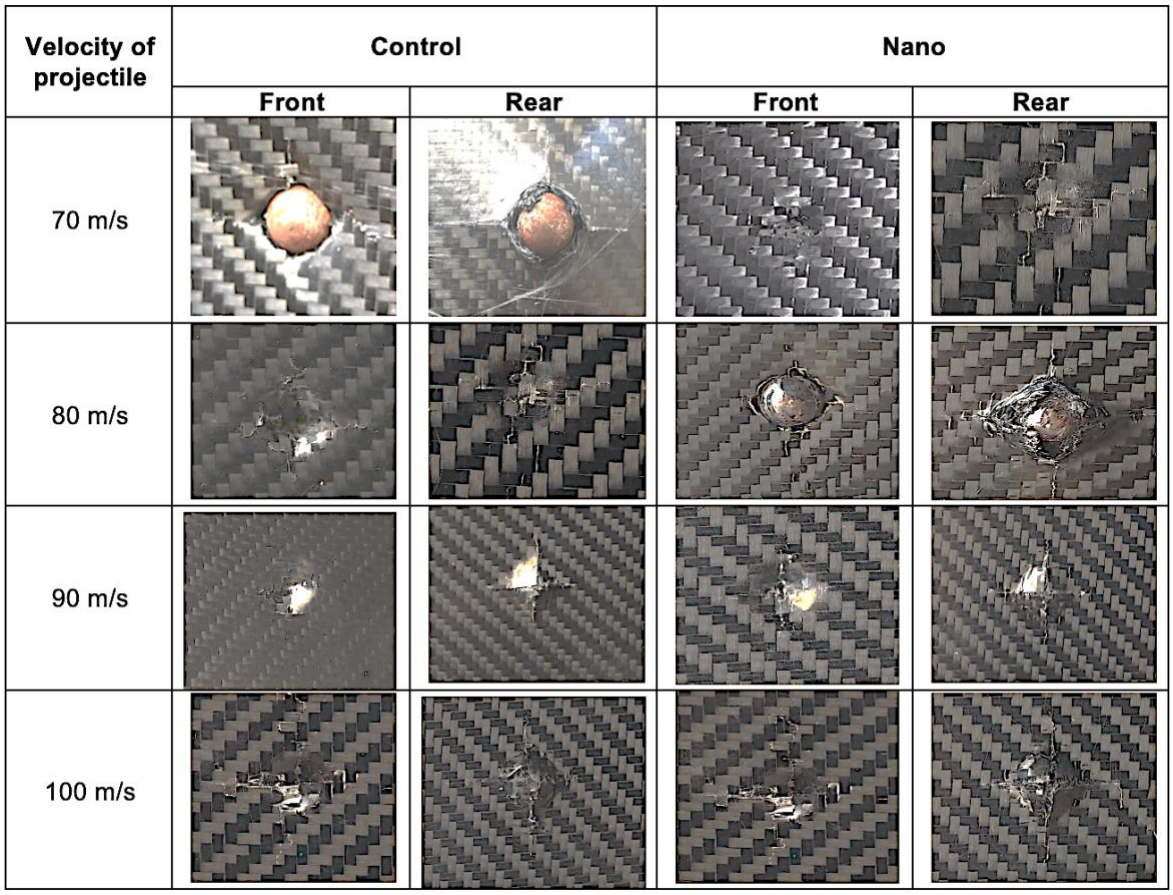

Figure 2. Post-impact damaged CFRP and CFRP-Nano composite specimens under different velocity

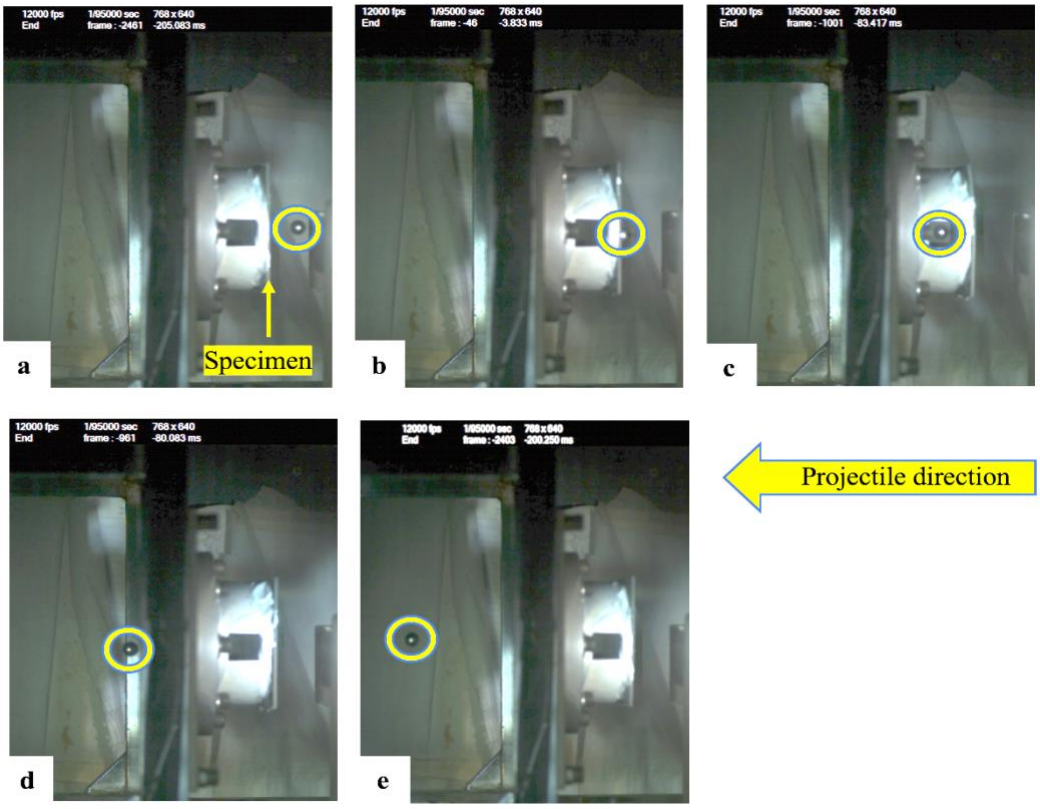

Figure 3. Representative high-speed camera footage for ballistic impact event

Experimental Study on Short-Term Flexural Behaviour of One-Way Seawater-Sea Sand Concrete Slabs Reinforced with GFRP under Impact Loading

Hai La-Hong [1], Long Nguyen-Minh [2] and Thong M. Pham [3]

[1] *Ph.D. Student, Faculty of Civil Engineering, Ho Chi Minh City University of Technology (HCMUT), Ho Chi Minh city, Vietnam; Lecturer, Faculty of Engineering - Technology, Tay Do University (TDU), Can Tho city, Vietnam; E-mail: lhhai@tdu.edu.vn.*

[2] *Associate Professor, Faculty of Civil Engineering, Ho Chi Minh City University of Technology (HCMUT), Ho Chi Minh city, Vietnam. E-mail: nguyenminhlong@hcmut.edu.vn*

[3] *Associate Professor, UniSA STEM, University of South Australia, Mawson Lakes, SA 5095, Australia. ORCID: https://orcid.org/0000-0003-4901-7113. Email: thong.pham@unisa.edu.au (Corresponding author)*

Seawater-sea sand concrete structures reinforced with fibre-reinforced polymer (FRP) have attracted considerable interest from researchers and engineers in recent years. This structural solution presents a viable alternative to traditional reinforced concrete (RC), particularly for coastal and island projects where freshwater and river sand resources are scarce. However, systematic understanding of the structural behaviour of seawater-sea sand concrete members reinforced with GFRP remains limited. This study investigates the short-term flexural behaviour of one-way seawater-sea sand concrete slabs reinforced with GFRP (GFRP-SC) under impact loading. An experimental program was conducted on five slabs: four slabs (two GFRP-SC and two RC) under impact loading and one GFRP-SC slab under static loading. All slabs had the same longitudinal GFRP reinforcement ratio (ρ_f) of 0.7% and dimensions of 1.0 m (width) × 0.1 m (height) × 2.0 m (span). The slabs were divided into two groups with concrete strengths of M350 (35 MPa) and M600 (60 MPa). The results show that increasing the concrete strength from normal to high improves the impact resistance and deformation behaviour (reducing deflection and the number of cracks) of GFRP-SC slabs. Under impact loading, GFRP-SC slabs exhibit different structural behaviour compared to static loading. Compared to RC slabs, the impact resistance and failure modes of GFRP-SC slabs are not significantly different, although the deformation of GFRP-SC slabs is greater than that of RC slabs.

Keywords: Seawater sea sand concrete, slabs, GFRP, flexural behaviour, impact loading.

Post-tensioned reinforced concrete column sections under impact loading

Ghazaleh Taheri[1], Petr Máca [1], Thomas Schubert[1], Nicholas Unger[1], Silke Scheerer[1], Birgit Beckmann[1], and Steffen Marx[1]

[1]*Institute of Concrete Structures, TUD Dresden University of Technology, Dresden, Germany*

Evaluating structural responses to dynamic loads, such as impact, is critical because these loads can cause severe damage to infrastructure and pose risks to human lives. Structurally important members, like bridge piers and building columns, are particularly vulnerable to impact loads from events such as vehicle collisions or rockfalls. To address these critical issues, we conducted experimental tests using a drop weight impact test to analyze the responses of post-tensioned reinforced concrete column sections under controlled impact loads. A drop tower was employed to accelerate a rigid cylindrical projectile with a flat nose, having a diameter of 100 mm and a length of 380 mm. The impactor's weight was 21.58 kg. Reaction forces were measured using load cells, while accelerometers captured dynamic responses during impact. Both the reinforced concrete columns and the impactor were equipped with a speckle pattern, facilitating Digital Image Correlation (DIC) analysis. The DIC system was used to track the impactor velocity throughout the event, as well as to measure deflections and observation of the cracking patterns on the column surfaces. In Figure 1, the impact test setup including high speed camera positions is shown. In total, six different column specimens were tested under two distinct impact velocities: 25 m/s and 33 m/s. The cross-section of the columns was 200 mm × 300 mm with a length of 1500 mm. The clear span was 1000 mm and the longitudinal and transverse reinforcement ratio were approximately 2 % and 0.7 %, respectively. The columns were post-tensioned to two levels of 34% and 67% of their axial capacity and compared to a reference specimen with no axial force. This range of axial force was chosen to have a detailed evaluation of how different levels of post-tensioning influenced structural performance, specifically in terms of reaction force, lateral deflection and cracking patterns under impact loading. We observed that the mass of debris generated by the impact increased with impact velocity. In most cases, the debris mass also increased with a higher axial force ratio. This trend is likely due to the release of elastic energy stored within the post-tensioned specimen during the impact event, which intensified the dynamic response. The post-tensioning seemed to induce significant vibrations within the columns. Specifically, we noted a pronounced scabbing of the concrete cover, primarily on the rear side of the impact, which led to the exposure of the

reinforcement. (Figure 2) The results of this study can serve as basis for analytical and numerical models and as guideline for testing additional parameters in similar specimens.

Keywords: drop-tower, impact loading, post-tensioning, columns, dynamic response, reinforced-concrete.

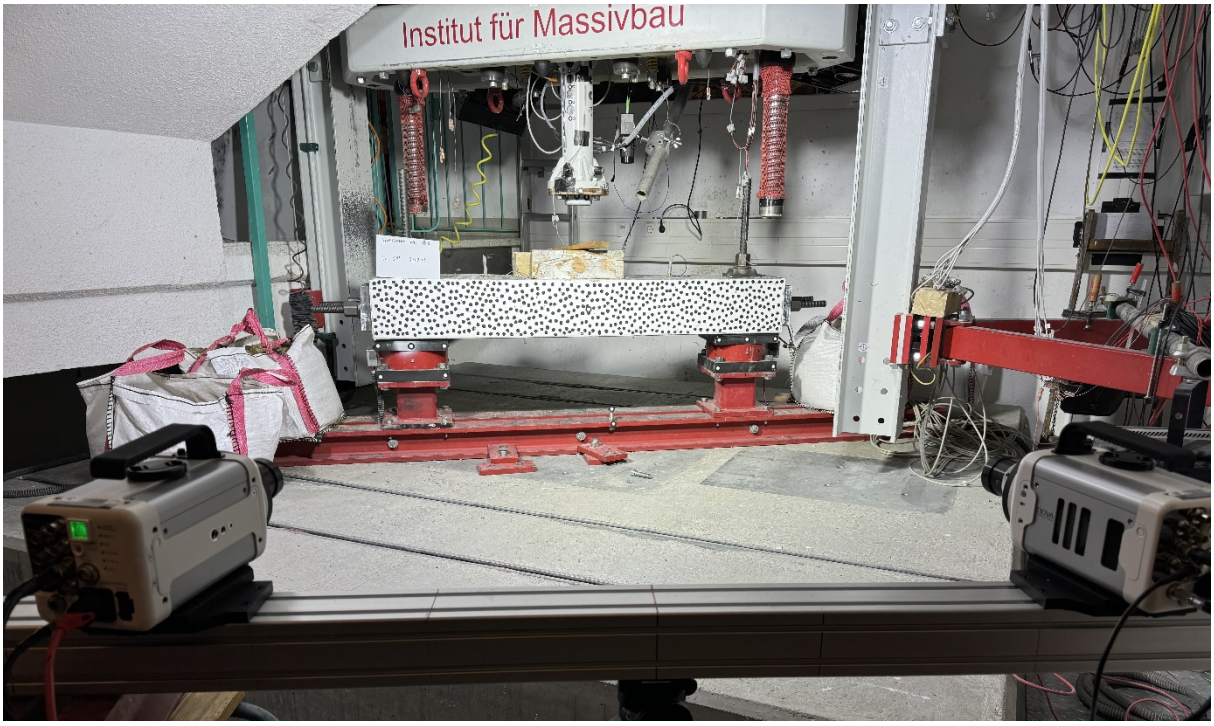

Figure 1: Post tensioned column in the Drop Tower of TUD ready for testing. From the view-point of the high speed cameras.

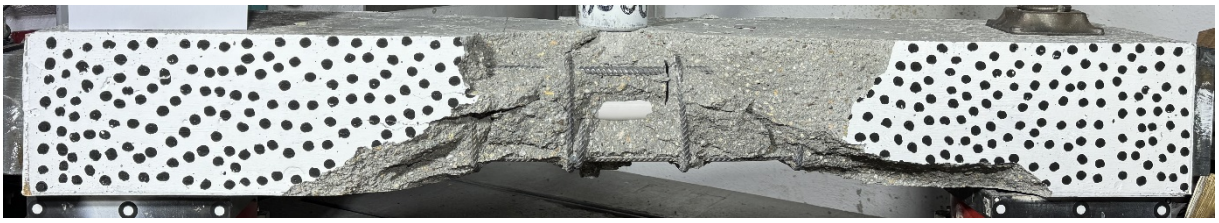

Figure 2: Damage to a specimen with an axial force ratio of 34 % after an impact test at a speed of 33 m/s.

Blast protective system for concrete walls: experimental tests and numerical simulation

María Chiquito[1], Anastasio P. Santos [1], Lina M. López[1], Ricardo Castedo[1], Alejandro Pérez-Caldentey[1,2], Luis Iglesias[1] and Iván Gil[1,3]

[1]*Universidad Politécnica de Madrid, Madrid, Spain*

[2]*FHECOR Consulting Engineers, Madrid, Spain*

[3]*National Institute of Aerospace Technology (INTA – Campus La Marañosa), Madrid, Spain*

In the search for protective solutions that improve safety in critical infrastructures, a novel system of protection based on changing the frequency of the protected structure is presented. The solution is based on protecting the structure with a low-frequency harmonic isolator wall, consisting in a massive steel sheet (40 mm thick) supported by a series of springs anchored on the wall to be protected and, at the bottom, on rollers. To test the system, a series of experimental tests were carried out on a concrete wall with dimensions of 2.50 m wide, 3.00 m high and 0.25 m thick. The steel sheet was connected to the concrete wall by 30 springs, spaced 0.5 m apart, both vertically and horizontally, with a diameter of 250 mm, 25 mm coil diameter and 14 coils. The spacing between the steel plate and the concrete wall was 1.20 m and the maximum spring stroke was 0.7 m. For comparison purposes, a concrete wall with the same dimensions and no additional reinforcement was tested at the same time. A total of 12 tests were performed on the walls separated into two testing phases. For the first phase, explosive charges between 10 and 50 kg TNT eq. were used at 3 m from the wall with the protective system, combining tests with centered and eccentric load. For the second phase, the charges varied between 50 and 70 kg TNT eq. located at 2 and 3 m from the wall. The trials were monitored with pressure gauges, accelerometers, photogrammetry for measuring wall displacements and two wire extensometers to monitor the displacement and damping of the steel sheet. Results showed that the change in the period of the structure through the interposition of the steel plate and the springs produced a significant reduction in the stresses transmitted to the concrete wall. The wall withstood the 12 tests without showing visible damage, which means that the protective system could be used to withstand successive explosions. As for the unreinforced wall, it showed a different behavior than expected because the anchors of the wall to the foundation slab failed. In addition to the experimental tests,

numerical modelling of the specimens tested was carried out using the finite element code LS-DYNA combined in some cases with the Viper Blast Computational Fluid Dynamics (CFD) solver. Results of numerical simulations were compared with the experimental data showing that, even with the simplifications used in the models, the results were in good agreement.

Keywords: blast loading, protective structure, full-scale tests, successive explosions.

Figure 1. High-speed camera image sequence.

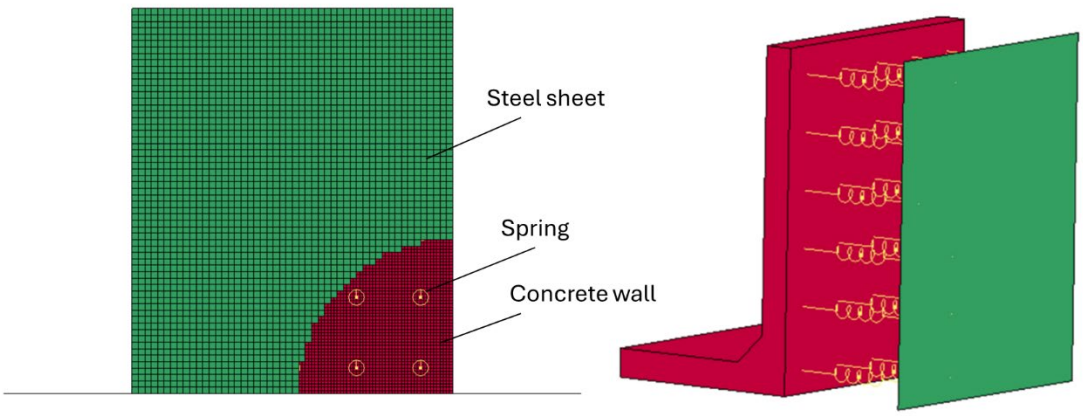

Figure 2. Numerical model of the protected wall.

Multiple Impact Behaviour of Nanoparticle Strengthened UHMWPE Composite Ballistic Helmet

M. D. Umbharatwala[1], Manmohan Dass Goel[1], Marcus Mäder [2] and Steffen Marburg[2]

[1]*Department of Applied Mechanics, Visvesvaraya National Institute of Technology, South Ambazari Road, Nagpur - 440 010, Maharashtra, India.*

[2] *Chair of Vibroacoustics of Vehicles and Machines, Department of Engineering Physics and Computation, TUM School of Engineering and Design, Boltzmannstr. 15, Garching 85748, Munich, Germany.*

This study presents a detailed numerical evaluation of the performance of a ballistic helmet made from carbon nanotube (CNT)-reinforced Ultra-High Molecular Weight Polyethylene (UHMWPE) fabric composites, based on experimental testing conducted at the Blast Impact Simulation and Testing Laboratory (BIST Lab) at Visvesvaraya National Institute of Technology (VNIT), Nagpur, India. Using LS-Dyna® finite element software, a series of simulations were carried out to model the behavior of the CNT-UHMWPE composite under ballistic impact conditions. The numerical model was validated by comparing its results to experimental data obtained from tests involving three identical fabric specimens. Each specimen was subjected to four sequential impacts from 10-gram ogive-shaped hardened steel projectiles, with impact velocities ranging from 538 m/s to 758 m/s. The tests provided crucial data on the material's response to high-velocity impacts, allowing for a comprehensive comparison between the simulated and experimental results. The simulations demonstrated that the addition of carbon nanotubes to the UHMWPE fabric significantly enhanced its mechanical properties, improving the fabric's ability to absorb and dissipate energy during impact. The CNT reinforcement contributed to a higher resistance to ballistic penetration, reducing the extent of deformation and preventing catastrophic failure. These findings highlight the effectiveness of CNT-UHMWPE composites as a promising material for ballistic protection, offering a balance between lightweight construction and high-impact resistance. Furthermore, the study emphasizes the importance of using a combination of numerical simulations and experimental validation to accurately predict the performance of advanced materials under realistic impact conditions. The results also provide insights into the potential for optimizing the composite's structure and material composition to further improve its ballistic protection capabilities. This research not only contributes to the development of more effective materials for ballistic helmets but also paves the way for future innovations in protective gear for military, law enforcement, and civilian applications. By advancing the understanding of composite behavior under high-velocity impacts, this study lays the foundation for designing next-generation protective components that are both lightweight and highly effective, satisfying the demand of modern-day security and defense applications.

Keywords: Ballistic Protection, Carbon Nanotubes, UHMWPE Composites, Finite Element Analysis, Impact Simulation, Protective Helmet.

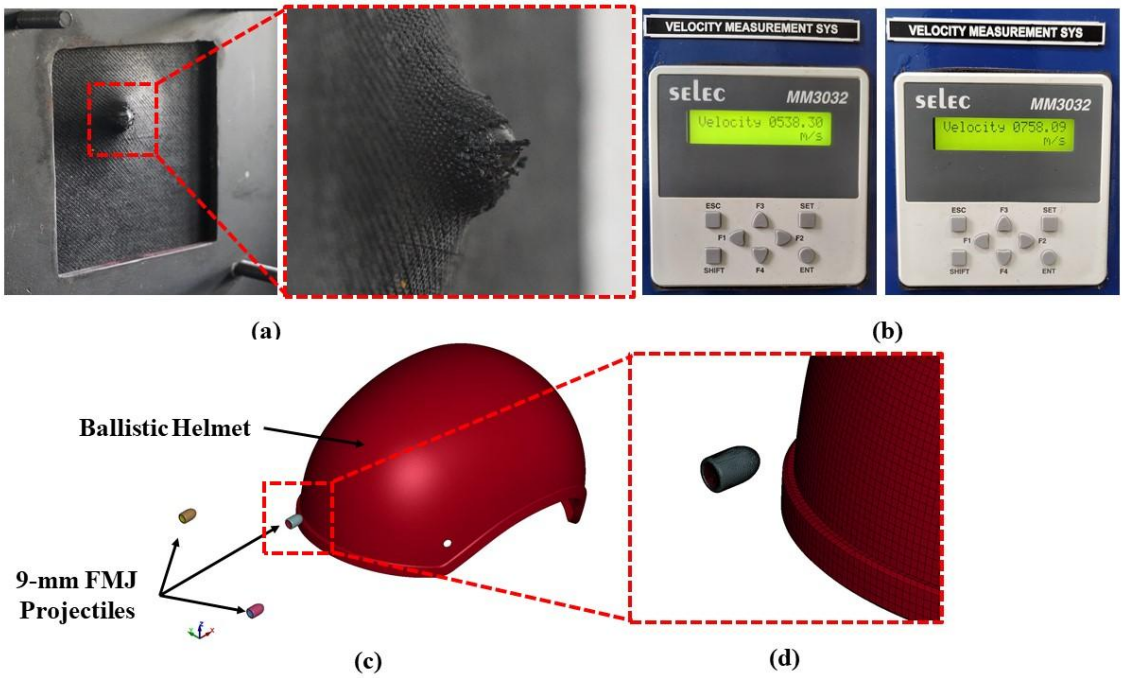

Figure 1. Details of Experiments and Numerical Model (a) Back Side of Composite Panel after Impact (b) Minimum and Maximum Velocities of Projectiles Impacted on the Composite Panel, and (c) Numerical Model of Ballistic Helmet Developed in LS-Dyna® for FE Simulation

Post-fire Impact Resistance of Ultra-high Performance Concrete Beams

Junjie Huang[1], Jun Li [1] and Chengqing Wu [1,2]

[1] *School of Civil and Environmental Engineering, University of Technology Sydney, NSW 2007, Australia*

[2] *Institute of Rock and Soil Mechanics, Chinese Academy of Sciences, Wuhan, 430071, China*

This study investigates the impact resistance of Ultra-high Performance Concrete (UHPC) beams after exposure to high temperatures between 600 °C and 1000 °C. UHPC reinforced with steel fibres showed a compressive strength of 129.5 MPa at room temperature, which dropped to 108.5 MPa and 32.8 MPa after 600 °C and 1000 °C thermal exposure, respectively. All the UHPC beams were heated in a horizontal furnace, after the target temperature was achieved, the beams were maintained at the target temperature for 120 minutes before cooling down in the furnace. Evident thermal spalling was observed on the surface of all the UHPC beams and the spalling depth increased with the exposed temperature. The beam static flexure capacity dropped by 22% after 600 °C exposure. The post-fire impact resistance was studied via a drop weight impact setup with a fixed drop weight of 641 kg and free-falling height from 0.25 m to 1 m. All UHPC beams failed under flexure. As expected, the impact resistance of UHPC beams reduced with the thermal exposure. Under the same impact scenario, i.e. 641 kg weight impacting the beam mid-span from 1 m height, the beam exposed to 600°C showed 73% higher peak mid-span deflection than non-heated beam.

Keywords: UHPC beam, fire exposure, impact loads.

BLAST PROTECTION OF STEEL-ALUMINUM FOAM SANDWICH STRUCTURES USING POLYUREA AND STIFFENER

ICPS6, Auburn University, May 2023

[1]Harshada Sharma, [2]Kusum Saini, [3]S. P. Singh, and [4]Vasant Matsagar

[1] *PhD Candidate, School of Interdisciplinary Research, Indian Institute of Technology (IIT) Delhi, Hauz Khas, New Delhi - 110 016, India. (Corresponding Author)*
Harshada.Sharma@sire.iitd.ac.in
[2] *Batch of 1969 Innovation Fellow, Department of Civil Engineering, Indian Institute of Technology (IIT) Delhi, Hauz Khas, New Delhi - 110 016, India.*
kusum.saini310@gmail.com
[3]*Professor, Department of Mechanical Engineering, Indian Institute of Technology (IIT) Delhi, Hauz Khas, New Delhi - 110 016, India.*
singhsp@mech.iitd.ac.in
[4] *Professor, Dogra Chair, and Head, Department of Civil Engineering, Indian Institute of Technology (IIT) Delhi, Hauz Khas, New Delhi - 110 016, India.*
matsagar@civil.iitd.ac.in

ABSTRACT

In current days, sandwich structures have become popular due to their flexibility with design requirements and excellent performance under extreme loads, such as blast. There are different strategies for enhancing the blast resistance of such sandwich structures. Including an additional layer of polyurea and stiffeners are widely used techniques that may enhance the performance of the panels under high-rate loadings. In this study, the effects of polyurea and stiffeners on the protection of a steel and aluminum foam sandwich panels is studied. Effective configuration of the panels with both polyurea and stiffeners are investigated. Here, different configuration cases of the sandwich panels: (a) panel without polyurea and stiffeners, (b) with polyurea applied on the rear face, (c) with stiffeners applied on the rear face, and (d) with polyurea and stiffeners on the rear face are investigated and compared. The finite element models of sandwich panels are developed, where steel facesheets, steel stiffeners, and polyurea are modeled with shell elements, and aluminum foam core is modeled with solid elements. Elastic-plastic, crushing foam, and hyperelastic material behaviors are implemented for steel, aluminum, and polyurea layers of the sandwich panels, respectively. The performance of the different configurations of the panels are compared in terms of the response quantities, i.e., deformation, equivalent von-Mises stresses, and energy absorption. Moreover, the damage patterns with fragmentation effect are depicted for all the considered sandwich panels. The results of the study show that both polyurea and stiffeners are the most effective configuration in protecting the sandwich structures. Moreover, the sandwich panel with stiffener is the most effective case for the highest reduction in equivalent von Mises stresses.

Keywords: Aluminum foam, Blast load, Polyurea, Protection strategy, Sandwich panel, Stiffener.

Submission ID: 2559

This study presents a numerical analysis of a high-rise building with 8 underground parking floors and 51 above-ground floors, focusing on its vulnerability to combined blast and progressive collapse scenarios. Extreme Loading for Structures (ELS) software, utilizing the Applied Element Method (AEM), is employed to simulate the building's response under extreme loading conditions. AEM is a powerful analysis technique that accurately models structural behavior by discretizing the structure into small elements connected by springs, allowing it to capture both large-scale deformations and fine-grained material failures. This capability makes AEM highly suited for simulating dynamic events like explosions, as it can model detailed interactions and sequential failures that occur after initial damage. In this study, each column at the ground parking level was analyzed under a blast loading scenario generated by a simulated car explosion, identifying high-risk zones where multiple columns sustained significant damage due to blast pressure. Using this damage data, a progressive collapse analysis was conducted on the global structural model, simulating the removal of damaged columns to understand potential collapse mechanisms. This approach provides an efficient alternative to full-model blast analysis, which can be computationally intensive and time-consuming. The results of this combined analysis reveal critical vulnerabilities, highlighting the building's susceptibility to collapse under extreme conditions. These insights provide essential data for engineers, risk managers, and policymakers seeking to enhance the resilience of high-rise buildings in urban environments against catastrophic events.

Effects of Triggering Event Characteristics on the Progressive Collapse Response of Reinforced Concrete Moment-Resisting Frames

Foad Kiakojouri[1], Elahe Zeinali[1] and Valerio De Biagi[1]

[1]*Department of Structural, Geotechnical and Building Engineering (DISEG) - Politecnico di Torino, Torino, Italy*

Progressive collapse can be defined as the spread of initial failure from one element to the next, ultimately leading to a collapse that is disproportionately larger than the initiating failure [1]. Upon reviewing major structural failures, it becomes evident that progressive collapse mechanisms are responsible for many of them [2]. Over the last two decades, our understanding of this phenomenon, as well as techniques to design and construct structures to resist it, has significantly improved. However, it should be noted that the body of knowledge has largely developed within a framework that ignores the triggering event, i.e., a threat-independent methodology [3]. While this approach facilitates code-based design and provides a simplified framework useful for practicing engineers, it does not account for the characteristics of the triggering event. The effects of this simplification, i.e., assuming the triggering event merely as an element removal, are not always clear, as they depend on the type of threat and the structural configuration [3].

Dynamic effects	Member loss	Damage to other members	Loading to other members	Upward forces on floors	Downward pressure on roof	Inward pressure on sides
Sudden column removal						
✓	✓	✗	✗	✗	✗	✗
Blast analysis						
✓	✓	✓	✓	✓	✓	✓

Figure 1. Comparison between the parameters involved in threat-dependent and threat-independent methodologies.

Considering the aforementioned framework, this study focuses on assessing progressive collapse in reinforced concrete structures subjected to blast scenarios. A numerical model of a 3D multi-story frame was developed, incorporating various blast scenarios with differing explosive charges and standoff distances. The structural responses were investigated using the

Applied Element Method, which effectively models extreme events and material behavior under such conditions. The results were compared with the threat-independent methodology, such as dynamic column removal, providing insights into the impact of triggering events and validating code-based approaches. The sources of differences between the two methodologies are highlighted in Figure 1.

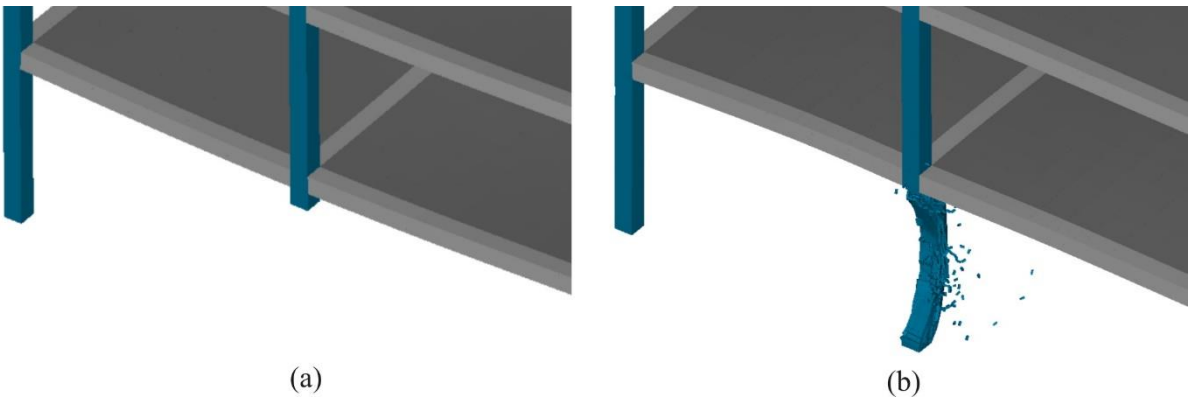

Figure 2. Initial damage regime for progressive collapse assessment: (a) sudden column removal, and (b) direct blast loading with 50 kg of C-4 explosive at a 1-meter standoff distance.

Based on the results, structural performance under blast scenarios is closely tied to the characteristics of the triggering event, which are functions of standoff distance and explosive charge weight. The removal policy does not always capture the actual initial damage regime, and blast-induced damage can differ significantly in both magnitude and nature compared to dynamic column removal. Figure 2 (a) and (b) present the cases for dynamic column removal and blast analysis, respectively, based on preliminary simulations. These findings are crucial for delineating the valid application range of code-based alternate load path analyses and emphasize key considerations for the performance of blast-loaded reinforced concrete moment-resisting frames.

Keywords: Blast, Progressive collapse, Extreme loading.

References

[1] Kiakojouri, F., De Biagi, V., Chiaia, B., & Sheidaii, M. R. (2020). Progressive collapse of framed building structures: Current knowledge and future prospects. *Engineering Structures*, *206*, 110061.

[2] Kiakojouri, F., Sheidaii, M. R., De Biagi, V., & Chiaia, B. (2021). Progressive collapse of structures: A discussion on annotated nomenclature. *Structures*, *29*, 1417-1423.

[3] Kiakojouri, F., De Biagi, V., Marchelli, M., & Chiaia, B. (2024). A conceptual note on the definition of initial failure in progressive collapse scenarios. *Structures*, *60*, 105921.

Experimental study on the anisotropic response of additively-manufactured polymeric lattices subjected to compression in different directions

Z.P. Sun[1*], Y.Y. Ding[1], and V.P.W. Shim[1,2]

[1]*Key Laboratory of Impact and Safety Engineering (MOE), Ningbo University, Ningbo, Zhejiang 315211, China*

[2]*Impact Mechanics Laboratory, Department of Mechanical Engineering, National University of Singapore, 9 Engineering Drive 1, Singapore 117575*

Lightweight lattice structures have been extensively studied, with the objective of enhancing their energy absorption performance. Consequently, a wide variety of different constituent cell geometries have been designed to yield high and stable stress plateaus during crushing. Much effort has been directed at fulfilling cubic symmetry of cell architecture, i.e., identical geometry when viewed from three orthogonal directions, to approximate quasi-isotropic compressive responses. Compared to other cellular materials that focus on enhancement of properties along a single direction, such as honeycombs, lattices with cubic symmetry are envisaged to provide better omnidirectional performance in protective applications, whereby the shielded object may sustain impact from any or multiple directions [1].

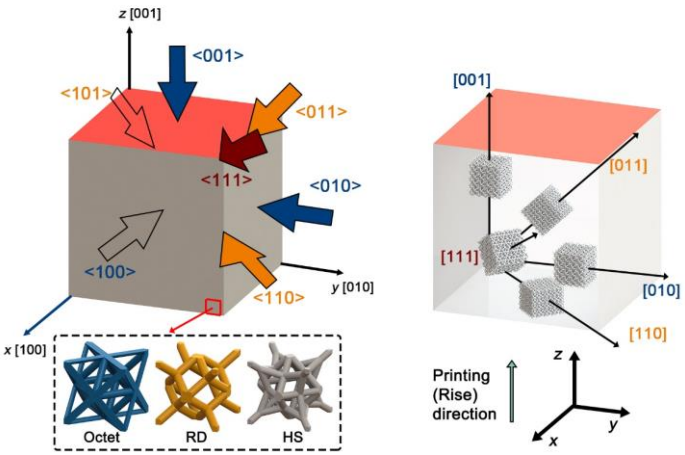

Fig. 1 Schematic diagram of lattices with different constituent cells, subjected to compression from directions other than along orthogonal axes of symmetry;

configurations of cubic lattice test specimens subjected to compression along various directions.

Both the lattice cell strut material properties and cell geometry govern the compressive responses of lattices [2]; hence, an understanding of the combined effects of these two factors is crucial. Firstly, orthogonal symmetry in the constituent cubic cell geometry does not ensure similar compressive responses of lattices loaded in directions not aligned with the axes of symmetry. Moreover, although advancements in additive manufacturing have enabled fabrication of lattices comprising sophisticated cell architectures, the layer-wise material deposition process involved results in non-uniform cell strut material properties. Thus, the compressive responses along the three orthogonal axes of symmetry are not identical, because the material properties of each cell strut depend on the angle to the direction of printing. Hence, attaining consistent omnidirectional crushing responses to achieve direction-independent energy absorption characteristics is challenging for lattices comprising cells with only cubic geometrical symmetry. Most previous studies have focused on the compressive response of lattices along a single axis of symmetry, i.e., the printing direction [3]; hence, it is instructive to gain an insight into the degree of anisotropy in response, for compression in different directions.

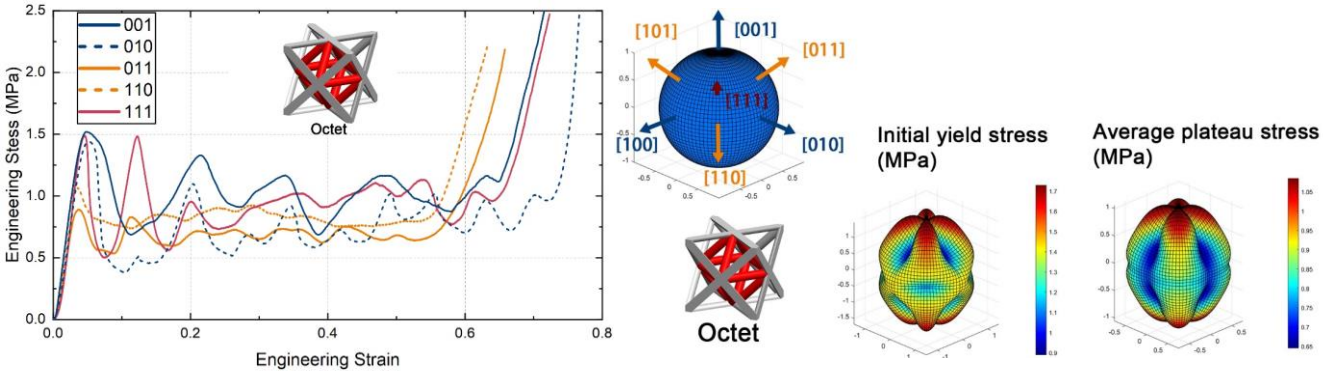

Fig. 2 Example of different stress-strain responses for an Octet lattice compressed in various directions; three-dimensional envelopes illustrating the degree of anisotropy in the initial yield stress and average plateau stress.

This study examines the classic truss-like Octet- and Rhombic Dodecahedron-based lattices, together with their hybrid descendant HS lattice, additively-manufactured using polylactic acid. Lattice samples with prescribed configurations were fabricated to facilitate quasi-static and dynamic uniaxial compression along orthogonal, face

diagonal and body diagonal directions. Dissimilar stress-strain responses, deformation patterns and energy absorption characteristics were observed, indicating different degrees of anisotropy associated with cell geometry. Furthermore, a comparison of the compressive responses along different directions which appear identical geometrically, i.e., [110] and [011] directions, highlights the influence of angle-dependent cell strut material properties in causing anisotropy. A reduced degree of anisotropy in the elastic and plastic responses of the novel HS lattice proposed, demonstrates its advantage in yielding more consistent and less direction-dependent behavior, in addition to a high energy absorption capacity and efficiency compared to its more conventional parent cell architectures.

Keywords: Lattice, compression, energy absorption, anisotropy, large deformation.

[1] Guo, X., Wang, E., Yang, H., & Zhai, W. (2024). Mechanical characterization and constitutive modeling of additively-manufactured polymeric materials and lattice structures. Journal of the Mechanics and Physics of Solids, 189. doi:10.1016/j.jmps.2024.105711

[2] Alkhatib, S. E., Xu, S., Lu, G., Karrech, A., & Sercombe, T. B. (2024). Rate-dependent behaviour of additively manufactured topology optimised lattice structures. Thin-Walled Structures, 198. doi:10.1016/j.tws.2024.111710

[3] Xiao, L., Li, S., Song, W., Xu, X., & Gao, S. (2020). Process-induced geometric defect sensitivity of Ti–6Al–4V lattice structures with different mesoscopic topologies fabricated by electron beam melting. Materials Science and Engineering: A, 778. doi:10.1016/j.msea.2020.139092

Characterization of a Modified Multi-material Auxetic Re-entrant Honeycomb for Protective Applications

Alexander Engel [1], Oraib Al-Ketan [2] and Anne Jung [1]

[1]*Protective Systems, Helmut Schmidt University / University of the Federal Armed Forces Hamburg, Hamburg, Germany.*

[2]*Core Technology Platforms, New York University Abu Dhabi, Abu Dhabi, United Arab Emirates.*

Auxetic structures are a class of mechanical metamaterials, characterized by their negative Poisson's ratio. This peculiar characteristic is a direct consequence of the structural design rather than the material it is composed of. Additionally, several other interesting properties, such as a low density, increased indentation resistance and high mass specific energy absorption capacity enable are shared upon auxetic structures, leading to diverse applications, including lightweight construction, ballistic protectors and shock absorbers upon many more. To achieve the desired characteristics and ensure structural integrity, an auxetic re-entrant structure has previously been optimized to maximize the mass specific energy absorption capacity for usage in lightweight construction by Bronder et al. [1]. This study, however, restricts itself to single material to compose the chosen structure, which limits the ability to exhibit auxetic deformation and show other beneficial effects due to vertical struts buckling. It has been shown that the use of multiple materials in the same structure can lead to severe improvements of the mechanical behavior for similar re-entrant honeycomb structures [2]. Nevertheless, this approach has yet to be investigated for a modified and optimized version of the re-entrant honeycomb. Hence, this contribution explores the possibility of using two different polymers, additively manufactured into the same 3D modified auxetic re-entrant structure, as shown schematically for a single unit cell in Figure 1. This leads to significant improvements of not only the auxetic effect itself, but also other performance related parameters by precisely alternating the deformation behavior. Figure 2 shows the comparison of the Poisson's ratios of the multi-material structure compared to each individual phase. The investigations go beyond quasi-static testing into the realm of low-velocity dynamic impact testing by utilizing a drop tower to cover a broader range of dynamic applications, with notable improvements being observed for all types of loading.

Keywords: Auxetic structures, re-entrant honeycomb, multi-material, low-velocity impact.

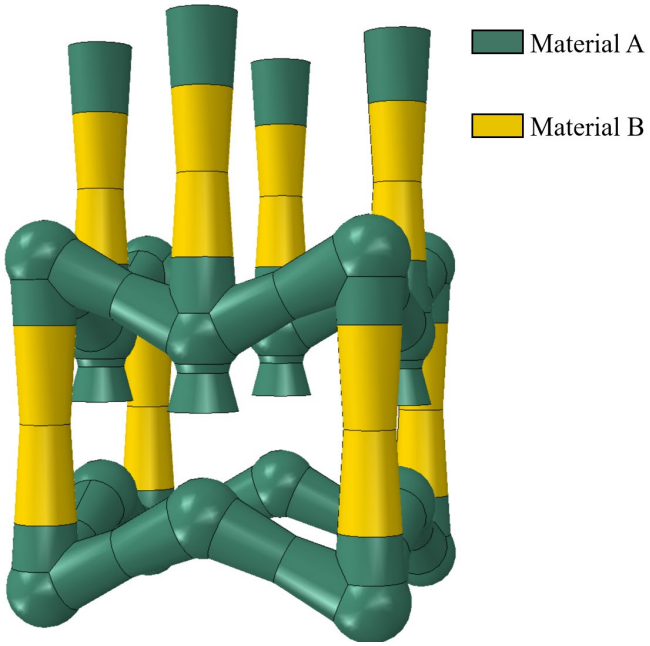

Figure 1: Schematic unit cell of a 3D modified auxetic re-entrant honeycomb utilizing a multi-material approach with two different materials.

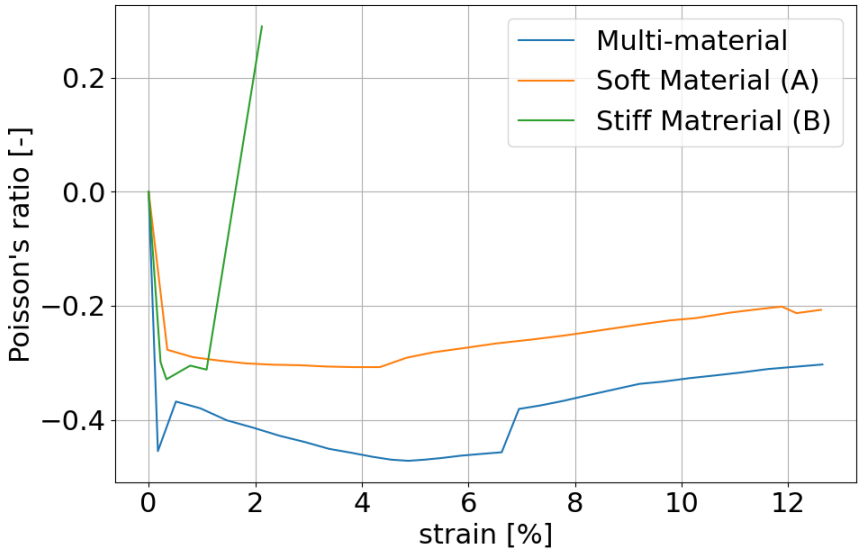

Figure 2: Poisson's ratios of the multi-material and each single material re-entrant structure.

[1] Bronder, S., Herter, F., Bähre, D., & Jung, A. (2022). Optimized design for modified auxetic structures based on a neural network approach. Materials Today Communications, 32, 103931, DOI: 10.1016/j.mtcomm.2022.103931.

[2] Chen, D., & Zheng, X. (2018). Multi-material additive manufacturing of metamaterials with giant, tailorable negative Poisson's ratios. Scientific reports, 8(1), 1-8, DOI: 10.1038/s41598-018-26980-7.

Investigating the effects of delaying the removal of frangible elements in CFD blast simulations.

Author 1 Gabriel Martin[1], Author 2 Laura Cannon [2], Author 3 Simone Vople[3]

[1]*WSP UK, London, United Kingdom*

[2]*WSP UK, London, United Kingdom*

[3]*WSP UK, London, United Kingdom*

"Frangible elements" play a critical role in CFD Blast simulations. These elements capture how design components such as glass, cladding or concrete walls are destroyed by blast events. Using such elements in a blast simulation has a series of advantages, such as better prediction on how a blast wave will travel through a damaged structural component, enabling the engineer to more accurately predict blast loading propagation.

In CFD blast simulations, frangible elements are typically modelled by defining Pressure-Impulse (PI) curves, which are representing pre-determined damage or critical failure conditions. Typically, simulations assume that failure occurs immediately when the thresholds outlined by the PI-curves are exceeded. However, in real-world conditions, structural failure does not occur instantaneously.

A Single Degree of Freedom (SDOF) analysis can be used to determine structural failure, such failure typically occurs when a structural element reaches a certain threshold, such as peak rotation or ductility ratio. Therefore, if the SDOF analysis is used to generate a PI-curve, it can also be used to derive a 'delay time' to be inputted into a CFD model. SDOF analysis can be conducted using software such as WINGARD PE, SBEDS or hand calculations from documentation such as UFC 3-340-02 or ASCE 59-22.

This study investigates the effects of introducing a delay in the removal of frangible elements within CFD simulations, using Viper::Blast. By integrating a delay between the time the PI-curves threshold is reached, and the actual removal of the elements from the analysis, the dynamic behavior of shockwave reflections and blast loading can be more accurately captured. SDOF analysis is used to determine the peak rotation capacity and the failure time of frangible elements. The failure time is then incorporated into the Viper::Blast CFD model to simulate delayed removal.

The delayed removal of frangible elements leads to additional shockwave reflections off surfaces prior to failure, influencing the propagation of the blast wave within the structure. This delay reduces shockwave loading downstream of the frangible elements, while simultaneously increasing the blast load reflected back into other critical structural components. A case study is presented to demonstrate these effects. The study compares models with and without delayed failure of frangible elements, summarizing the key differences in blast response. The case study uses PI-charts generated from WINGARD PE for a Polycarbonate panel, and an internal 30kg TNT blast event.

The findings of this study suggest that incorporating a delay in element failure alters the propagation and attenuation of shockwaves within the structure, affecting both the timing and magnitude of the blast load on critical components. The 2 figures show an example model, with Pressure-Time loading plotted for two key points, internal and external to the structure. The results show a substantial reduction in blast loading onto the external wall, and a minor increase in blast loading onto the internal wall when a failure-delay time is imposed on the frangible elements.

The study provides insights into the impact of delayed failure on protective structures and underscores the importance of accounting for non-instantaneous failure in CFD blast simulations. Further discussion on the methodology, results and conclusions of the study will be presented.

Keywords: Blast simulation and modelling, Response of structural elements to explosion loads, Computational Fluid Dynamics simulation, Frangible elements, PI-charts

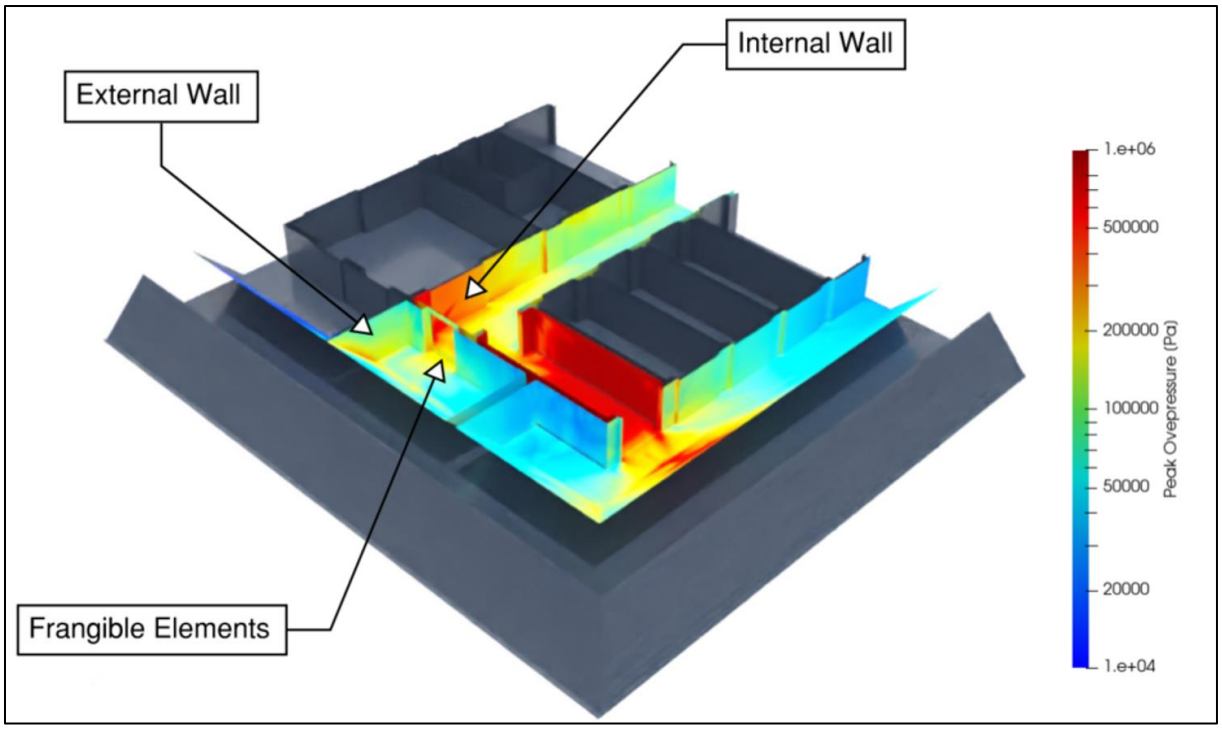

Figure 1 CFD Peak Overpressure Render

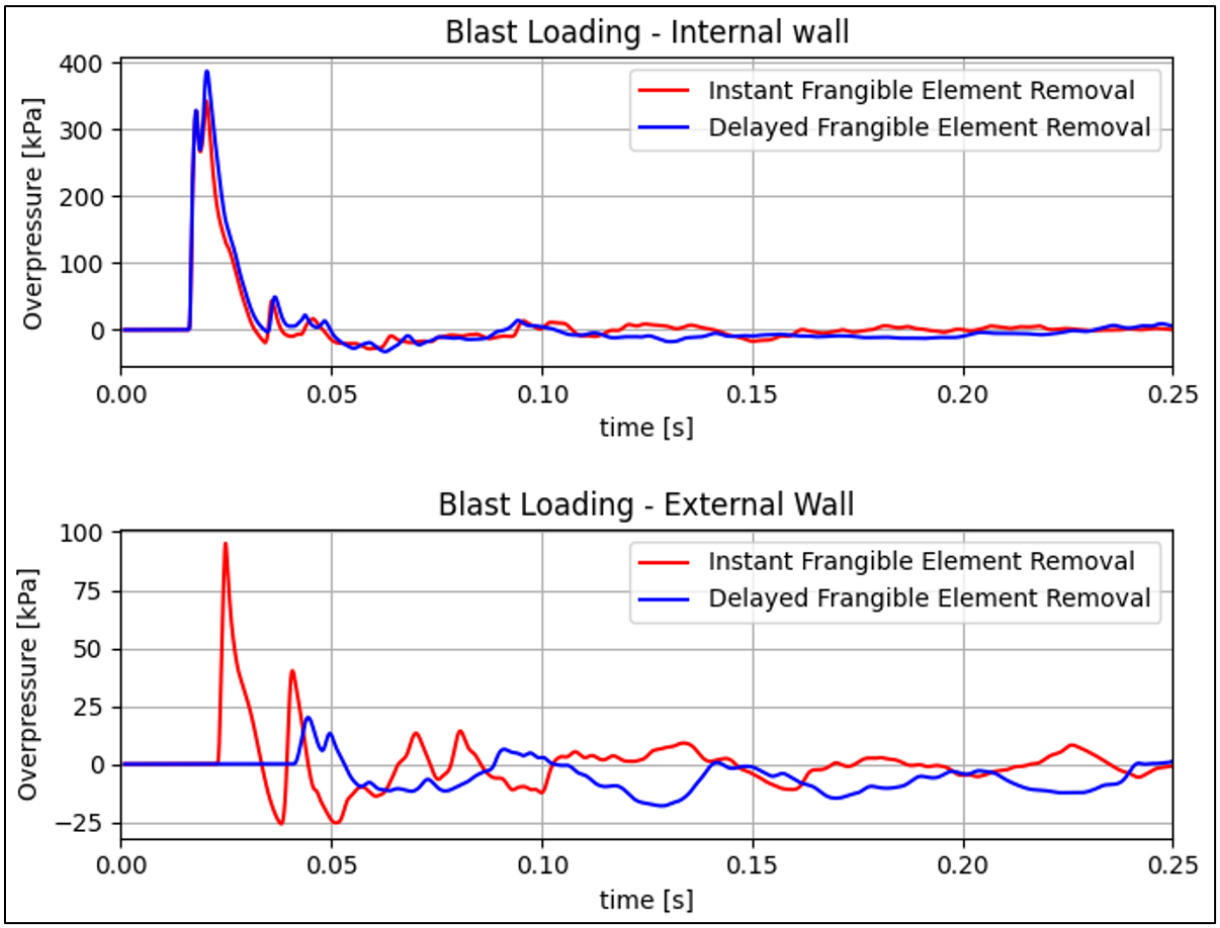

Figure 2 Blast Loading Comparison

Multiscale modelling of the structural response of plain-woven composites

Ziwen Xu[1], Yanhong Chen[1], Zhongwei Guan[2], Wesley Cantwell[3]

[1]*Harbin Institute of Technology, Harbin, People's Republic of China*

[2]*Technology Innovation Institute, Abu Dhabi, United Arab of Emirates*

[3]*Khalifa University, Abu Dhabi, United Arab of Emirates*

Composites have drawn significant attention in various modern industries due to their exceptional mechanical properties. However, owing to their inherently inhomogeneous and anisotropic nature, composites often exhibit scaling effects, where the mechanical performance may vary with geometric size. Therefore, obtaining a clear understanding of the scaling effects of composites is crucial for achieving the successful design of composite structures. Compared to laminated counterparts, woven composites have a superior resistance to delamination and are frequently used for impact applications. This research investigated the scaling effects of a plain woven composite under dynamic loading scenarios based on a combined experimental and numerical approach. On the experimental part, both low-velocity tests (on a drop-weight tower) and high-velocity impact tests (on a single-stage gas gun) were conducted to examine and quantify the relationships between a few response parameters (such as the load-displacement response, crack length, and energy absorption) and the primary input parameter, i.e. the characteristic length). It was found that, at the same impact velocity, the peak impact load of the composite specimens was inversely correlated with the characteristic length, while the energy absorption and crack length were positively correlated with the specimen size. Apart from the experimental study, a multiscale model was developed to simulate the experimental tests and thus provide information which is difficult to acquire, e.g. the velocity of crack propagation. The multiscale model includes an analytically parameterized unit cell (UC) proposed to homogenize woven composites from the mesoscale to the macroscale (Fig. 1). In the proposed UC model, the Hashin failure criteria [1] was generalized to model the failure of the yarns, while the Goldberg model [2] was employed to describe the nonlinearity and rate dependence of the matrix phase. The proposed multiscale model was implemented into the commercial finite element (FE) software ABAQUS by developing a user-defined material

subroutine VUMAT. FE simulations were conducted following the validation of the proposed model (Fig. 2), and the results indicate that the larger specimens tend to have a higher crack propagation speed during the impact. It is worth noting that the numerical work not only addressed the challenge of experimentally monitoring the damage evolution of the specimens but also provided a meaningful explanation of the observed scaling effects of the composite. The findings of the present research offer valuable insights for designing woven composite structures intended for load-bearing applications.

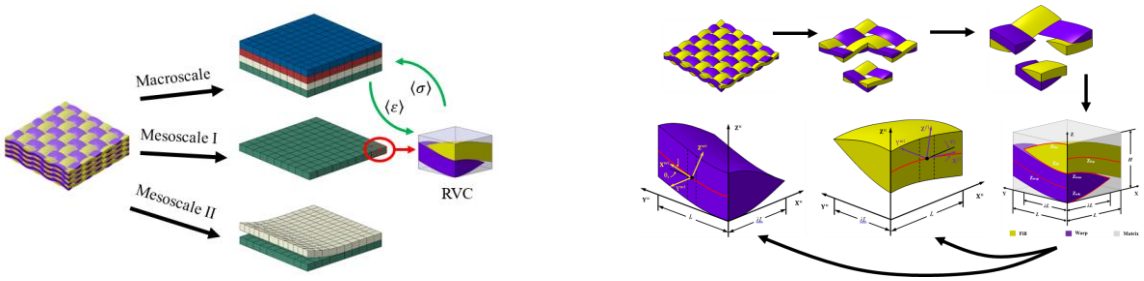

(a) Overall modelling strategy (b) Parameterised modelling of unit cell

Figure 1: Multiscale modelling strategy based on a parameterised unit cell

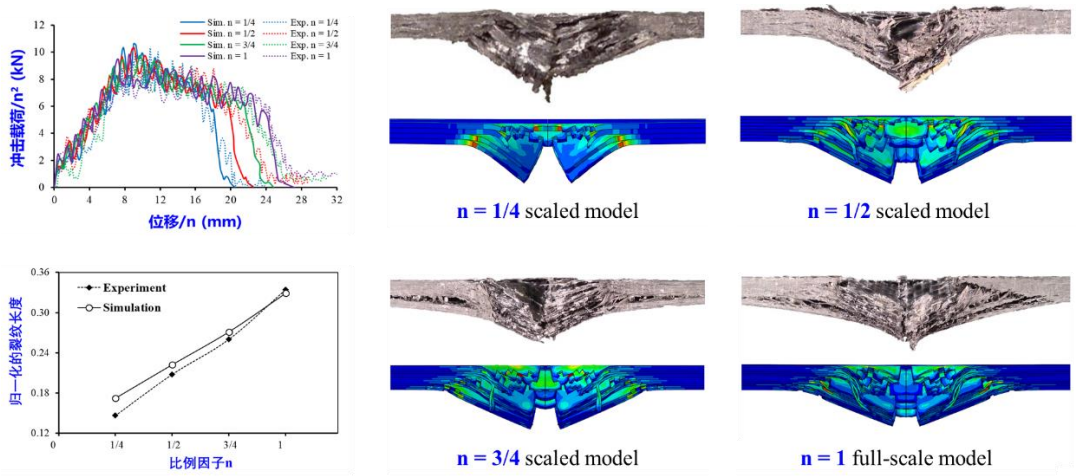

Figure 2: Comparison between the predicted outcome against experimental results

Keywords: Woven Composites, Scaling Effects, Impact, Multiscale Modelling

[1] Hashin, Z. (1980). Failure criteria for unidirectional fiber composites. Journal of Applied Mechanics, 47, 329-334.

[2] Goldberg, R. K., Roberts, G. D. (2004). Analytical studies of the high strain rate tensile response of a polymer matrix composite. Journal of Advanced Materials, 36, 14-24.

Equivalency method for evaluating the high-velocity impact performance of composite panels

Chunlin Du[1,2,3], Chao Zhang*[1,2,3]

[1]*School of Civil Aviation, Northwestern Polytechnical University, Xi'an 710072, China*

[2]*Key Laboratory on the Impact Protection and Safety Assessment of Civil Aviation Vehicle, Taicang, Jiangsu 215400, China*

[3]*Joint International Research Laboratory of Impact Dynamics and its Engineering Applications, Xi'an, Shaanxi, 710072, China*

Abstract: Advanced composites, such as aramid and carbon fiber-reinforced polymers (AFRP, CFRP), are critical for impact protection in aerospace structures due to their high specific strength and modulus. However, the variability in material properties and impact responses across different composites and between composites and metals poses challenges in rapidly evaluating their equivalency under diverse impact conditions. This study addresses these challenges by developing a unified method for equivalency assessment, focusing on composite-composite and composite-metal comparisons. For composite-composite equivalency, impact tests, and validated numerical simulations were employed to analyze the ballistic response of AFRP and CFRP laminates. A predictive isoenergetic model based on ballistic limits and projectile residual energy was established to quantify the impact performance equivalency of composite laminates across varying thicknesses and velocities. A ballistic-limit formula for subcritical penetration velocity conditions complements the model. Extending this framework to composite-metal equivalency, a novel method was developed to correlate the energy absorption characteristics of metallic (Al2024, Ti64) and CFRP panels. By integrating experimental data and validated numerical models for heterogeneous materials, the method derives equivalent thicknesses for metal panels across a broad velocity range. Dimensionless parameters—area density ratio Π_{AD} and velocity ratio Π_{V}—were introduced to link normalized thickness and velocity. Findings reveal that the Ti64 panel exhibits superior impact resistance to Al2024, while CFRP woven laminates outperform both metals in energy absorption when $\Pi_{AD} > 1$. The proposed equivalency models, validated through experimental and numerical results, provide a rapid method for evaluating impact resistance and structural protection.

Keywords: composites panels, energy-equivalency method, ballistic limit, high-velocity impact.

1. Introduction

Laminated composites, known for high strength, hardness, and low density, are ideal for protective structures in aerospace and ground transport, enduring impacts at various velocities [1]. Traditional tests based on samples fail to capture complex structural-level impact resistance. Increasing thickness leads to localized impact properties due to higher energy dissipation [2]. Composite thickness significantly influences ballistic limit and energy absorption, crucial for impact resistance [3][5]. Carbon/epoxy composites excel in high-velocity impacts compared to steel [6]. A non-linear relationship between ballistic limit and panel thickness exists [7]-[8], emphasizing the need for impact-resistant composites. Predicting laminate panel ballistic limits is essential for defining perforation conditions. Figucia found aramid fiber fabric's energy absorption proportional to surface density [9]. The effectiveness of FRP in reducing impact loads is still being studied, with Impact resistance material selection critical. Few studies have analyzed impact behavior and energy absorption equivalence, especially for anisotropic composites. This paper introduces a thickness prediction method based on ballistic limit and energy similarity, validating impact behavior and energy absorption equivalence for composite-composite or composite-metal structures.

2. Methodology

The Lambert-Jonas approximation was used for terminal ballistic impact. This reveals an L–J correlation between impact velocity and both residual and ballistic limit velocities [10]:

$$V_{\mathrm{R}} = a\left(V_{\mathrm{I}}^{p} - V_{\mathrm{bl}}^{p}\right)^{1/p}, \qquad V_{\mathrm{I}} > V_{\mathrm{bl}} \tag{1}$$

where p and a represent the empirical constant chosen to best fit the data when employing the least squares method and where V_{I} and V_{R} are the initial velocity and residual velocity of the projectile impacting the target panels, respectively. The ballistic limit velocity, denoted as V_{bl}, is defined as the impact velocity required for the impactor to exit the target with a zero velocity.

$$E_{\mathrm{R}} = \frac{1}{2} m_{\mathrm{p}} a^{2} \left(V_{\mathrm{I}}^{p} - V_{\mathrm{bl}}^{p}\right)^{2/p} \propto V_{\mathrm{bl}}^{2} \tag{2}$$

where m_{p} is the mass of the projectile and the residual energy of the projectile E_{R} exhibits a linear relationship with the ballistic limit velocity V_{bl} of the target panel. The model based on impact energy criteria was applied to estimate the residual velocity of the projectile, the absorbed energy by the target, and the ballistic limit. The residual energy equivalent is obtained using the following formula:

$$E_{R\_AFRP} = E_{R\_CFRP} \tag{3}$$

where E_{R_AFRP} and E_{R_CFRP} are the residual energies of the AFRP and CFRP panels, respectively.

3. Results

The ballistic limit formula establishes the relationship between target panel thickness h and ballistic limit in Fig. 1. As thickness increases, the ballistic limit difference ($\triangle V_{bl}$) between the two types of composite materials also increases. However, the growth rate gradually decreases, indicating that as thickness becomes larger, the improvement in penetration resistance slows down. The model predictions of the ballistic limit correlate well with the conclusions of the nonlinear relationships in the Ref.[11]. In Fig. 1, the region above the blue solid curve predicted by the analytical model (red area) indicates that AFRP exhibits superior penetration resistance, while the region below the blue curve (blue area) signifies that CFRP demonstrates better penetration resistance. The trend of the curve predicted by the ballistic limit equivalency model aligns closely with the discrete data points (red dots) calculated by the simulation model, showcasing well correlation.

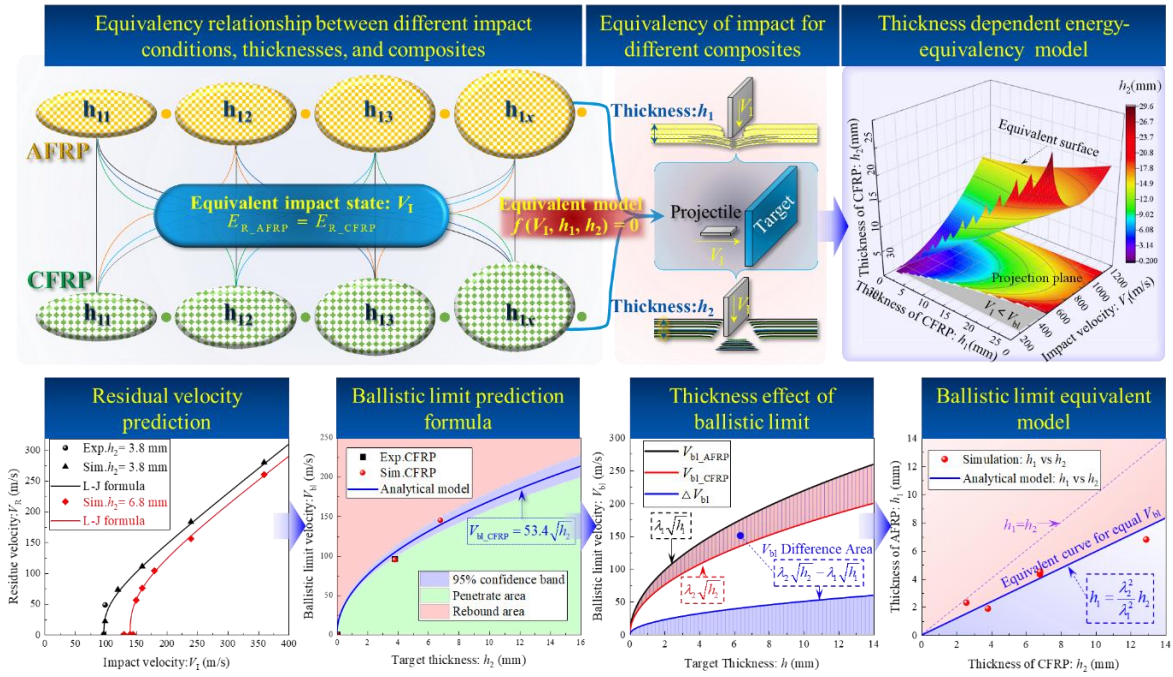

Fig. 1. Equivalency methods for the impact of different composites

4. Conclusions

This investigation presented a novel equivalent method to analyze the high-velocity impact behavior equivalence of different composites at varying plate thicknesses. Through systematic integration of experimental measurements and numerical simulations with the ballistic limit

formula, we established precise quantitative relationships between panel thickness and ballistic limit velocity for both AFRP and CFRP. Key findings revealed that while ballistic limit velocity increases with panel thickness, this relationship exhibits a diminishing growth trend characterized by asymptotic convergence. The energy absorption coefficient (η) demonstrated an exponential decay pattern relative to impact velocity, with its dissipation behavior governed by both intrinsic material properties and ballistic limit parameters. The energy-equivalent method shows that AFRP has better energy absorption and penetration resistance than CFRP after the projectile penetrates the same thickness of the target plate. The proposed equivalence paradigm further elucidated fundamental relationships between equivalent thickness ratios and impact velocities through normalized area density and velocity parameters. Findings reveal that the Ti64 panel exhibits superior impact resistance to Al2024, while CFRP woven laminates outperform both metals in energy absorption when $\Pi_{AD} > 1$.

Reference

[1] Sanchez-Saez S, Barbero E, Zaera R, et al. Compression after impact of thin composite laminates. Compos Sci Technol 2005;65(13):1911–9.

[2] Reis PNB, Sousa P, Ferreira LM, et al. Multi-impact response of semicylindrical composite laminated shells with different thicknesses. Compos Struct 2023;310:116771-.

[3] Wang, W; Chouw, N; Jayaraman, K. Effect of thickness on the impact resistance of flax fibre-reinforced polymer. Journal of Reinforced Plastics and Composites 2016;0(0):1-13.

[4] Kayaaslan M, Coskun T, Unlu UM, et al. Effects of thickness, fiber orientation, and fabric textile on the low-velocity impact performances of thermoset and thermoplastic composites. Journal of Thermoplastic Composite Materials 2023.

[5] Li H, Zhang X. An equivalent target plate damage probability calculation mathematics model and damage evaluation method. Def Technol 2024;41:82-103.

[6] Gao Y, Shi L, Lu T, et al. Ballistic and delamination mechanism of CFRP/aluminum laminates subjected to high-velocity impact. Eng Fract Mech 2024;295:109797,

[7] Gellert EP, Cimpoeru SJ, Woodward RL. A study of the effect of target thickness on the ballistic perforation of glass-fibre-reinforced plastic composites. Int J Impact Eng, 2000;24(5):445–56.

[8] Wen HM. Penetration and perforation of thick FRP laminates. Compos Sci Technol 2001;61(8):1163–72.

[9] Figucia F. Energy Absorption of Kevlar (trade name) Fabrics under Ballistic Impact. Energy Absorption of Kevlar Fabrics Under Ballistic Impact, 1980.

[10] Ben-Dor G, Dubinsky A, Elperin T. A class of models implying the Lambent–Jonas relation. International Journal of Solids & Structures 2001;38(40):7113–7119.

[11] Shim VPW, Tan VBC, Tay TE. Modelling deformation and damage characteristics of woven fabric under small projectile impact. Int J Impact Eng 1995;16(4):585–605.

DESIGN AND DEVELOPMENT OF AN INTERCHANGEABLE CLAMP FOR TENSILE TESTING OF UHMWPE COMPOSITES WITH 3D DIC

Alia Ruzanna Aziz, Naresh Kakur, Henrique Ramos, Rafael Santiago

Advanced Materials Research Centre, Technology Innovation Institute, Abu Dhabi, United Arab Emirates, alia.aziz@tii.ae (corresponding author)

ABSTRACT

Ultra-high molecular weight polyethylene (UHMWPE) laminate composites are widely used in impact-resistant structures due to their high specific strength and exceptional energy absorption capabilities. However, previous studies encountered challenges in characterizing the tensile properties of UHMWPE composites, including specimen slippage, stress concentrations, and failures outside the gauge length. This work presents the design and development of an interchangeable clamp for the tensile testing of UHMWPE composites. This clamp guarantees secure gripping and uniform load transfer across the UHMWPE specimens. The developed clamp can be used interchangeably in quasi-static and high-strain-rate devices, facilitating the evaluation of a broad range of strain rates. The tensile properties of two UHMWPE composites were subsequently assessed using this clamping system, with strain measured through three-dimensional digital image correlation (3D-DIC). The effectiveness of a 3D-DIC technique for measuring strain in the UHMWPE composite is demonstrated. The tests reveal that the designed clamp enables reliable measurements, with tensile strength values reaching approximately 1300 MPa. The measured tensile properties are useful for the input data of numerical simulations, providing valuable insights for developing highly efficient protective structures.

Keywords: UHMWPE, tensile properties, quasi-static, digital image correlation.

Ultra-high performance curved concrete slabs against blast loading

Manish Kumar[1], Alok Dua[2] and Shreya Korde[1]

[1]*Department of Civil Engineering, Indian Institute of Technology Bombay, Mumbai, India*

[2]*Royal Military College, Canada*

Protective military bunkers are designed to sustain small arms, mortar, and light and medium artillery fire. The protection provided by bunkers made of conventional materials are inadequate due to the advancement in weaponry systems over last few decades. This research focussed on development of curved roof panels of modular bunkers using ultra-high performance fibre-reinforced concrete (UHPFRC) and normal strength concrete (NSC). The UHPFRC has been experimentally proven to be much more robust, durable and ductile than NSC. A detailed experimental study was conducted on 22 UHPFRC & NSC flat and curved slabs (without steel rebars) subjected to airblast to determine their blast resistance capability and fragments mitigation. The experimental investigations were conducted on 1200 mm × 750 mm × 75 mm and 1200 mm × 750 mm × 125 mm slabs made of NSC and UHPFRC. A height-to-width ratio of 0.25 was provided for the curved panels. This experimental work aimed to determine the efficacy of flat and curved slabs in resisting blast loads and subsequently arrive at the optimum slab depth which can sustain blast load of given intensity. Additionally, one 75 mm UHPFRC panel was provided with CFRP confinement on the distal face to investigate the efficacy in mitigating the effects of blast loading. The experimental setup for the blast tests is shown in Figure 1 and the failure mode of the curved under blast loading is shown in Figure 2. The UHPFRC flat slabs could sustain blast loads up to scale distances one-third and one half of the NSC flat slabs for 75 mm and 125 mm thicknesses, respectively, thereby confirming the enhanced performance due to UHPFRC material. The curved NSC slab could withstand blast load up to a smaller scaled distance (~20%) compared to flat NSC slab for 75 mm and 125 mm thickness. Similar performance enhancement was observed for 75 mm UHPFRC curved slab over the flat slab as well. However, the 125 mm curved slab could sustain the blast load up to a scale distance that was half of the corresponding flat slab. These results indicate that the maximum benefit of curved shape is realized for a minimum threshold thickness of the slab and higher compressive strength of concrete. Hence, UHPFRC is particularly suited for curved slab applications and can effectively be utilized as roof panels in modular bunkers against blast loading.

Figure 1: Curved 125 mm thick UHPFRC slab under blast load

Figure 2: Failure after the blast load

Keywords: UHPFRC, Concreted, Curve, Blast, Bunkers, Modular

Study of a protective structure made of soil-cement using weight dropping device for an impact resistance

Toshiyuki Horiguchi[1], Ichiro Kuroda[2]

[1]*Dept. Civil Engineering, National Defense Academy, Yokosuka, Japan*

[2]*Dept. Civil Engineering, National Defense Academy, Yokosuka, Japan*

In recent years, Japan has faced numerous disasters caused by abnormal weather patterns, including localized heavy rainfalls and typhoons that bring prolonged rainfall over wide areas. Boulder debris flows, which generate significant impact forces, have caused substantial damage. To mitigate such damage, erosion control dams that means sediment and/or soil, granular control structures have been constructed as countermeasures. The soil cement composed of generated soil has some advantages of reducing the amount of sediment transported, reducing costs by using local sediment, and the construction method considers zero emission in the environment [1]. Figure 1 shows erosion control dams as protective structures using soil-cement. The strength of soil cement is typically evaluated based on compressive strength obtained from the uniaxial compression test. However, evaluations aren't conducted about dynamic load evaluation as boulder debris flow. Furthermore, in terms of absorbing the impact load of debris flows, soil-cement, which has lower rigidity compared to concrete, is expected to demonstrate a cushioning effect in Sabo dams like protective structure [2]. However, there is a lack of fundamental experiments and dynamic test data from this perspective, and many aspects remain unclear at present.

The objective of this study conducts an impact loading experiment against soil cement specimen to examine impact resistance. During the experiment, dent of the specimen was observed after impact. Figure 2 shows post-impact images of specimens A and C, revealing that

Figure 1 Sabo dam using soil-cement

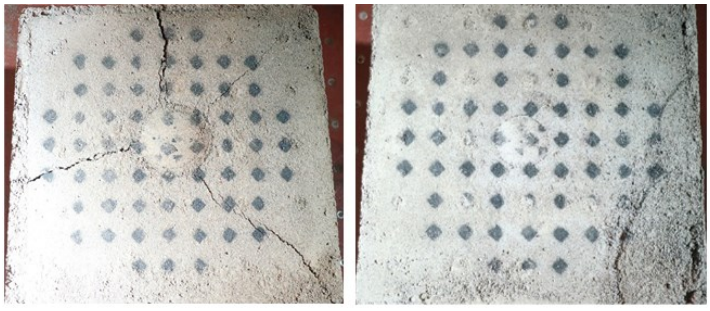

(a) A-specimen (b) C-specimen

Figure 2 Depression sample of loading experiment

specimens with higher compressive strength exhibited less settlement. Additionally, to study the impact resistance possessed by the Sabo soil-cement, the relationship between dropping weight accumulation energy and a collapsed volume and the relationship between dropping weight energy and compressive strength were summarized.

In these results, the larger the compressive strength, the larger the accumulated weight energy. Besides, there is a proportional relationship between the collapsed volume and dropping weight accumulation energy. The relationship between maximum impact load and weight energy increases linearly until it cracks in the specimen. However, when the internal properties of the specimen change, the minimum impact load doesn't increase due to the dissipating energy. In addition, the impact spectrum of the specimen possessed a small compressive strength is found to have the effect of reducing the impact load on the collision surface. Therefore, if the compressive strength of the soil cement is large, the soil-cement has large impact resistance against impact load on the collision surface. On the other hand, if the compressive strength of that is low, soil-cement possesses the effect of reducing the impact force.

Keywords: soil-cement, protective structure, debris flow impact, contact mechanism

[1] SABO & LANDSLIDE CENTER, (2016). Erosion Control Soil Cement Construction Handbook, 2016 Edition, Nissei Ebro Inc.

[2] Joji Sima, Yoshikuni AKIYAMA, Takahisa MIZUYAMA, (2015). Proposed minimum management strength to ensure INSEM hydration reaction, Journal of the Japan Society of Erosion Control Engineering, Vol.68, No.2, pp.14-22, doi.org/10.11475/sabo.68.2_14_22

Blast Resistance and Fragility Analysis of RC Columns with Chloride-induced Corrosion

Yu Liu [1], Hong Hao [1,2] and Yifei Hao [3]

[1]*Earthquake Engineering Research and Test Center, Guangzhou University, Guangzhou, China*

[2]*School of Civil and Mechanical Engineering, Curtin University, Perth, Australia*

[3]*School of Civil and Transportation Engineering, Hebei University of Technology, Tianjin, China*

Chloride-induced corrosion is one of the key factors affecting the lifecycle performance and loading capacity of reinforced concrete (RC) structures. The corrosion degrades the mechanical properties of reinforcement and the bonding ability between reinforcement and concrete, leading to cracking in concrete. When analyzing reinforced concrete structures that may be exposed to explosion hazards, considering the influences of chloride-induced corrosion of reinforcement can provide quantitative insight into the lifecycle performance of structures against blast loads.

This study presents the blast resistance and fragility analysis of RC columns with corrosion damage. Effects of corrosion on the dynamic bond behaviour between steel reinforcement and concrete were investigated. Corrosion damage affects the pull-out failure mode and the dynamic bond strength. Three failure modes were observed in the tests, i.e., pull-out failure without splitting, splitting failure and splitting failure along corrosion cracks. With the increase of strain rate and corrosion level, the failure modes tend to change from ductile failure to brittle failure.

The post-blast damage of corroded RC columns considering dynamic bond-slip between rebar and concrete was quantified. The corrosion effect was modelled by considering the deterioration of rebar diameter and yield strength, bond strength between rebar and concrete, and rust expansion pressure effect. The blast damage mode may change from combined shear and flexural damage to substantial concrete spalling damage with the increment of corrosion degree. Corrosion damage reduces column blast resistance capacity and its influence becomes more pronounced when blast loading is larger.

Parameters of reinforcement and concrete and the blast load uncertainties were considered in the Monte Carlo simulations to estimate the damage probabilities. The fragility curves of three example RC columns with different dimensions and reinforcement ratios corresponding to the 0 to 90 years of uniform and pitting corrosion damage were generated. The fragility of higher damage level is more sensitive to corrosion damage because concrete contributes the most to resisting low blast loads that cause only small damages, but both concrete and reinforcement contribute to resisting large blast load that cause severe damages. Uniform corrosion damage causes more blast loading capacity reduction initially when the corrosion damage intensity is relatively small, but pitting damage leads to more significant column capacity reduction when the damage level is large.

Keywords: RC column, dynamic bond-slip, blast fragility, chloride-induced corrosion.

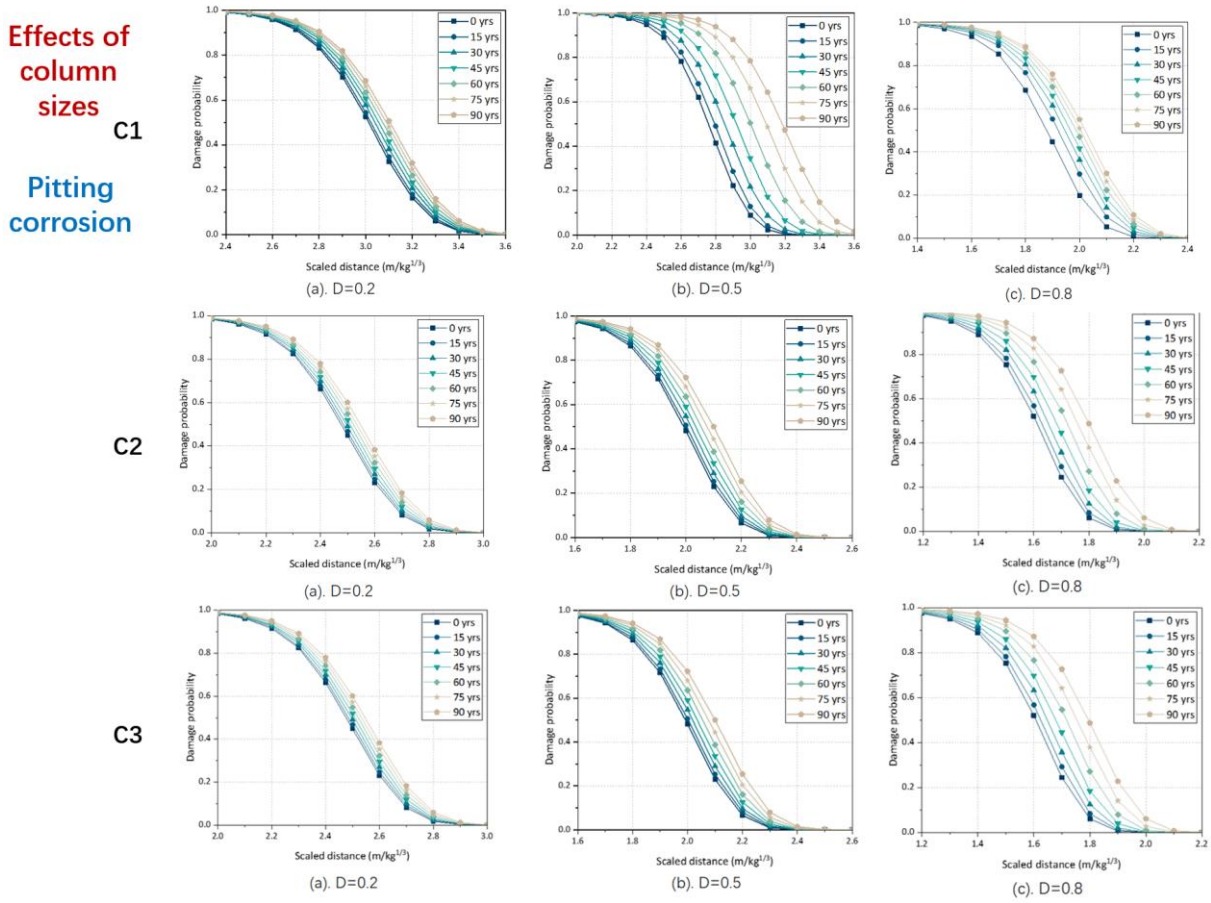

Figure 1. Effect of column sizes on blast fragility curves of the RC columns with pitting corrosion

Figure 2. Dynamic pullout test and failure modes of the RC pullout specimens

Submission ID: 3334

7th International Conference on Protective Structures (ICPS7)
12th – 15th May 2025, Abu Dhabi, UAE

Ballistic Penetration Resistance of Reinforced and Non-Reinforced Concrete Formulations under High-Velocity Gas-Gun Impact

Henrique Ramos[1,2], Felipe Rodrigues de Souza[1,3], Nikolaos Nikos[1], Omar Ba Nabila[1], Rafael Savioli[1], Flavio de Andrade Silva[3], Rafael Santiago[1]

[1]Advanced Materials Research Center, Technology Innovation Institute, Abu Dhabi, United Arab Emirates, henrique.ramos@tii.ae (corresponding author)

[2]Department of Mechatronics and Mechanical Systems Engineering, Group of Solid Mechanics and Structural Impact, University of Sao Paulo, Brazil

[3]Department of Civil and Environmental Engineering, Pontificia Universidade Catolica do Rio de Janeiro (PUC-Rio), Brazil

ABSTRACT

This study investigates the ballistic performance of sixteen concrete formulations subjected to high-velocity impact loading using a 12.7×99 mm armour-piercing projectile fired from a single-stage gas gun at an impact velocity of 850 m/s. The experimental campaign evaluated the depth of penetration (DOP), mass loss, and failure morphology of both reinforced and non-reinforced concretes under the same test conditions. Concrete types included ordinary concrete (OC), steel and basalt fibre-reinforced mixes, ultra-high-performance concrete (UHPC), strain-hardening cementitious composites (SHCC), rubber aggregate concretes (RSC), and cement-modified variants. Visual inspections, high-speed camera sequences, and three-dimensional (3D) scanning images were used to evaluate the impact response of each concrete configuration. Results show that UHPC formulations exhibited the best ballistic resistance, with DOP values reduced by nearly 50% compared to ordinary concrete. Steel fiber-reinforced concretes showed a fiber-dosage-dependent improvement in DoP and material retention, with SF120 emerging as the most balanced solution. In contrast, rubber-modified and SHCC mixes demonstrated high DOP values but effectively limited surface scabbing. These findings highlight the importance of material composition in optimising ballistic performance and guide the selection of concrete systems for infrastructure protection applications.

Keywords: Ballistic, concrete, gas gun, high-velocity impact

Fast Prediction Model for Explosion Loads in Complex Scenarios

Suwen Chen [1,2], Yang Huang [1] and Dingkun Luo [1]

[1]*College of Civil Engineering, Tongji University, Shanghai 200092, China*

[2]*Disaster Reduction in Civil Engineering, Shanghai 200092, China*

Rapid and precise acquisition of overpressure loads in complex explosion scenarios is critical for blast-resistant structural design and post-blast safety assessment. Explosion-induced overpressures are characterized by significant spatial and temporal variations influenced by the propagation of shock waves and the evolution process of detonation products, which pose challenges to achieving an accurate description of the loads. Traditional methods, such as empirical models or numerical simulations, are insufficient for calculating explosion loads with high accuracy and low computational cost, while existing deep learning-based models exhibit limited practicability for predicting overpressure loads from complex explosion scenarios. To address these challenges, this paper presents the recent progress of our research group in the fast prediction models for explosive loads in complex explosion scenarios. Firstly, a deep learning-based framework for reconstructing explosion pressure fields was proposed to achieve high-fidelity explosion pressure distributions and overpressure time histories based on low-resolution numerical simulation results. The network adopted a novel super-resolution strategy, which concatenates high-resolution channels that record flow field boundaries and flow regions with the low-resolution channel to improve the computational performance and training stability of the super-resolution model. Then, a physical model-guided deep learning approach was presented to realize pressure history prediction in fully and partially confined explosion scenarios. Two physical models, the method of images and the simplified Bernoulli method, were utilized as the network input to consider the dynamic pressure fluctuations caused by the propagation process of shock waves and the quasi-static pressure influenced by the afterburning effect. Finally, a deep learning-based model that balances the precision of explosion flow field and pressure histories was proposed to realize rapid and accurate prediction of explosion loads in 3D typical street scenarios. The model utilizes a 3D convolutional neural network (CNN) and integrates both the spatial and temporal information to enhance its prediction accuracy in diverse explosion scenarios. Evaluation results demonstrate that incorporating physical model information is crucial for ensuring robust network performance. The proposed models can not only provide high-credibility pressure fields and pressure time histories but also exhibit

excellent generalization capabilities for explosive scenarios beyond the training dataset, thereby providing reliable and efficient methods for practical applications in explosion analysis.

Keywords: Deel learning; Explosive load; Complex scenario; Fast calculation model.

Derivation of P-I diagram for UHPC protective wall against gaseous explosion based on calibrated K&C model and machine learning

Di Chen [1, 2], Chengqing Wu [1,2], Jun Li [2], Xue Kong [1]

[1] *Institute of Rock and Soil Mechanics, Chinese Academy of Sciences, Wuhan, 430071, China*

[2] *School of Civil and Environmental Engineering, University of Technology Sydney, Sydney, NSW, 2007, Australia*

Gaseous fuels, such as natural gas and hydrogen, are fundamental energy sources in modern society, powering various sectors including industry, residential, and transportation. Despite their benefits, gaseous explosions remain a significant hazard worldwide, frequently leading to severe casualties and extensive economic losses. Unlike high explosives, which are typically associated only with detonation, gaseous explosions can manifest in two forms: detonation and deflagration. Detonation is characterized by a rapid, high-intensity explosion with a sharp pressure peak and short duration, while deflagration features a notably longer duration, a slower pressure rise, a flatter pressure peak, and a greater impulse. These differences in explosion behavior have crucial implications for designing structures that can effectively withstand such hazardous events. In this study, a K&C constitutive model was calibrated for ultra-high performance concrete (UHPC), which has a compressive strength of up to 150 MPa, based on experimental data. This model was then used to simulate the structural behavior of a UHPC cantilever protective wall subjected to explosion loads. The blast loads generated by both detonation and deflagration were simplified for ease of analysis. Specifically, the detonation load was modeled as a right triangle, while the deflagration load was represented as an isosceles triangle. These simplified representations of the explosion loads were applied to the protective wall to assess its structural response under varying conditions. A detailed parametric study was conducted to examine the effects of wall thickness, wall height, and reinforcement (rebar) on the performance of the protective wall under different types of blast loads. Given the substantial amount of data required to explore these variables, an artificial neural network (ANN) was employed to fit the parametric data and generate additional data points. This process enabled the efficient generation of a pressure-impulse (P-I) diagram, which significantly reduced the computational time and effort typically required for such analyses. The findings of this study provide valuable insights into the design of UHPC protective walls, particularly in their capacity to resist both detonation and deflagration-type explosions. The findings from this study offer valuable insights into the design of UHPC protective walls, particularly in their ability to resist both detonation and deflagration-type explosions, ultimately improving safety and resilience against gaseous explosion hazards.

Keywords: UHPC, gas explosion, P-I diagram, ANN.

Submission ID: 3546
(Full Paper)

7th International Conference on Protective Structures (ICPS7)
12th – 15th May 2025, Abu Dhabi, UAE

COMPARISON OF ALE, LBE, AND THE IDEALIZED TRIANGULAR LOADING METHOD FOR EVALUATING AN EDST BLAST LOADING ON A LABORATORY-SCALE RC COLUMN

Walid Ben Kraiem
Structures and Effects of Explosions Department, Royal Military Academy, Brussels, Belgium
(walid.benkraiem@mil.be)
Mohamed Ben Rhouma
Mechanics of Materials and Constructions Department, Vrije Universiteit, Brussels, Belgium
Structures and Effects of Explosions Department, Royal Military Academy, Brussels, Belgium
(mohamed.benrhouma@mil.be)
Bachir Belkassem
Structures and Effects of Explosions Department, Royal Military Academy, Brussels, Belgium
(bachir.belkassem@mil.be)
David Lecompte
Structures and Effects of Explosions Department, Royal Military Academy, Brussels, Belgium
(david.lecompte@mil.be)

ABSTRACT

The collapse of buildings during explosions or other extreme events is often linked to the failure of key structural elements such as columns. As vertical load-bearing members, reinforced concrete (RC) columns are essential for maintaining the stability of structures but are also among the most vulnerable components when exposed to blast loads. This study focuses on the numerical prediction of the dynamic behavior of RC columns subjected to explosive-driven shock tube (EDST) loading. The analysis is based on an experimental campaign using a laboratory-scale RC column specimen with a height of 1500 mm and a circular cross-section of 100 mm, tested under blast loading generated by 30 g C4 charge. To simulate the structural response and optimize computational performance, three finite element techniques are evaluated and compared: Multi-Material Arbitrary Lagrangian-Eulerian (MM-ALE), Load Blast Enhanced (LBE), and the Idealized Triangular Loading (ITL) method. All three models are validated against experimental data. In terms of mid-span out-of-plane displacement, MM-ALE showed the best accuracy with a 2.1% discrepancy, followed by LBE at 8.8%, and ITL at 10.6%. Regarding computation time, MM-ALE required 12 hours, while LBE was three times faster and ITL was six times faster than MM-ALE. The LBE method present a balance between speed and accuracy but relies on precise input values for reflected pressure and impulse, which are typically derived from MM-ALE simulations or analytical expressions. The ITL method, while computationally efficient, tends to overestimate peak displacements due to its simplified and uniform pressure application. Among the three approaches, MM-ALE remains the most accurate.

Keywords: Multi-Material Arbitrary Lagrangian-Eulerian (MM-ALE), Load Blast Enhanced (LBE), Idealized Triangular Loading (ITL), Blast Loading, Explosive Driven Shock Tube.

Investigating Fragmentation Risk in ARMOX 440T Steel plates Under Localized Blast Loading

Haleimah Alabdouli [1,2], Richard Curry[1] and Genevieve Langdon [1]

[1]*School of Mechanical, Aerospace and Civil Engineering, University of Sheffield, Mappin Street, Sheffield S1 3JD, UK*

[2]*Technology Innovation Institute, PO Box: 9639, Masdar city, Abu Dhabi, UAE*

Abstract

Steel is a popular choice for blast protection systems due to its strength and rigidity. However, when subjected to blast loading, steel can be susceptible to fragmentation, which poses a significant hazard. Under localized blast loads, for example, steel may deform, forming a central bulge with a narrow band of thinning that eventually leads to the ejection of a fragment, known as 'capping'. In this work, Armox 440T steel, a high-strength armour steel grade commonly used in protective structures, was experimentally tested under localized blast loads to determine its fracture mechanisms and assess its fragmentation risks.

Keywords: Armox 440T, localized blast loading, capping, fragmentation.

Introduction

Armox 440T is an armour steel grade with a minimum yield strength of 1100 MPa, a minimum hardness of 420 HBW, and a minimum tensile strength of 1250 MPa [1]. This grade is widely used in protective structures due to its exceptional penetration and impact resistance. Its excellent hardness-to-toughness ratio makes it an obvious choice for ballistic protection [1]. This work considers its failure and fragmentation behaviour when subjected to localized blast loads.

Methodology

Disk-shaped charges of PE10 plastic explosive, placed at a 13 mm standoff distance, were used to create localized blast loading, with charge masses ranging from 50 to 60 g. The charge mass and SOD were selected based on research by MacDonald [2], who evaluated rupture thresholds of various high-strength steels using PE4 charges at similar standoffs. The square test plates, having a side length of 400 mm, were clamped to a large frame. Two synchronized Photron high-speed cameras were used to capture stereo images of the back face, enabling post-processing using the Digital Image Correlation (DIC) method to infer transient out-of-plane

displacement, velocity, and strain measurements [3]. A high-speed side-view camera also recorded the cap detachment from the plate's centre during the event. Strawboard plates were positioned behind the rig as a soft capture system for the ejected caps. The side-on camera images were used to estimate the velocity of the cap post-fracture.

Results

Table 1 summarizes the blast load conditions and key results for each test. The equivalent cap diameter is calculated based on cap mass and plate density, while the projected cap diameter is the measured diameter averaged from several measurements. The cap detachment speed, measured with Photron FASTCAM Analysis software, was approximately 390 m/s for a 60 g charge and 356 m/s for a 55 g charge, generating an impulse of 7–9 N·s. This substantial impulse poses a serious injury risk. Observations also indicated inconsistent cap trajectories across tests due to tumbling. High-speed footage showed that, in some cases, the cap petals outward as fractures spread from the initiation site, leading to rotation upon separation. The time required for the cap to fully fracture around its periphery varied between tests.

Table 1: Summary of Test Conditions and Results

Test ID	Charge Mass (g)	Charge Diameter (mm)	Equivalent Cap Diameter (mm)	Projected Cap Diameter (mm)	Hole size (mm)	Cap mass (g)
T01	50	50	30.28	33	34.5	22.6
T02	50	50	27.32	32	32.5	18.4
T03	60	50	30.94	33	43.5	23.6
T04	55	50	29.05	32	33.5	20.8
T05	55	50	28.2	32	34	19.6
T06	55	50	26.42	30	32	17.2

Figure 1 shows the front and back views of selected tested panels and the detached caps from each test. Armox 440T exhibited localized thinning at the fracture initiation site, where cracks progressed circumferentially, leading to complete cap separation, with additional features such as shear lips and radial cracks. Increasing the charge mass to 60 g caused the fractured steel to 'petal' outward. This ejected the cap more violently (at high velocity) and created larger out-of-plane deformation around the fractured region, resulting in a larger permanent hole. The higher charge mass also led to multiple radial cracks, producing tiny flying fragments along with the cap.

Figure 2 displays the shear strain contour obtained using DIC at the capping location just prior to fracture. A white square marks the fracture initiation site. Notably, transient shear strains

diverged in opposite directions on either side of the thinning area, with the fracture initiation site in the liminal region. This highlights the role of shear strains in driving the capping fracture mechanism in Armox 440T, supporting MacDonald's post-test observation that slant shear failure was the primary fracture mode responsible for initial rupture, as confirmed by scanning electron microscopy of the fracture surface [2].

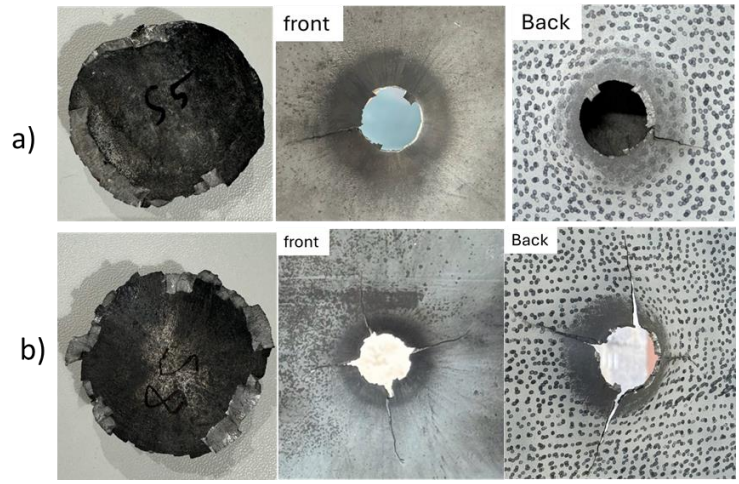

Figure 1: photographs showing the front and back views of Armox 440T plates tested at a 13 mm standoff distance with (a) 50 g and (b) 60 g PE10 cylindrical plastic explosive charges.

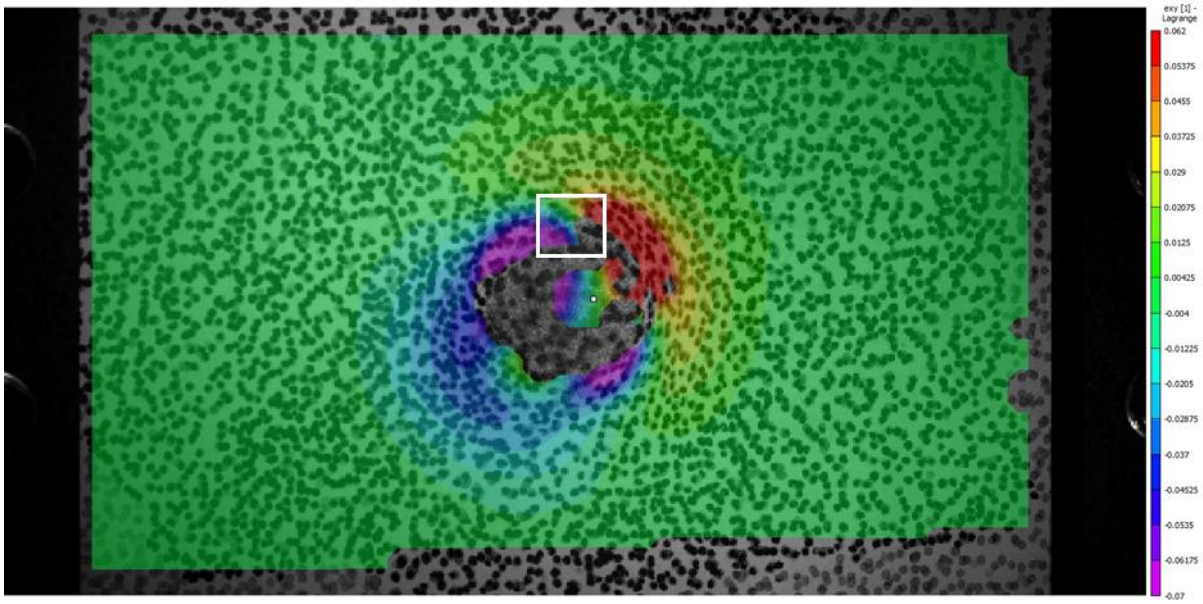

Figure 2: Shear strain contour at the capping location of an Armox 440T plate just before fracture (50 μs post detonation), the fracture initiation site is indicated by the white square.

Conclusion

The results of localized blast tests of ARMOX 440T plates revealed significant fragmentation risks characterized by high detachment speeds (over 300m/s) and unpredictable fragment trajectories. These findings suggest that additional safety measures may be needed in protection designs incorporating ARMOX 440T plates when localized blast loading is a likely threat. The role of shear strain was significant, highlighted in the transient shear distribution on the rear surface of the plate immediately prior to fracture.

References

[1] SSAB (2017), 'Armox® 440t'. Data sheet 173en, 19 April 2017. URL: https://www.ssab.com/en-gb/brands-and-products/armox/product-offer/armox-440t

[2] McDonald, B., Bornstein, H., Langdon, G. S., Curry, R., Daliri, A., & Orifici, A. C. (2018). Experimental response of high strength steels to localised blast loading. International Journal of Impact Engineering, 115, 106-119.

[3] Curry, R. J., & Langdon, G. S. (2017). Transient response of steel plates subjected to close proximity explosive detonations in air. International Journal of Impact Engineering, 102, 102-116.

Utilizing LiDAR to Effectively Assess Residual Capacity of Damaged Structures

Samuel Benson[1], Samuel Keys, [1] and Dr. Eric Williamson [1]

[1]*United States Military Academy, West Point, NY, USA*

In modern military operations, the goal is not simply to target the enemy and eliminate their forces. Armed conflict requires strategic decision making against one or more opposing militias. Such decisions include, but are not limited to, assessing the enemy objectives, enemy composition, enemy capabilities, surrounding terrain, and how friendly forces can affect or be affected by each of these factors. One common way to control the enemy is to limit their possible maneuver and transportation routes. When unable to concentrate friendly troops to secure or defend an objective, it is commonplace to damage infrastructure such as roadways and bridges to restrict enemy movement, thereby influencing, directing, or forcing them to use routes that aid friendly objectives.

The objective of this project is to determine the residual capacity of damaged small-scale bridge components. The specimens designed for the current study extend prior work conducted at the U.S. Military Academy in West Point, NY. The aim is to create a more accurate and expedient method than what was previously developed. A primary goal of this project is to establish a method for military commanders in an operational or field setting to rapidly and accurately assess the remaining capacity of infrastructure damaged by armed conflict (to include blasts, small arms munitions, etc.) and to determine if it is still sufficient for use. This information is of critical importance to units with large vehicles that must cross bridges.

Previous research on this topic has utilized photogrammetry, which involves taking pictures and having computer software develop a three-dimensional image that can be manipulated and analyzed. What the previous research lacked was comprehensive imaging of the complete structure. The missing data often required the modeling software to incorrectly interpolate or guess where the missing parts of the structure were located or just leave a gap in the data. Instead of relying on photogrammetry, the current effort uses LiDAR to capture accurate and dense data as a point cloud, which can then be analyzed using finite element analysis (FEA) software to estimate the remaining capacity of a damaged structure. To validate the finite element modeling approach, the research team is conducting tests on scaled bridge components.

The bridge specimens will be damaged from blast or ballistic effects, then statically loaded to failure to determine their remaining capacity.

The research team will evaluate the effectiveness of LiDAR relative to past attempts using photogrammetry. Additionally, operational considerations, such as the relative trade-off in accuracy and speed from stationary LiDAR units (used as a baseline) compared to mobile scanners, will be evaluated. Finally, finite element modeling guidelines for accurately and efficiently predicting residual structural capacity of damaged infrastructure will be provided.

Figure 1: Intact, Small-Scale Bridge Pier used in the project

Figure 2: LiDAR-developed Point Cloud Model of an Intact, Small-Scale Bridge Pier in Cloud Compare

Keywords: point cloud, finite element analysis, residual structural capacity

Blast Response of Masonry Wall Under Contact Explosion Using CFRP as Externally Bonded Reinforcement: Experimental and Numerical Analysis

Azer Maazoun[1,2,3], Oussema Atoui[1,2],Mohmed Ben Rhouma[4], Ahmed Siala [2]
Bachir Belkassem[4], Stijn Matthys[3] and David Lecompte [4]

[1]*Civil Eng Department, Military Academy of Fondouk Jedid, Nabeul, Tunisia*
[2]*Defense Science and Technology, Military Research Center, l'Aouina, Tunisia*
[3]*Department of Structural Eng and Building Materials, Ghent University, Gent, Belgium*
[4] *Structural and Blast Engineering Department, Royal Military Academy, Brussels, Belgium*

Masonry walls are commonly used in construction due to their strength and durability. However, when subjected to blast loads, walls can be vulnerable to extensive damage or even collapse. To address this issue, researchers and engineers have been working on developing state-of-the-art techniques to improve the performance of masonry walls under blast loads. This article discusses the blast response of masonry walls subjected to a contact explosion and investigates the efficiency of carbon fiber reinforced polymer (CFRP) as externally bonded reinforcement (EBR) in order to improve the blast resistance of the masonry wall. Four simply supported walls are subjected to an explosion of 50g of C4 suspended at the center of the wall. One of the walls is used as a reference specimen and the three remaining ones are retrofitted with different amounts of CFRP. High-speed camera is used to capture the damage progression during the explosions, and a shock accelerometer, is fixed to the rear surface of the walls, to monitor out-of-plane vibrations. Additionally, detailed numerical simulations using the finite element software LS-DYNA is also carried out using the finite element (FE) software LS-DYNA to complement the experimental findings of the blast campaign. The results indicate that bonding CFRP strips on the surface opposite to the explosion is an effective way to reduce the acceleration and to limit the damage levels in the walls. A reduction of 29% and 58% in the damage levels is recorded for the wall retrofitted with 2 wraps and 4 wraps at both sides of the wall, respectively. The propagation of the blast wave causes spalling effect and fragmentations, triggering local debonding between the CFRP wrap and the bricks during the explosion. Damage levels and crack distribution predicted by the numerical analysis are in good agreement with the experimental results.

Keywords: Masonry walls, Damage mitigation, CFRP, Blast resistance, Numerical analysis.

(a)

(b)

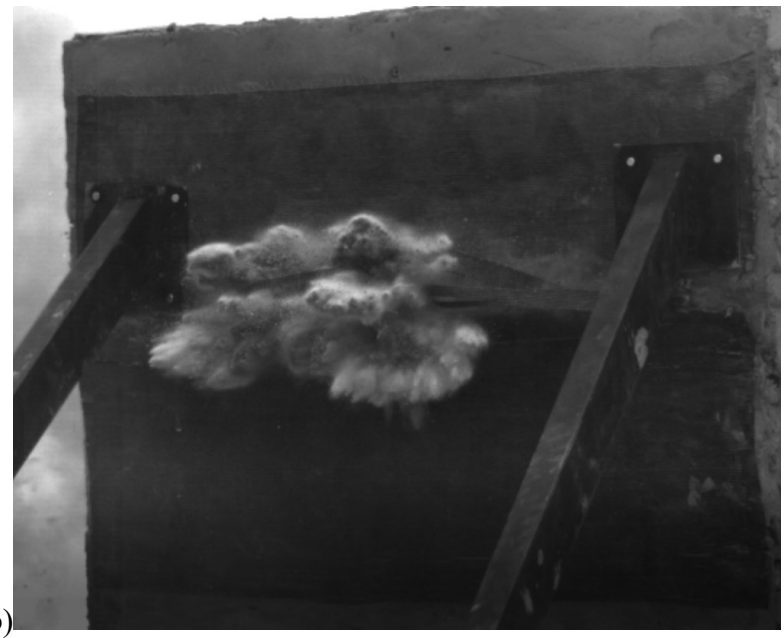

Figure 1. (a) Damage Evolution of a Masonry Wall without CFRP Reinforcement
(b) Damage Evolution of Masonry wall with a single wrap of Unidirectional CFRP

Engineering model to determine the residual static load-bearing capacity of reinforced concrete and steel fibre reinforced concrete structures after contact detonation

Vahan Zohrabyan[1], Thomas Braml[1]

[1]*Institute of Structural Engineering, University of Bundeswehr Munich, Germany*

Increasing safety requirements in critical infrastructure require a deeper understanding of the structural behaviour of concrete elements under extreme loads such as contact detonations. In particular, the estimation of the residual capacity after such an event is challenging for reinforced concrete and steel fibre reinforced concrete structures. In this paper, an engineering model is developed that takes into account the complex damage mechanisms during detonations. The model integrates both experimental investigations (non-destructive tests, 3-point bending test 3PB) and numerical simulations (FEM LS-Dyna) to provide a reliable estimate of the residual strength. Particular attention is paid to material properties, reinforcement/concrete matrix interactions and cracking and its influence on residual strength. The developed model should help engineers to assess the damage to structures after explosions more quickly and accurately, and thus to make informed decisions about the further use or strengthening of components.

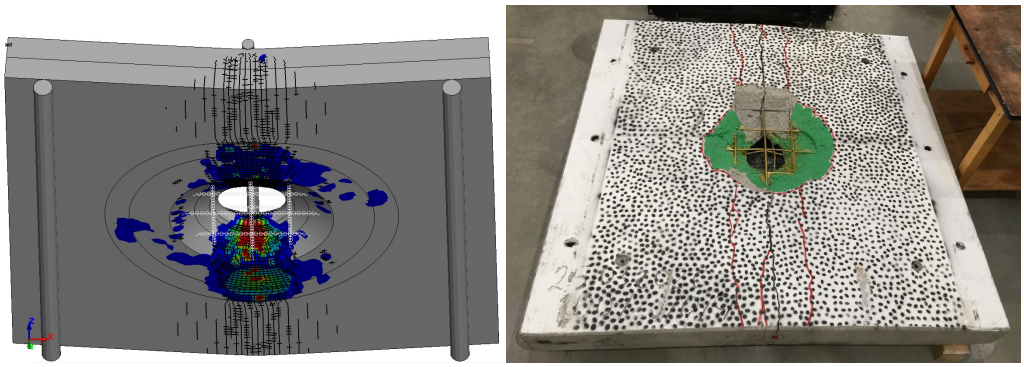

Figure 1. Cracking on the protective side of the reinforced concrete slab (d = 20 cm, 1000 g SEMTEX10).

Keywords: Contact detonation, residual static load-bearing capacity, non-destructive testing, 3D-scan, impact-echo, ultrasound, engineering model, 3-point bending test, LS-Dyna.

SUBTERRANEAN PIPE RESPONSE TO ABOVE-GROUND BLAST: PART 2 – NUMERICAL ANALYSIS

Chris Taggart[1], Alex Rogers[1] and Sam Chacksfield[1]

[1]*AWE, Aldermaston, Reading, Berkshire, RG7 4PR, United Kingdom*

Numerical modelling and experimental testing are employed extensively to study the response of critical national infrastructure to explosive effects. This may include either super- or sub-terranean equipment subject to explosions initiated either above or below ground. Although considerable data is available in the literature on the response of above ground structures to above ground blast, less work has been conducted to study the response of below ground structures subject to loadings originating from above ground blast.

In view of this, an experimental trial and associated numerical modelling was undertaken to enhance understanding of this type of scenario. This paper will focus on the numerical aspects of this work, a sister paper [1] discusses the related experimental trial.

Each of the shots fired during the trial was replicated using numerical simulation, and comparison was made of equivalent simulation and trial results. This validation exercise enabled the accuracy of the modelling techniques that were employed to be assessed, which, in turn, informs the degree of confidence that can be placed in their application to similar studies in the future.

The trial was carried out to generate data on the relative performance of structures when submerged in various media, and to provide validation data for numerical modelling. Each shot consisted of a spherical PE4 charge suspended above three galvanized steel pipes laterally offset from each other. The pipes were held off the ground in a steel frame and fixed to the frame by circular brackets at their ends. The media in which the pipes were submerged varied depending on the shot between air, water and dry sand. An enclosure was constructed around the pipes to contain the water and sand in the relevant shots.

The majority of the modelling was undertaken using LS-Dyna, making use of its Structured ALE (Arbitrary Lagrangian Eulerian) and coupled Fluid-Structure Interaction (FSI) capability. For computational efficiency, a multistage approach was employed. The detonation of the charge and the initial blast propagation were modelled in 2D axisymmetry until interaction of

the blast with the pipes/water/sand. The final state of the 2D model was then mapped into a 3D quarter symmetry domain to capture the blast interaction with the pipes (see Figure 1). The pipes were simulated using shell elements and their ends were constrained using springs and nodal rigid bodies. This permitted the small amount of slip and rotation of the pipes in the end clamps that occurred in the trial without the need for representing the interface between them explicitly. Separate hydrocode modelling was also undertaken to predict the free-field pressure data.

Strong agreement between the simulations and tests was exhibited with respect to the final deformation of the pipes across all media (see Figure 22). Good agreement was also seen between free-field pressure-time histories, although the simulations underpredicted the peak pressures, and overpredicted the arrival times, slightly. Strain gauge data was not used as a validation metric but did highlight potential inconsistencies in the charge construction/positioning from shot to shot. This helped account for some of the variation in final pipe deformation observed between some repeat shots. Overall, the findings provide confidence that the modelling techniques employed reliably captured the physics of the event, and that the same methods could be effectively employed to predict structural response in similar scenarios in the future.

[1] C. Taggart, A. Rogers and S. Chacksfield “Subterranean Pipe Response to Above Ground-Blast: Part 1 – Experimental Testing”, 7th International Conference on Protective Structures (ICPS 7), Abu Dhabi, 2025.

Keywords: Blast, Hydrocode, Finite Element Analysis, Pipes, Structures, Modelling, Simulation.

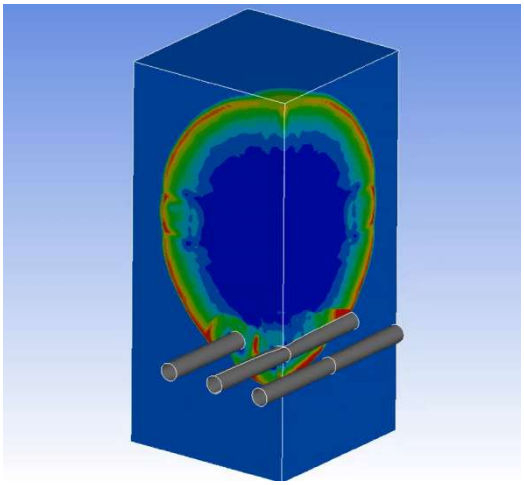

Figure 1: Blast interaction with pipes in air simulation

Figure 22: Comparison of simulation (left) and test (right) pipe response to blast when buried in sand

Shock Tube Tests and Modeling of Buildings Materials and Structural Components Exposed to Critical Blast Loads

Mohsen Sanai*, Waylon M. Weber, Joe Crepeau, and Sean P. Cooper
Applied Research Associates, Test Technology Division, Albuquerque, NM, USA.

*Corresponding author e-mail: msanai@ara.com

In support of the Department of Defense (DoD) blast and impact research, Applied Research Associates, Inc. (ARA) has designed, developed, and built an explosives test site that accommodates two operating shock tube facilities: a 165-ft-long, 8-ft-diameter Medium Scale Shock Tube (MSST) and a 65-ft-long, 10-inch-diameter Small Scale Shock Tube (SSST), shown in Fig. 1. The MSST is powered by a compressed air driver section and can produce peak overpressures in the 2-60 psi range and impulses in the 0.1-1.5 psi-sec range. The SSST is powered by an explosive driver that can produce free field overpressures in the 20-600 psi range and reflected pressures up to 6,000 psi. Both shock tubes are equipped with advanced instrumentation including synchronized high-speed video cameras that can track fragments and debris in three dimensions, piezoelectric and piezoresistive pressure transducers that provide an accurate measure of static, stagnation and dynamic pressure, and a flexible testbed that can be configured to measure the effect of groundcover on blast environments. ARA supports all its shock tube research with advanced modelling and simulation using its leading-edge computational fluid dynamics (CFD) code, SHAMRC, and the computational structural dynamics code (CSD), LS-DYNA.

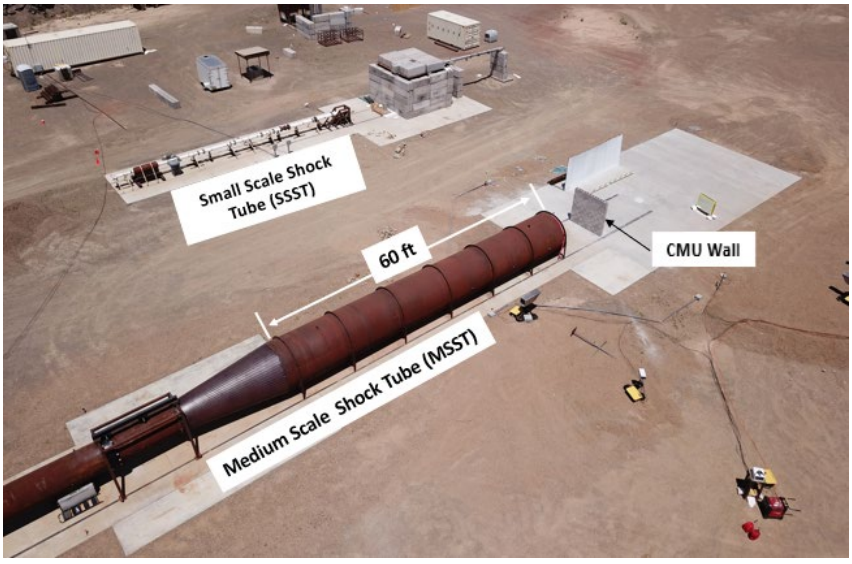

Figure 1. Aerial view of the MSST and SSST facilities.

Examples from tests conducted in each shock tube are presented herein. The lower right portion of Figure 1 shows an 8-ft-square wall built with Concrete Masonry Unit (CMU) blocks erected 11 ft from the muzzle end of MSST. The initial driver pressure of 125 psi produced a peak overpressure of 10.5 psi at the muzzle end. Figure 2(a) shows the measured static overpressure waveforms inside the 8-ft-diamter section of MSST. The pressure waveform at 25 ft upstream

of the muzzle end (top left of Fig. 2(a)) contains a flat top that becomes a peaked waveform as it reaches the muzzle end (lower right plot of Fig. 2(a)). Figure 2(b) shows ground-level pressures measured in front and back of the CMU wall. The difference between the front and back pressures indicates that an initial impulse of approximately 0.3 psi-sec was applied to the base of the wall.

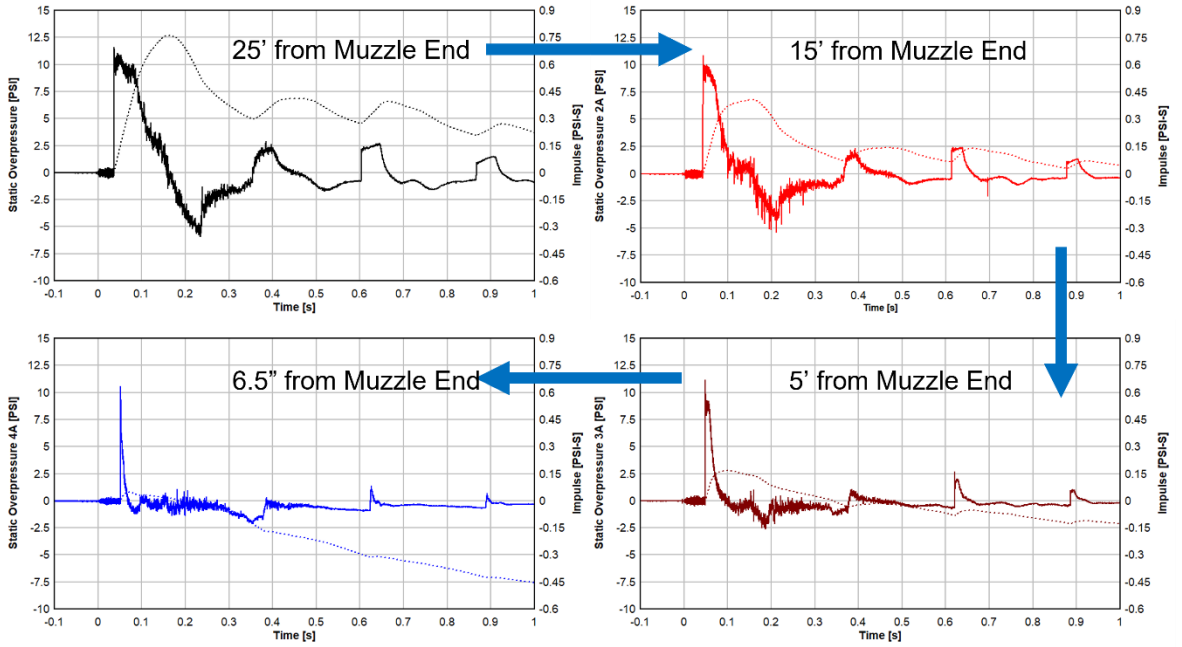

Figure 2(a). Blast wave propagation inside the driven section of MSST.

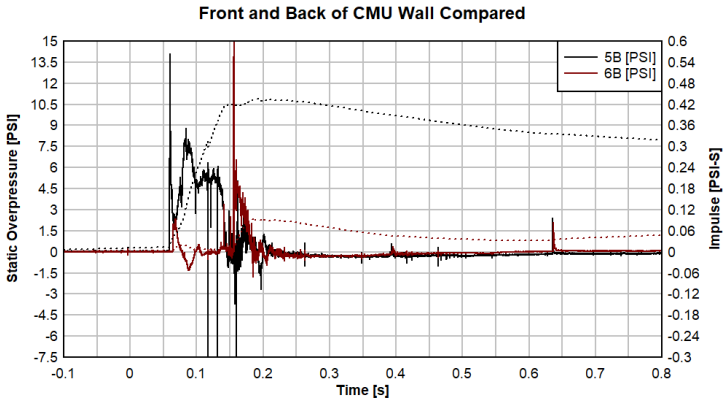

Figure 2(b). Overpressures measured in front (black) and back of (red) the CMU wall in MSST test, using transducers mounted flush in the concrete pad at the base of the wall.

ARA supports all its shock tube research with advanced modelling and simulation codes including SHAMRC and LS-DYNA. SHAMRC predictions of overpressure showed excellent agreement with measured pressures inside the shock tube and with pressures measured in front and back of the CMU wall. The early breakup of the CMU wall modifies the applied pressure loads, so ARA has coupled the LS-DYNA code, that primarily models structural response, with SHAMRC that calculates the blast environment, into a code called Tether to provide accurate predictions of structural response under complex loading conditions. This rare capability allows ARA to predict blast-related structural response even when the structure is not motionless because of elemental failures or because the whole structure is in motion as a rigid body. As an example of Tether coupled code application, Fig. 3 shows the CMU wall response for MSST

driver pressures of 125-psi and 150-psi. The predicted fragments and debris include intact and broken blocks that disperse laterally as they move downstream. Figure 3 shows that the CMU blocks in the lower portion of the wall are broken into smaller pieces whereas the bricks in the upper portion have remained mostly intact. This breaking pattern was expected due to the magnified applied pressure when the flow stagnates near the base of the wall. The 25-psi increase in driver pressure has resulted in significantly greater fragment dispersion, smaller fragments, and fewer intact CMU blocks. The predicted dispersion angle is in qualitative agreement with the debris field observed after the test.

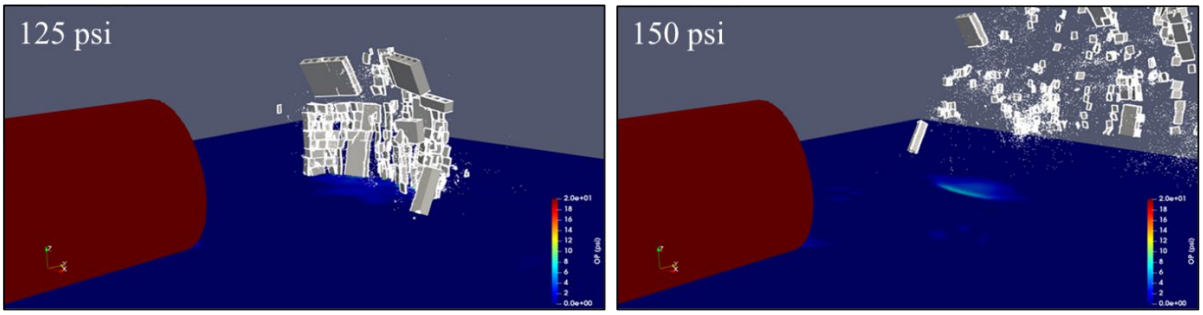

Figure 3. Coupled SHAMRC-LSDYNA calculations for 125-psi (left) and 150-psi (right) driver pressures at 149 ms.

The SSST was used to investigate the breakup and fragmentation of building materials exposed to high pressures. In a typical test, a 14-inch-diamter disc specimen consisting of common building materials, such as concrete and glass, is held in place by a ring bolted to the exit portal flange of the shock tube. The incident shock strength is adjusted by the amount of energetic material distributed in the driver (up to 22 lb net explosive weight (NEW)). Upon firing the shot, the specimen is exposed to the reflected shock pressure, which is measured by wall-mounted pressure transducers located a short distance upstream of the specimen location. Several advanced high-speed video cameras are used to capture stereoscopic images of the fragments against a white backdrop panel. Example images are shown in Figure 4 that were obtained once the fragments and debris have exited the opaque cloud formed by the detonation products. Utilizing the ProAnalyst® image analysis software, high-resolution images from two synched video cameras are used to obtain 3D distributions of the fragments' size and velocity.

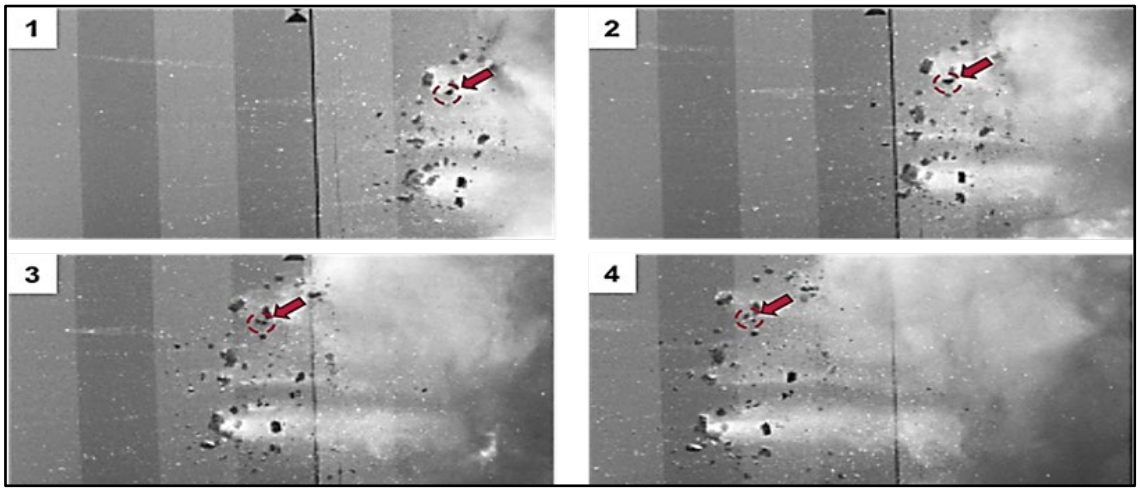

Figure 4. High-resolution, still-video images showing propagation of the debris field moving from right to left. The red arrows indicate potential debris breakup during the flight.

Video cameras running at up to 40,000 frames/second were also used to observe the early stages of fragmentation of facade and other building materials, including concrete and glass shown in Fig. 5. As shown in the middle panel of Fig. 5, these images were digitized to compare with computer simulations that modelled the fracture and formation of fragment surfaces.

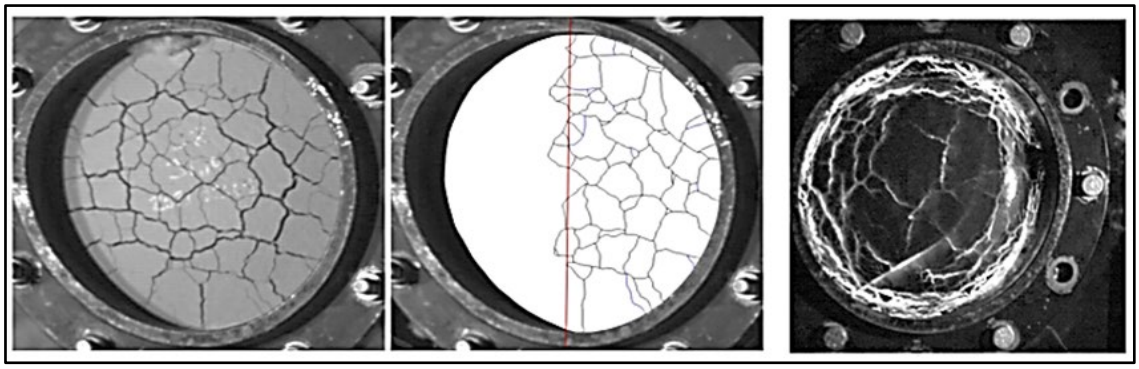

Figure 5. Images from high-speed camera footage focused on the outside face of fragmenting specimens: a 2-inch-thick concrete specimen exposed to 2240 psi (left) and a 3/8-thick glass (at 7.8 ms) exposed to 2350 psi (right).

The shock tube facilities discussed above allow ARA to investigate the response of building materials and structural components to a variety of blast environments. ARA's capability to model such tests with a fully coupled blast code combined with advanced instrumentation capability has furthered the understanding of structural response to blast loads and reduced the technical risks associated with large, more expensive field tests.

The authors wish to express their appreciation for the funding and technical support from Defense Threat Reduction Agency (DTRA), especially the current technical monitors MAJ W. Michael Meier and Dr. John W. Englert.

Modelling vehicular impact for threat-dependent progressive collapse assessments

Gioele Montalbetti[1,*], Alex Sixie Cao[1,2] and Andrea Frangi[1]

[1]*ETH Zurich, Institute of Structural Engineering, Stefano-Franscini-Platz 5, 8093 Zurich, Switzerland*

[2]*Empa, Swiss Federal Institute of Materials Science and Technology, Structural Engineering Research Laboratory, Ueberlandstrasse 129, 8600 Dübdendorf, Switzerland*

**Corresponding author*

The notional column removal method is a common approach to assess the robustness of building structures. Different codes address vehicular impact through prescriptive values depending on the vehicle type [1] and simplified models [1][2]. Due to the uncertainties related to vehicular impact loading, the peak impact force and energy-related phenomena during impact may be severely underestimated with prescriptive values. This may result in the unintentional loss of multiple columns, posing greater danger to the structural integrity. In this context, the response of building structures subjected to successive column removals is not well understood.

In this paper, an approach is presented to estimate the time histories of the kinetic energy of a vehicular impact that captures relevant energy dissipating mechanisms of the vehicle and structure. On the vehicular side, the kinetic energy is reduced from deceleration phenomena and through plastic deformations. The energy dissipation from plastic deformations is derived from an energy-equivalent approach of the crushing behaviour from relevant literature [2][3][4]. On the structure side, the kinetic energy is reduced from the partial or complete rupture of a column, including rigid-body motion of the ruptured column [5]. The structural response of the column is based on full-size tests of timber beams subjected to impact loading using reaction force- and energy-based analytical models [6]. This approach enables the estimation of the time of failure of columns in a vehicular impact scenario, which can be used to assess threat-dependent damage scenarios for progressive collapse analyses.

As shown in Figure 1, the application of the time history of the kinetic energy is exemplified in a case study of a timber building subjected to vehicular impact in a city environment. Using the aforementioned approach, the time of column failure is determined and used to remove ground-floor columns in the structure at specific instances of time, as depicted in Figure 2. The structural response to the successive removal of ground-floor columns is assessed using a state-

of-the-art framework to model progressive collapse of building structures [7]. Based on the results, practical implications of the threat-independent approach to vehicular impact loading scenarios are discussed.

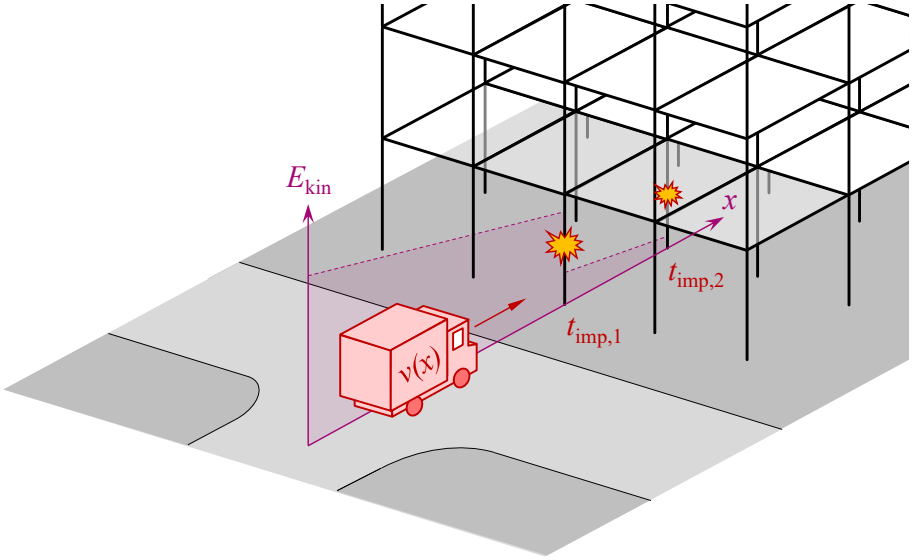

Figure 1: Time history of the kinetic energy of a vehicle for impact loading.

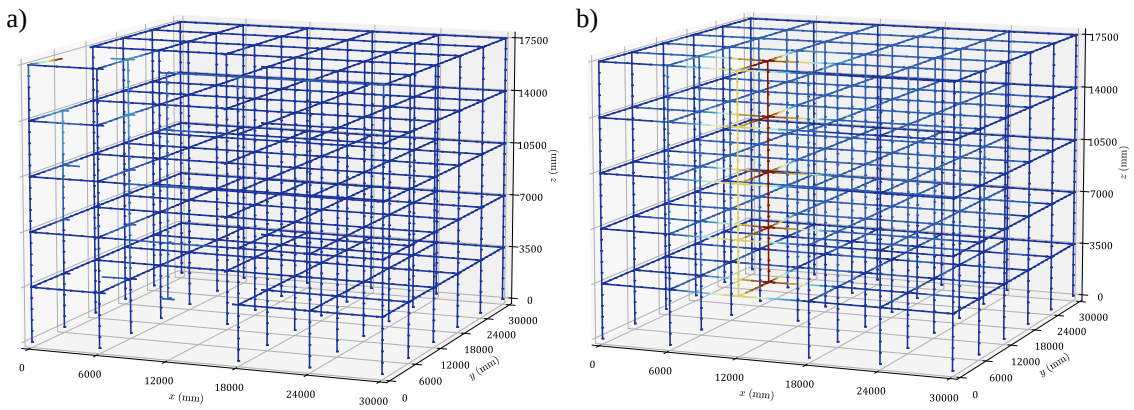

Figure 2: Progressive collapse assessment of a frame structure subjected to the loss of multiple columns. (a) Initial damage state. (b) Final damage state

Keywords: Vehicular impact, energy dissipation, loss of multiple columns, progressive collapse

[1] Taushanov, A., & Spasova, E. (2024). Determination of Vehicle Impact Loads according to different Design codes. Annual of the University of Architecture, Civil Engineering and Geodesy Sofia, 57, 739.
[2] Comité Européen de Normalisation (CEN/TC). (2016). EN 1991-1-7:2006 - Eurocode 1: Actions on structures, General actions - Accidental actions (No. EN 1991-1-7:2006; Version 2016-07).
[3] Bare, C., Peterson, D., Marine, M., & Welsh, K. (2013). Energy Dissipation in High Speed Frontal Collisions. SAE International. https://doi.org/10.4271/2013-01-0770
[4] Kodsi, S., Selesnic, S., Attalla, S., & Chakravarty, A. (2017). Vehicle Frontal Crush Stiffness Coefficients Trends. Accident Reconstruction Journal, 27.
[5] Cao, A., Houen, M., & Frangi, A. (2024). Impact loading of glued laminated timber beams without finger-joints. Computers & Structures, 296, 107278. https://doi.org/10.1016/j.compstruc.2024.107278
[6] Cao, A., & Frangi, A. (2023). Dynamic strength increase of glued laminated timber beams subjected to impact loading. 10th International Network on Timber Engineering Research. https://doi.org/10.3929/ethz-b-000653637
[7] Cao, A., Esser, L., & Frangi, A. (2024). Modelling progressive collapse of timber buildings. Structures, 62, 106279. https://doi.org/10.1016/j.istruc.2024.106279

Coupled Effect of Temperature and Impact Loading on the Mechanical Properties of Ultra High Performance Concrete

Gabriel Erlacher[1], Flavio Silva[1] and Cardoso Daniel[1]

[1]*Departament of Civil and Environmental Engineering, Pontifical Catholic University of Rio de Janeiro, Rio de Janeiro, Brazil*

The pursuit of more robust and durable structures has driven the development of ultra high performance concrete (UHPC). However, extreme conditions, such as fires and explosions, expose the material to environments where its high brittleness and susceptibility to thermal spalling may compromise its ability to provide the required structural safety. In this context, hybrid reinforcement with dispersed metallic and polymeric fibers has emerged as an effective strategy to enhance toughness and prevent thermal spalling. This study investigates the elasticity modulus, compressive strength, and flexural tensile strength of UHPC reinforced with 2% straight steel fibers, with and without the addition of 0.2% polypropylene (PP) fibers, after exposure to temperatures of 200°C, 400°C, 600°C, 800°C, and 1000°C for 2 hours. Furthermore, the residual flexural tensile strength of the composite is evaluated after drop-weight impact tests, with strain rate of approximately $9.3s^{-1}$, after exposure to different temperatures to assess the combined effects of temperature and impact on the material. Results show that polypropylene fibers did not affect compressive strength, with both mixtures exceeding 155 MPa. However, they reduced the elastic modulus from 51.2 GPa to 46.7 GPa, a decrease of approximately 9%. Nevertheless, 0.2% PP fibers effectively prevented the explosive spalling observed before 400°C in the mixture without them, preserving 31.5 MPa of compressive strength and 6.5 GPa of elastic modulus after exposure to 1000°C. As for the flexural tensile strength, the composite material was greatly affected by the degradation of the fibers that occur after 400ºC, leading to even more significant reduction, from 15.9 MPa to only 1.2 MPa, after 1000ºC. The properties of the material under static loadings remained constant or increased until 400ºC, which can be a result of the later reaction of anhydrous cement particles, and decreased steeply for higher temperatures. On the impact tests, the temperature range between 400°C and 600°C appears to be critical as well, as none of the specimens exposed to these or higher temperatures withstood the drop-weight impact test. All specimens containing

PP fibers resisted the impact test at room temperature and after exposure to 200°C, whereas most specimens without PP fibers failed after 200°C, which suggests that the use of PP fiber may also help postpone thermal degradation on UHPC.

Keywords: ultra high performance concrete, fiber reinforced concrete, impact loading, temperature, residual properties.

Experimental and numerical investigation on the protective performance of polymeric pre-layered steel targets under high-velocity ballistic loadings

Teresa Fras[1]

[1]*French-German Research Institute of Saint-Louis (ISL), Saint-Louis, France*

teresa.fras@isl.eu

By adding a front pre-layer, the ballistic limit velocity of armour steel plates against fragments may increase significantly as presented in [1-3], for example. The goal of the presented ballistic tests was to find out how a polymeric pre-layer affects the ballistic resistance of a high-hardness armour steel plates. On target plates, armour-piercing and fragment-simulating projectiles were fired, aiming to observe the performance of target configurations. Further, the entry and exit crater diameters, as well as the residual velocity were measured. The experiments revealed the residual velocity's dependencies as a function of impact velocity and the pre-layer. In order to gain insight into the mechanisms involved in the penetration process, the conducted impact tests were also modelled in a FEM simulation. The investigation revealed the potential for multiple effects to interplay when a pre-layer is coated onto the substrate steel plate, subjected further to blunt projectile impacts. The synergic effect of two much different materials resulted in an enhanced protective performance of the tested structures.

Keywords: terminal ballistics, impact modelling, FSP, PU, pre-layered steel plates.

[1] Roland, CM, Fragiadakis, D, Gamache RM, (2010). Elastomer–steel laminate armor, Composite Structures 92.

[2] van der Wal, R, Carton, E, Hilvers, F, (2018). The performance of armour steels with pre-layers against fragment simulating projectiles. EPJ Web of Conferences 183.

[3] Karl, J, Kirsch, F, Faderl, N, Perko, L, Fras, T, (2020). Optimizing viscoelastic properties of rubber compounds for ballistic applications. Applied Sciences, 10(21).

Experimental and Numerical Characterization of Annealed Glass under High Strain Rate Loading

Nexia Murali[1], Roouf Un Nabi Dar[1], Kaviarasu K[1*], and Alagappan P[1*]

[1]*Department of Civil Engineering, Indian Institute of Technology Madras, Chennai, India*

*Corresponding author: alagappan@iitm.ac.in, ce19d023@smail.iitm.ac.in

Annealed glass plays a critical role in various structural and protective applications, such as architectural glazing, vehicle windshields, and protective barriers in defense and industrial systems. In such scenarios, the material is often subjected to extreme dynamic loading conditions, such as blast wave impacts or ballistic strikes. These high-strain-rate scenarios induce unique mechanical responses and failure mechanisms in annealed glass, which are crucial to understanding for optimizing material performance and ensuring structural safety. Despite its widespread use, the behavior of annealed glass under such conditions remains underexplored due to its brittle nature and the complexity of its fracture dynamics.

This study combines experimental and numerical approaches to investigate the high-strain-rate behavior of annealed glass. Experimentally, a Split Hopkinson Pressure Bar (SHPB) apparatus was employed to replicate dynamic conditions representative of blast and ballistic events. The SHPB setup was calibrated to achieve strain rates ranging from 10^2 to 10^3 s^{-1}, enabling precise characterization of the material's stress-strain response, energy dissipation capacity, and failure patterns. The results demonstrated a pronounced strain-rate sensitivity in annealed glass, with observed increases in apparent compressive strength and stiffness at higher strain rates. Failure was characterized by brittle fracture, involving rapid crack initiation and propagation, often leading to catastrophic fragmentation.

To complement the experimental findings, numerical simulations were performed using finite element modeling to replicate and further explore the observed phenomena. A damage-based constitutive model for annealed glass was implemented, capturing the material's strain-rate-dependent behavior and fracture characteristics. The numerical model was validated against experimental data, achieving strong agreement in stress-strain predictions, crack evolution patterns, and energy absorption metrics. The combined experimental and numerical investigations revealed key insights into the dynamic response of annealed glass, including the influence of microstructural features, surface flaws, and loading conditions on its mechanical performance. The study also highlighted the role of annealed glass in mitigating dynamic loads through energy dissipation mechanisms, providing a framework for improving its performance

in high-strain-rate environments. These findings have significant implications for the design and optimization of glass-based systems in applications requiring resistance to blast and ballistic impacts. The results contribute to the development of safer and more reliable protective structures, enabling better material selection and improved design methodologies. Overall, this study offers a holistic approach to the study of annealed glass under high-strain-rate loading, addressing the critical need for accurate material characterization in extreme environments. By elucidating the mechanical response and failure mechanisms of annealed glass, this study lays the groundwork for future advancements in the design of blast-resistant and impact-resistant systems.

Keywords: annealed glass, high strain rate, material characterization, blast and ballistic resistant.

Submission ID: 4543

7th International Conference on Protective Structures (ICPS7)
12th – 15th May 2025, Abu Dhabi, UAE

Design and optimization of ballistic panels for light armored vehicles

Rafael Celeghini Santiago, Alia Ruzanna Aziz, Fengbo Han, Rafael Savioli, Naresh Kakur, Rubayea Alameri, Nikolaos Nikos, Henrique Ramos

Advanced Materials Research Centre, Technology Innovation Institute, Abu Dhabi, United Arab Emirates, rafael.santiago@tii.ae (corresponding author)

ABSTRACT

Ballistic panels are used to protect occupants in both military and civilian vehicles. These panels are designed to be effective against various types of ammunition, from light firearms to armor-piercing (AP) rounds. Metallic panels are frequently employed for vehicle protection, they significantly increase the vehicle's weight, which can adversely affect performance and payload capacity. This study focuses on optimizing a reference ballistic steel (BS500 + BS600) panel with ultra-high molecular weight polyethylene and ceramics to meet STANAG 4569 Level 3 requirements while minimizing areal weight. For this purpose, material characterization was conducted on reference materials using the Split-Hopkinson Pressure Bar and Universal Testing Machine to evaluate material performance at various temperatures, strain rates, and failure modes across different triaxiality levels. The material constitutive parameters were identified and used to develop explicit numerical models, which were validated and subsequently applied to optimize several panel designs. After that, the identified promising configurations were manufactured and tested using a gas gun projectile launcher. As a result of this work, two panel designs were developed with a reduction in areal weight of more than 20% compared to the reference ballistic steel (BS500 + BS600) panel while providing superior ballistic protection.

Keywords: Ballistic panel, ammunition, vehicle armor, high strain rate, numerical simulation

Enhanced Anchorage Techniques for Smooth Surfaced Nitinol-SMA Rebars

Moustafa Basha[1], Anas Issa[1] , and Ahmed Bediwy[1]

[1] Civil and Environmental Engineering Department, United Arab Emirates University, Al Ain P.O. Box 15551, Abu Dhabi, United Arab Emirates

Over the past decades, Shape Memory Alloys (SMAs), have revolutionized the field of seismic and structural engineering, offering their unprecedented unique properties such as superelasticity, energy dissipation, and the ability to undergo remarkable deformations and reverting to their original shape. The origins of SMA date back to the 1930s when Swedish scientist Arne Ölander initiated revolutionary research on iron alloys, exploring the distinctive characteristics of Iron-Manganese (Fe-Mn) alloy. Ever since, researchers have extensively investigated the mechanical properties of SMAs, leading to increasingly utilizing them in a wide variety of applications, including self-centering braces, structural elements, and systems frequently exposed to harsh working conditions, such as in regions susceptible to earthquakes and dynamic loading. These studies have demonstrated the remarkable advantages SMAs offer, such as their corrosion resistance, durability, and ability to withstand repeated loading cycles without significant degradation. However, a critical limitation has emerged, particularly those made of Nitinol (Nickel–Titanium), which possesses a smooth surface that makes it hard to implement in most structural elements, therefore anchorage systems are often required. Consequently, this smooth surface increases the possibility for slippage, therefore conventional methods to anchor steel reinforcement bars may not be applicable. The process of anchoring the Nitinol rebars involves securing them within different structural components to guarantee effective load transfer and enhanced structural performance. A few recent studies have investigated the anchorage of SMA rebars, but there is still a big research gap. To address this research gap, this paper presents an experimental test to evaluate the possible anchorage systems for smooth-surfaced Nitinol-SMA rebars. The experimental testing includes uniaxial tensile testing, with 6% strain, different loading rates, and two types of anchorage systems. The key challenge associated with this research is finding a suitable anchorage system to solve the slippage dilemma to exploit SMA bars' unique characteristics. This paper's key findings include ultimate tensile strength, force/displacement relationship, and stress/strain relationship under different loading rates. This paper highlights the need for a more thorough investigation of innovative anchorage systems that might be suitable with SMA bars to pave the way for researchers to enable their wider application in more structural elements.

Keywords: Slippage, Anchorage, SMAs, Superelastic, Self-Centering

Development of the BLADE tool for blast load assessment and damage evaluation

Vasilis Karlos[1], Orestis Ioannou[2], Ralf Schumacher[1], Martin Larcher[1]

[1]*European Commission, Joint Research Centre, Ispra-Italy*

[2]*Steel Structures Laboratory, School of Civil Engineering, National Technical University of Athens, Athens-Greece*

The European Commission's priority of enhancing the resilience of critical infrastructure and safeguarding public spaces has driven the development of the BLADE tool by the Joint Research Centre (JRC). This tool is designed to support stakeholders in assessing the potential consequences of terrorist attacks involving explosives on critical infrastructure and public spaces.

The BLADE tool utilizes pressure-impulse (P-I) diagrams to evaluate the response of structures and various components under blast loads, allowing users to customize parameters to suit their specific needs. It provides a user-friendly interface that offers a comprehensive overview of the selected components and their expected performance under the chosen blast loads.

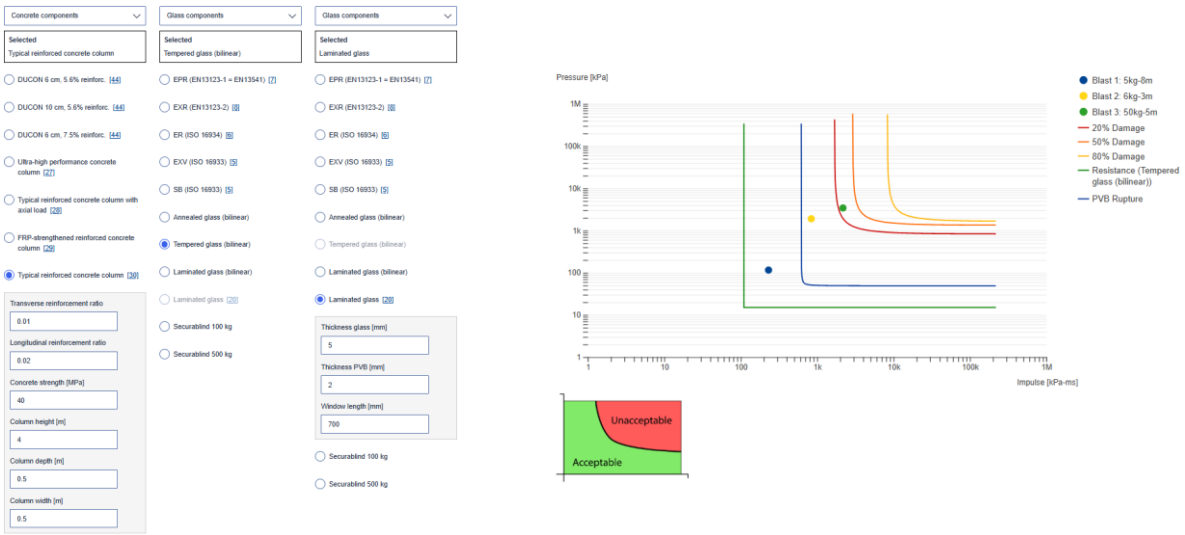

Figure 1. Selection of components and their parameters in BLADE and the resulting P-I diagram for three different blast scenarios.

The tool has been expanded to include single-degree-of-freedom (SDOF) models, enabling the analysis of steel beams and columns, as well as cross-laminated timber (CLT) components. Additionally, it addresses the effects of contact detonations on concrete slabs, a scenario that has gained significant importance due to the increasing ability of Unmanned Aircraft Systems (UAS) to transport explosive loads.

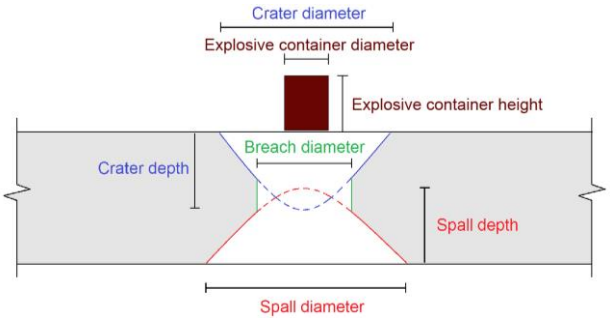

Figure 2: Representation of the failure modes on concrete slab facing a contact detonation

The BLADE tool has been developed through a comprehensive literature review and incorporates existing analytical, closed-form formulations for P-I applications. The tool includes a wide range of components, such as glass, concrete, steel, masonry, and soil, as well as effects on humans and vehicles.

The tool's ability to provide fast and reliable predictions of failure or fatality due to an explosion makes it an essential resource for enhancing the resilience of critical infrastructure and safeguarding public spaces. The BLADE tool is a valuable resource for stakeholders to assess the potential consequences of terrorist attacks and implement appropriate safeguarding measures.

The development of the BLADE tool demonstrates the JRC's commitment to supporting the European Commission's priority of enhancing the resilience of critical infrastructure and safeguarding public spaces. The tool is expected to be widely used by stakeholders, including architects, engineers, and security experts, to assess the potential consequences of terrorist attacks and implement effective protective measures.

Keywords: BLADE, P-I diagrams, contact detonations, blast damage assessment, critical infrastructure, public spaces, terrorist attacks, explosives

Temperature Distribution in Underground Structure Subjected to Blast and Subsequent Fire Loads

Abhishek Mohapatra[1], Sunita Mishra[2], Wensu Chen[3]

[1]*Ph.D. Student, Department of Mining Engineering, IIT Kharagpur, India.*

[2]*Assistant Professor, Department of Mining Engineering, IIT Kharagpur, India.*

[3]*Assoc. Prof., School of Civil and Mechanical Engineering, Curtin University, Australia*

The scarcity of space above ground has compelled human society to embrace subterranean habitats for sustainable living. Beyond the need for space, the factor of comfort plays a pivotal role in the development of underground structures. However, it is of utmost importance to recognize that underground structures, especially tunnels, are susceptible to the impact of explosive loading and fire in case of terrorist attacks. The escalation of temperature resulting from a fire, due to external threats such as bomb detonations or missile strikes, has the potential to adversely affect the temperature distribution at the point of occurrence. Consequently, it becomes imperative to conduct comprehensive numerical investigations to evaluate the impact of these external hazards on subterranean structures. This study aims to perform a holistic analysis of the combined effects of blast and fire on a tunnel constructed within sandstone rock. The primary objective of the present study is to predict the resulting temperature distribution across the longitudinal-sectional area of the tunnel. To achieve this, a three-dimensional nonlinear finite element model of 200 × 200 × 200 m^3 is developed with a circular tunnel diameter of 5.6 meters situated at a depth of 20 m below the ground surface using a strain rate dependent finite element numerical tool, ABAQUS and is shown in Figure-1. The investigation begins with a blast analysis, simulating a 50-kg PETN (Pentaerythritol Tetranitrate) explosion at the tunnel's center. Subsequently, a thermal analysis is conducted, involving the application of a time-varying heat flux profile at the central portion of the tunnel. The outcomes of this comprehensive study reveal that the degradation of strength in the tunnel's periphery is due to the combined effect of blast and thermal loads. It was observed that the tunnel reaches a maximum temperature of 381.93°C at the center of the tunnel roof and 344.36°C at the center of the tunnel sidewall when exposed to a fire load for 900 seconds as shown in Figure 2. The temperature gradually decreases towards the boundaries along the length of the tunnel. These

findings serve to illuminate the design considerations for constructing resilient underground structures that prioritize enhanced safety measures.

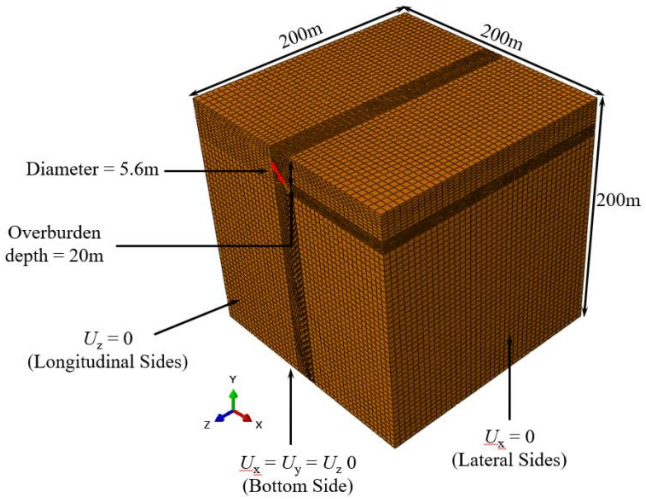

Figure 1. 3D Finite element meshed model of tunnel showing boundary conditions**.**

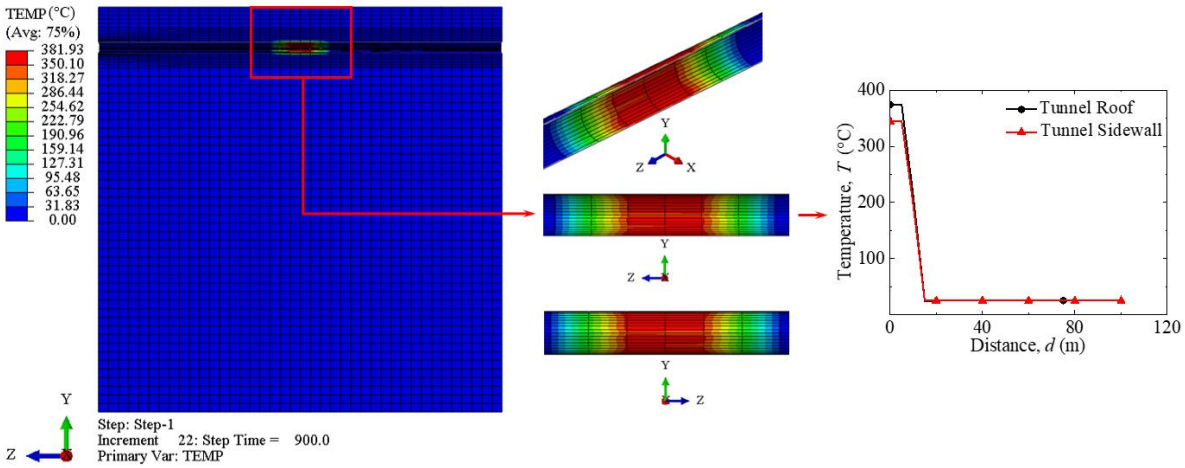

Figure 2. Temperature distribution (°C) along the tunnel at 900s.

Keywords: Blast Load, Fire Loads, Numerical Simulation, Temperature Distribution, Underground Tunnel

Numerical Investigation of Close-in Blast Loads in Partially Confined Spaces

Hwee Kiat YEO

Home Team Science & Technology Agency, 1 Stars Ave, #12-01, Singapore 138507,

YEO_Hwee_Kiat@HTX.gov.sg

(Corresponding author)

Swee Hong TAN

PhD, PE(S'pore), CEng(UK), MIStructE, MASCE

Home Team Science & Technology Agency, 1 Stars Ave, #12-01, Singapore 138507,

TAN_Swee_Hong@HTX.gov.sg

Structural components, such as beam, wall and column, when subjected to overpressures and impulses arising from far-range detonations, are typically idealised as individual Single-Degree-Of-Freedom (SDOF) dynamic systems under uniformly distributed loads. Such assumption is practical, because at scaled distances over 1.2m/kg$^{1/3}$, the blast profile is nearing planar in elevation with minimal disparities across the component spans. In the context of fully confined spaces, to further account for the secondary effects due to wave interactions with surrounding surfaces, procedures set out in standards, such as UFC 3-340-02, recommend the use of amplification factors to determine ultimate design loads. Complexities in the prediction of blast propagation manifest substantively when the focus is shifted to partially confined spaces, especially at close-in standoffs. First, the assumption of uniformly distributed loads no longer holds. The same SDOF idealisation can be applied, only if stringent limits regarding the spatial distribution of blast loads are met before a meaningful impulse equivalence can be drawn. Second, the component of interests is more likely to be within the immediate plume of detonation products. The gas pressures arising from build-up of detonation products in close vicinity need to be accounted for, through combined shock-and-gas load-histories for design.

In this contribution, a series of findings from Computational Fluid Dynamics (CFD) simulations of blast propagation within partially confined spaces are presented. Multi-material Euler-Godunov grids are employed to create numerical domains representative of configurations of carparks commonly found in Singapore. Not only the movement of both air and explosives constituents are comprehensively tracked, the combined shock-and-gas load-histories on

specific pre-decided locations within the virtual environments, can also be directly calculated and thereafter consolidated for post-simulation regression analyses. Furthermore, to maximise utilisation of finite processing and memory capacities, the usual routine of remapping blast propagation from 1D and 2D axial symmetrical models to the eventual 3D numerical domains is carried out. This is to ensure that the best numerical resolution is accorded rightfully to the calculations of the highly localised detonation phenomena, including the formation of shock front, followed by subsequent propagation and interactions with surrounding surfaces. Finally, the Richardson Extrapolation Method is considered for mesh refinement studies. This is to address the importance of the need to quantify discretization errors in numerical simulations.

Keywords: blast propagation, computational fluid dynamics, partially confined spaces, close-in, scaled distance

Enhancing Ballistic Resistance of High-Performance Fiber-Reinforced Concrete Panels Using Polyurethane Coatings and Epoxy Composites

Petr Hála [1], Přemysl Kheml [1], Alexandre Perrot [2], Jiří Mašek [3] and Radoslav Sovják [1]

[1]*Czech Technical University in Prague, Faculty of Civil Engineering, Experimental Centre, Prague, Czech Republic*

[2]*SYNPO, a.s., Pardubice, Czech Republic*

[3]*SPOLCHEMIE - Spolek pro chemický a hutní výrobu, a.s., Ústí nad Labem, Czech Republic*

This study introduces an innovative ballistic protection system based on high-performance fiber-reinforced concrete (HPFRC) panels reinforced with polyurethane (PU) coatings and epoxy composite layers. The lightweight, modular panels are designed for rapid assembly into structures such as freestanding walls, checkpoints, and mobile barriers, offering flexibility and ease of deployment. The research investigates the ballistic performance of the HPFRC panels, focusing on the impact of applying polyurethane coatings and glass/epoxy or aramid/epoxy composites to enhance protection against projectile impacts. The results confirmed that PU coatings significantly reduce secondary fragmentation, enhancing safety for personnel and equipment. The addition of composite layers allowed for a reduced panel thickness and weight, without compromising ballistic performance. This research paves the way for optimizing the design of protective structures, with future work focusing on improving blast resistance.

Keywords: ballistic protection, HPFRC, polyurethane coating, glass/epoxy.

Introduction

A new ballistic system has been developed for use in checkpoints, fortified posts, and mobile barriers. It consists of lightweight, high-performance fiber-reinforced concrete (HPFRC) panels that can be easily assembled into different structures, such as freestanding walls or outposts with varying angles, see Figure 1. The panels lock together, allowing rotation and flexibility in shape. Assembly is quick, requiring only two people and no heavy equipment. The test results of system's resistance to bending, shearing, blasting, and ballistic impacts confirmed its effectiveness [1].

Figure 1. The mobile ballistic system consisting of bulletproof panels

HPFRC, known for its high energy absorption and radial cracking mitigation, offers promising applications in protective structures compared to conventional concrete [2,3]. These enhanced properties are attributed to its dispersed fiber reinforcement and fine material composition, making it highly effective against projectile impacts. However, slim, uncoated panels may still generate debris during impacts, posing a risk of secondary injuries or damage.

Polyurethane (PU) coating has been used to increase the ballistic resistance of many protective panels, such as carbon fiber reinforced plastic panels [4] or low carbon alloy steel panels [5]. It has also been used in conjunction with concrete to mitigate fragmentation under blast [6]. Glass/Epoxy (G/E) laminates [7] and Kevlar/Epoxy (K/E) composites [8] have been tested under projectile impact, but not in combination with HPFRC and PU layers. This research addresses this gap by exploring the potential benefits of the protective layers made of polyurethane or epoxy composite in enhancing the ballistic resistance of HPFRC panels.

Methodology

The proposed sandwich structure consists of an HPFRC core, glass/epoxy or aramid/epoxy composite layers, and polyurethane (PU) coatings containing 30% filler. The HPFRC used in this study was made from a multifunctional dry prefabricated cementitious composite with 2% volume of 13×0.14 mm steel fibers. The epoxy composites were made by combining glass (type INTERGLAS™ twill 2/2) or aramid (type Twaron®, twill 2/2) fibers with epoxy (type CHS-EPOXY® 582 + TELALIT® 0542) resin. The PU elastomer was a two-component thermoset, comprising a telechelic polyol thinned with castor oil and an aromatic isocyanate. Additives like defoamer, zeolite paste, and an accelerator were included.

Ballistic tests were initially conducted at a public firing range and later verified at a certified military range. The tests evaluated the samples' resistance to various projectiles at different velocities to develop designs for multiple levels of ballistic protection. A high-speed camera captured the projectile's impact on the target. The shooter aimed at the center of the specimen, which was mounted in a steel frame, and no yaw or pitch angles were detected during the shots.

Results

Table 1 shows the thickness of individual layers in sandwich panels that meet the selected ballistic classes of the European standard EN 1522 (FB4-FB7), and the NATO Standardization Agreements STANAG 2280 (A2, A4) and STANAG 4569 (K2). Figure 2 displays typical results from numerical simulations using the LS-DYNA solver, where the color indicates damage to the HPFRC, with red areas representing complete failure.

Table 1. Thicknesses in mm of sandwich panels required to meet ballistic class requirements

	FB4	FB5	FB6	FB7	A2	A4	K2
Polyurethane	2×5	2×5	2×5	2×5	2×3	2×5	2×5
Glass/Epoxy	2×3	2×5	2×5	2×5	2×5	-	-
Aramid/Epoxy	-	-	-	-	-	2×5	2×5
HPFRC	30	40	60	70	40	160	70
Total	46	60	80	90	56	180	90

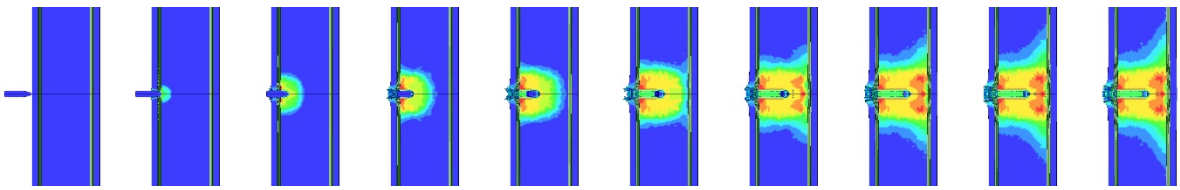

Figure 2. Simulation of a sandwich panel resisting penetration by a 5.56×45 projectile

Conclusions

The aim of this study was to develop and assess a novel ballistic protection system composed of high-performance fiber-reinforced concrete panels reinforced with polyurethane coatings and epoxy composite layers. The following conclusions can be drawn from the study: (1) The polyurethane (PU) coating enhances the ballistic resistance of high-performance fiber-reinforced concrete (HPFRC) panels. (2) Applying PU to the back of the panel prevents the formation of secondary fragments, reducing the risk of injury or property damage behind the structure. (3) Although the front PU coating doesn't fully stop fragment formation, it narrows the fragment spread, limiting the affected area in front of the structure. (4) Adding glass/epoxy

and PU layers allowed for a thinner HPFRC core, reducing the panel's overall weight by 13%. (5) Numerical models, developed independently from ballistic tests, accurately predict the panels' ballistic performance using conventional data. (6) The newly designed panels are mobile, bulletproof, and eliminate scabbing. Future work will optimize them for blast resistance and explosion exposure.

Acknowledgements

This publication was supported by the Technology Agency of the Czech Republic [grant number FW03010141], the Czech Science Foundation [grant number 23-06352S], and the Grant Agency of the CTU in Prague.

References

[1] Mára, M., Talone, C., Sovják, R., Fornůsek, J., Zatloukal, J., Kheml, P., & Konvalinka, P. (2020). Experimental investigation of thin-walled UHPFRCC modular barrier for blast and ballistic protection. Applied Sciences, 10(23), 8716, doi: 10.3390/app10238716.

[2] Sovják, R., Vavřiník, T., Zatloukal, J., Maca, P., Mičunek, T., & Frydrýn, M. (2015). Resistance of slim UHPFRC targets to projectile impact using in-service bullets. International Journal of Impact Engineering, 76, 166-177, doi: 10.1016/j.ijimpeng.2014.10.002.

[3] Máca, P., Sovják, R., & Konvalinka, P. (2014). Mix design of UHPFRC and its response to projectile impact. International Journal of Impact Engineering, 63, 158-163, doi: 10.1016/j.ijimpeng.2013.08.003.

[4] Liu, Q., Guo, B., Chen, P., Su, J., Arab, A., Ding, G., ... & Guo, F. (2021). Investigating ballistic resistance of CFRP/polyurea composite plates subjected to ballistic impact. Thin-Walled Structures, *166*, 108111 , doi:10.1016/j.tws.2021.108111.

[5] Zhang, P., Wang, Z., Zhao, P., Zhang, L., Jin, X. C., & Xu, Y. (2019). Experimental investigation on ballistic resistance of polyurea coated steel plates subjected to fragment impact. Thin-Walled Structures, *144*, 106342, doi:10.1016/j.tws.2019.106342.

[6] Iqbal, N., Sharma, P. K., Kumar, D., & Roy, P. K. (2018). Protective polyurea coatings for enhanced blast survivability of concrete. Construction and Building Materials, 175, 682-690, doi:10.1016/j.conbuildmat.2018.04.204.

[7] Wu, E., & Chang, L. C. (1995). Woven glass/epoxy laminates subject to projectile impact. International Journal of Impact Engineering, 16(4), 607-619, doi:10.1016/0734-743X(95)00001-Q.

[8] MathusoothanaperumalSukanya, N., & Sundaram, S. K. (2024). Investigations on low-velocity ballistic impact behaviour of Kevlar/Epoxy composites reinforced with chopped wet spun fibers intruded with nanofillers. Thin-Walled Structures, 198, 111665, doi: 10.1016/j.tws.2024.111665

The use of high-performance fiber reinforced cement based composites to strength concrete structures under impact loading

Felipe Souza[1], Júlio Nunes[1], Victor Lima[2] and Flávio Silva[1]

[1]*Pontifícia Universidade Católica do Rio de Janeiro, Rio de Janeiro, Brazil*

[2]*University of Stavanger, Stavanger, Norway*

Concrete structures can be subjected to impact loadings of varying magnitudes and durations throughout their service life, ranging from minor vehicular collisions to more severe events such as aircraft crashes, earthquakes, and warfare attacks. Fiber-reinforced concretes (FRC) have proven effective in enhancing the performance of structural elements under impact loads by reducing crack formation and propagation, minimizing scabbing and spalling, and limiting mass loss while preserving the stiffness and rigidity of the structure. This is due to the fibers' ability to disperse stress across the element. Additionally, the application of thin external strengthening layers using Strain-Hardening Cementitious Composites (SHCC) and Ultra-High-Performance Concrete (UHPC), as well as their combinations with carbon textiles (TSHCC and TUHPC), significantly improves impact resistance. These materials enhance energy dissipation through multiple cracks, thereby contributing to the structure's resilience under high-strain rate loads. This study aims to deepen the understanding of the behavior of concrete structures reinforced with these advanced materials under impact loading. A state-of-the-art drop-weight impact test machine, equipped with piezoelectric load cells, accelerometers, and a data acquisition system capable of recording 2 million samples per second, was used to conduct the experiments. Impact energies ranging from 300 J to 1,700 J were applied to the center of 600 mm x 600 mm x 100 mm concrete panels supported at four points. The concrete used had a compressive strength of 35 MPa and was reinforced with steel fibers. Thin strengthening layers of SHCC, UHPC, and TSHCC (incorporating two layers of carbon textiles) were applied to the bottom face of the panels to enhance their impact resistance. A Digital Image Correlation (DIC) stereo high-speed system was employed to measure displacement and strain on the panels' underside. Results indicate that steel fibers reduced crack formation and spalling, though significant damage and cracking still occurred. SHCC layers improved energy absorption, while TSHCC with carbon textiles significantly enhanced energy dissipation and

minimized crack formation due to the material's multiple-cracking behavior. The TUHPC combination withstood several successive impacts beyond the limits of SHCC, maintaining structural integrity throughout testing. These findings demonstrate the superior performance of these materials in protecting concrete structures from impact loads.

Keywords: fiber reinforced concrete, strain-hardening cementitious composite, ultra-high performance concrete, impact loading, high-strain rate.

25 Years of concrete modeling: Some key lessons learned for predictive simulations in hydrocodes

Werner Riedel[1], Christoph Grunwald [1]

[1]*Ernst-Mach-Institut (EMI), Fraunhofer Society, Freiburg, Germany*

Modeling of concrete under dynamic loading situations in hydrocodes for real-world application scenarios, such as ballistics, aircraft impact and explosion effects on protective structures - covering effects from rate-dependence to shock loading, from quasi-plastic behavior to fragmentation - has considerably advanced in the past decades. The main drivers were, aside advancing dynamic test methods, better constitutive laws, evolving best practices for modeling and discretization and the exponential increase in computing power.

25 years ago, a concrete model was developed at Fraunhofer EMI by Riedel, Hiermaier and Thoma (RHT) [1,2]. It helped the German community of infrastructure protection to achieve better predictiveness in numerous research works and industrial applications. The introduction as standard models in ANSYS-Autodyn around 2001 [3] and LS-Dyna in 2011 [4,5] made it available to innumerable users world-wide, leading to hundreds of citations, see Figure 1. The continuous and wide-spread work with this model lead to a better understanding of the necessary key phenomenology, which will be highlighted on three aspects:

First, the pressure-dependence will be discussed regarding dynamic strength and wave propagation. Studies of concrete-type masonry materials with very low strength (uniaxial compressive strength f'_c~3MPa) reveal projectile instability effects similar to hydraulic ram in fluids, because of the extremely low strength and wave speed [6]. In contrary, ultra-high-performance concretes (UHPC, f'_c~160MPa), feature so high strength values that meridian behavior is hardly measurable at relevant pressures, which makes constitutive modeling and dynamic predictions difficult.

Second, replica scaling of concrete damage and failure will be investigated. While it is undebated, that in static loading scaling is hardly applicable to concrete structures, transient dynamic experiments scale much better, as shown repeatedly by experimental evidence. The role of key material and structural properties in scaling laws, notably the fracture energy, and the influence on rebars will be discussed based on experimental studies and modeling analysis.

Third, concrete damage and fracture, debris formation in quantitative simulations will be canvassed as most recent results and outlook. Not only that mesoscale simulations are beneficial studying shock waves in the heterogenous composite [7], but they can also provide substantial progress towards quantitative simulation of concrete damage and fragmentation [8], bridging predictions even to debris ejection and safety distances [9], see Figure 2.

The proposed contribution will thus provide, based on more than two decades of experience, insights on achievements and remaining limitations in modeling reinforced concrete under dynamic loading in hydrocodes, together with an outlook on chosen latest developments.

Keywords: Concrete, hydrocodes, RHT

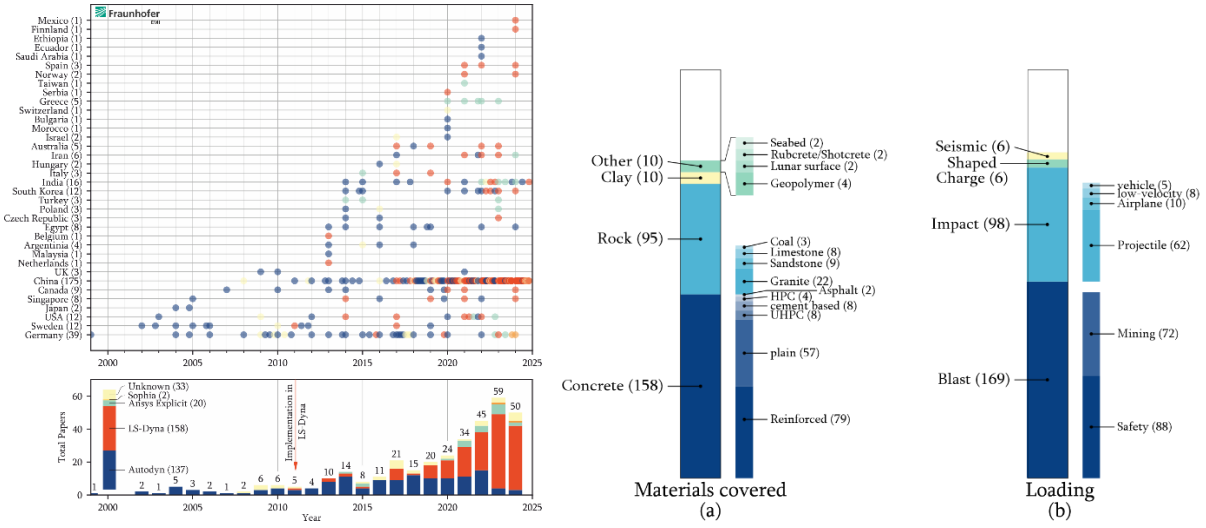

Figure 1. Citation numbers and applications using the RHT concrete model over the past 25 years.

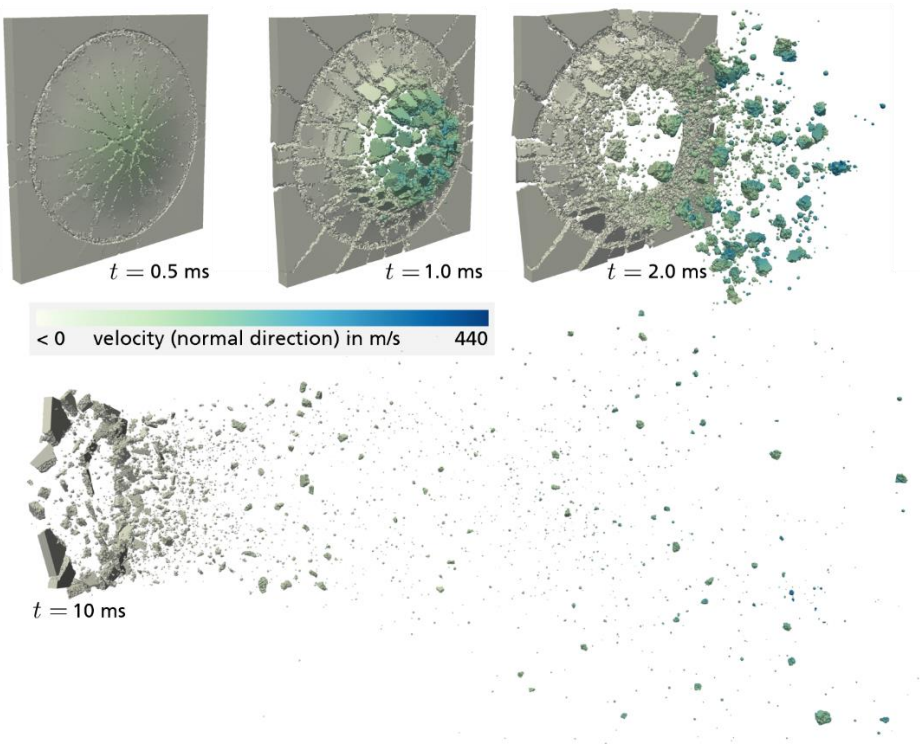

Figure 2. Latest mesoscale simulations for quantitative concrete fragmentation and debris size predictions under blast [9].

[1] Riedel, W. et. al. (1999). Penetration of Reinforced Concrete by BETA-B-500, Numerical Analysis using a New Macroscopic Concrete Model for Hydrocodes. Proc. 9. International Symposium Interaction of the Effects of Munitions with Structures - ISIEMS, CD-ROM.

[2] Riedel, W. (2004). Beton unter dynamischen Lasten: Meso- und makromechanische Modelle und ihre Parameter, Hrsg.: Fraunhofer-Institut für Kurzzeitdynamik, Ernst-Mach-Institut EMI, Freiburg/Brsg., Fraunhofer IRB Verlag, ISBN 3-8167-6340-5.

[3] Riedel, W. et al. (2009). Numerical Assessment for Impact Strength Measurements in Concrete Materials, Int J Impact Engn **36**, pp. 283-293, doi: 10.1016/j.ijimpeng.2007.12.012.

[4] Borrvall, Th., Riedel, W. (2011). The RHT Concrete Model in LS-Dyna, 8th European LS-DYNA Users Conference, Strasbourg, Session 12, Paper 1.

[5] Grunwald, Chr. et al. (2017). A General Concrete Model in Hydrocodes – Verification and Validation of the RHT model in LS-Dyna, Int J Protective Structures **8** (I), 58-85, doi: 10.1177/2041419617695977.

[6] Sauer, Chr. et al. (2017) Stability of tungsten projectiles penetrating adobe masonry, Int J Impact Engn **109**, pp67-77, doi: 10.1016/j.ijimpeng.2017.06.001.

[7] Riedel, W. et al. (2008) Shock Properties of Conventional and High Strength Concrete, Experimental and Mesomechanical Analysis, Int J Impact Engn **35**/3, pp. 155-171 doi: 10.1016/j.ijimpeng.2007.02.001.

[8] Knell, S. et al. (2012). Mesoscale simulation of concrete spall failure, European Physical Journal **206** (1), 139-148, doi:10.1140/epjst/e2012-01595-1.

[9] Grunwald, Chr. et al. (2025). Simulating the break-up, debris formation and throw of concrete structures under explosive loading, Int J Impact Engn (accepted manuscript).

Numerical Evaluations on the Blast Response Behavior of Cross-Laminated Timber Panels

Erkan Mutlu [1], James Davidson [1], David Roueche [1], and Kadir Sener [1]

[1]*Civil and Environmental Engineering, Auburn University, Auburn, Alabama, USA*

Engineered wood products (EWP) have increasingly attracted attention as sustainable and efficient alternatives to traditional building materials in protective structural applications. Among these, cross-laminated timber (CLT) has emerged as a particularly promising material due to its unique two-way resistance capability, achieved through orthogonal plies of glued laminations. This configuration enhances its performance under multi-directional loading, making it suitable for protective structures. However, research on the blast resistance of CLT panels remains limited, with only a handful of studies addressing their potential in high-strain rate environments. The resistance of CLT panels to out-of-plane loads is influenced by a complex interplay of factors, including aspect ratio, support conditions, and the nature of blast events (far-field or close-in), all of which can lead to brittle failure modes such as rolling shear or flexure as shown in Figure 1.

To bridge these knowledge gaps, a systematic experimental program was undertaken to investigate the failure mechanisms of CLT panels subjected to static out-of-plane loading. Key parameters evaluated included panel thickness (3, 5, 7, and 9 plies), shear-span-to-depth ratios (2.0, 3.0, 4.0, and 5.0), panel widths (12, 24, and 36 inches), ply orientations (major and minor axes), and loading configurations (three- and four-point bending). The experimental findings provided critical data for developing benchmark finite element models capable of replicating the mechanical behavior of CLT panels. These numerical models captured the initial stiffness, peak load, post-peak response, and distinct failure modes with high accuracy, as demonstrated in Figure 2.

Building on these validated models, a comprehensive parametric study was conducted to assess the influence of various geometric and material properties on the blast performance of CLT panels. Computational simulations extended the understanding of both one-way (beam-like) and two-way (plate-like) behaviors, incorporating rate-dependent stress-strain models

developed in a companion study. These models also facilitated the replication of blast test results from prior research, further enhancing their reliability for predictive analysis.

The findings demonstrate that CLT panels can effectively resist blast loads, with their behavior strongly influenced by geometric properties, material configurations, and boundary conditions. This research significantly advances the understanding of CLT performance under dynamic loading, establishing its potential as a sustainable and resilient material for protective structural applications. The outcomes provide a foundation for the broader adoption of CLT in scenarios demanding robust resistance to extreme loading conditions, aligning with growing sustainability goals in construction.

Figure 1 – CLT Beam Typical Failure Mode

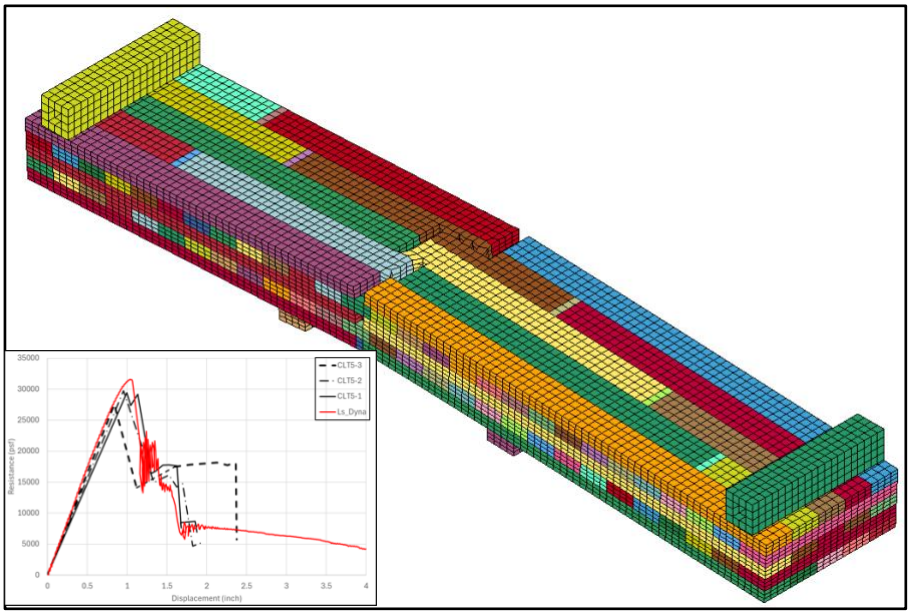

Figure 2 – CLT Beam Modeling Approach and Comparison with Test Data

The ballistic performance of composite walls made of 3D printed concrete

Richard Dekker[1], Dieter van der Pol[1], Erik Carton[1] , Elfi van Zeijl[1] and Hugo Dijkers[1]

[1]*TNO – Defence, Safety and Security, Den Haag, Netherlands*

Additive or digital concrete manufacturing is increasingly used in the construction of buildings. Sculptures, bridges, industrial buildings and houses have already been constructed from 3D printed concrete (3DPC). Additive manufacturing of concrete structures can also be of interest for military applications in remote and potentially hostile areas. However, printing with locally sourced materials is still an ongoing research topic, as the mechanical properties and printability of 3DPC depend highly on the mortar constituents. Therefore, pre-mixed externally sourced materials are still needed, which increases the costs and worsens the environmental impact. Innovative composite wall solutions can aid to reduce the required amount of pre-mixed material for 3DPC by incorporating local filler material. At the same time, composite walls may offer interesting protective design solutions. Together, such composite solution can help overcome some critical downsides of 3DPC in military applications.

This research is a continuation of the work performed by Dijkers et al. [1], who investigated the ballistic resistance of blocks made of regular cast concrete and 3DPC with and without polyvinyl alcohol (PVA) fibres against 12.7 mm AP M2 projectiles. Dijkers et al. found that the blocks made from regular cast concrete showed the highest ballistic performance in terms of residual velocity, which was most likely due to the presence of aggregates. On the other hand, the fibre-reinforced 3D printed concrete showed the least amount of damage, which is generally considered positive for the multi-hit performance.

In the current research, different 3DPC hollow blocks are filled with widely available sand and gravel, and their ballistic performance is compared to blocks with regular cast concrete filling. The hollow blocks have either one or two sand/gravel filled cavities. The 3D printed mortar is reinforced with PVA fibres in order to increase the material toughness, thereby reducing the size of the damage zone and enhancing the multi-hit performance. For the purpose of making a fair comparison, all the wall configurations are given the same areal density. The goal is to

identify the most efficient wall configurations to resist the impact of a 12.7 mm AP M2 projectile in terms of residual velocity and damage area.

Keywords: 3D printed concrete, ballistic testing, composite wall

[1] Dijkers, H.P.A, (2023). Material characteristics of 3D printed concrete subjected to highly dynamic loading, 6th International Conference on Protective Structures (ICPS6)

Projectile impact behaviour of geopolymer-based ultra-high performance concrete (G-UHPC)

Kefo Qu [1 2], Jian Liu [1 2]

[1] *Earthquake Engineering Research and Test Center, Guangzhou University, Guangzhou 510405, China*

[2] *Key Laboratory of Earthquake Resistance, Earthquake Mitigation and Structural Safety, Ministry of Education, Guangzhou 510405, China*

Geopolymer-based ultra-high performance concrete (G-UHPC) represents a novel advancement in UHPC, developed to address the growing demand for ultra-high-strength, cost-effective, and environmentally friendly construction materials. This study provides a preliminary investigation into the dynamic response of fibre-reinforced G-UHPC slabs under projectile impact. Experimental tests were conducted to evaluate the anti-penetration performance of G-UHPC slabs reinforced with 1.8% steel fibres, achieving a compressive strength of 128 MPa. The slabs, measuring 400 mm × 400 mm in plan dimensions, were fabricated with thicknesses of 50 mm, 75 mm, 100 mm, and 150 mm. The projectile, manufactured from 40CrNiMoA steel, had a diameter of 25 mm, a length of 110 mm, and a mass of approximately 330 g, with a calibre-radius-head (CRH) ratio of 3. It was launched using a light gas gun at a striking velocity of approximately 350 m/s. Key experimental data included residual projectile velocity, penetration depth, crater diameter ($d_{c,f}$), scabbing diameter ($d_{c,r}$) and mass loss of the slabs. The results were analysed to evaluate the applicability of existing empirical and semi-empirical formulas for predicting the penetration and perforation behaviour of G-UHPC slabs. Numerical models simulating projectile penetration into G-UHPC slabs were developed and validated against the experimental findings.

Keywords: Geopolymer-based ultra-high performance concrete (G-UHPC), Projectile impact test, Empirical and semi-empirical formulae, Numerical model.

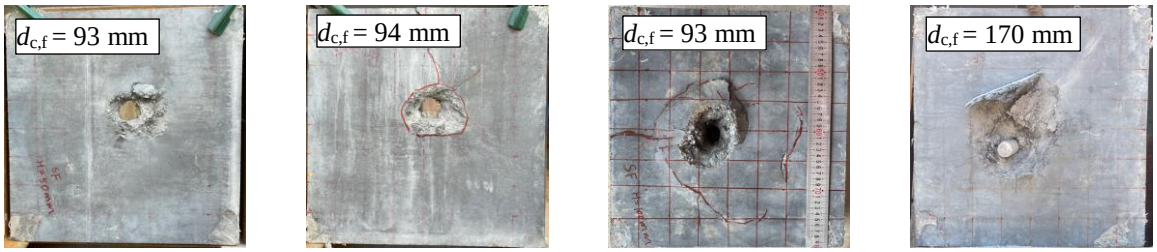

(a) SF-50-348 (b) SF-75-346 (c) SF-100-343 (d) SF-150-352

Figure 1 Crater damage of G-UHPC slabs after projectile impact

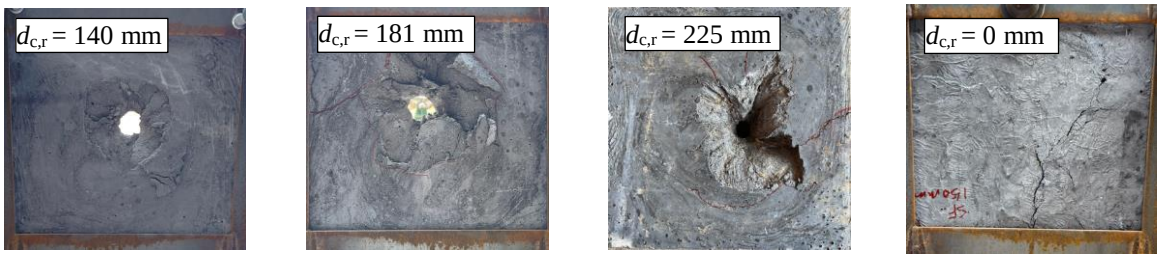

(a) SF-50-348 (b) SF-75-346 (c) SF-100-343 (d) SF-150-352

Figure 2 Scabbing damage of G-UHPC slabs after projectile impact

Restraining Effect for Scabbing Fragments of RC Slab Subjected to Projectile Impact by Polyurea Resin and Aramid Fiber Sheet

Koki Mori[1], Masuhiro Beppu[1], Hiroyoshi Ichino[1], Koji Harada[2] and Yoshitsugu Goto[3]

[1]*Department of Civil and Environmental Engineering, National Defense Academy, Yokosuka, Japan*

[2]*NISHIMATSU CONSTRUCTION CO., LTD., Tokyo, Japan*

[3]*Denka Company Limited, Tokyo, Japan*

Structural damage caused by the volcano and tornado missiles has been reported. Although occurence probability of the disasters is relatively low, the missiles could cause serious damage to human lives and structures. Therefore, an evaluation of impact resistant performance and reinforcement methods for protective structures against the missiles is necessary. Projectile impact by the missiles generates local failure such as cratering, scabbing and perforation. Scabbing and perforation are unacceptable failure mode because the failures endanger human lives and equipment inside the structures. Mitigation methods for local failure of RC slabs, such as application of the use of fiber reinforced concrete, high-strength concrete, and attachment of steel plates, resins or fiber sheets on the rear surface of RC slabs, have been proposed. In this study, polyurea resin coating and attachment of an aramid fiber sheet were investigated. This study experimentally investigated restraining effect, by the polyurea resin coating and aramid fiber attachment, for scabbing fragments of RC slabs subjected to projectile impact. Impact tests were carried out using an 8.3 kg projectile with an impact velocity of approximately 40-90 m/s. The dimension of RC slab was 1100 mm in length and width, and 150 mm in thickness. Polyurea resin was sprayed and an aramid fiber sheet was attached on the rear surface of the RC slabs. The tensile strength and rupture elongation of polyurea resin were 9.9 MPa and 276%, respectively. The tensile strength and rupture elongation of aramid fiber sheet were 2060 MPa and 2%, respectively. The thickness of the polyurea resin was varied 2 mm and 4 mm. The density of aramid fiber sheet was set 180 g/m^2, 330 g/m^2 and 650 g/m^2. Scabbing of the RC slab without polyurea resin coating and aramid fiber sheet attachment occurred at an impact velocity of approximately 60 m/s. At an impact velocity of approximately 90 m/s, scabbing occurred in 2mm- and 4mm-thick polyurea resin coated RC slabs, but the coating restrained scattering of

fragment in which the 2mm coat was partly ruptured and the 4mm coat was not broken at all. At an impact velocity of approximately 70 m/s, all of the aramid fiber sheet attached RC slabs exhibit scabbing, but the aramid fiber sheet contained the fragments. These results indicated the polyurea resin coating and aramid fiber sheet attachment effectively restrained the scabbing fragments.

Keywords: Local failure, RC slab, Rear surface reinforcement, Polyurea resin, Aramid fiber sheet.

Assessment of precast prestressed concrete beams subjected to blast loading

Anqi Chen[1], Jin Zhang[2] and Gauthier Stiegler [1]

[1]*Arup, London, UK*

[2]*Arup, Singapore*

Precast concrete structures are often viewed negatively in blast design due to the inherent weakness in the continuity of reinforcement in beam-to-column connections. Prestressed precast elements are typically considered too brittle to withstand blast loads. The US Army Corps of Engineers provides some analysis guidance for precast prestressed concrete elements in UFC-3-340-20 and PDC TR-06-08 based on single degree of freedom (SDOF) models, with stricter performance criteria compared to non-prestressed cast in-situ concrete structures. However, current analysis guidance has limitations: (1) simple support is often assumed for precast prestressed elements, and (2) there is no clear guidance for close-in stand-off distances ($Z < 2.0$ m/kg$^{1/3}$).

With the increasing demand for productivity and sustainability benefits of off-site construction, precast concrete elements are becoming the preferred solution for more high-profile projects worldwide. However, these projects often face heightened threats from improvised explosive devices (IEDs). This paper presents a holistic assessment methodology for precast prestressed concrete beams under blast loading, enabling wider application of precast concrete elements in such high-threat environments.

A two-method solution is proposed: (1) a modified SDOF model with generalized support conditions based on connection design for mid to far-range stand-off distances, and (2) a multi-stage detailed finite element model of precast prestressed beam for close-in blast loads. In method 1, the resistance of the SDOF model is determined by considering both the precast beam and its connections based on Component-Based Mechanical (CBM) model [1], leveraging wet or dry precast connections that would have previously been assumed to be pinned in UFC 3-340-02. Due to the highly nonuniform blast load distribution at close-in stand-off distances, method 2 utilizes a detailed finite element model to assess the effects of blast loads on precast prestressed beams. This approach also incorporates CFD for accurate blast load calculations,

providing greater insight into the local response of the prestressed concrete material, its connections, and the prestressing tendons.

Overall, this methodology contributes to the broader application of precast structures in projects subject to blast threats, allowing for greater use of precast concrete elements in structures exposed to explosion risks. This enables the economic and sustainability benefits of precast construction to be realized in a wider range of high-profile development projects.

Keywords: pre-cast, prestressed, close-in blast loading, component-based joint model, advanced SDOF model

[1] Bao, Y., & Tan, K. H. (2023). Experimental and numerical study on performance of precast concrete wet and dry joints under progressive collapse scenario. Journal of Building Engineering, 74, 106739. https://doi.org/10.1016/j.jobe.2023.106739

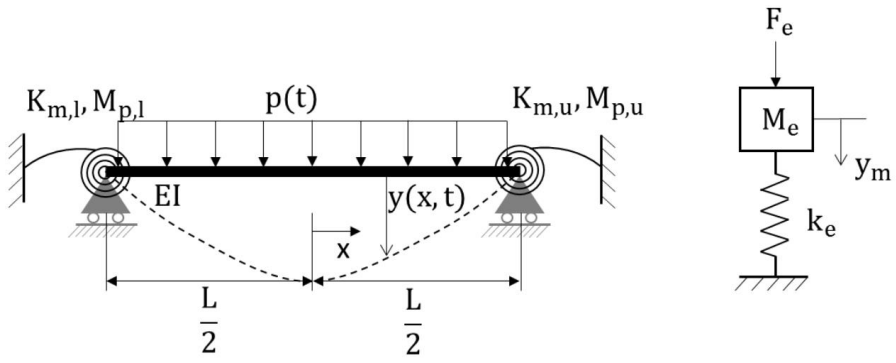

Figure 1 Equivalent single degree of freedom model for precast prestressed element with generalized support conditions

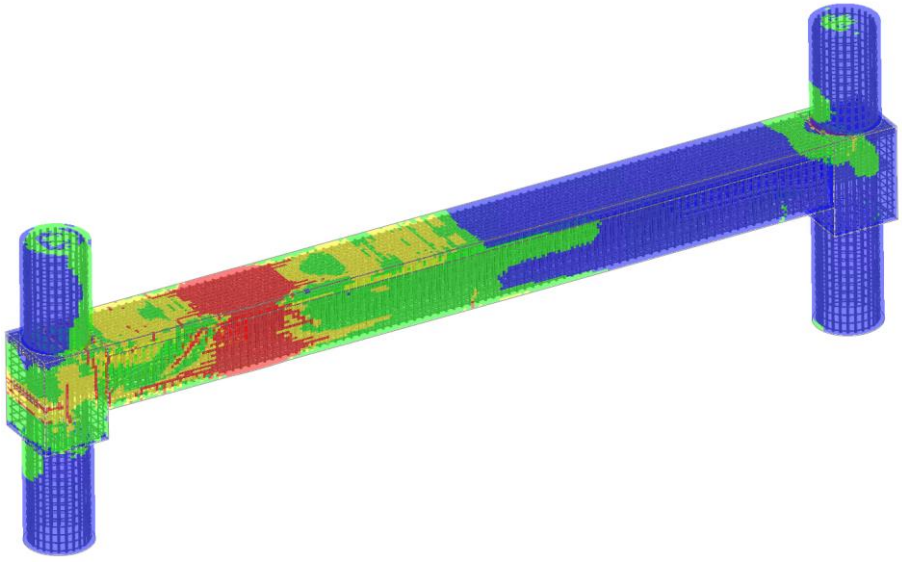

Figure 2 Full detailed precast prestressed concrete beam under close-in blast load in LS-DYNA

A Constitutive Model of Heavyweight Concrete for Blast Simulation

Chunyuan Liu[1], Yifei Hao[1*], Xueqiang Li[1], Siyao Wang[1], Guowei Ma[1]

[1]*School of Civil and Transportation Engineering, Hebei University of Technology, Tianjin, China*

**Presenter. E-mail: yifei.hao@hebut.edu.cn*

Heavyweight concrete (HWC), characterized by a unit weight exceeding 2800 kg/m^3, is essential for nuclear power plants and military installations, due to its superior radiation attenuation properties. Recent conflicts have underscored the vulnerability of such structures under extreme loads, highlighting the urgent need for further analysis, which is currently hindered by the lack of suitable constitutive models of HWC. To address this limitation, comprehensive constitutive studies of HWC with densities ranging from 3000 to 6000 kg/m^3 were conducted and presented in this study. A series of quasi-static tests were conducted. Strength, modulus and other key mechanical parameters were determined. The hydrostatic pressure-volumetric strain relationship, compressive and tensile meridians were established. Impact tests were performed to investigate the dynamic properties of HWC. The true dynamic increase factor (DIF)-strain rate relationships of HWC with different densities were then obtained. Based on the observed mechanical behavior, a constitutive model incorporating plasticity and damage was developed for HWC. To verify and validate the model, TNT blast tests of HWC slabs were conducted, and the results were compared with numerical simulations. The proposed model accurately captured the complex mechanical behavior of HWC and predicted the dynamic response and damage of the HWC slabs. This study contributes a reliable constitutive model for HWC, enabling more accurate predictions of blast response and improved design of protective structures.

Keywords: Heavy weight concrete, mechanical behavior, constitutive model, blast loading

Investigation into the Effects of Blockage and Frangible Tunnel Sections on Blast Pressure Profiles

Aljo Jose[1], Chris Taggart[1], John Adams[1]

[1]*AWE, Aldermaston, Reading, Berkshire, RG7 4PR, United Kingdom*

AWE is tasked with substantiating the performance of numerous systems in diverse environments. Often this involves both experimental trials and numerical analysis undertaken in an integrated manner. One area in which this approach has been applied is the assessment of structural response to blast loading. Experimental testing is undertaken using blast tunnels/tubes to generate surrogate environments and obtain appropriate load profiles. AWE's Air Blast Tunnel (ABT) – a unique facility for generating large-scale long duration blast waves – is commonly employed for this purpose. Modelling activities, including finite element analysis (FEA), hydrocode analysis and engineering calculations, are performed in conjunction with the trials to optimise their output. Data collected during the tests is subsequently exploited to facilitate model validation. Validated models are then used to study the true environments of interest.

To complement the ABT and provide a facility in which new and novel test methods and technologies can be explored, the 'Mini Air Blast Tunnel' (MABT) was designed and constructed by AWE. One of the first applications of this facility was to support exploration of methods to engineer blast profiles and scale to larger tunnels; an area of ongoing interest. 18 shots were fired with various configurations of frangible section and/or tunnel blockage to study their effect on the blast profiles obtained. This study was accompanied by complementary analysis employing coupled Fluid-Structure Interaction (FSI). Pressure data recorded during the experimental trial were used to validate the model prior to it being exploited to consider further configurations that were not tested. The analysis revealed the influence of the thickness and strength of the frangible section on pressure-time histories within it, as well as the impact of blockage on increasing load on the test item in addition to the internal radial load applied to the tunnel structure.

An overview of the trial and modelling activities will be provided whilst highlighting key similarities and differences between model and test results. The challenges and limitations encountered in the study and its potential future direction will also be discussed.

Keywords: Blast Tunnel, Hydrocode Modelling, FEA, Fluid Structure Interaction

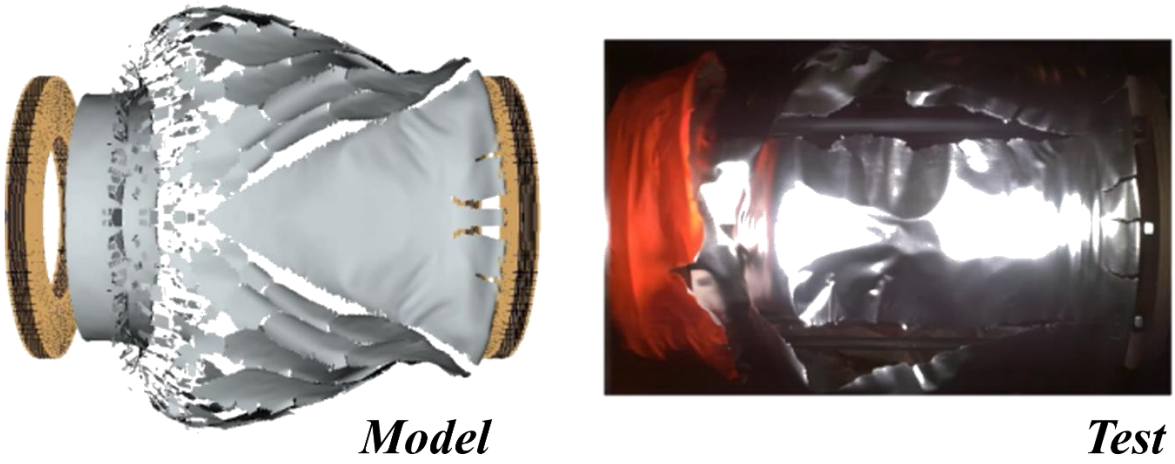

Figure 1: Model to test comparison of frangible tunnel section

Figure 2: Setup of frangible section attachment to the Mini Air Blast Tunnel

Numerical Investigation of Hydrogen Leakage Dispersion and Explosion Consequences under Coupled Factors at Refueling Stations

Yanchao Shi[1], Ziyu Zhong [1], Zhong-Xian Li[1] and Jian Cui[1]

[1]*School of Civil Engineering, Tianjin University, Tianjin, China*

Hydrogen refueling stations are crucial for the supply of hydrogen energy. However, incidents of leaks and explosions at these stations continue to occur sporadically. This study establishes numerical models based on real-world hydrogen refueling stations to investigate the evolving patterns of hydrogen clouds induced by hydrogen leakage under the combined influence of wind speed and leak angles, identifying the formation of worst-case scenarios and analyzing the explosion consequences based on these scenarios. The results indicate that as leak angles and headwind speeds increase, the effective volume of flammable clouds within the refueling station initially increases before decreasing. Leak angles dominate in the combined effects, and the fitted response surface shows high confidence in predicting flammable cloud volumes. The ignition location significantly impacts overpressure within the scenario; ignition at the unbounded edge of the gas cloud results in the most destructive outcomes and produces maximum overpressure on the constrained side. This research provides valuable insights for assessing the risks of leaks and explosions at hydrogen refueling stations and offers guidance for mitigating explosion-related consequences.

Keywords: Hydrogen refueling station, Hydrogen leakage, Hydrogen diffusion, Hydrogen explosion, Response surface methodology, blast overpressure

An experimental investigation on the low velocity impact response of novel thermoplastic and thermoset sandwich composite structures

Laila Alhadary, Mahmoud Mohamed, Haibin Ning, Selvum Pillay

The University of Alabama at Birmingham, Birmingham, Alabama, USA

Sandwich composites structures are extensively used in a various of applications and industries due to their distinct advantages such as high strength to weight ratio. While they are primarily designed are designed to resist bending loads, they also exhibit excellent energy absorption capabilities. Their ability to absorb substantial impact energy from a blast while maintaining structural integrity make them a preferred choice for applications such as military shelters and aerospace vehicles where blast resistance is critical.

This study presents a comparative experimental study on the low-velocity impact behavior of thermoplastic and thermoset sandwich composite structures. The thermoplastic sandwich panel (TP-SP) consists of E-glass fiber reinforced polypropylene prepreg face sheets and thermoplastic syntactic foam as the core material. The formulation of the thermoplastic syntactic foam consists of Adflex resin, polypropylene polymer, micro glass balloons, and some other additives. In contrast, the thermoset sandwich panel (TS-SP) is composed of woven E-glass reinforced polyurethane face sheets and a polyurethane core foam. In thermoplastic sandwich panel (TP-SP), the thermoplastic syntactic core was initially manufactured using extrusion compression molding process. Next, the prepreg for the bottom face sheet were stacked into the mold in a 0/90 configuration, followed by the placement of the preformed core. The prepreg for the top face sheet is then stacked into the mold in the same 0/90 configuration. Finally, the complete assembly was placed into a press, followed by the application of heat and pressure (see figure 1). For the thermoset sandwich panel (TS-SP), an innovative manufacturing technique was employed during the manufacturing process. The face sheets were first fabricated using vacuum assisted resin transferred molding (VARTM) process. After curing, the two face sheets where held together using 3D printed spacers. Finally, a polyurethane foam was poured between the two face sheets allowing it to expand and cure forming the thermoset sandwich panel (TS-SP) (see Figure 2). Thermoplastic and thermoset sandwich composite panels were manufactured to the size of 12” x12” with comparable core and face sheets thicknesses to ensure a fair comparison. The sandwich panels were cut, and low velocity impact tests were performed

in accordance with ASTM D7136. Several low velocity impact tests were performed using different impact energies. Damage was characterized and maximum peak load was recorded after the test. Various failure modes were observed in the sandwich structures, including fiber breakage, matrix cracking, foam crushing, and debonding. The results of this study are presented with consideration of the advantages of both systems for strategic energy absorption applications for protective structures.

Keywords: low-velocity impact, thermoplastic, thermoset, sandwich composite, glass fiber, low velocity impact test.

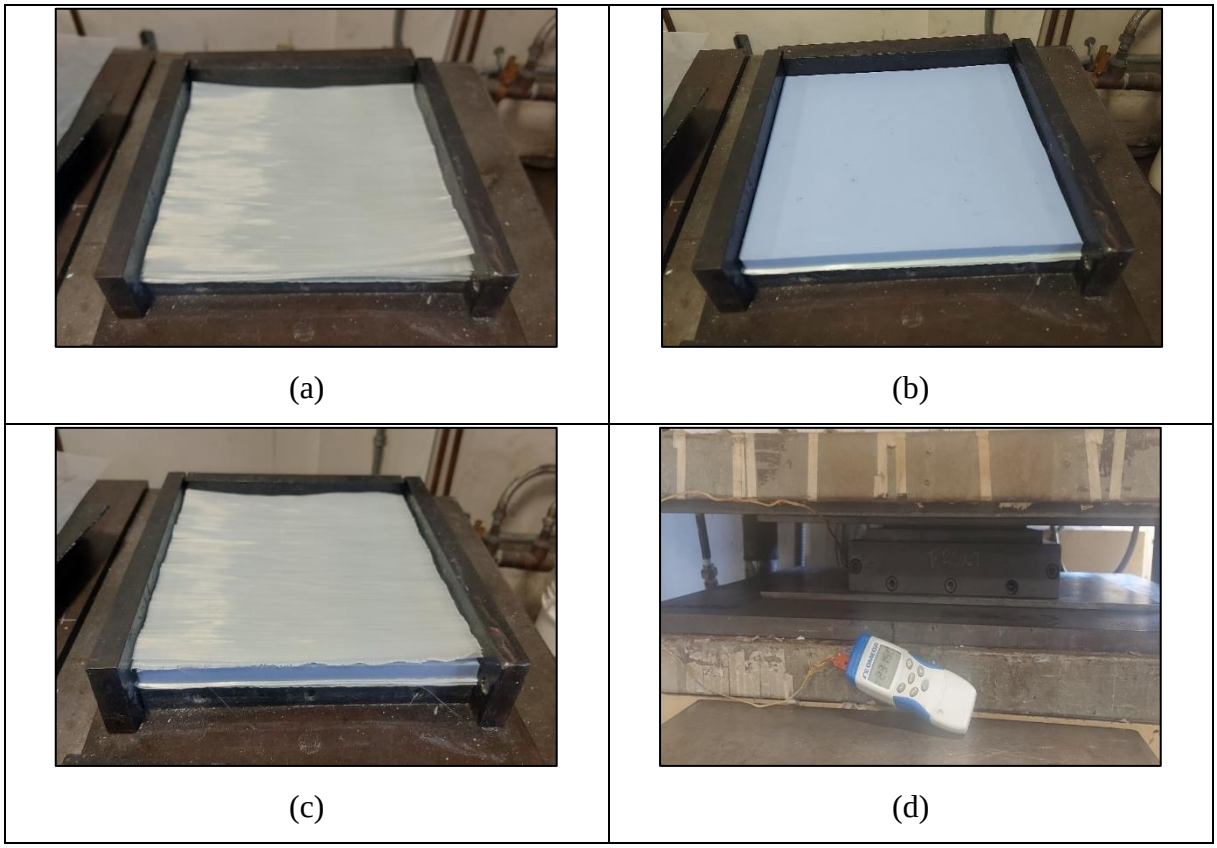

Figure (1) manufacturing steps of thermoplastic sandwich panel (TP-SP). (a) Stacking Bottom face sheet, (b) adding preformed core, (c) Stacking top face sheet, and (d) consolidating sandwich panel in press.

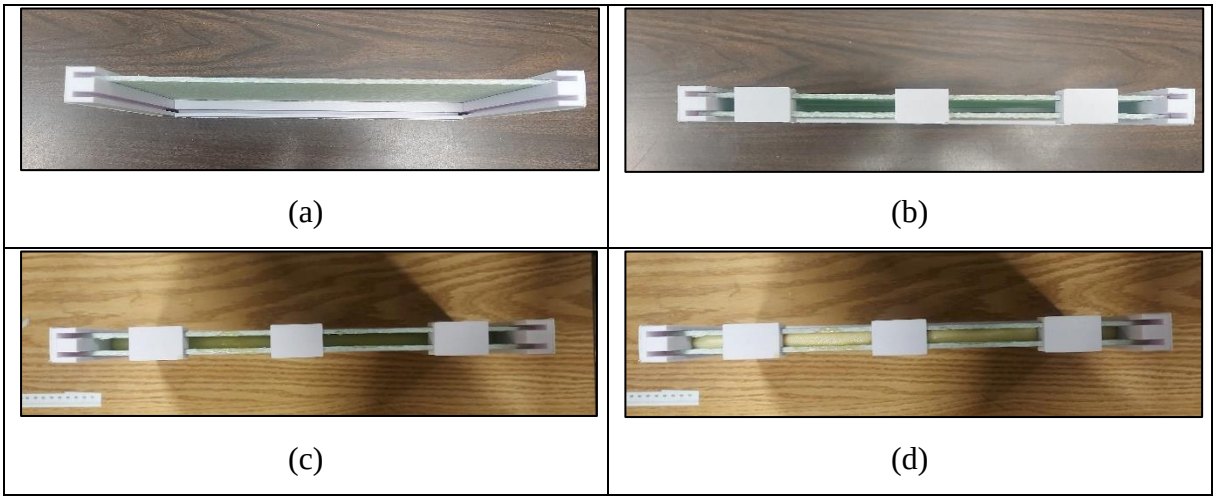

Figure (1) manufacturing steps of thermoset sandwich panel (TS-SP). (a) face sheet installation into 3D printed spacers, (b) both face sheets hold in place, (c) PU foam poured, and (d) Foam expansion.

Submission ID: 5813
(Full Paper)

7th International Conference on Protective Structures (ICPS7)
12th – 15th May 2025, Abu Dhabi, UAE

DYNAMIC RESPONSE OF BFRP BARS SUBJECTED TO IMPACT LOADING AT HIGH STRAIN RATES

Zeinah Elnassar
PhD student, Materials Science and Engineering program, American University of Sharjah, Sharjah, UAE, g00062755@aus.edu

Maen Alkhader
Professor, Department of Mechanical Engineering, American University of Sharjah, Sharjah, UAE, malkhader@aus.edu

Farid Abed
Professor, Department of Civil Engineering, American University of Sharjah, Sharjah, UAE, fabed@aus.edu, (corresponding author)

ABSTRACT
Fiber-reinforced polymers (FRP) bars have gained widespread recognition as a viable alternative to steel reinforcement in concrete structures over the past decades due to their advantages in corrosion resistance, durability, and lightweight properties. However, existing research and current design codes do not adequately address the dynamic compressive response of FRP bars under high-impact loading conditions. This gap in knowledge presents a significant challenge in accurately predicting the response of FRP-reinforced structures under extreme loading events. Therefore, it is essential to investigate the response of FRP bars under dynamic loading conditions across a range of strain rates to improve design codes and ensure the reliability and safety of structures subjected to such conditions. This study presents an experimental program conducted on basalt FRP (BFRP) bars subjected to dynamic testing using the Split Hopkinson Pressure Bar (SHPB) apparatus. The 12-mm BFRP bars are subjected to impact loading at high strain rates ranging from 400 to 770 s^{-1}. These varying strain rates are achieved by adjusting the pressure of the impact bar. A high-speed camera is employed to capture the failure mechanisms and provide visualization of the deformations during loading. The study focuses on evaluating the stress-strain relationship and failure modes of the tested BFRP bars under various loading rates. The results revealed that at higher strain rates of ~770 s^{-1}, BFRP bars lost 40% of its compressive strength when compared to its quasi-static strength (tested at 0.00035 s^{-1}). At lower strain rates (~400 s^{-1}), 20% of the quasi-static strength is lost. At intermediate strain rates (~580 s^{-1}), one sample showed a strength reduction of 10%, while another sample showed a strength gain of 10%. This proves that BFRP bars are highly strain-rate dependent. Additionally, the results show relatively significant variation in the behavior of the samples at similar strain rates, indicating microstructural differences between them.

Keywords: Dynamic, Impact, BFRP, Strain rate

INTRODUCTION

Steel reinforcement corrosion is among the most significant durability issues affecting reinforced concrete structures. Chloride ions, commonly originating from marine environments or de-icing salts, can migrate through the concrete and reach the reinforced steel bars. When chlorides accumulate around the reinforcement, they disrupt the protective oxide layer on the steel surface, even in high pH environments, which leads to pitting corrosion of the steel rebars [1]. The expansion of corroded steel leads to spalling of the concrete cover, ultimately compromising the structural capacity and shortening the lifespan of the structure. To address this issue, replacing conventional steel rebars with non-corrosive reinforcement materials has been widely explored. The non-metallic fiber-reinforced polymer (FRP) bars have attracted attention as an effective alternative due to their corrosion resistance. In addition to their noncorrosive properties, FRP bars offer advantages such as low density and a high strength-to-weight ratio [2]. FRP bars are commonly manufactured using glass, basalt, carbon, or aramid fibers. FRP properties are influenced by various factors such as the type and orientation of the fibers, the volume of fibers used, the type of resin, and the level of quality control applied during manufacturing [3].

FRP composites differ significantly from traditional steel reinforcement in their mechanical behavior. Unlike steel, which shows inelastic and ductile performance, FRP bars exhibit a linear elastic manner until failure, leading to a brittle failure [4]. As a result, the conventional ACI 318 design code [5] is not applicable to FRP-reinforced concrete. To accommodate these differences, a separate design guideline, ACI 440 [6], was introduced to address the unique behavior of FRP-reinforced structures. However, ACI 440 does not currently cover the dynamic compressive performance of FRP bars under high-impact loading. More specifically, the research on BFRP bars is even more scarce [7]. This study seeks to address this gap by experimentally investigating the dynamic response of sand-coated BFRP bars under varying strain rates.

Numerous studies have explored the long-term performance and durability of BFRP bars embedded as internal reinforcement in concrete structures [8,9]. El Refai et al. [8] studied different types of BFRP bars, specifically ribbed and sand-coated, by performing pullout tests after subjecting the bars to harsh environmental environments. The results demonstrated the promising performance of BFRP bars as reinforcing materials. Sand-coated BFRP bars demonstrated superior bond strength, better adherence to concrete, and reduced slippage at peak stress levels in comparison to ribbed bars. Moreover, elevated temperatures up to 80°C had a minimal impact on their bond strength. Elgabbas et al. [9] studied the tensile behavior of BFRP bars after being immersed in an alkaline solution at 60°C for up to 3000 hours to replicate concrete-like conditions. The findings showed that the basalt fibers and resins remained unaffected by the conditioning process. The observed reduction in strength was attributed primarily to degradation at the fiber–matrix interface.

To evaluate the mechanical properties of BFRP-reinforced concrete structures, Alkhraisha et al. [7] studied the flexural strength of concrete beams reinforced with BFRP bars under severe exposure conditions. The results showed that that the exposure did not notably impact the strains experienced by the BFRP reinforcement. Strain values were consistent across all BFRP beams with comparable reinforcement ratios, irrespective of the exposure conditions. As for columns reinforced with BFRP bars, results showed that these columns exhibited only 17% less strength than their steel-reinforced counterparts [10].

MATERIALS AND EXPERIMENTAL PROCEDURE

To assess the dynamic response of BFRP bars under high strain rates, the Split Hopkinson Pressure Bar (SHPB) apparatus was used (Figure 1). In this setup, a stress wave generated by the impact of a striker bar

propagates through the incident and transmission bars to apply controlled high strain-rate loading to the specimen.

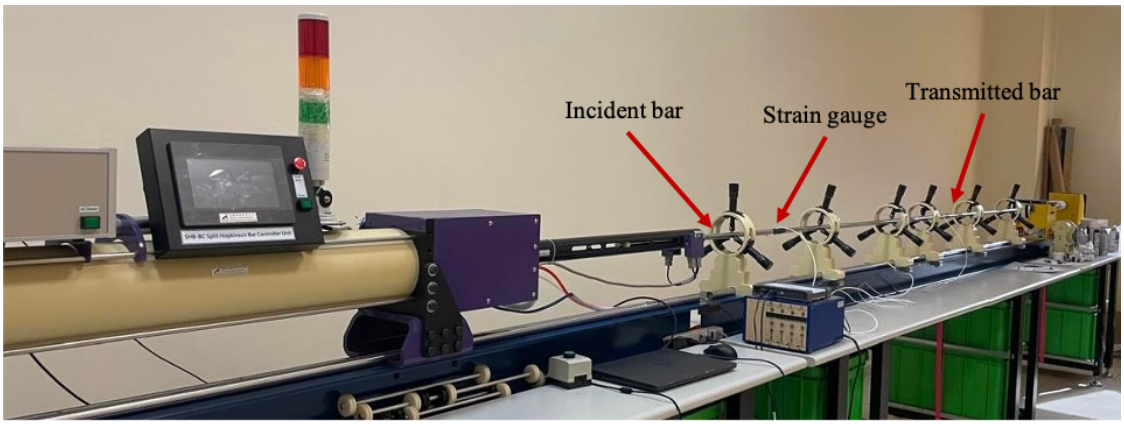

Figure 1. SHPB test set-up

All the BFRP specimens studied in this research have identical dimensions, with both length and diameter equal to 12 mm. A BFRP sample is shown in Figure 2, with its material properties summarized in Table 1.

Figure 2. BFRP bar sample

Table 1. BFRP bar material properties [7]

Diameter (mm)	Length (mm)	Area (mm^2)	Ultimate tensile strength (MPa)	Modulus of elasticity (MPa)
12	12	121.3	1118.6 ± 31	46.6 ± 1.7

The experimental program (Table 2) includes four BFRP samples. Sample B1 is characterized by a lower strain rate of 400 s^{-1}, while B2 is tested at a higher strain rate of 770 s^{-1}. Two additional samples, with similar properties, are tested to simulate an intermediate strain rate of 580 s^{-1}.

The stress-strain results for samples B1 and B2 are presented in Figure 3. Compared to the quasi-static compressive strength of BFRP at room temperature (500 MPa) [11], sample B1 exhibited a 22% reduction in strength, whereas sample B2 showed a 38% reduction. Another noteworthy difference in the stress-strain response is the sudden drop in stress observed in the sample subjected to the lower strain rate (B1). This behavior is attributed to local deformations occurring under low-speed impact. In contrast, sample B2

showed no indication of local failure, likely due to the effect of inertia at high-speed impact, which suppresses localized deformation.

Table 2. Experimental program

Bar ID	Striker velocity (m/s)	Pressure (bar)	Strain rate (s^{-1})
B1	9.6	0.25	400
B2	18.4	0.6	770
B3	14	0.4	580
B4	13.8	0.4	575

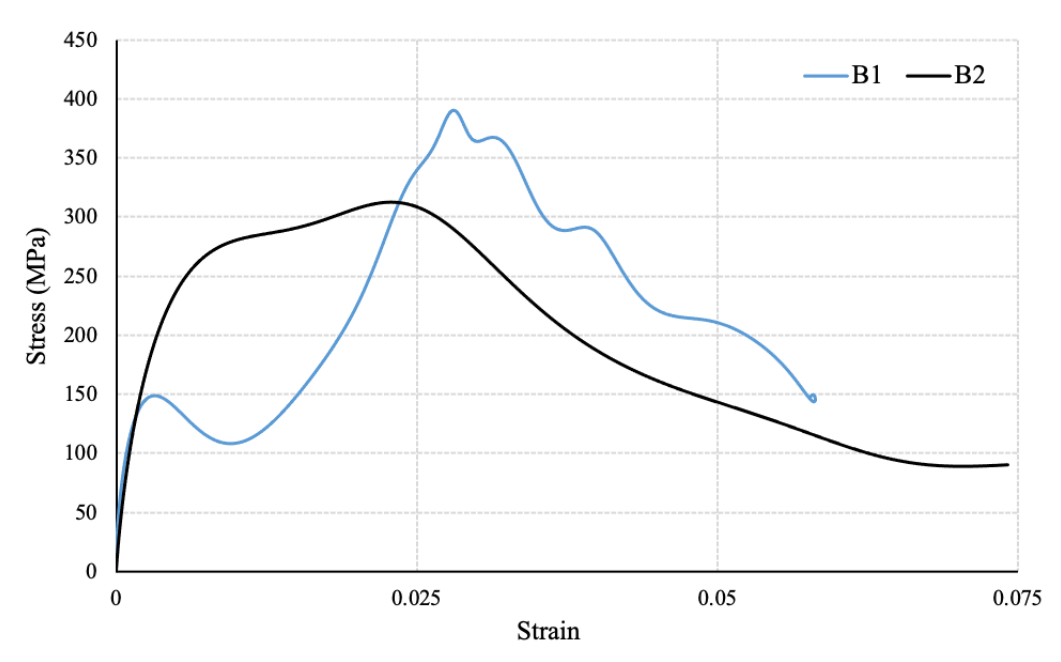

Figure 3. Stress versus strain response for BFRP bars with varying strain rates

Figure 4 and Figure 5 show the deformation at the end of the test for samples B1 and B2, respectively, as captured by the high-speed camera. The failure mode was observed to vary with strain rate. At higher strain rates, severe fragmentation occurred.

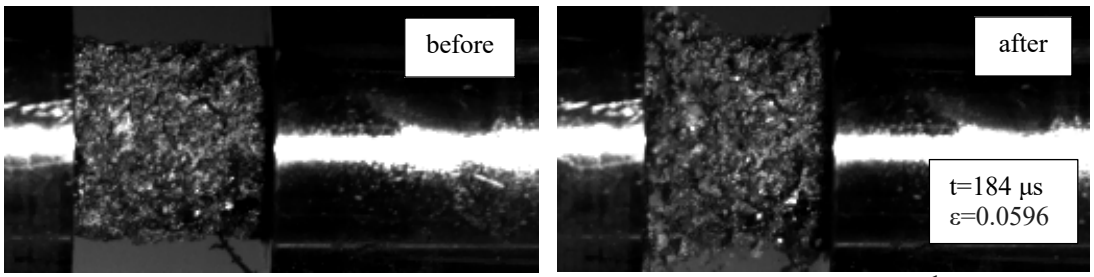

Figure 4. Failure mode at the end of the impact (strain rate = 400 s^{-1}) - B1

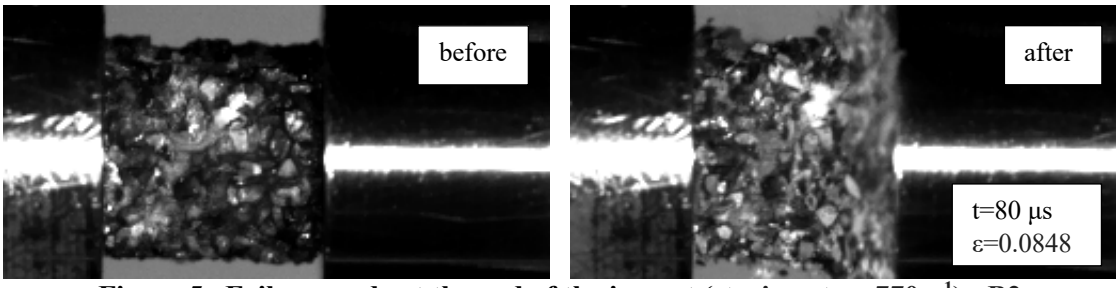

Figure 5. Failure mode at the end of the impact (strain rate = 770 s^{-1}) - B2

Figure 6 shows the stress-strain response of two bars tested at the same intermediate strain rate of 580 s^{-1}. Despite having similar properties and testing conditions, the results reveal a noticeable difference between the two samples. Sample B3 gained 10% additional strength compared to the quasi-static tests, while sample B4 showed a 10% reduction. This significant variation between bars made from the same material and tested under similar conditions suggests the presence of microstructural differences between the samples. Therefore, testing a larger number of specimens is necessary to ensure reliable and consistent results. Aside from the strength variation, both stress-strain curves follow the same general trend.

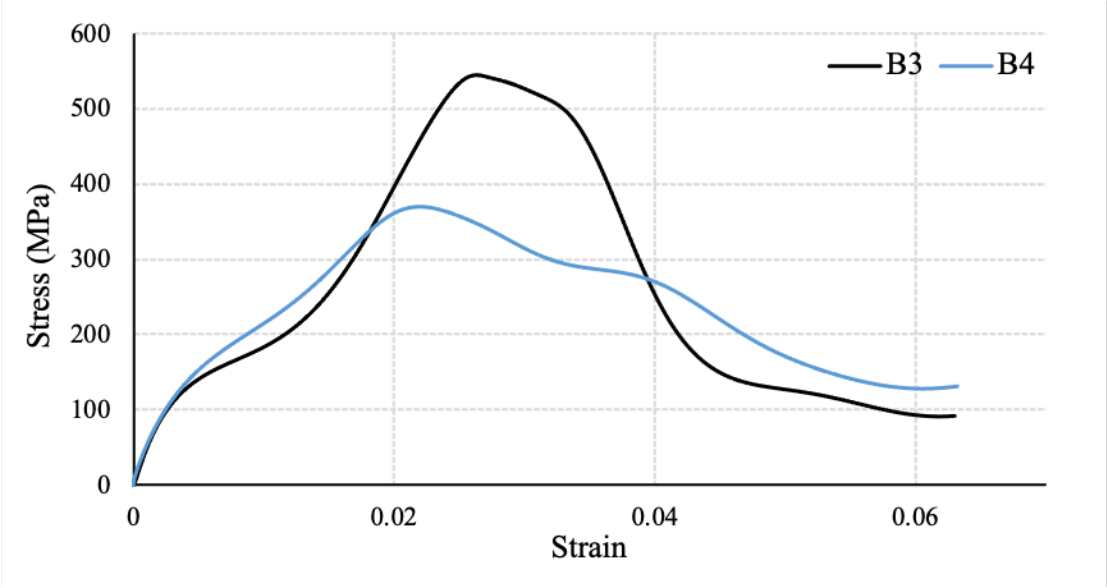

Figure 6. Stress versus strain response for BFRP bars with intermediate strain rates

CONCLUSIONS

This study examined the dynamic compressive behavior of sand-coated BFRP bars under high strain rates using the Split Hopkinson Pressure Bar (SHPB) apparatus. Results showed a clear strain rate dependency, where strength reductions increased with higher strain rates, reaching up to 40% at approximately 770 s^{-1} and 20% at around 400 s^{-1}. At intermediate strain rates (~580 s^{-1}), inconsistencies between samples indicated possible microstructural variations, despite identical testing conditions.

Failure modes also varied with strain rate, where samples tested at lower rates were more prone to local deformation, while those tested at higher rates suffered more fragmentation. These findings highlight the need to incorporate strain-rate effects into design codes and emphasize the importance of testing a larger number of specimens for reliable characterization.

REFERENCES

1. Gowripalan N, and Mohamed HM (1998) Chloride-ion induced corrosion of galvanized and ordinary steel reinforcement in high-performance concrete. *Cement and Concrete Research* 28(8): 1119-1131.
2. Feng G, Zhu D, Guo S, Rahman MZ, Jin Z, and Shi C (2022) A review on mechanical properties and deterioration mechanisms of FRP bars under severe environmental and loading conditions. *Cement and Concrete Composites* 134: 104758.
3. ACI (American Concrete Institute) (2015) Guide for the Design and Construction of Structural Concrete Reinforced with Fiber-Reinforced Polymer Bars; Farmington Hills, MI, USA.
4. Han S, Fan C, Zhou A, and Ou J (2022) Simplified implementation of equivalent and ductile performance for steel-FRP composite bars reinforced seawater sea-sand concrete beams: Equal-stiffness design method. *Engineering Structures* 266: 114590.
5. ACI (American Concrete Institute) (2019) Building code requirements for structural concrete and commentary. ACI 318-19. Farmington Hills, MI, USA.
6. ACI (American Concrete Institute) (2015) Guide for the design and construction of structural concrete reinforced with fiber reinforced polymer (FRP) bars. ACI 440.1R-15. Farmington Hills, MI, USA.
7. Alkhraisha H, Mhanna H, Tello N, and Abed F (2020) Serviceability and flexural behavior of concrete beams reinforced with basalt fiber-reinforced polymer (BFRP) bars exposed to harsh conditions. *Polymers* 12(9): 2110.
8. El Refai A, Abed F, and Altalmas A (2015) Bond durability of basalt fiber–reinforced polymer bars embedded in concrete under direct pullout conditions. *Journal of Composites for Construction* 19(5): 04014078.
9. Elgabbas F, Ahmed EA, and Benmokrane B (2015) Physical and mechanical characteristics of new basalt-FRP bars for reinforcing concrete structures. *Construction and Building Materials* 95: 623-635.
10. Elmesalami N, Abed F, and Refai AE (2021) Concrete columns reinforced with GFRP and BFRP bars under concentric and eccentric loads: Experimental testing and analytical investigation. *Journal of Composites for Construction* 25(2): 04021003.
11. Abed F, Elnassar Z, Abuzaid W, and Alhoubi Y (2023) Compressive response of GFRP and BFRP bars at different temperatures and quasi-static rates. *Mechanics of Advanced Materials and Structures*, 31(27): 1-8.

Impact Response of Steel Tubular Columns: Role of Axial Load, Connecting member Stiffness, Projectile Mass, and Span Length

Prithvi Sangani[1], and Anil Agarwal[2]

[1]*Research Scholar, Indian Institute of Technology, Hyderabad, Sangareddy, India*

[2]*Associate Professor, Indian Institute of Technology, Hyderabad, Sangareddy, India*

The use of steel tubular columns is on the rise in modern construction due to their excellent structural efficiency. However, these columns are often subjected to impact loads, which makes their behavior under such extreme conditions a critical area of concern. Given that tubular compression members are typically thin-walled members, the magnitude of axial load acting on the member during the accidental impact loading is also likely to significantly influence their impact responses. This study focuses on investigating the effects of projectile impact on steel tubular columns through finite element (FE) analysis. Initially, an FE model was developed and calibrated against benchmark experiments available in the literature. A Johnson-Cook material model was utilized for these tubular sections and implemented in Abaqus for FE simulations. Numerical analyses were performed with a rigid projectile of mass 100 Kg, impacting tubular column at a velocity of 20 m/s.

To comprehensively investigate the behavior of the columns, parameters such as column thickness, cross-sectional shape (circular and square), and axial load levels were varied in FE analysis. The influence of other factors, such as the projectile's mass and the column's span length, was also examined. Results indicate that as column thickness increases, the column's lateral deformation decreases and maximum impact force increases. Increased axial compressive loading resulted in a reduced maximum impact force and increased deformation of the column.

The study also examined the occurrence of negative reaction forces (whiplash effect), particularly in columns with longer spans (see Figure 1). Displacement profile along the span length was used to explain this behavior. Additionally, the reaction force response in columns with longer spans was found to have a more significant delay. This delay can be attributed to the time taken for the stress wave to propagate from the point of impact to the end of the column. A significant discrepancy between impact force and reaction force was observed when a lower mass projectile impacted the column, compared to a higher mass projectile. This indicates that

inertial forces play a predominant role for lower mass projectiles. Furthermore, the effect of alternate load path on column behavior was modeled using a spring that was connected to the column and represented the stiffness of the neighboring elements connected to the column against column shortening. The results indicated that stiffer members reduce damage to the column by providing an alternate load path after the column losses some part of its axial stiffness. However, when the normalized stiffness ratio, which is defined as the ratio of spring stiffness to axial stiffness of the column exceeds 1, no significant increase in impact resistance was observed (see Figure 2).

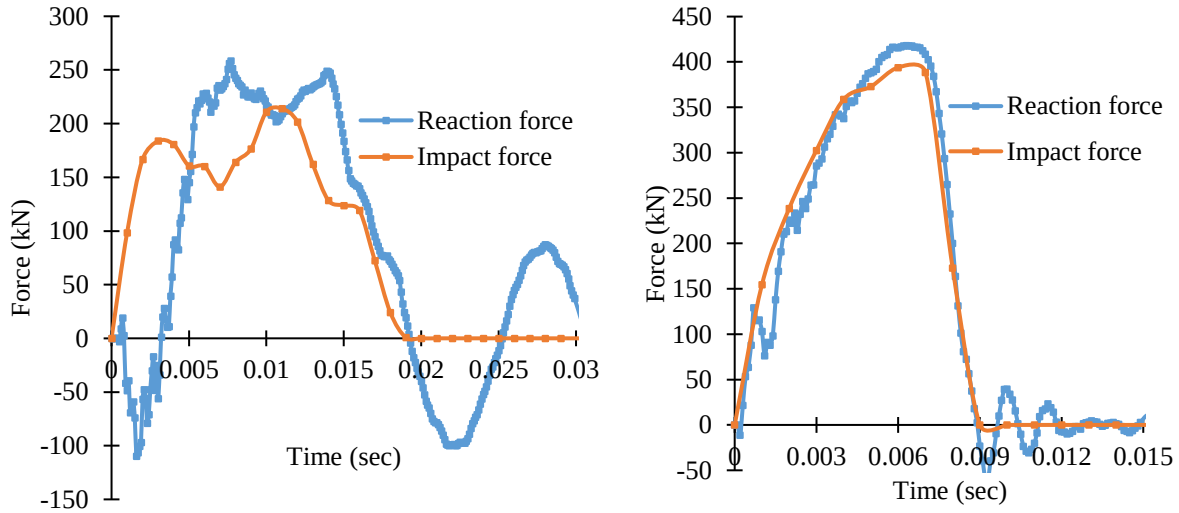

(a) Span 3.6m (b) Span 0.9m

Figure 1. Impact force and reaction force histories for columns with span length of 3.6 m and 0.9 m

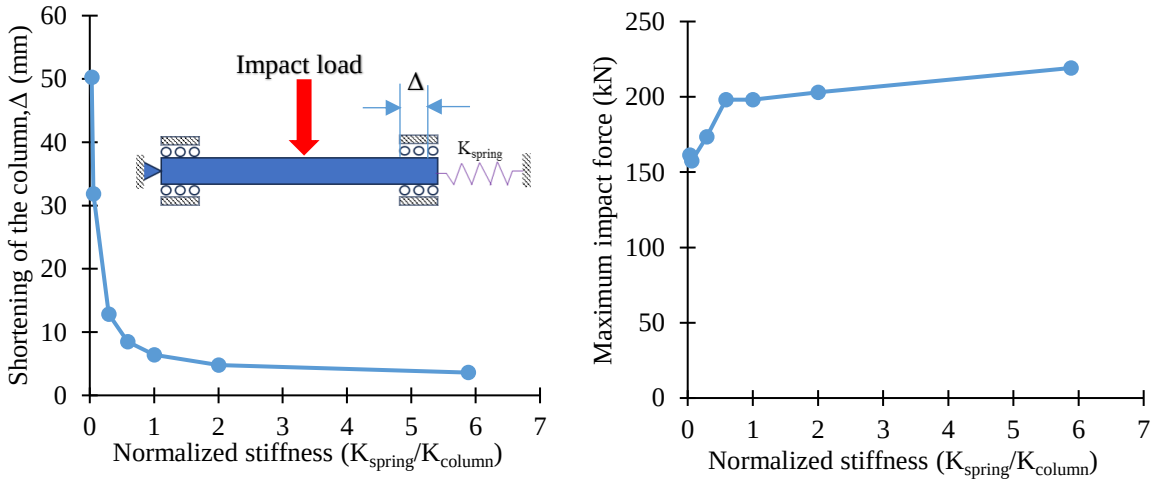

(a) (b)

Figure 2. Influence of normalized spring stiffness on (a) post impact shortening of column and (b) maximum impact force resisted by column

Keywords: Finite element analysis, Johnson-Cook model, Negative reaction force, Rigid projectile impact, Steel tubular columns

SUBTERRANEAN PIPE RESPONSE TO ABOVE-GROUND BLAST: PART 1 – EXPERIMENTAL TESTING

Chris Taggart[1], Alex Rogers[1] and Steve Fay[1]

[1]AWE, Aldermaston, Reading, Berkshire, RG7 4PR, United Kingdom

Numerical modelling and experimental testing are employed extensively to study the response of critical national infrastructure to explosive effects. This may include either super- or sub-terranean equipment subject to explosions initiated either above or below ground. Although considerable data is available in the literature on the response of above ground structures to above ground blast, less work has been conducted to study the response of below ground structures subject to loadings originating from above ground blast.

In view of this, an experimental trial and associated numerical modelling was undertaken to enhance understanding of this type of scenario. This paper will focus on the experimental aspects of this work, a sister paper [1] discusses the related numerical analysis.

The trial was used to generate data on the relative performance of structures when submerged in various media, and to provide validation data for associated numerical modelling activities. Each shot consisted of a spherical PE4 charge suspended above three galvanized steel pipes laterally offset from each other (see Figure 1). The pipes were held off the ground in a steel frame and fixed to the frame by circular brackets at their ends. The media in which the pipes were submerged varied depending on the shot between air, water and dry sand. An enclosure was constructed around the pipes to contain the water and sand in the relevant shots. Suitable charge masses and standoffs distances for each medium were calculated using preliminary numerical modelling to ensure a moderate amount of pipe damage was caused. Trial instrumentation included high-speed video (HSV), free-field pressure sensors and strain gauges. 3D scans of the pipes pre- and post- shot were also taken.

Six shots were initially planned (two per medium), but some unexpected results from the early air shots necessitated further investigation. Ultimately, eight shots were conducted with the pipes in air, two shots with the pipes in water, and two shots with the pipes in dry sand.

The setup proved to be practical, cost-effective, and repeatable. The amount of pipe damage from each shot was appropriate to allow for meaningful comparison to simulation results (see

Figure 2), and the instrumentation fielded enabled quantitative evaluation of modelling output. The data from the trial and the associated modelling provide valuable insight into the effects of different media on the attenuation of above ground blast. They also inform how analysis of similar scenarios can most effectively be conducted in the future.

[1] C. Taggart, A. Rogers and S. Fay "Subterranean Pipe Response to Above Ground-Blast: Part 2 – Numerical Analysis", 7th International Conference on Protective Structures (ICPS 7), Abu Dhabi, 2025.

Keywords: Blast, Trials, Pipes, Structures, Validation, Modelling

Figure 1: Air shot pipe setup pre-firing

Figure 2: Air shot pipes post-firing

Impact Loading of Isotropic Shell-Based Stochastic Cellular Metamaterials Fabricated via Additive-Enabled Casting

Oraib Al-Ketan[1*], Valentina Ortiz[1], Nejc Novak[2], Anja Mauko[2], Lovre Krstulović-Opara[3], Shigeru Tanaka[4], Kazuyuki Hokamoto[4], Reza Rowshan[1], Rashid Abu Al-Rub[5], Matej Vesenjak[2], Zoran Ren[2]

[1] *Core Technology Platforms Operations, New York University Abu Dhabi, Abu Dhabi, UAE*

[2] *Faculty of Mechanical Engineering, University of Maribor, Maribor, Slovenia*

[3] *Faculty of Electrical, Mechanical and Shipbuilding Engineering, University of Split, Split, Croatia*

[4] *Kumamoto University, Kumamoto, Japan*

[5] *Mechanical Engineering Department, Khalifa University, Abu Dhabi, UAE*

Lattice-mimicking structures exhibit promising physical properties. However, they also exhibit highly anisotropic properties. In this work, a design procedure to create shell-based stochastic cellular materials based on implicit functions is presented. Then, samples were fabricated using additive manufacturing – enabled casting process and Aluminum AlSi10Mg alloy. Finite element analyses (FEA) were employed to assess the mechanical properties and isotropy of the designed structures. The samples were then tested under quasi-static and dynamic (impact) compressive loading conditions up to a strain rate of 11000 s−1 to evaluate their mechanical behaviour.

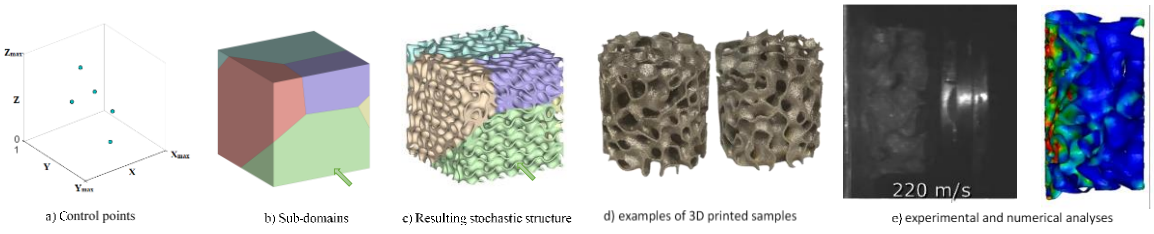

Figure 1. a-c) Design procedure, d) additively manufactured samples, and e) experimental and numerical deformation pattern at high strain rates.

Quasi-static experimental results showed that the stochastic cellular materials exhibit a stretching-dominated mode of deformation where samples deform collectively with no shear band formation. The samples exhibited attractive Specific Energy Absorption (SEA) capacity in the shock deformation mode at a strain rate of 11000 s−1. Thus, the combined proposed design and manufacturing approach has great potential for impact and blast mitigation applications. The developed and validated computational models offered a more detailed analysis of the deformation mechanism and provided means to predict the sample's behaviour at very high strain rates. The current study allows for further investigation of non-metallic and metallic stochastic cellular materials and their deployment in different engineering disciplines.

Micro-CT scan analysis for ballistic cement-based composites

Omar Ba Nabila[1],Felipe Rodrigues[1] ,Ana Jimenez[1]

[1]*Technology Innovation Institute, Masdar City, Abu Dhabi, UAE*

Abstract

Recently, the need for impact resistance in concrete structures has been increasing due to war and terrorism. Common failure mechanisms of concrete structures against firearm attacks can be visualized using X-ray Computed Tomography (XCT). XCT provides detailed microscopic information about concrete quality and aggregate distribution in both two-dimensional and three-dimensional forms. Cement, water, and aggregates (fine and coarse) are the main constituents of concrete. The fine aggregate is sand, while the coarse aggregates include particulate fibers (steel, glass, basalt, etc.). The ballistic impact properties of concrete structures can vary based on the size, shape, aggregate distribution, and volume fraction of these particulate fiber additions in concrete. In this research, gas gun tests were conducted on cylindrical concrete samples in a steel mold with a 300 mm diameter, 300 mm length, and 12 mm thickness, as shown in Figure 1. The samples were tested by armor-piercing projectiles of 12.7 x 99 mm at a velocity of 850 m/s. Four concrete types were tested, namely ordinary concrete, basalt fiber concrete with [insert basalt fiber concentration], steel fiber concrete with [insert steel fiber concentration], and ultra-high-performance concrete. Following that, XCT analysis was deployed for all samples to visualize fiber distribution, voids within the structure, and projectile orientation. Moreover, some issues related to XCT analysis and scanning were highlighted. The XCT analysis results demonstrated steel fiber orientation and distribution. It was possible to measure fiber concentration and voids (including cracks) within the structure. However, it was not possible to detect basalt fibers since they have a similar atomic number to cement aggregates. Moreover, it was challenging to separate cracks from voids and analyze them individually. It is important to investigate the high-impact properties of concrete, particularly ultra-high-performance concrete, to utilize their full potential effectively for defense applications.

Keywords: X-ray Computed Tomography, Concrete, impact, Projectile

(a)Sample in Gas Gun (b) Sample After impact (c) Reconstructed Concrete (XCT)

Figure 1. (a) sample placed inside Gas Gun Chamber with steel mold, (b) Basalt fiber sample after 12.7 AP projectile impact, and (c) Reconstructed Basalt fiber concrete using Avizo software

References

[1] Das N, Nanthagopalan P. Ballistic impact resistance of ultra-high-performance concrete (UHPC): A comprehensive experimental investigation and parametric analysis. International Journal of Impact Engineering. 2024;187.

[2] Taheri-Shakib J, Al-Mayah A. Applications of X-ray computed tomography to characterize corrosion-induced cracking evolution in reinforced concrete: A review. Journal of Building Engineering. 2024;90.

[3] https://www.heidelbergmaterials.co.uk/en/ready-mixed-concrete/technical-information/concrete-constituents.

[4] Dapper PR, Ehrendring HZ, Pacheco F, Christ R, Menegussi GC, Oliveira MFd, et al. Ballistic Impact Resistance of UHPC Plates Made with Hybrid Fibers and Low Binder Content. Sustainability. 2021;13(23).

Kinetic Energy Penetrator (KEP) impact on confined concrete

Hakim Abdulhamid[1], Fabien Plassard[1], Jérôme Mespoulet[1] and Paul Deconinck[1]

[1]*Shock Physics Department, Thiot Ingenierie, 830 route Nationale, 46130 Puybun, France*

Understanding concrete response facing warheads threats is important for both the design of strategic infrastructure protection and the prediction of warhead performances. This ongoing study aims at building a robust approach for the characterization of concrete behavior under ballistic impact of Kinetic Energy Penetrator (KEP). A set of tests has been identified and performed to fit the main parameters of the Johnson Holmquist Concrete (JHC) material model. Highly instrumented tests are conducted to improve the model prediction capability and to identify its limits. After a brief description of the test configuration and the model, the paper focus on the analysis of an impact test and presents the preliminary results from the simulation.

Keywords: concrete, dynamic behavior, impact.

1 Introduction

Design of strategic infrastructures requires the evaluation of its performance against warhead threat. Similarly, the question may also be raised for existing buildings as threats evolve. Predicting the response of concrete under such ballistic penetration and/or blast events requires a model with a good representation of some non-linear phenomena like compaction, cracks and spalling. Due to its rock like behavior, concrete material shows unconventional mechanical behavior since its response is highly depended on pressure (higher pressure leads to higher strength). Meshing choice is also as important; for example, using finite elements may affect the compaction behavior in case of element erosion. Another difficulty for conducting simulation is related to the unavailability of a full set of material. Dynamic characterization data and ballistic tests results are not generally available for a specific concrete. Characteristics of two different batch of concrete may differ especially as they evolve in time and with storage conditions.

Focusing on a KEP impacting a highly confined concrete, this study aims at developing and validating an approach for the development of a concrete model able to predict such event. The model should require a reasonable amount of data for it to be usable in an industrial context. The Holmquist-Johnson-Cook Concrete model (HJC) [1] available in IMPETUS AFEA™ is used. To reduce some sources of uncertainties, both dynamic characterization tests and ballistic impact are realized. All the specimens of the study have been manufactured from the same

batch. The concrete is modelled with recent type of meshless method called γ-SPH that reveals its efficiency in fragmentation and hypervelocity impacts [2]. This paper shows some preliminary results from a ballistic non-perforating impact and its simulation.

2 Concrete modelling

The HJC model has been chosen for its limited number of parameters to reduce the necessary characterization tests. It can be summarized with two main equations: volume strain response (EOS) represented by a pressure compaction relationship and the strength vs pressure dependency of intact and damage concrete. The major phenomena during impact which are the large compaction around the projectile nose and possible spalling of the target back side can therefore be fairly represented. The concrete specimen is represented with γ-SPH elements and the remaining parts are modelled with finite elements.

3 KE penetrator impact test and simulation

The test consists in an impact of a 520 g KEP on a cylindrical concrete specimen 100 mm diameter and 200 mm length. The specimen is inside a metallic jacket of 5 mm thickness to represent the confinement provided by concrete reinforcements. The impact velocity is 400 m/s. A high-speed camera records the event from the top side of the target.

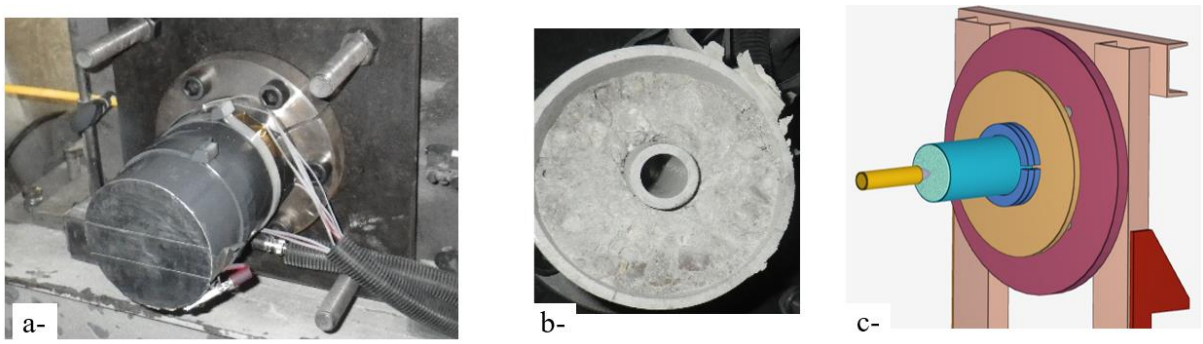

Figure 1. a-Test configuration, b-post-mortem image of the target, c- numerical model

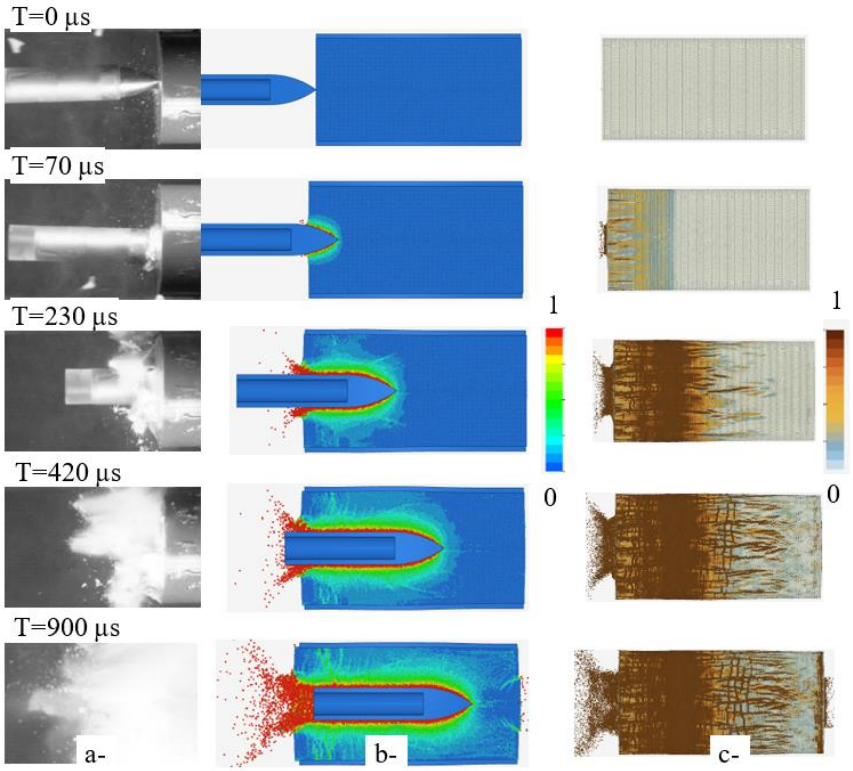

Figure 2. Comparison of test with simulation: a-Images from high speed camera, b-Simulated concrete internal strain, c-Simulated concrete external damage

Figure 1 and 2 compare some experimental data with the simulation. As observed, the front side of the concrete is completely fragmented and ejected from its jacket. The penetrator did not completely perforate the target, the depth of penetration is 160mm. The built model has reproduced similar results (165mm). Large deformation is observed around the penetrator due to a compaction of the concrete. The model also predicts a beginning of spalling forming on the back side of the target which cannot be observed on the impacted specimen. The concrete damage is characterized by diffuse failure on its first half and fewer large cracks on the second half. The diffuse damaged part can be easily ejected from the jacket sometime after the impact. The model projectile deceleration in Figure 3 correlates with the test measurements obtained from the high-speed camera images. The use of γ-SPH discretization is important because it improves the modelling of projectile/target contact interaction. The concrete confinement is better reproduced as no element is deleted.

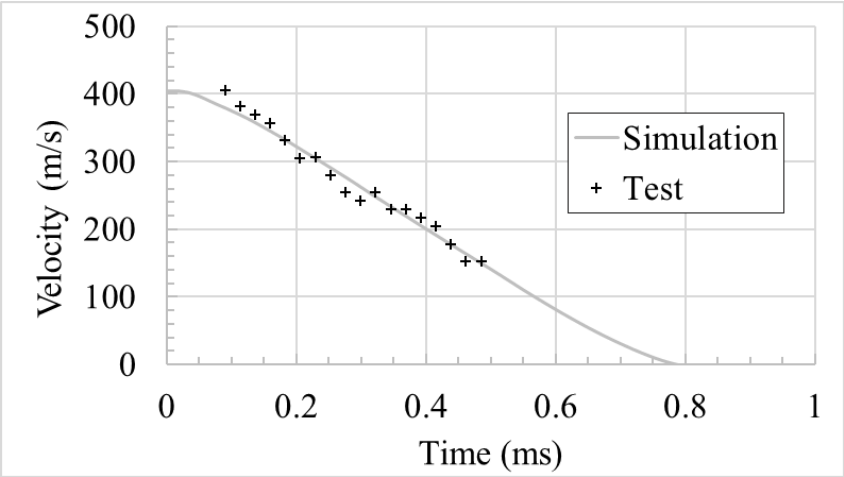

Figure 3. Projectile deceleration during penetration

4 Conclusion

This paper shows some preliminary results of a down scaled KE penetrator impact on highly confined cylindrical concrete. Both characterization tests and hypersonic impact tests are conducted to calibrate and evaluate a numerical model combining a γ-SPH discretization with HJC material model. The first simulations give very good results in terms of penetrator/concrete interaction. Projectile depth of penetration and deceleration are reproduced by the model as well as the concrete damage. In perspective, simulations of all the remaining tested configurations will be conducted to evaluate the residual velocity in case of perforation and the robustness of the model for a range of impact velocity between 300 and 900 m/s.

Acknowledgments

The authors thank Thiot Ingenierie laboratory team for performing all the tests.

References

[1] Holmquist, T.J., Johnson, G.R., Cook, W, (1993). A Computational Constitutive Model for Concrete Subjected to Large Strains, High Strain Rates and High Pressures, 14th Int. Symp. on Ballistics, Québec, Canada.

[2] Collé, A., Limido, J., Villa, J.P., (2018). An Accurate SPH Scheme for Dynamic Fragmentation modelling, 12th International DYMAT Conference, EPJ Web of Conferences, 183, 01030.

Effects of eccentric impacts and corrosion on the structural behaviour of retaining wire ring nets

Francesco Pimpinella[1], Maddalena Marchelli [2] and Valerio De Biagi [1]

[1]*Department of Structural, Geotechnical and Building Engineering (DISEG), Politecnico di Torino, Torino, Italy*

[2]*Department of Environment, Land and Infrastructure Engineering (DIATI), Politecnico di Torino, Torino, Italy*

Anti-Sub-Marine (ASM) nets, also called ring nets, are commonly used as intercepting component. In flexible rockfall barriers, and in general in structures which need to dissipate large amounts of energy, wire ring nets have the role of transmitting the dynamic load to other structural components in a quasi-homogeneous manner, avoiding load concentrations in structural components and providing flexibility to the whole system.

The scientific literature has mainly focused on describing the structural behaviour of single rings, rings chains, and portions of ring nets making use of experimental tests. Numerous analytical models have been introduced at the single ring scale [1][2], eventually being extended and validated on the entire flexible rockfall barrier considering perfectly centered impacts. Existing studies [3] have also shown the possibility to estimate, with good adherence to experimental results, the energy absorption capacity of ring nets by modeling the net by means of fibers, whose properties are derived from experimental tests on three-rings chains. This powerful approach, however, could not take into account the occurrence of eccentric impacts and the influence of ageing on the overall behavior of the net.

In this paper, the equivalent fibers approach was used and improved (where needed) in order to include eccentric impacts. The dynamic impact of a generic mass on the ring net is seen as an imposed displacement of the mass-net contact points. Considering that at each step of the displacement the equilibrium of the forces has to be fulfilled in every direction, the position of the impacting mass at each step can be estimated, both in terms of eccentricity inside the panel and rock inclination. This allows to estimate the forces transmitted to the external flexible boundary (generally constituted by steel wire ropes) by the fibers at each displacement step,

finally identifying the failure. Hence, the force-displacement behaviour and the energy absorbed by the net for a generic impact can be estimated. The existing literature has already tackled the capacity reduction of steel wire rings caused by corrosion and partially correlated the laboratory results to the site conditions [4]. Hence, the effect of corrosion can be considered in this study by modifying the structural behaviour associated to the fibers which simulate the ring net. The model was initially applied on a 3 m x 3 m net panel and validated with experimental tests available in literature with wire ring nets constituted by different number of windings and both flexible and rigid boundary.

Then, the model was applied on a 10 m x 4 m, i.e. a module of a rockfall barrier, for various impacting positions and validated by comparing the obtained results with the outcomes of a numerical model built in Abaqus CAE 2024, where the net is modelled following the equivalent membrane approach [5]. Sensitivity analyses on impact position and net ageing were performed evaluating the effects on the net energy absorption capacity. It is seen that impact eccentricities can cause significant load concentrations and potential local damages; useful indications for the dimensioning of retaining structures are proposed.

Keywords: Analytical model for ring nets, eccentric impacts, corrosion effect

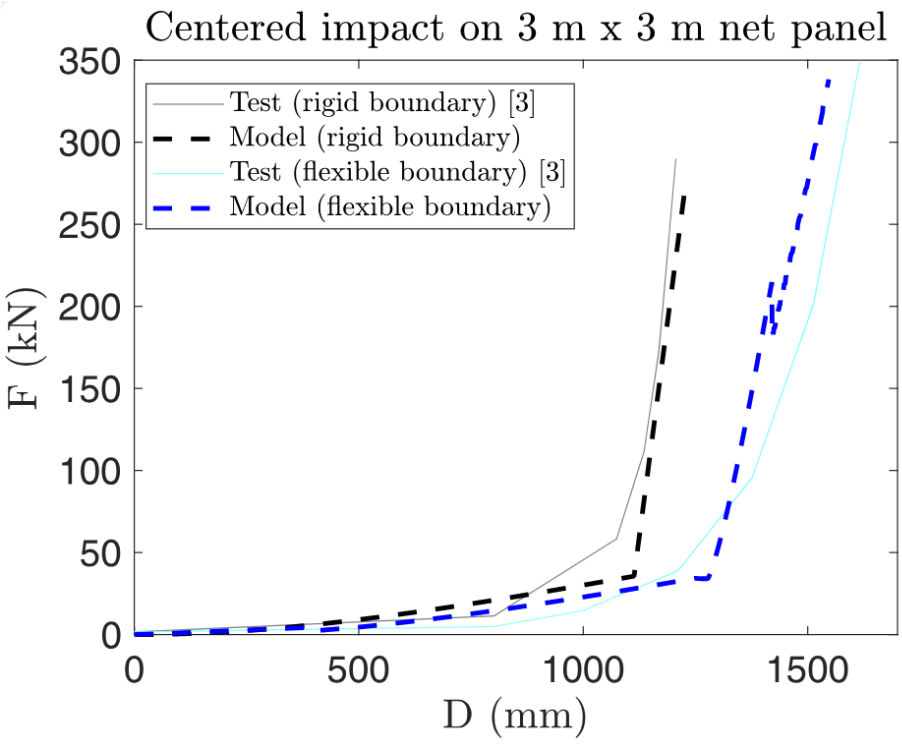

Figure 1 – Application of the fibers equivalent model to a 3 m x 3 m net panel considering ring R5/3/300: the energy dissipated by the wire ring net can be estimated by calculating the area below the load-displacement curve

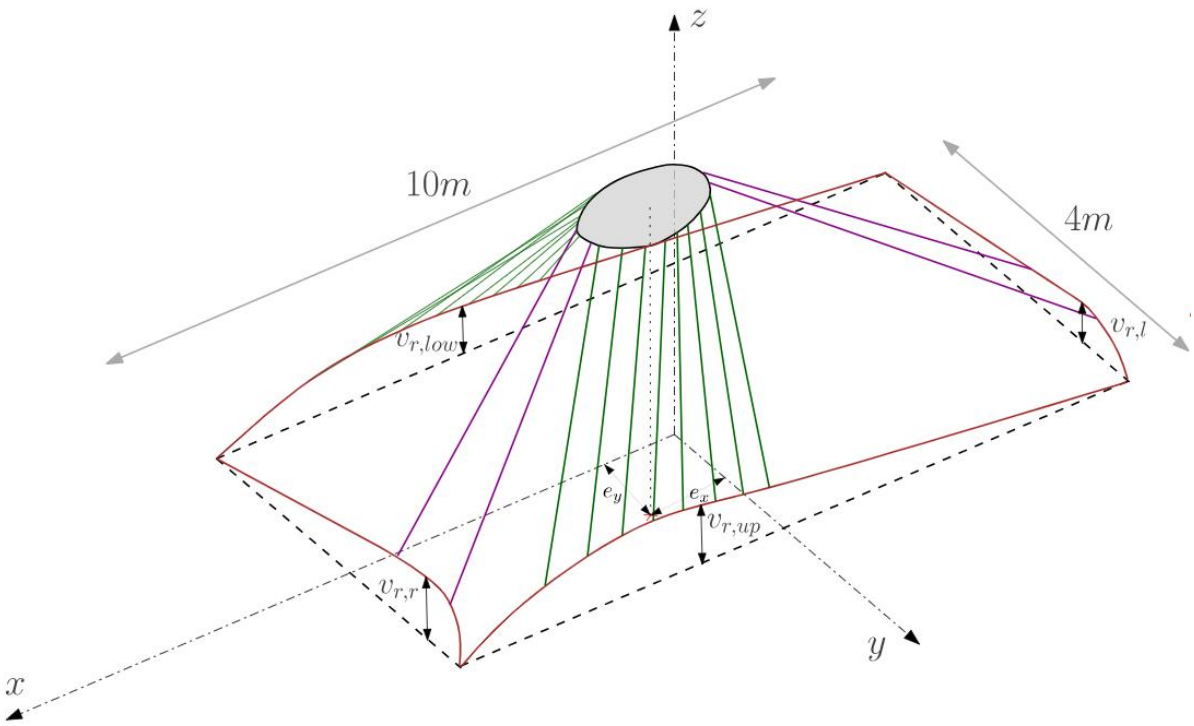

Figure 2 – Graphic representation of the analytical model in case of eccentric impact: the displacement is imposed to the initial points of the equivalent fibers and the wire ropes deflection is calculated at each step with an iterative procedure

[1] Coulibaly, J., Chanut, M., Lambert, S. & Nicot, F (2017). Nonlinear Discrete Mechanical Model of Steel Rings, American Society of Civil Engineers, https://doi.org/10.1061/(ASCE)EM.1943-7889.0001303.

[2] Boulaud, R. & Douthe, C. (2022). A comparative assessment of ASM4 rockfall barrier modelling, Engineering Structures, https://doi.org/10.1016/j.engstruct.2021.113512.

[3] Guo, L., Yu, Z., Jin, Y., Liao, L & Luo, L. (2022). An analytical method for evaluating the deflection and energy absorption capacity of rockfall ring nets considering multifactor influence, Advanced Steel Construction http://dx.doi.org/10.18057/IJASC.2022.18.3.1.

[4] Xu, H., Cheng, Y., Zhao, L., Liu, Y. & Yu, Z. (2024). Experimental Study on Bearing Capacity Reduction of the Steel Wire-Rings in Flexible Barriers Due to Corrosion, Construction and Building Materials, https://doi.org/10.1016/j.conbuildmat.2024.137341.

[5] Jin, H., Yu, Z., Luo, L., Guo, L. & Zhang, L. (2021). A membrane equivalent method to reproduce the macroscopic mechanical responses of steel wire-ring nets under rockfall impact, Thin-Walled Structures, https://doi.org/10.1016/j.tws.2021.108227.

Key Considerations and Methodology for analyzing LVBIED Blast Events on Long-Spanning Roof Diagrid Structures

Author 1 Gabriel Martin[1], Author 2 Laura Cannon [2], Author 3 Simone Vople[3]

[1]*WSP UK, London, United Kingdom*

[2]*WSP UK, London, United Kingdom*

[3]*WSP UK, London, United Kingdom*

This study explores the key and unique considerations and structural impacts of Large Vehicle-Borne Improvised Explosive Device (LVBIED) blast events on long-spanning roof diagrid structures. The case presented involves a complete envelope including a roof structure complete with curtain walling systems, subjected to significant blast loading originating from an LVBIED.

The key objective of the analysis is to assess risk of progressive collapse and to determine the required framing forces to be implemented to ensure structural resilience.

A critical aspect of the study is the behavior of the curtain walling system under blast loading.

As the glass in the curtain wall fails, the blast wave propagates through the resulting openings, exerting both upward and downward blast pressures on the structure. The propagation of the blast across the large roof span takes a relatively long time, which introduces additional complexity in predicting structural response. Potential failure modes include local failures, such as the failure of support elements, as well as global instability and plastic deformation across the entire structure.

To address these considerations, the study utilizes a semi-coupled CFD-FEA (Computational Fluid Dynamics – Finite Element Analysis) system, implemented using Abaqus FEA and Viper::Blast CFD simulations. The semi-coupled approach is appropriate due to the relatively low displacements expected from the structure under blast loading. The frangible glazing elements, modelled using WINGARD PE PI-curves, help to predict the extent of glazing failure and assess which areas will experience significant uplift forces.

The system applies the blast loading incrementally over time to simulate the dynamic response of the structure. Throughout the analysis, plastic deformation is evaluated, and both sectional and reaction forces are measured to assess the performance of the diagrid under the extreme loading conditions. The study also evaluates the impact of glazing failure on the propagation of the blast and the subsequent loading experienced by the roof structure.

The figures demonstrate the extent of the glazing damage caused by the blast loading, and the shockwave propagation across the FEA model.

The study compares the CFD-FEA approach used with a simplified global Kingery-Bulmash loading demonstrates the substantial reduction in blast loading damage prediction. Such reduction can be used to optimize structural design, reduce material costs, improve aesthetics and reduce total embodied carbon. Further discussion on the results and detailed analysis of connection forces and collapse mechanisms will be provided.

Keywords: Response of structures to explosion loads, collateral damage estimation, numerical simulation and modelling, structural collapse mitigation strategies, computational fluid dynamics, finite element analysis, multi-physics coupling, structural blast analysis,

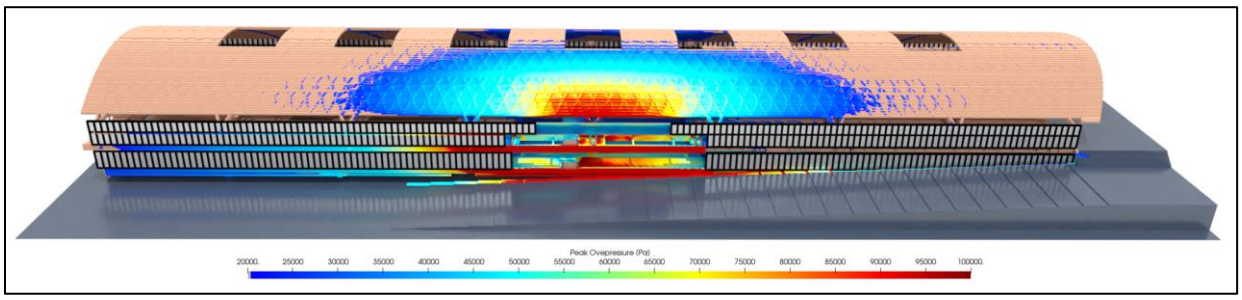

Figure 1 CFD Peak Overpressure Render

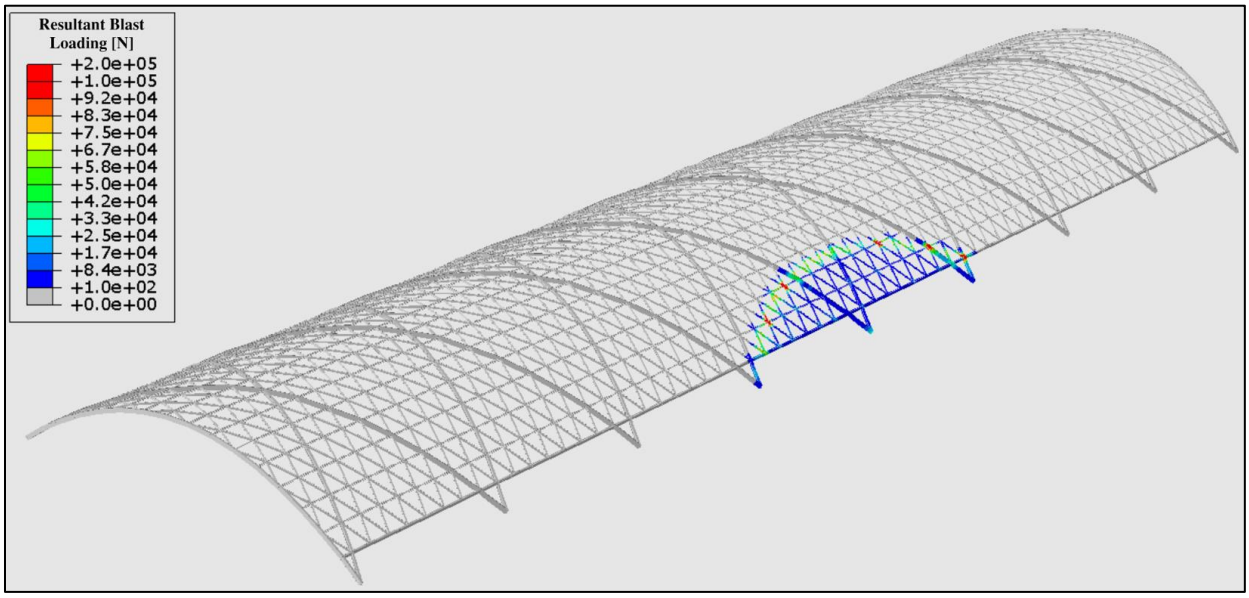

Figure 2 FEA Blast Loading Propagation

Underexcitation prevents crystallization of granular assemblies subjected to high-frequency vibration

Sara AlMahri[1,2], Ivan Grega [2] and Vikram Deshpande [2]

[1]*Technology Innovation Institute, Abu Dhabi, UAE*

[2]*Department of Engineering, University of Cambridge, Cambridge, UK*

Crystallization of dry particle assemblies via imposed vibrations is a scalable route to assemble micro/macro crystals. It is well understood that there exists an optimal frequency to maximize crystallization with broad acceptance that this optimal frequency emerges because high-frequency vibration results in overexcitation of the assembly. Using measurements that include interrupted X-ray computed tomography and high-speed photography combined with discrete-element simulations we show that, rather counterintuitively, high-frequency vibration underexcites the assembly. The large accelerations imposed by high-frequency vibrations create a fluidized boundary layer that prevents momentum transfer into the bulk of the granular assembly. This results in particle underexcitation which inhibits the rearrangements required for crystallization. This clear understanding of the mechanisms has allowed the development of a simple concept to inhibit fluidization which thereby allows crystallization under high-frequency vibrations.

Mesoscale in-situ methods for characterizing the interfacial properties of the 3DWC

Licheng Guo [1], Qingsong Zong [1], Jinzhao Huang [1,2],Yunpeng Gao [1]

[1]*Department of Astronautic Science and Mechanics,*
Harbin Institute of Technology, Harbin, China
[2] *Department of Mechanical Engineering,*
National University of Singapore, 9 Engineering Drive 1, Singapore

The 3D woven composites (3DWCs) are typical high-performance composites with promising applications in the aerospace industry due to their superior out-of-plane properties and high damage tolerance. Studies have shown that the yarn/matrix interfacial properties are crucial to the mechanical performance of 3DWCs[1–5]. However, characterizing the interfacial properties of 3DWCs is still difficult and rarely done. To this end, this study proposed a mesoscale in-situ experimental method to characterize in-situ interfacial properties of 3DWCs.

First, the stable propagation of the mode II crack along the interface was achieved by the unique specimen design. Then a highly restored finite element (FE) model of the specimen was established, and the virtual crack closure technique (VCCT) was adopted to calculate the interfacial Mode II fracture toughness (G_{IIC}). The strain field at the crack tip exhibited a distinct strain release phenomenon, facilitating the identification of crack propagation onset and overcoming the challenge of observing mode II cracks. By comparing experimental and simulation results, the in-situ interfacial G_{IIC} was determined.

Furthermore, the in-situ interfacial shear strength was then obtained using the same methodology. A type of off-axis tensile specimen incorporating a typical interfacial structure was designed. The crack surface morphology observed under an optical microscope indicates that the interfacial debonding is the dominated failure mode and shear stress is a key factor in interfacial fracture. Then, the bilinear cohesive zone model (CZM) was employed to simulate the interfacial fracture. The obtained G_{IIC} simplified the simulation process, enabling the determination of the in-situ interfacial shear strength.

The results of the high-resolution mesoscale DIC analysis validated the reliability of the experimental design and provided a reference for verifying the accuracy of the FE model. Experimental and simulation results for specimens with different off-axis angles validated the effectiveness of the proposed methods. The analysis results of multiple information fields, including digital image correlation (DIC), scanning electron microscopy (SEM), computed tomography, and simulations, demonstrated the rationality of the experimental design. This article provides a systematic evaluation method for the in-situ performance of the interface within 3DWCs and provides reliable parameter sources for the mechanical model of the interface in simulation works.

Keywords: Interface; In-situ; Strength; Fracture toughness; 3D woven composites.

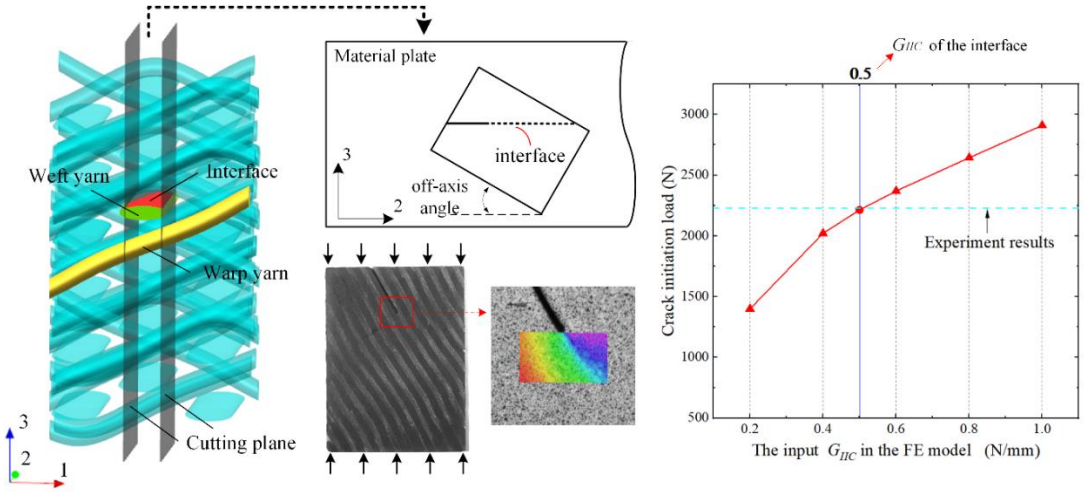

Figure 1 Method for obtaining the in-situ interfacial Mode II fracture toughness of 3DWCs.

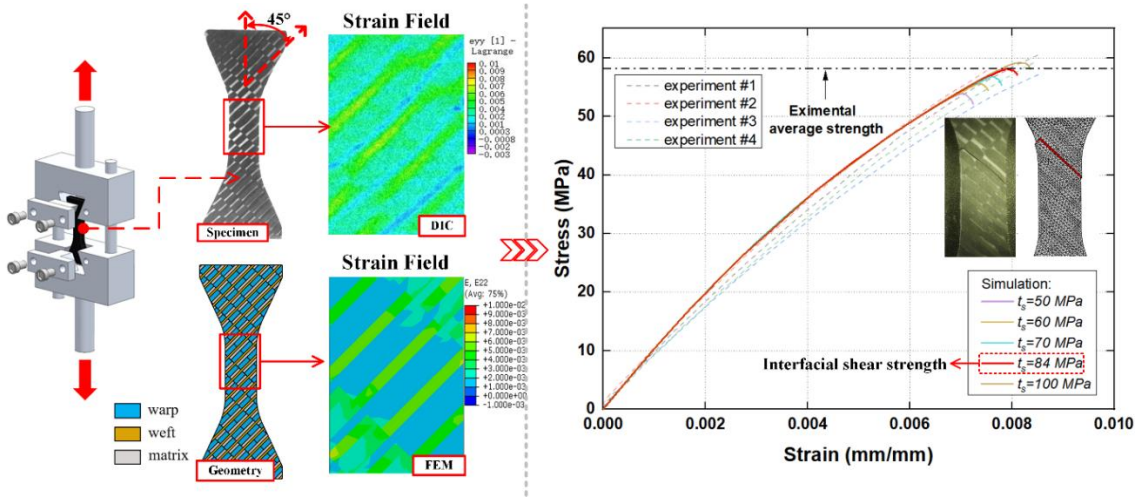

Figure 2 Method for obtaining the in-situ interfacial shear strength of 3DWCs.

[1] Guo L, Huang J, Zhang L, Sun X. Damage evolution of 3D woven carbon/epoxy composites under tension-tension fatigue loading based on synchrotron radiation computed tomography (SRCT). International Journal of Fatigue 2021;142:105913.

[2] Huang J. Damage evolution of 3D woven carbon/epoxy composites under the tension–compression fatigue loading based on multi damage information. International Journal of Fatigue 2022.

[3] Li Z, Guo L, Zhang L, Wang Q. In situ experimental investigation on the out-plane damage evolution of 3D woven carbon-fiber reinforced composites. Composites Science and Technology 2018;162:101–9.

[4] Sun R, Guo L, Li Z, Zhang L, Zheng T. A novel approach to assessing yarn/matrix (or yarn/yarn) in situ interfacial strength in 3D woven composites. Composites Science and Technology 2021;213:108893.

[5] Sun R, Zheng T, Yao Y, Li D, Si H, Guo L. Experimental investigation on shear damage evolution of 3D woven composites using in situ computed tomography and multi-scale digital image correlation. Composite Structures 2023;319:117159.

Submission ID: 6368

Finite Element Analysis of Gusset Plate and Joint Sections for Buckling Restrained Braced Frames under Seismic Loading

Brwa BEBANI[1], Mieczysław KUCZMA[1]
[1]Institute of Building Engineering, Poznan University of Technology, Poznan, Poland

Abstract

Buckling Restrained Braced Frames (BRBF) are widely used for their ability to withstand seismic loads through high ductility and energy dissipation. To enhance their seismic resilience, this study focuses on optimizing gusset plate design and connection details, which are critical for preventing out-of-plane buckling and ensuring stable frame behavior. Finite element analysis was performed to evaluate various gusset plate geometries and connection strategies under cyclic loading, following the guidelines of the AISC-2016 Seismic Provisions. Results show that gusset plates with balanced dimensions and reinforced connections improve axial force transfer and eliminate out-of-plane buckling, maintaining stable hysteretic response. These findings provide practical recommendations for designing BRBF systems with improved stability and reliability under seismic conditions.

Keywords: buckling restrained braced frames (BRBF), finite element analysis, seismic analysis, connection details of gusset plates, cyclic loading, out-of-plane buckling, Abaqus.

[1*] Corresponding author: Institute of Building Engineering, Poznan University of Technology, Pl. M. Skłodowskiej-Curie 5, 60-965 Poznan, Poland, mieczyslaw.kuczma@put.poznan.pl, +48616652155

Dynamic response and failure mechanism of Double-Double laminate under high-speed ballistic impact

Lijun Xiao[1], Hong Zhen[1] and Weidong Song[1]

[1]*State Key Laboratory of Explosion Science and Safety Protection, Beijing Institute of Technology, Beijing, China*

The unique ply design of Double-Double (DD) laminates breaks the constraints of traditional ply angles, endowing the composite laminates with more balanced mechanical properties and higher design flexibility, which provides new insights for structural lightweight design and strength optimization. Currently, most research focused on the quasi-static and low-velocity impact response of DD structures [1−3], while limited on their response under high-velocity impacts. Herein, the mechanical response of DD laminates under high-speed ballistic impact was explored by experiments. The anti-penetration performance and damage characteristics of DD laminates were compared with traditional QUAD laminates. The results indicated that DD laminates exhibited more superior impact resistance in high-velocity impact tests, specifically demonstrated by their higher energy absorption capacity and more uniform damage mode. Furthermore, numerical simulations were also performed to investigate the dynamic response of DD laminates under high-velocity impacts, which were in good agreements with the experimental results. The mesoscopic energy absorption and damage mechanism of DD laminates were analyzed accordingly. This research not only deepens the understanding regarding the dynamic properties of DD laminates, but also provides potential technical support for their application in aerospace and other fields..

Keywords: Double-Double laminate, High-speed penetration, Numerical simulation.

[1] Vermes B, Tsai SW, Massard T, et al. Design of laminates by a novel “double−double” layup. Thin-Walled Structures, 2021, 165: 107954. https://doi.org/10.1016/j.tws.2021.107954

[2] Shabani P, Li L, Laliberte J. Low-velocity impact (LVI) and compression after impact (CAI) of Double-Double composite laminates. Composite Structures, 2025, 351: 118615. https://doi.org/10.1016/j.compstruct.2024.118615

[3] Kappel E, Boose Y, Missbach M. A CAI study on transition zones of conventional and Double-Double laminates. Composites Part C: Open Access, 2024, 14: 100450. https://doi.org/10.1016/j.jcomc.2024.100450

Modeling of Confined Explosions: an Uncoupled Eulerian-Lagrangian Approach for Blast Wave Propagation and Structural Assessment

Edison Shehu[1], Luca Lomazzi[1] and Andrea Manes[1]

[1]*Politecnico di Milano, Department of Mechanical Engineering, Via Giuseppe La Masa, 1, Milan, 20156, Italy*

Blast waves represent an extreme loading condition that poses significant challenges during the modelling phase, especially when structural response is investigated. The pressure histories resulting from blast wave interactions with structures are highly influenced by the level of confinement and the geometry of the impacted structure. Fully confined blast events are more severe than their unconfined counterparts due to multiple wave reflections and residual quasi-static pressures, which result in prolonged shock-structure interactions and complex pressure profiles (Edri et al., 2011; Feldgun et al., 2011, 2012). Most experimental studies have primarily focused on spherical or hemispherical blast waves in free-field conditions, supporting simplified models like the CONWEP algorithm (Hyde D., 1988), commonly integrated into Finite Element (FE) solvers for unconfined explosions. However, this approach is unsuitable for more complicated scenarios, such as explosions in confined scenarios. Over the years, numerous methodologies have been developed to handle these configurations. Among these, recent advancements in Computational Fluid Dynamics (CFD) codes have demonstrated the capability of high-fidelity modelling of energetic materials and their interactions with surrounding structures. The current study presents a synergistic approach that integrates CFD with a FE framework. The methodology is applied to investigate blast wave propagation in structures with an increasing degree of confinement. This study focuses on extending the capabilities of the FE solver *Abaqus/Explicit* to handle these complex load histories, which are beyond the scope of its default built-in configurations. User-defined subroutines are developed to enable an Uncoupled Lagrangian-Eulerian (UEL) framework. CFD simulations are performed independently to calculate pressure histories, then they are subsequently mapped onto structural FE models as input loads (Figure 1). This approach allows for creating the uncoupled framework and its application to scenarios with varying degrees of confinement. Finally, the structural response of blast-loaded metal plates was evaluated under confined and unconfined conditions, highlighting the differences in pressure load, impulse profile and structural performance (Figure 2).

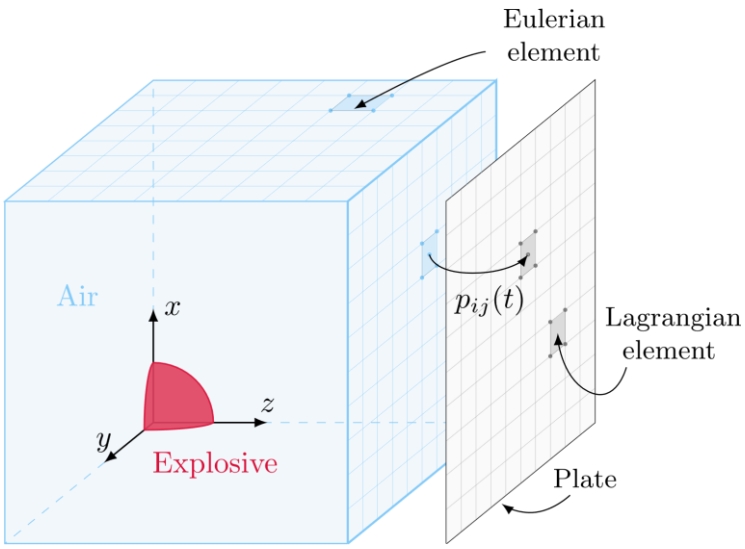

Figure 1. Uncoupled Eulerian Lagrangian approach where pressure field is mapped onto the plate.

The results demonstrate that the proposed framework significantly extends the range of scenarios that can be analysed for blast wave propagation and its effects on structures. By employing this uncoupled approach, diverse structural simulations can be performed using a single FE model. This is achieved by varying the pressure load histories corresponding to different degrees of confinement in the surrounding environment where the blast wave interacts. This methodology offers enhanced flexibility in analysing complex confined blast scenarios.

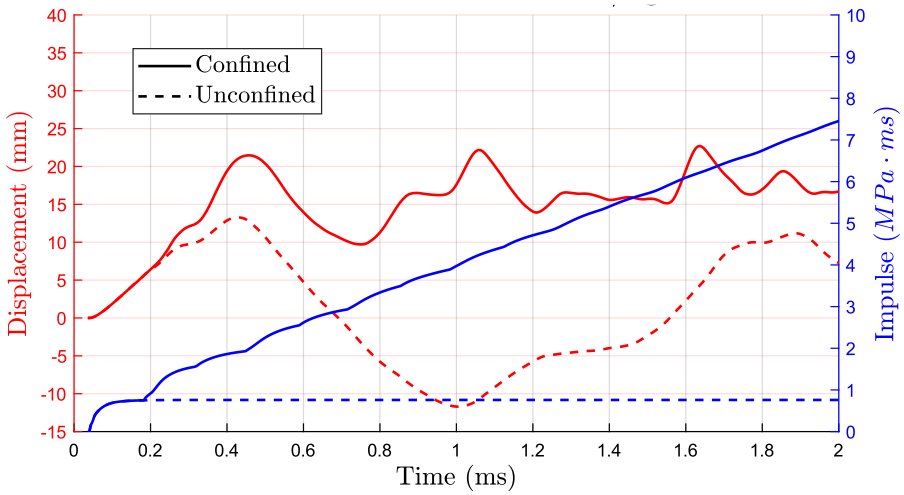

Figure 2. Comparison between midpoint displacement of a blast-loaded metal plates over time and impulse; two cases are reported: unconfined and fully confined blast events.

In conclusion, this study provides a numerical tool for simulating confined explosions, with applications in industrial safety and structural design. The findings contribute to a deeper understanding of blast wave behaviour in different geometrical environment, facilitating improved engineering designs for mitigating blast effects.

Keywords: Blast wave, Confined explosion, Uncoupled Eulerian Lagrangian, Structural Assessment

Edri, I., Savir, Z., Feldgun, V. R., Karinski, Y. S., & Yankelevsky, D. Z. (2011). On Blast Pressure Analysis Due to a Partially Confined Explosion: I. Experimental Studies. International Journal of Protective Structures.

Feldgun, V. R., Karinski, Y. S., Edri, I., Tsemakh, D., & Yankelevsky, D. Z. (2012). On Blast Pressure Analysis Due to a Partially Confined Explosion: II. Numerical Studies. International Journal of Protective Structures.

Feldgun, V. R., Karinski, Y. S., & Yankelevsky, D. Z. (2011). Some characteristics of an interior explosion within a room without venting. Structural Engineering and Mechanics, 38(5), 633–649. https://doi.org/10.12989/sem.2011.38.5.633

Hyde D. (1988). Microcomputer Programs CONWEP and FUNPRO, Applications of TM 5-855-1, 'Fundamentals of Protective Design for Conventional Weapons.

Field Tests of Square RC Column under Vehicle Impact Loads

Sanghee Kim[1]

[1]*Department of Architectural Engineering, Kyonggi University, Suwon 16227, Rep. of Korea*

Damage and destruction of structural members due to vehicle collisions frequently occur domestically and internationally. Approximately 15% of bridge damage in the United States and China is reportedly caused by collisions with ships or vehicles [1]. To prevent structural damage due to vehicle collisions, ASCE, AASHTO, and EUROCODE suggest various protective loads [1, 2]. Numerous experiments and studies have been conducted by many researchers, but most focus on large circular columns of bridges, leaving a gap in research on columns of smaller buildings. In Republic of Korea, many small piloti structures exist, with their ground floors used as parking lots, exposing road columns to potential vehicle collision loads. To address this, we conducted full-scale experiments simulating vehicle collisions with RC columns of piloti buildings. The tests involved a passenger car, a 1-ton truck, and a 2.5-ton truck colliding with an RC column (cross-section: 400 x 400 mm²) at speeds of 50 km/h, 50 km/h, and 30 km/h, respectively. To measure column deformation, we captured the collision moment using a high-speed camera and tracked lateral displacement using YOLOv5. Additionally, we scanned the column using a 3D scanner to compare deformation before and after the vehicle crash load. Maximum displacements for the passenger car, 1-ton truck, and 2.5-ton truck collisions were approximately 34 mm, 39 mm, and 59 mm, respectively. Post-experiment, the columns exhibited permanent lateral displacements of approximately 7 mm, 11 mm, and 24 mm, respectively, without significant visible damage. Notably, we observed torsional deformation in addition to lateral displacement. This finding suggests that when designing structural members subjected to vehicle crash loads, it is crucial to account for both lateral and torsional loads.

Keywords: field tests, vehicle impact loads, YOLOv5, 3D scanning, Square RC column

[1] Chen, L. Wu, H., and Liu T. (2021). Vehicle Collision with Bridge Piers: A State-Of-The-Art Review, Advances in Structural Engineering, Vol. 24, No. 2, 385-400.

[2] Chen, L., Wu, H., and Liu, T. (2020) “Shear Performance Evaluation of Reinforced Concrete Piers Subjected to Vehicle Collision,” Journal of Structural Engineering, Vol. 146, No. 4, Article No. 04020026.

Deformation Behavior of Additively Manufactured Cellular Metamaterials at Different Strain Rates

Zoran Ren[1], Anja Mauko[1], Oraib Al-Ketan and Nejc Novak[1]

[1] *University of Maribor, Maribor, Slovenia*

[2] *Core Technology Platform, New York University Abu Dhabi, United Arab Emirates*

This work reviews and synthesizes recent advances in the study of high strain rate mechanical behavior of metallic cellular metamaterials, focusing on uniform/hybrid and stochastic Triply Periodic Minimal Surface (TPMS) structures built by using advanced additive manufacturing techniques.

Uniform and hybrid TPMS structures, explored in Novak et al. [1], included Diamond, Gyroid, IWP, and Primitive topologies, along with Gyroid–Diamond hybrids, Figure 1 a,b,c,d, e, respectively. The sample structures were fabricated using a powder bed fusion method with 316L stainless steel. The samples were then tested under quasi-static and dynamic (impact) compressive loading conditions using the Direct Impact Hopkinson Bar (DIHB) setup, Figure 2, to evaluate their mechanical behavior. They exhibited strain rate hardening and distinct deformation modes influenced by their geometric configuration. SEA values for Diamond and IWP structures increased significantly during shock loading, reaching up to 40.8 J/g, a fivefold increase compared to quasi-static conditions. Hybrid TPMS structures, combining softer and stiffer regions, showed orientation-dependent behavior, allowing tailored mechanical

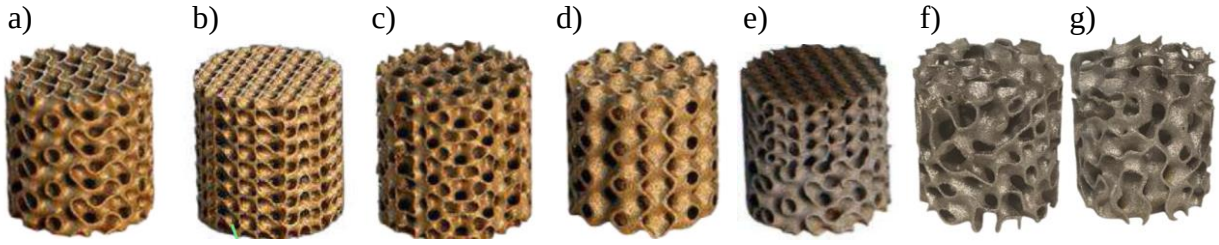

Figure 1. Studied TPMS structures

responses. Computational models, validated against experimental data, extended the strain rate analysis to 35,000 s^{-1}, predicting enhanced energy absorption and dynamic stability.

Stochastic TPMS structures, as presented in Novak et al. [2], Figure 1 f and g, were also fabricated from 316L stainless steel, achieving relative densities between 13% and 21%. These structures demonstrated isotropic mechanical behavior due to their randomized unit cell

orientation. Experiments across different strain rates showed consistent plateau stress behavior, particularly beneficial for energy absorption applications. The Specific Energy Absorption (SEA) of stochastic materials increased dramatically under impact loading, with values rising from 9.2 J/g in quasi-static conditions to 35 J/g under shock deformation. Computational models validated against experimental results further revealed critical loading velocities (25–32 m/s and 43–56 m/s for the first and second modes, respectively), where the deformation transitioned from quasi-static to shock modes.

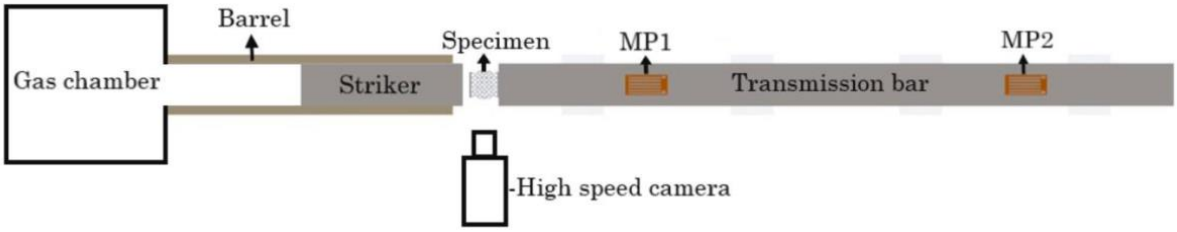

Figure 2. Schematic representation of the DIHB experimental setup

Key findings from both studies highlight the influence of cellular architecture on deformation behavior. Stochastic structures excel in isotropy and dynamic performance, while TPMS architectures provide tunable, geometry-dependent responses. Both classes demonstrate promising applications in crashworthiness and blast mitigation due to their lightweight and energy-absorbing capabilities. Future work should focus on optimizing fabrication techniques to minimize defects and further refining computational models for complex deformation scenarios.

References

[1] N. Novak, S. Tanaka, K. Hokamoto, A. Mauko, Y. Emre, High strain rate mechanical behaviour of uniform and hybrid metallic TPMS cellular structures, Thin-Walled Struct. 191 (2023) 111109. https://doi.org/10.1016/j.tws.2023.111109.

[2] N. Novak, O. Al-Ketan, A. Mauko, Y.E. Yilmaz, L. Krstulović-Opara, S. Tanaka, K. Hokamoto, R. Rowshan, R.A. Al-Rub, M. Vesenjak, Z. Ren, Impact loading of additively manufactured metallic stochastic sheet-based cellular material, Int. J. Impact Eng. 174 (2023) 104527. https://doi.org/10.1016/j.ijimpeng.2023.104527.

Keywords: cellular metamaterials, deformation behavior, different strain rates.

Numerical Analysis of Energy Dissipation and Temperature during Impact Tests on S235 Steel Specimens at Various Impact Angles

Maciej Klosak[1], Michal Grazka[2] and Leopold Kruszka[3]

[1]*Laboratory for Sustainable Innovation and Applied Research, Technical University of Agadir, Universiapolis, Agadir 80000, Morocco*

[2]*Faculty of Mechatronics, Armaments and Aeronautics, Military University of Technology, Warsaw 00-908, Poland*

[3]*Faculty of Civil Engineering and Geodesy, Military University of Technology, Warsaw 00-908, Poland*

The material under investigation, i.e. S235 steel, is a typical construction material. The S235 steel tested under perforation investigation, subjected to impacts of moderate velocity demonstrated its mechanical properties are also beneficial for the development of engineering applications in the domain of the so-called critical infrastructure. The presented numerical work was focused on the thermal response of the material subjected to impact within a wide range of temperatures and using different angles between the projectile and specimen during impact. The numerical analysis was preceded by the experimental programme in which the specially designed thermal chamber heated specimens before impact. The range of available temperatures was from the ambient temperature to ~300 ˚C. The ballistic properties of the material impacted by a conical nose shape projectile were studied experimentally and those results were then extended by numerical simulations. The general-purpose software Abaqus/Explicit was used to verify the implemented constitutive relation coupled with a failure criterion and then to extrapolate experimental results to other projectile-specimen configurations. Different angles between the projectile and specimen were studied, from 0˚ (projectile perpendicular to specimen) to 60˚. The numerical analysis of the energy dissipation induced during impact was reported as a function of the projectile-specimen angle configuration. Good correlation is reached between numerical and experimental results concerning the failure mode.

Keywords: perforation tests, S235 steel, thermal chamber, numerical simulations, Abaqus.

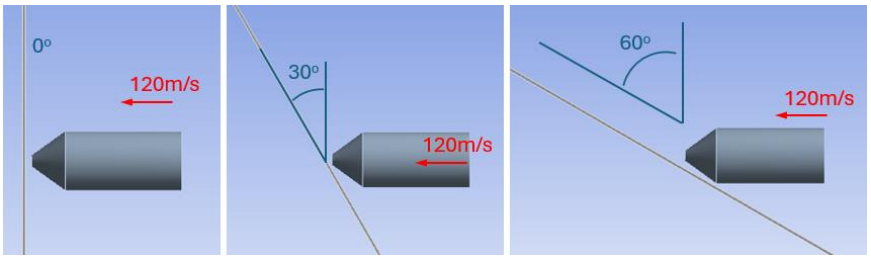

Figure 1. Projectile-specimen configuration for numerical model

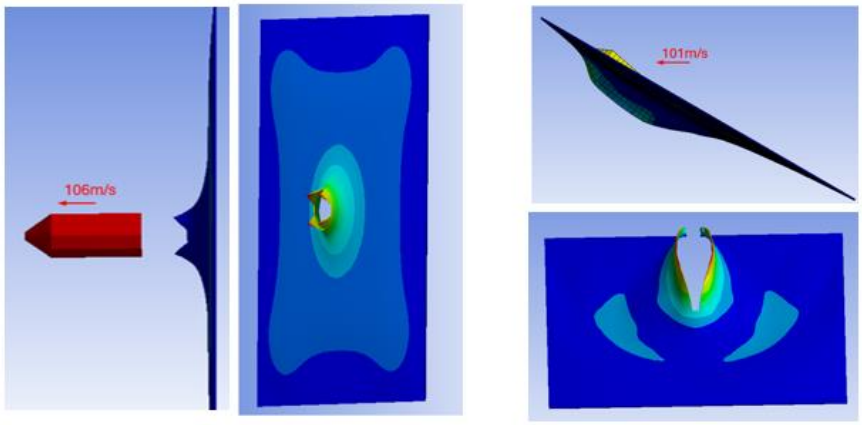

Figure 2. Numerical simulation of impact at different angles with visible change of residual velocities V_R (impact velocity V_0 = 120 m/s)

[1] Klosak, M, Grazka, M, Kruszka, L, Mocko, W, (2021). Perforation analysis of S235 steel sheets up to 573 K using experimental and numerical methods, Archives of Civil Engineering, vol. LXVII, no 3, p. 639-659, DOI: 10.24425/ace.2021.138075.

[2] Kruszka, L, Kubíková, Z. (2019). Critical Infrastructure Systems Including Innovative Methods of Protection", in Critical Infrastructure Protection. NATO Science for Peace and Security Series D: Information and Communication Security, Kruszka, L, Klosak, M, Muzolf, P, (eds), IOS Press, Amsterdam, DOI: 10.3233/978-1-61499-964-5-1.

[3] Jankowiak, T, Rusinek, A, Kpenyigba, KM, Pesci, R, (2014). Ballistic behaviour of steel sheet subjected to impact and perforation, Steel and Composite Structures, vol. 16, no 6, p. 595–609, DOI: 10.12989/scs.2014.16.6.595.

[4] Kruszka, L, Janiszewski, J, (2015). Experimental analysis and constitutive modelling of steel of A-IIIN strength class, EPJ Web of Conferences, vol. 94, 05007, DOI: 10.1051/epjconf/20159405007.

[5] Massaq, A, Rusinek, A, Klosak, M, Abed, F, El Mansori, M, (2016). A study of friction between composite-steel surfaces at high impact velocities, Tribology International, vol. 102, p. 38–43, DOI: 10.1016/j.triboint.2016.05.011.

[6] Rosenberg, Z, Vayig, Y, (2021). On the friction effect in the perforation of metallic plates by rigid projectiles, International Journal of Impact Engineering, vol. 149, 103794, DOI: 10.1016/j.ijimpeng.2020.103794.

Study of the uncertainty in the experimental evaluation of the TNT equivalent of a plastic explosive and numerical validation

Lina M. Lopez[1], Maria Chiquito[1], Anastasio P. Santos[1], Ricardo Castedo[1], Ana Lopez[1], Andrew Nicholson[2], Peter McDonald[2], Chris Stirling[2]

[1] *Universidad Politécnica de Madrid, Madrid, Spain*

[2] *Viper Applied Science, 272 Bath Street, Glasgow, United Kingdom*

The TNT equivalent is a very useful engineering tool when comparing explosives: it gives us a universal pattern, of relative simplicity in its calculation, to establish equivalences between substances that can exhibit different behaviours. The experimental TNT equivalent concept is the most widely used for the design of resistant structures. However, not always is possible to get this equivalence by experimental methods. Therefore, numerical methods appear as a good alternative to evaluate and calculate a reliable equivalency to TNT. The calibration of the methodology would allow the evaluation of equivalents without the need for testing for a certain scaled distance range. The experimental TNT equivalence for PG3, a plastic explosive with RDX, has been evaluated. Pressure sensors were placed at three distances, and spherical charges were tested covering a range of 1.79 to 9.01 m/kg$^{1/3}$ scaled distance. Equivalents have been evaluated based on a total of 54 pressure signals, the arrival time and average shock velocity data, based on high-speed camera images. Since 6 experimental data are available for each scaled distance, the uncertainty in the measurements has been evaluated with average values of 0.9% for the arrival time, 2.7% for the peak pressure and 1.9% for the impulse. The equivalents have been calculated based on pressure, impulse, arrival time and shock velocity. The uncertainty in the measurements of the different equivalents evaluated has been studied and it has been observed that the parameter that offers the least uncertainty in the equivalent for a given scaled distance is the impulse (average uncertainty of 2.2%). However, the variation of the impulse-based equivalent with the scaled distance within the range of the tests presented, is patent, a situation that does not occur with the pressure-based equivalent, which shows a constant trend.

After the analysis of the experimental results, these tests have been simulated using the finite volume code Viper::Blast to validate the methodology of the TNT equivalence based on pressure and impulse. The numerical simulation has been carried out reproducing the

experimental setup. The experimental pressure curves and those obtained by simulation show an average difference of 5.2%. The pressure-based TNT equivalent found experimentally was 1.330 and the one found by simulation results was 1.333.

Keywords: TNT equivalent, plastic explosive, shockwave parameters, uncertainty, Viper::Blast.

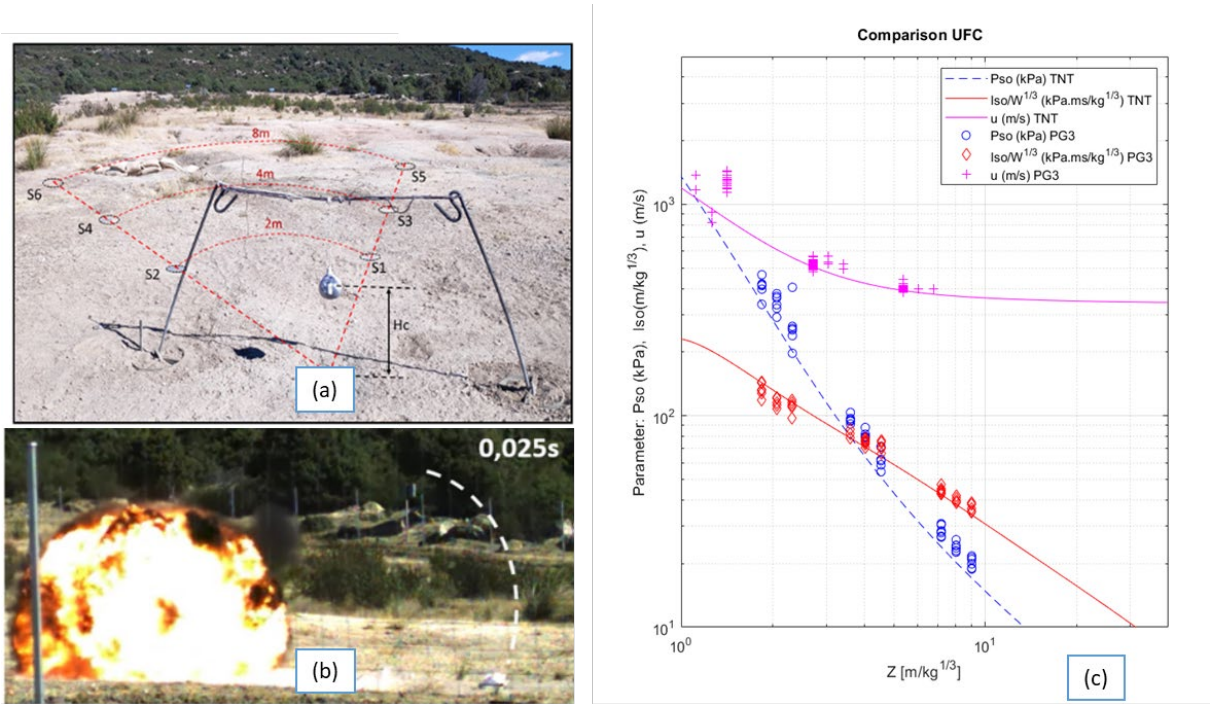

Figure 1. Experimental setup, high-speed camera image, shock wave parameters compared to TNT (UFC 3-340)

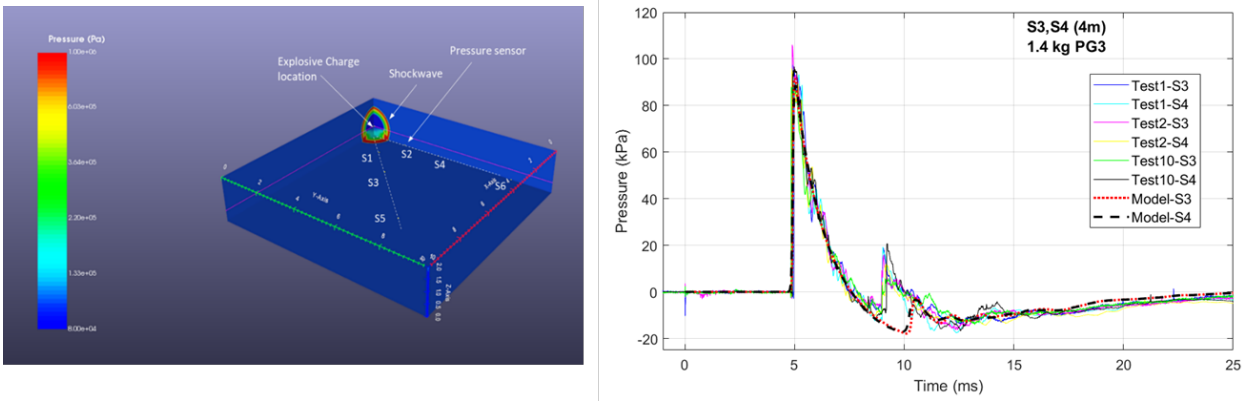

Figure 2. Simulation with Viper, Pressure signal comparison.

A novel hydro-elastoplastic model for concrete-like materials under impact and explosion loadings considering modulus damage

Junfeng Wang [1,2], Li Chen [1,2]

[1] *School of Civil Engineering, Southeast University, Nanjing, 210096, China*

[2] *Engineering Research Center of Safety and Protection of Explosion & Impact of Ministry of Education (ERCSPEIME), Southeast University, 211189, Nanjing, China*

The conduct of impact or explosion experiments is limited by many conditions, therefore numerical simulation methods are currently the main means of studying impact and explosion problems. It is well known that material constitutive models play a crucial role in numerical predictions. Under the action of impact or explosion loads, concrete materials exhibit extremely complex nonlinear dynamic mechanical behaviors. The development of high-fidelity concrete constitutive models has always been a key focus and challenge in research. This paper proposes a new constitutive model for concrete based on the theoretical framework of hydro-elastoplastic model. Based on a large amount of triaxial compression test data for concrete, a high-pressure dynamic strength model was established that includes an initial yield surface, a maximum strength surface, and a residual strength surface. The model also takes into account pressure dependence, Lode angle effects, and strain rate effects. Based on the hydrostatic compression damage mechanism of concrete, an analytical equation of state for high-pressure conditions has been developed, which takes into account nonlinear volumetric compaction and unloading behavior. The damage model includes volumetric compressive damage, shear damage, and tensile damage. It takes into account the degradation of the initial modulus of concrete due to volumetric compressive damage, as well as the reduction in shear strength and tensile strength. The new constitutive model also considers the shear compaction and dilation effects of concrete under high confining pressure. To validate the new model, numerical tests were conducted on concrete under uniaxial and triaxial compression, uniaxial and isotropic tension, monotonic and cyclic hydrostatic compression, as well as uniaxial compression and tension after hydrostatic compression. Compared to commonly used concrete constitutive models, the model proposed in this paper demonstrates high computational accuracy. Finally, numerical predictions of concrete under projectile penetration and explosive loading were carried out using the proposed

model. The results show that the numerical predictions are in excellent agreement with experimental data.

Keywords: Concrete constitutive model, Impact and explosion loadings, High-pressure dynamic strength model, Nonlinear volumetric behavior, Damage model.

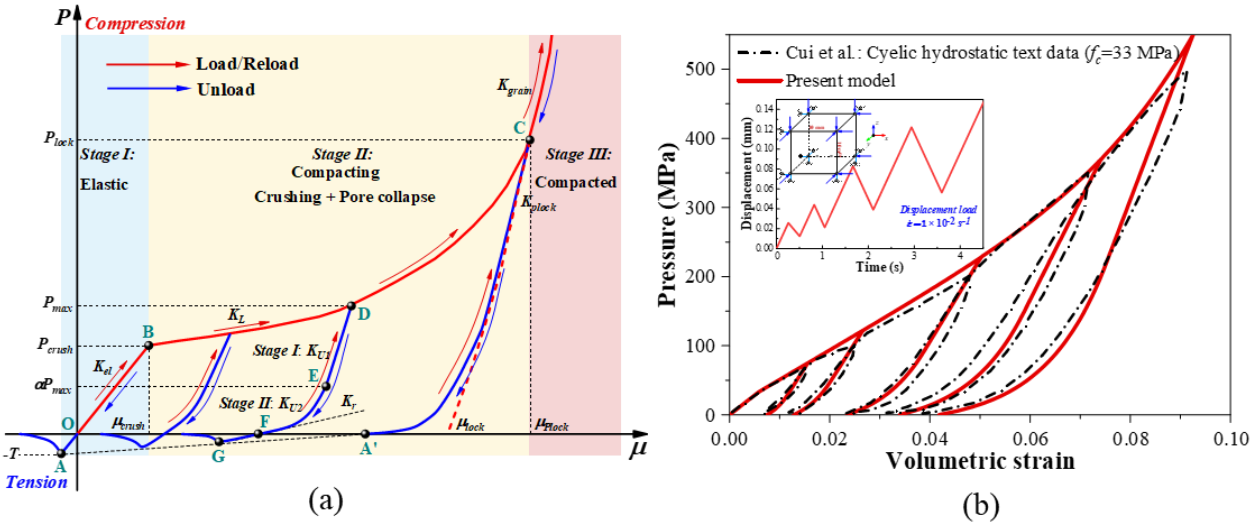

Fig.1 Equation of state and cyclic hydrostatic compression single-element test.

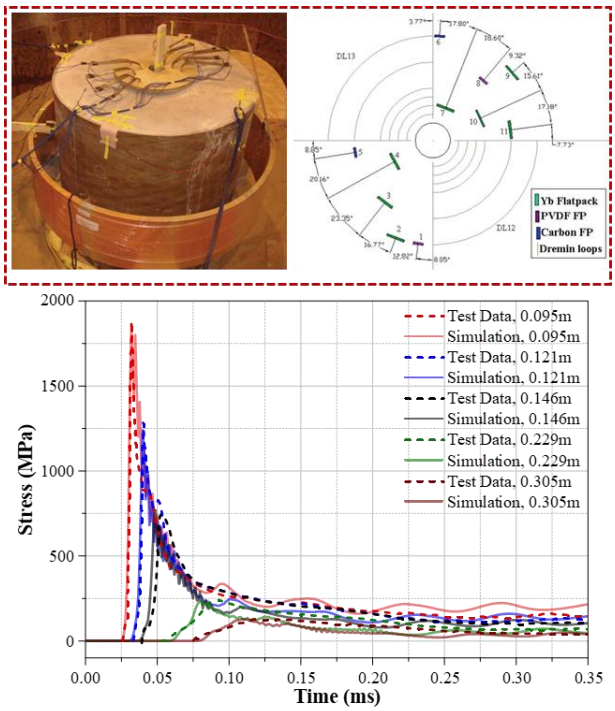

Fig.2 Simulation of stress wave propagation from spherical charge explosion in concrete.

A Dimensionless Metric for Quantifying Fluid-Structure Interaction in Blast-Loaded Plates

Giovanni Marchesi[1], Luca Lomazzi[1], Vegard Aune[2], Andrea Manes[1] and Trevor John Cloete[3]

[1]*Politecnico di Milano, Department of Mechanical Engineering, Via La Masa n.1, 20156 Milan, Italy*

[2] *Structural Impact Laboratory (SIMLab), Department of Structural Engineering, NTNU – Norwegian University of Science and Technology, NO-7491 Trondheim, Norway*

[3] *Blast Impact and Survivability Research Unit (BISRU), Department of Mechanical Engineering, University of Cape Town, Rondebosch 7700, South Africa*

The numerical modelling of blast-loaded structures is highly complex due to fluid-structure interaction (FSI) effects (Aune et al., 2021; Lomazzi et al., 2023). When a blast wave encounters a structure, it causes a rapid increase in pressure, followed by a gradual decay. The response of the structure in turn influences the blast load, resulting in a mutual interaction that significantly increases the computational burden of numerical simulations, which must address coupled fluid-structure problems. For this reason, in typical air blast analysis, an inexpensive uncoupled approach is preferred, in which the structural response is assumed not to affect the blast load. However, when significant FSI effects are present, uncoupled analyses lose accuracy as the structural response is notably overestimated (Børvik et al., 2009).

In the outlined scenario, this work aims to define a procedure for obtaining an initial estimate of the error incurred when using an uncoupled approach compared to a coupled one. The procedure is specifically tailored for blast-loaded plates constrained at their outer edges – as this is the type of structure most likely to experience FSI effects – and yields a dimensionless number that estimates the difference in deflection calculated using the two approaches.

The primary advantage of this method is that the dimensionless number can be derived from a single uncoupled simulation, providing analysts with an effective tool to assess whether more costly coupled analyses are necessary. This dimensionless number is estimated based on a limited set of parameters related to the blast load and the structural response. The expression is formulated analytically by modelling the plate's centre as a free-standing plate, as illustrated in Figure 1. Large inelastic deformations characterise the response of the plates considered in this work, and the proposed analytical model remains valid until the plastic hinge formed at the boundary reaches the centre of the plate (Cloete & Nurick, 2019). Furthermore, the proposed

framework allows gas dynamics to be considered through a reduced one-dimensional model (Seigel, 1965).

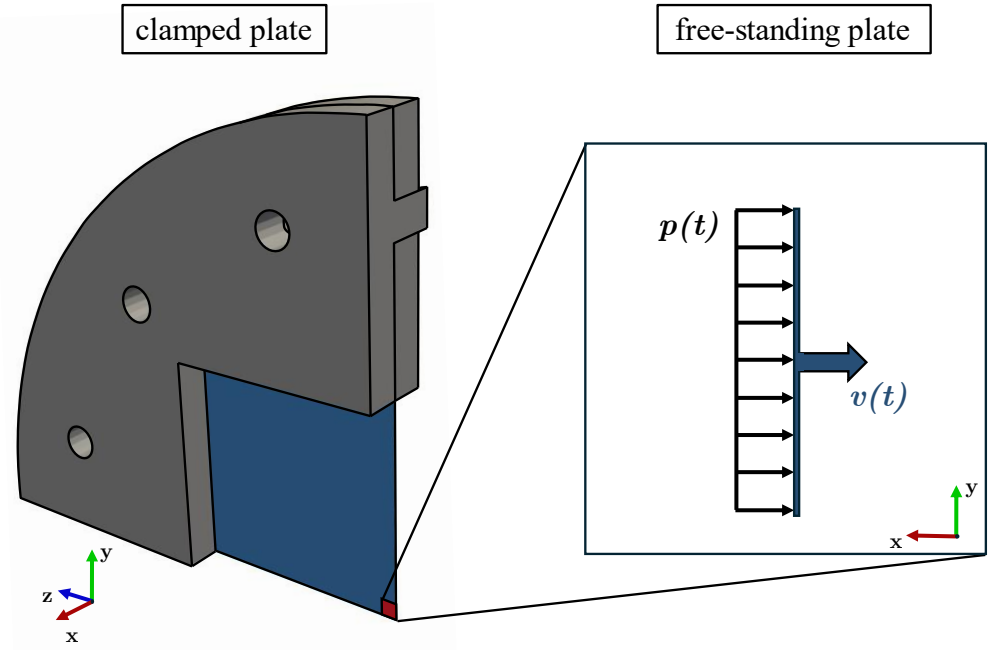

Figure 1. Representation of the analytical framework for a free-standing plate.

The procedure and the validity of the dimensionless number were demonstrated and subsequently tested on experimental case studies conducted in a dedicated shock tube facility (Aune et al., 2016). For each case study, both coupled and uncoupled analyses were conducted to determine the exact value of the dimensionless number $\Delta\varpi_{num}$, calculated as a deflection difference and used for comparison. A representative result is presented in Figure 2a, where the midpoint deflection of the plate is shown for both the coupled and uncoupled approaches, along with the exact value ($\Delta\varpi_{num}$). Additionally, the outputs of the uncoupled simulation were employed to calculate the analytical trends displayed in Figure 2b, following the procedure developed in this work. These curves provided an estimate of the dimensionless number $\Delta\varpi_{estimate}$, which is the primary outcome of the proposed procedure. This estimate accurately quantifies the FSI effects, demonstrating its effectiveness in capturing the relevant trends.

In conclusion, this work presents a new dimensionless metric for analysts to determine whether more computationally intensive coupled simulations are necessary. In doing so, the derived number highlights the key quantities governing FSI effects, providing valuable insights that can be employed to develop blast protection strategies.

Keywords: fluid-structure interaction, dimensionless number, blast loading, numerical simulations.

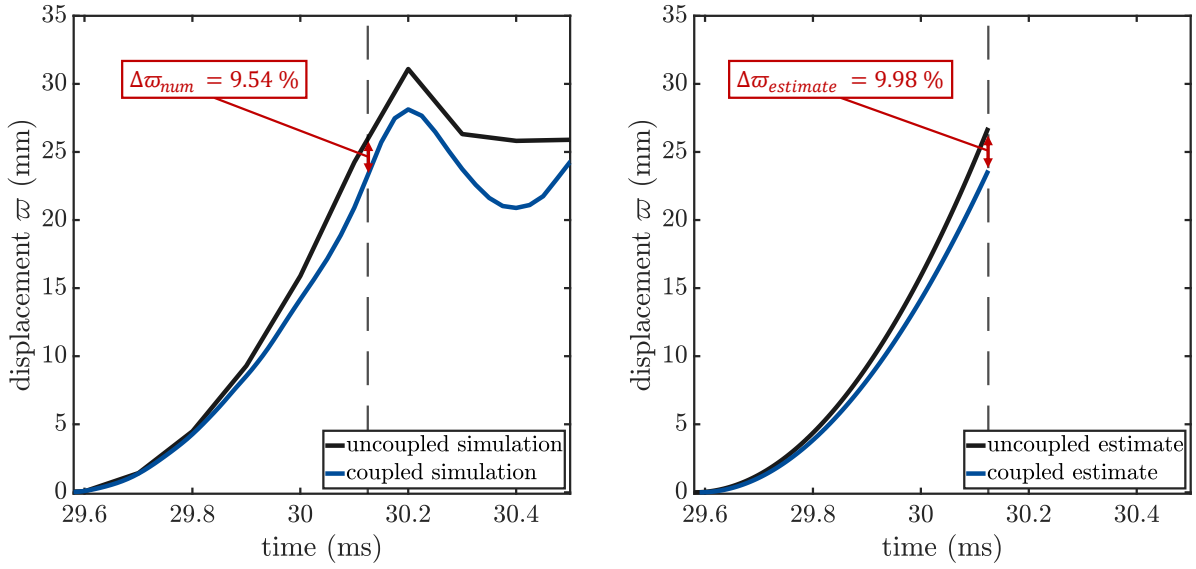

Figure 2. Midpoint plate deflection and dimensionless number computed from both coupled and uncoupled simulations (a), and from the analytical trends based on the uncoupled simulation (b).

Aune, V., Fagerholt, E., Langseth, M., & Børvik, T. (2016). A shock tube facility to generate blast loading on structures. *International Journal of Protective Structures*, *7*, 340–366.

Aune, V., Valsamos, G., Casadei, F., Langseth, M., & Børvik, T. (2021). Fluid-structure interaction effects during the dynamic response of clamped thin steel plates exposed to blast loading. *International Journal of Mechanical Sciences*, *195*, 106263. https://doi.org/10.1016/j.ijmecsci.2020.106263

Børvik, T., Hanssen, A. G., Langseth, M., & Olovsson, L. (2009). Response of structures to planar blast loads – A finite element engineering approach. *Computers & Structures*, *87*(9), 507–520. https://doi.org/10.1016/j.compstruc.2009.02.005

Cloete, T. J., & Nurick, G. N. (2019). A dimensionless number for shock-structure interaction. *Advances in Engineering Materials, Structures and Systems: Innovations, Mechanics and Applications*. https://api.semanticscholar.org/CorpusID:214280362

Lomazzi, L., Morin, D., Cadini, F., Manes, A., & Aune, V. (2023). Deep learning-based analysis to identify fluid-structure interaction effects during the response of blast-loaded plates. *International Journal of Protective Structures*, *0*(0). https://doi.org/10.1177/20414196231198259

Seigel, A. E. (1965). *The theory of high speed guns*. https://api.semanticscholar.org/CorpusID:117774109

A Comparative Study for Evaluating Secondary Debris Throw of Building Components from an Internal Explosion

Xiao Ding Bu[1] and Anay Raibagkar[2]

[1]*Structural Project Consultant, BakerRisk, Burlington, Canada*

[2]*Structural Principal Engineer, BakerRisk, Burlington, Canada*

For facilities processing and storing fuels and high explosives, potential internal explosion can be a major source of hazard. Unless the building envelope is designed to withstand and contain the potential explosion, secondary fragment debris from failure of building is expected. For example, if corrugated metal panels are used to construct the walls or the roof of the donor building, they can be more vulnerable to failure than reinforced concrete or masonry components and hence are more prone to generate secondary debris at lower internal blast loads. This failure is not limited to light panels, but to any building element that is susceptible to failure at relatively low ductility values.

Three decades ago, Department of Defense Explosives Safety Board (DDESB) technical paper No. 13 [1] (TP13) provided a numerical method to estimate the critical hazardous distance for various types of building components. The TP13 method assumes the debris from the failure of a large corrugated metal panel, with the initial velocity estimated based on the applied impulse and panel weight. TP13 recommends the use of a program, called “MUDEMIMP” [2], to estimate the travel distance of the secondary debris in a statistical manner. The hazardous distance can hence be estimated based on given kinetic energy criteria.

However, the TP13 method is statistical-based, and the input of the statistical parameters will significantly affect the output. Hence, it will be difficult to visualize the actual behavior of the debris. Besides, this method requires access to MUDEMIMP, which might not be readily available.

In this study, a simplified method of calculating the secondary building debris is proposed. Specifically, light metal cladding components are used to illustrate the method. The simplified method evaluates the initial velocity of the panel debris using a single-degree-of-freedom (SDOF) analysis methodology [3, 4]. When the equivalent SDOF system of the panel is predicted to fail, the corresponding failure velocity is taken as the initial velocity of the debris.

Projectile motion physics is used to calculate the trajectory path of the debris, from which the hazardous distance can be evaluated, see Figure 1.

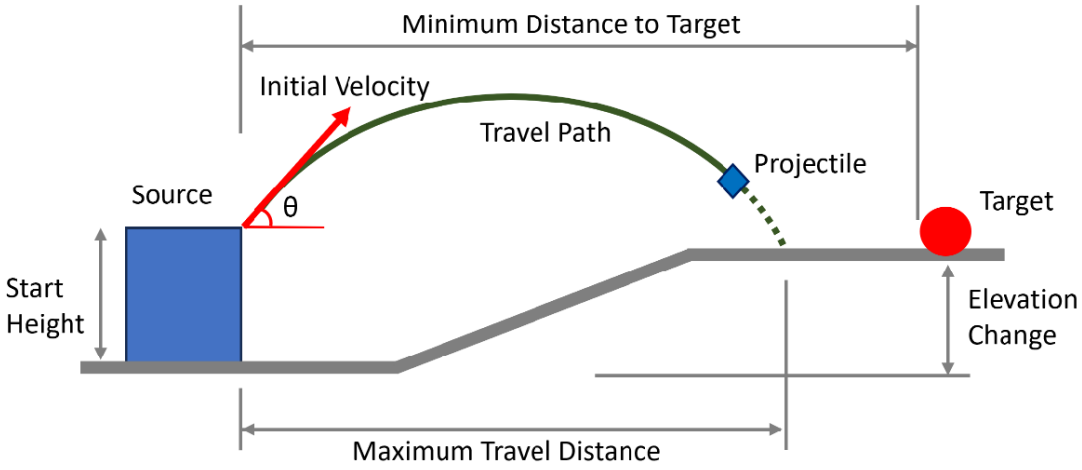

Figure 1.Projectile Motion

This simplified method is further calibrated with Finite element (FE) method (ANSYS LS-DYNA 2024R2), where 3D models of multiple panes of corrugated metal panel are built, and the panels are loaded with standard bilinear pressure time-history loads. Sample FE model is shown in Figure 2. The behavior of the debris, such as size, and initial velocity is recorded after failure. The trajectory of the debris is then calculated and compared against the corresponding critical hazardous distances given by MUDEMIMP. For a comprehensive understanding of the behavior of the panel debris, the following parameters are varied for a parametric study: (i) the panel gauge; (ii) the blast load; (iii) the panel size; and (iv) the support type.

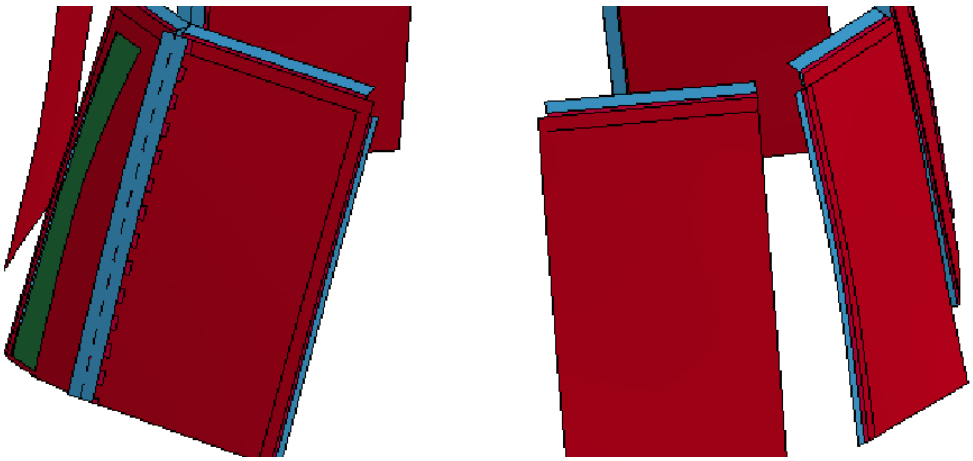

Figure 2. Sample FE Model on Secondary Debris Throw

The proposed method is more useful than a statistical approach as it can account for specific situations such as charge weight, stand-off distance, venting in a building, structural capacity, and response limits of building components.

Keywords: corrugated metal panel, secondary debris, internal explosion, single-degree-of-freedom, finite element analysis, hazardous distance

[1] Department of Defense Explosives Safety Board (DDESB), (1991). Prediction of Building Debris for Quantity-Distance Siting, Technical Paper 13.

[2] Ibrahim, Y. and Wager, P. (2010). DDESB TP13 Software Update, 2010 DDESB Seminar, Port Hueneme, California.

[3] Biggs, J. D., (1964). Introduction to Structural Dynamics, McGraw-Hill Publishing Company, New York, 1964.

[4] ASCE Task Committee on Blast-Resistant Design, (2010). Design of Blast-Resistant Buildings in Petrochemical Facilities, Second Edition, American Society of Civil Engineers, New York.

Submission ID: 6786

Machine learning prediction of fragment distribution with graph neural networks

Zhijie Zhang[1], Qiushi Yan[1], Yeqing Chen[2], Mengnan Dai[2], Longyun Zhou[2]

[1]*Key Laboratory of Urban Security and Disaster Engineering under the Ministry of Education, Beijing University of Technology, Beijing 100124, China;*

[2]*State Key Laboratory of Target Vulnerability Assessment, Institute of Defense Engineering, AMS, PLA,Beijing 10036, China*

Abstrast: The rapid and reliable prediction of fragment distribution is essential for the design and damage assessment of cased charges, as well as for the blast and impact-resistant design of structures. Traditional numerical simulation methods, such as finite element methods and meshless approaches, have been widely applied in the modeling of fragment distribution. However, these methods require complex modeling and parameter settings and consume substantial computational resources, especially with fine mesh sizes, making it difficult to meet the demands of large-scale computation and real-time prediction. Current machine learning models have demonstrated effectiveness in predicting the velocity distribution of fragments; however, they remain inadequate for comprehensive predictions of the fragmentation evolution, geometry, velocity, and mass of cased charges, which are essential for accurate assessment. In this study, the Smooth Particle Hydrodynamics (SPH) algorithm was utilized to discretize the casing and explosive into particles, preventing element failure due to material distortion and enabling the simulation of dynamic fragmentation under internal explosion. The fragmentation state of the casing was characterized using particle dynamic parameters (velocity, mass, and plastic strain) at various time points. Additionally, a convex hull algorithm was applied to reconstruct the three-dimensional geometry of the fragments, providing a more detailed description of their shape and distribution characteristics. The dataset used for model construction comprised 108 cases, each containing approximately 500 particle states, and considered the influence of casing thickness, aspect ratio, and diameter on fragmentation behavior under internal explosion. Based on this dataset, a predictive model for natural fragment distribution was developed using a Graph Neural Network (GNN) approach. The results indicated that, compared with traditional numerical simulation methods, GNN could effectively predict the geometry, mass, and velocity of natural fragments, significantly reducing computational cost. Furthermore, the GNN model exhibited excellent generalization capability when input parameters extended beyond the training data range. This study demonstrates the significant potential of GNN in predicting fragment distribution,

providing an efficient and scalable solution for cased charge design and damage assessment, as well as for the blast and impact-resistant design of structures.

Keywords: Case charge, Fragment distribution, Machine learning, Graph neural networks

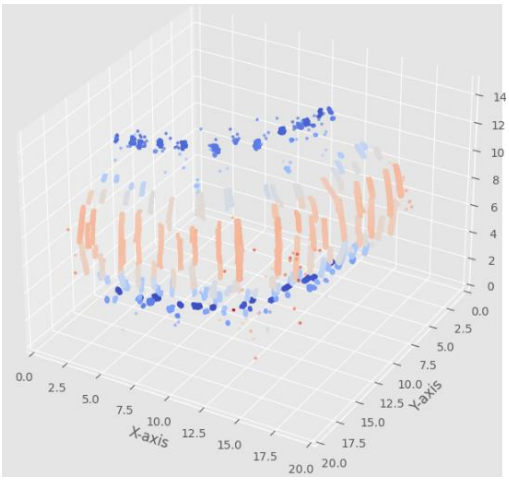

Fig.1. Sph simulation

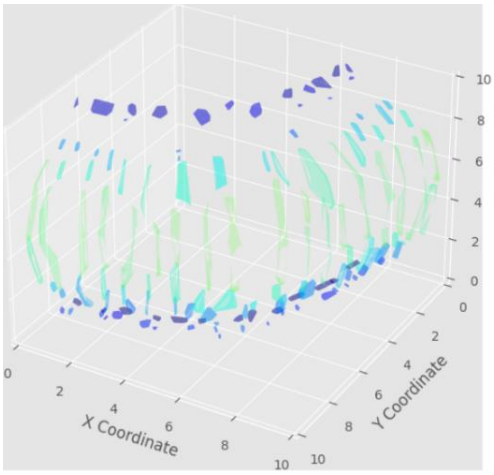

Fig.2. GNN prediction results

Dynamic Analysis of Lattice-Based Metamaterials for Impact Protection

Salvatore Annunziata [1], Edison Shehu [1], Luca Lomazzi [1] and Andrea Manes [1]

[1] *Politecnico di Milano, Department of Mechanical Engineering, Via Giuseppe La Masa, 1, Milan, 20156, Italy*

The use of metamaterials in protective structures has gained significant attention due to their unique mechanical properties, offering promising solutions for energy absorption and lightweight design in impact protection applications. Recent studies have sought to capture the behaviour of these materials under impact loading. For instance, Ramos et al. studied the response of gyroid lattice structures under impact, highlighting that minor modifications to their topology lead to substantially different impact responses **(Ramos, Santiago, Soe, Theobald, & Alves, 2022)**. Moreover, experimental evaluations of metamaterial structures have been performed to assess their response to blast loading **(Ramos, et al., 2023)**.

However, the dynamic behaviour of such structures, particularly under dynamic loading conditions, requires further investigation to optimize their performance and modelling approaches. Current research has explored various lattice-based architectures and their deformation mechanisms, emphasizing their potential advantages over traditional materials like foams. Several researchers have demonstrated that it is possible to design core architectures that offer greater strength and stiffness-to-weight ratios than those of traditional foam materials **(Shen, et al., 2010) (Chiras, et al., 2002)**. Traditional foams dissipate energy through cell collapse, viscoelastic behaviour, and plastic deformation, while metamaterials rely on lattice geometry, local buckling, and the interaction between material properties and structural features **(Shim, 2013)**. Despite these advances, limitations remain in understanding the trade-offs between computational efficiency and predictive accuracy when modelling such materials.

This study presents a numerical analysis of different unit cell architectures for lattice-based metamaterials, as shown in **Figure 1**, utilizing finite element models to evaluate their performance under dynamic loading conditions.

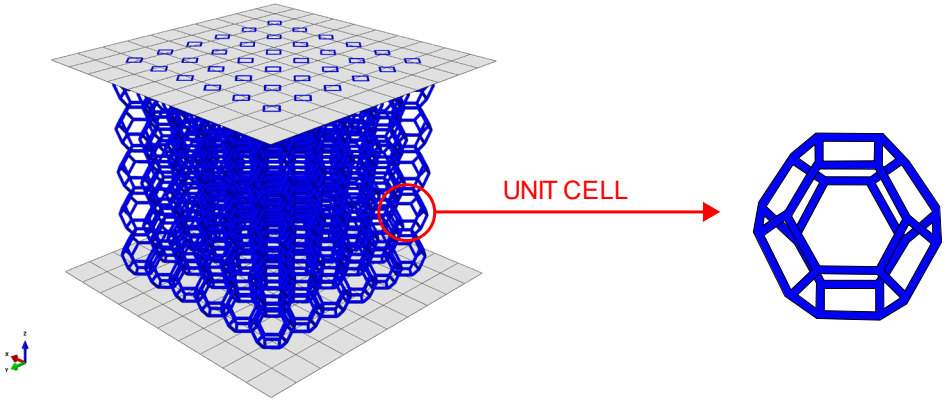

Figure 1. Lattice-based metamaterial and its unit cell

Two modelling methodologies are compared: beam elements, which offer computational efficiency, and 3D solid elements, which provide greater accuracy. The impact of these approaches on simulation precision and computational resource requirements is analysed to identify optimal strategies for highly dynamic loading scenarios.

Additionally, a comparative assessment is performed between lattice metamaterials and traditional foam materials to evaluate their energy absorption capacity (**Figure 2**).

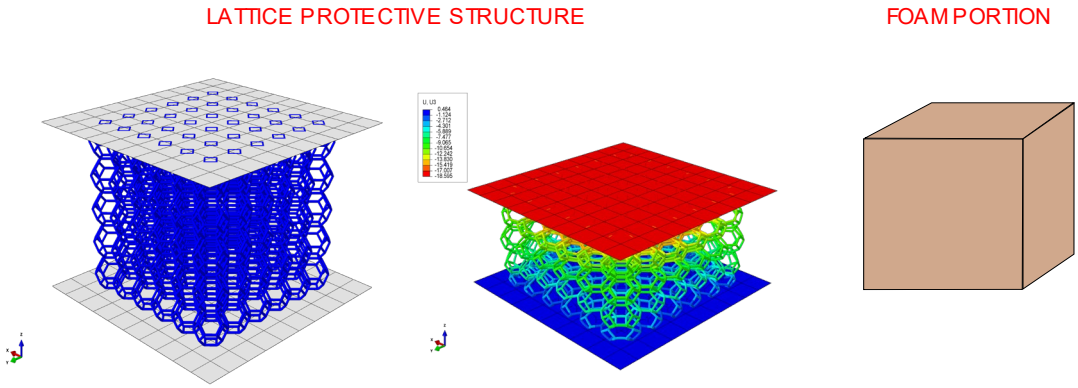

Figure 2. Representation of a lattice metamaterial and a model of a foam material

The study highlights key differences in deformation mechanisms, structural efficiency, and adaptability, aiming to determine whether metamaterials can surpass foams in protective applications.

The results offer valuable insights into the strengths and limitations of various architectures and modelling methodologies. This preliminary research provides a foundation for designing next-

generation protective materials that balance energy absorption, lightweight properties, and computational efficiency to meet the demands of modern engineering applications.

Keywords: Protective structures, Unit cells, Lattice, Foams, Energy absorption, Impact loading

Chiras, S., Mumm, D., Evans, A., Wicks, N., Hutchinson, J., Dharmasena, K., & Wadley, H. &. (2002). The structural performance of near-optimized truss core panels. *International Journal of Solids and Structures*, 4093-4115. doi:https://doi.org/10.1016/S0020-7683(02)00241-X

Ramos, H., Erik, P., Sara, A., Kapil, K., Jide, O., Zhongwei, G., . . . Rafael, S. (2023). Experimental evaluation of hybrid lattice structures subjected to blast loading. *Additive Manufacturing*. doi:https://doi.org/10.1016/j.addma.2023.103751

Ramos, H., Santiago, R., Soe, S., Theobald, P., & Alves, M. (2022). Response of gyroid lattice structures to impact loads. *International Journal of Impact Engineering*. doi:https://doi.org/10.1016/j.ijimpeng.2022.104202

Shen, Y., Mckown, S., Tsopanos, S., Sutcliffe, C., Mines, R., & Cantwell, W. (2010). The Mechanical Properties of Sandwich Structures Based on Metal Lattice Architectures. *Journal of Sandwich Structures & Materials*, 159 - 180. doi:https://doi.org/10.1177/1099636209104536

Shim, C. Y. (2013). Design of protective structures with aluminum foam panels. *International Journal of Steel Structures*, 1-10. doi:https://doi.org/10.1007/s13296-013-1001-1

High Velocity Impact Studies of Ceramic/UHMWPE Composite Ballistic Plate Configurations

Rubayea Alameri, Naresh Kakur, Rafael Savioli, Nikolaos Nikos, Rafael Santiago

Advanced Materials Research Center, Technology Innovation Institute, Abu Dhabi, United Arab Emirates, rubayea.alameri@tii.ae (corresponding author)

ABSTRACT

Recently, ceramics and metal-armed structures have been replaced by ceramics combined with ultra-high molecular weight polyethylene (UHMWPE) composite laminated structures for National Institute of Justice (NIJ) level III and level IV body armor applications. This shift is due to the superior specific energy absorption capabilities of the ceramics/UHMWPE composites compared to traditional ceramics and metal armor; however, it comes at a higher cost. Manufacturing body armor that offers higher specific energy absorption at a lower cost is challenging. As the thickness of UHMWPE increases, the specific energy absorption and the overall cost of the body armor increase. Additionally, there is limited experimental data to evaluate the thickness of ceramics and UHMWPE to explore the performance of NIJ level III body armor, indicating that further research is needed. In this study, six different types of ballistic plate configurations were manufactured. Following that, high velocity impact tests were conducted to investigate the effects of front and back layer thicknesses of UHMWPE (Type 1 to Type 3 plates), the effects of foam material (Type 4 plate), and the effects of different thicknesses of boron carbide (B_4C) ceramic strike face (Type 5 and Type 6 plates) on the back face signature (BFS) of the ballistic plate. It was found that the BFS of Type 5 and Type 6 ballistic plate configurations is lower by 12% and 8.5%, respectively, compared with that of the Type 4 UHMWPE/polyvinyl chloride low-density foam ballistic plate. However, the Type 5 option is cost-effective and easy to manufacture, making it the preferred choice over the Type 6 variant.

Keywords: Ballistic plate; ceramic tiles; UHMWPE; high velocity impact; back face signature

Submission ID: 7043
(Full Paper)

Enhanced Penetration Through Two-Stage Double-Blunt Projectile

Shaima Alhosani, Afsar Husain, Sanan H Khan
Department of Mechanical and Aerospace Engineering,
United Arab Emirates University, Al Ain, United Arab Emirates

Abstract

This study introduces a novel double-blunt projectile design featuring a reduced-diameter primary nose (6.40 mm) followed by a larger secondary diameter (12.80 mm). The penetration performance is compared with conventional single-blunt projectiles through ABAQUS/Explicit finite element analysis. At 100 m/s impact velocity, the double-blunt configuration demonstrates significantly higher penetration efficiency, absorbing only 3.64 J energy compared to 15.21 J for the single-blunt design. This improved performance is achieved through a strategic two-stage perforation process that optimizes stress distribution and minimizes resistance during penetration.

Keywords: Impact mechanics, Double-blunt projectile, Two-stage penetration, Finite element analysis.

The finite element investigation [1] employs quarter-symmetry modeling to analyze penetration behavior at impact velocities ranging from 35-100 m/s. As shown in Table 1, at 100 m/s impact velocity, the double-blunt projectile demonstrates remarkably improved performance over the single-blunt design.

Table 1: Comparative Performance Analysis at 100 m/s Impact Velocity

Parameter	Single Blunt	Double Blunt
Initial Velocity (m/s)	100	100
Residual Velocity (m/s)	92.17	96.36
Energy Absorption (J)	15.21	3.64
Penetration Efficiency (%)	92.17	96.36
Maximum Deformation (mm)	8.3	8.07
Perforation Mechanism	Single Stage	Two-Stage

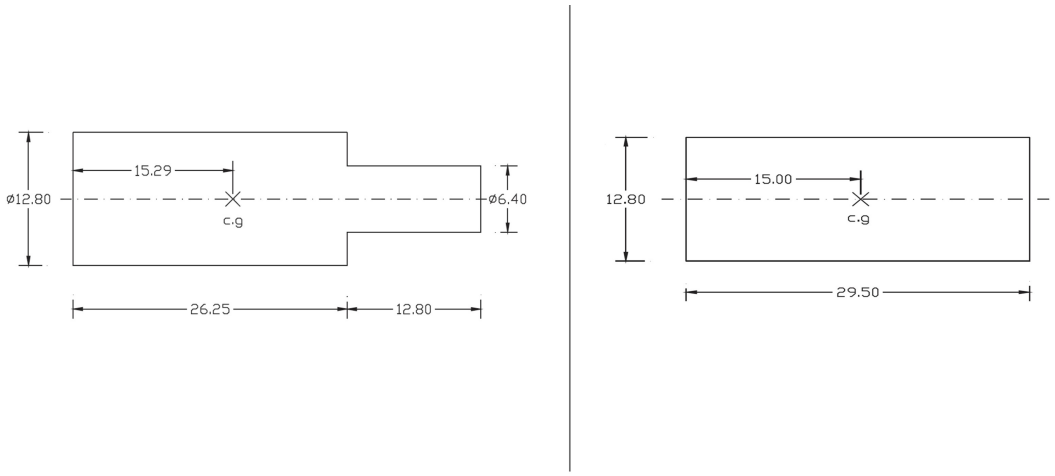

Figure 1: Schematic showing double blunt projectile design (left) with reduced primary diameter and conventional single blunt projectile (right) [2]

The key performance differences include:

- 76% reduction in energy absorption (3.64 J vs 15.21 J)
- Higher residual velocity (96.36 m/s vs 92.17 m/s)
- Reduced target deformation (8.07 mm vs 8.3 mm)
- More efficient two-stage perforation process

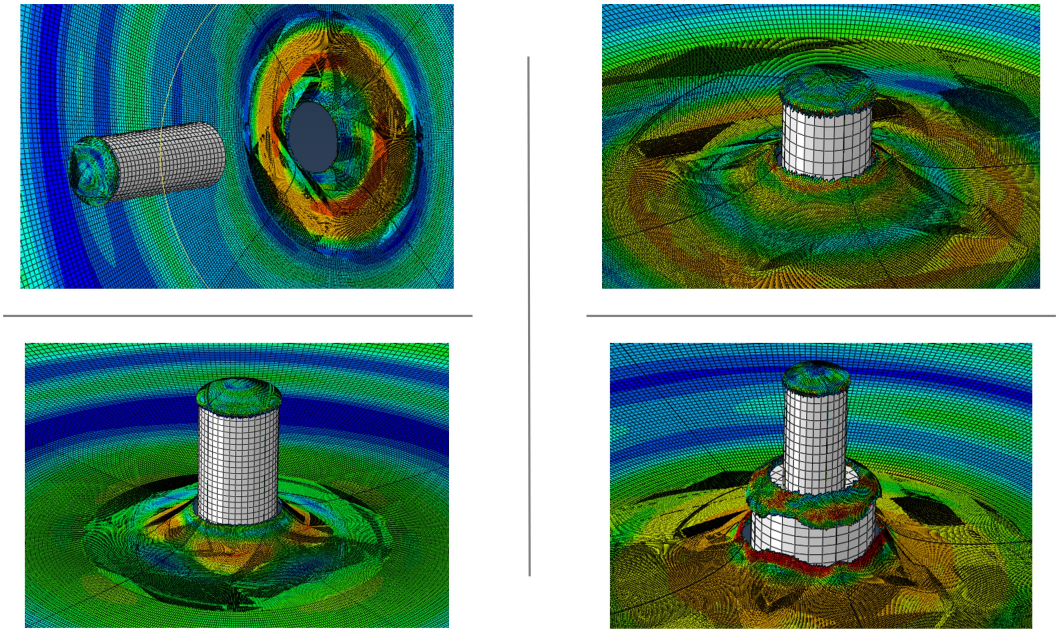

Figure 2: ABAQUS/Explicit analysis showing penetration progression and stress distribution for both projectile designs

This enhanced performance can be attributed to the innovative two-stage penetration mechanism:

1. Initial Stage: The reduced-diameter nose (6.40 mm) initiates penetration with minimal resistance, creating a pilot hole.
2. Secondary Stage: The larger diameter section (12.80 mm) follows through the pre-damaged material, completing the perforation process with optimized energy utilization. The study demonstrates that geometric optimization through the double-blunt configuration significantly enhances penetration performance. The strategic reduction in initial contact area, followed by controlled secondary penetration, results in substantially lower energy absorption while maintaining higher residual velocities. These findings represent a significant advancement in projectile design, particularly for applications requiring efficient penetration with minimal energy loss.

References:

[1] S. H. Khan, S. K. Agnihotri, A. A. Khan, and A. Husain, "Finite Element Modeling and Simulation of Projectile Impact on Ductile Target," *Lecture Notes in Mechanical Engineering*, pp. 429–437, 2020, doi: 10.1007/978-981-15-1071-7_36/COVER/.

[2] M. A. Iqbal, S. H. Khan, R. Ansari, and N. K. Gupta, "Experimental and numerical studies of double-nosed projectile impact on aluminum plates," *Int J Impact Eng*, vol. 54, pp. 232–245, Apr. 2013, doi: 10.1016/J.IJIMPENG.2012.11.007.

Energy-Based Monitoring Technique for Progressive Collapse Prevention in Complex Structures

Lorenza Abbracciavento[1], Valerio De Biagi[1]

[1]*Department of Structural, Geotechnical and Building Engineering, Politecnico di Torino, Turin, Italy*

This research addresses key challenges in progressive collapse prevention by introducing an advanced method to enhance the complex structural systems monitoring. The study focuses on variation of deformation work patterns with the aim to identify the most critical load paths while a random element within the structure undergoes damage. A comprehensive mathematical model has been developed to analyze changes in load paths due to damage in structural elements. The method utilizes an energy-based metric introduced by De Biagi and Chiaia (2013) [1], allowing for a detailed assessment of damage progression. The damage is simulated through the alteration of the stiffness of structural elements by applying progressive cross section reduction. The predictions of the model were validated through its application to simple systems composed of rods, where changes in load paths were observed as damage advanced in random elements. For more complex structural systems, the method was applied using numerical simulations, providing a detailed evaluation of its performance in more load cases scenarios. The proposed metric effectively captures the effects of localized damage and its propagation through the system, offering valuable insights for the monitoring and prevention of progressive collapse. The method yields two significant outcomes: first, mapping the variation of deformation work with respect to the damage allows for the visualization of the variation in the load path during the damage of a random element within the structure, thus, identifying which elements are loaded and which are unloaded; second, the study of evolution of the variation of deformation work with respect to the damage for different stiffnesses allows identifying the value of critical stiffnesses that determine whether the element remains part of the main load-bearing path.

In this work, the method is applied to 2D and 3D truss systems, which are representative of critical infrastructure like bridges and towers, as well as to ad hoc designed structural schemes created to highlight specific aspects and demonstrate the effectiveness of the method. The aim of the method is not only to ensure the safety of vital infrastructure by improving resilience

against catastrophic events, but also to offer practical insights by identifying the most critical areas for sensor placement, enabling optimal monitoring and early detection of failure points.

Keywords: progressive collapse, robustness, structural complexity, energy metrics.

Images:

The 2 main outcomes of the proposed methodology

1) Load path variations within the structure during the random damage of elements

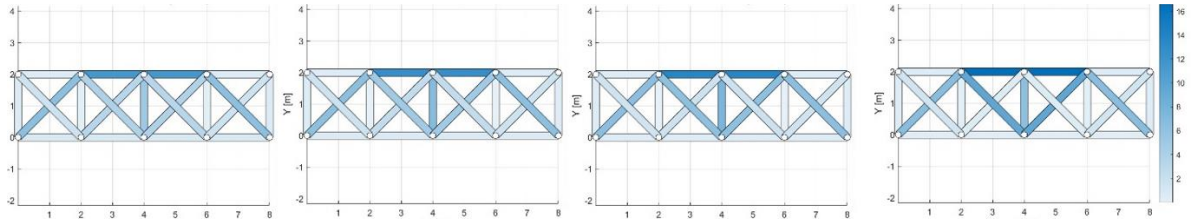

Figure 1. *Mapping the parameter $\partial W/\partial \xi$. Load path redistribution due to the damage to the central vertical rod. Colour variations indicate how load paths change in response to incremental damage. Each colour represents a different level in the variation of deformation work in members.*

2) Critical stiffness value

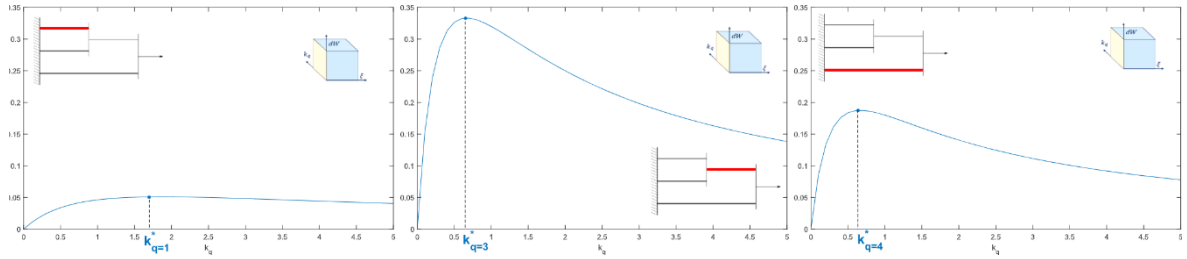

Figure 2. *The study of the parameter $\Omega\ (k_q)$. The variation of deformation work, by varying the stiffness value of the element of the system presents a bell-shape curve. The peak of the curve represents the critical value of stiffness that determines when the element is part of the preferential path load (right side of the peak) or not (left side of the peak).*

References:

[1] V. De Biagi, B. M. Chiaia, Damage tolerance in parallel systems, International Journal of Damage Mechanics 25 (7) (2016) 1040–1059.

Estimation of the probability distribution of rockfall barriers energy absorption capacity through a global analytical model

Francesco Pimpinella[1], Maddalena Marchelli [2] and Valerio De Biagi [1]

[1]*Department of Structural, Geotechnical and Building Engineering (DISEG), Politecnico di Torino, Torino, Italy*

[2]*Department of Environment, Land and Infrastructure Engineering (DIATI), Politecnico di Torino, Torino, Italy*

Flexible rockfall barriers are worldwide commonly used in alpine and coastal environment to protect structures and infrastructures, reducing the risk below an acceptable threshold value. The risk depends on the spatial and temporal occurrence of the rockfall phenomenon and on the exposure, vulnerability and value of the potentially affected elements [1]. The risk reduction after a flexible rockfall barrier installation depends on the system's ability of intercepting and withstanding the impacting block, which is complementary to the system's failure probability [2].

In the current design approaches, the performance of the barrier is assessed through standardized impact tests according to the EAD 340059-00-0106, which presupposes an impact in the center of the central module of the barrier. The system is considered failed whenever the block kinetic energy exceeds the system nominal capacity. This approach is not able to describe the real capacity of the system, which depends on many factors, such as the rockfall size [3] and/or impacting position [4], and the system ageing. Reaching a more refined estimation of the energy absorption capacity cumulative density function (CDF) and its change over time can lead to more sophisticated residual risk assessments. Consequently, funds for new installations and maintenance of existing barriers could be allocated in a more targeted way.

The estimation of the CDF related to energy absorption capacity is not trivial. First of all, the function should be specific of each system typology. For this reason, in our work we introduced and applied a procedure which is replicable for any system, but was validated for a commonly installed technology, only. The idea was to build a global analytical model in which all the relevant rockfall barriers components (intercepting structure, wire ropes, steel posts, energy

dissipators, ropes end terminations) are assembled and mutually connected. The basic components properties also depend on the system aging, making it possible to study the barrier performance over time. The generic rockfall impact is simulated in the model with displacement impositions on the intercepting structure. Consequently, all the elements are progressively loaded until one of them fails, causing the inefficiency of the system. At that point, the energy absorbed by the barrier for that generic rockfall impact simulated on a barrier with a given service life can be estimated through the analytical model related to each component. The complete energy absorption capacity cumulative density function can be estimated after several applications of the model in which the impact position, the block size and the components' properties are extracted by appropriate distributions, allowing for the execution of a statistically sound process.

The application of the introduced framework to other commonly installed rockfall barriers technologies can lead to the introduction of more efficient maintenance procedures. An example of application is proposed to explain the capabilities of the approach.

Keywords: rockfall barriers, energy absorption capacity, global analytical model, system degradation.

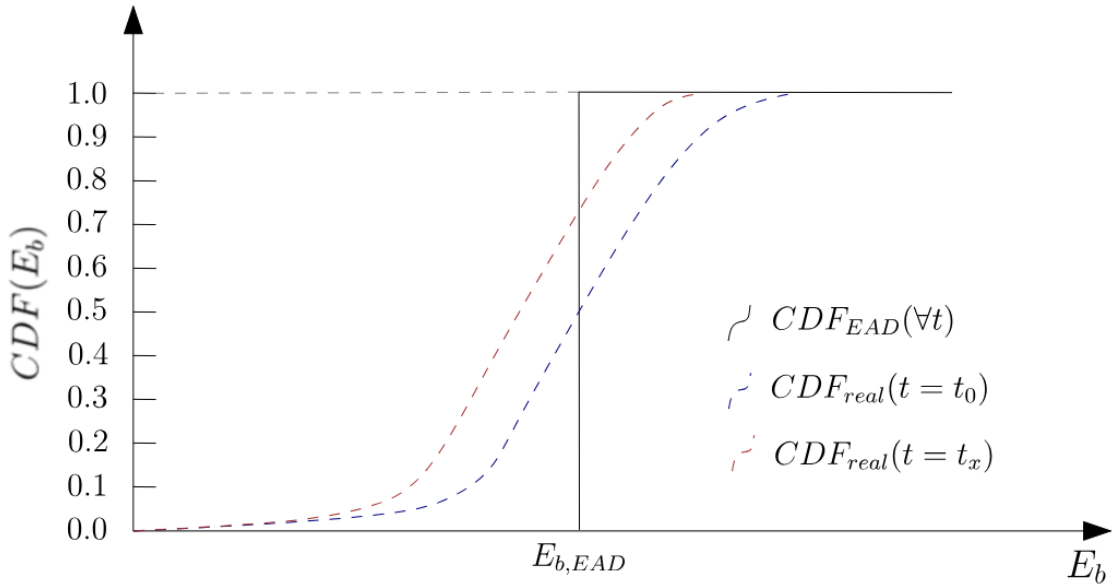

Figure 1 - Cumulative distribution functions of energy absorption for rockfall barriers: the approach currently used in the risk evaluation is graphed in black, while the expected CDF shape and its modification over time are plotted in blue and red dashed lines, respectively.

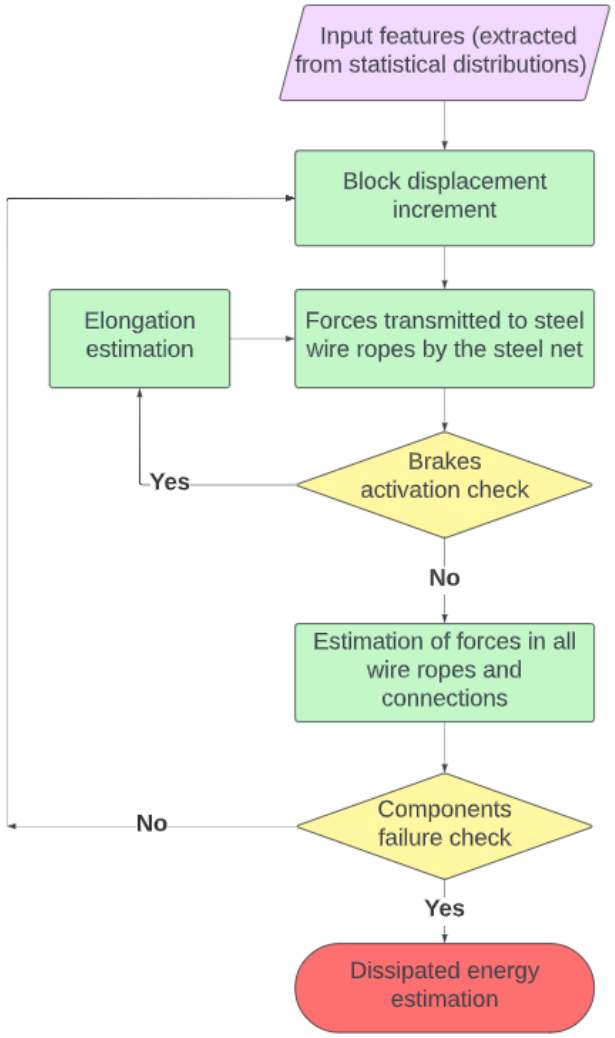

Figure 2 – Process used in the global analytical model to estimate the energy absorption capacity of a generic barrier with a given service life and for a generic impact

[1] Marchelli, M., De Biagi, V., Bertolo, D., Paganone, M., & Peila, D. (2021). A mixed quantitative approach to evaluate rockfall risk and the maximum allowable traffic on road infrastructure, Georisk: Assessment and Management of Risk for Engineered Systems and Geohazards, https://doi.org/10.1080/17499518.2021.2010097.

[2] De Biagi, V., Marchelli, M. & Peila, D. (2020). Reliability analysis and partial safety factors approach for rockfall protection structures, Engineering Structures, https://doi.org/10.1016/j.engstruct.2020.110553.

[3] Koo, R, Kwan, J., Lam, C., Ng, C, Yiu, J, Choi, C, Ng, A, Ho, K, Pun, W (2017). Dynamic response of flexible rockfall barriers under different loading geometries, Landslides, https://doi.org/10.1007/s10346-016-0772-9.

[4] Zhao, L., Yu, Z. X., Liu, Y. P., He, J. W., Chan, S. L., & Zhao, S. C. (2020). Numerical simulation of responses of flexible rockfall barriers under impact loading at different positions. Journal of Constructional Steel Research, https://doi.org/10.1016/j.jcsr.2020.105953.

Response of Gradient Hexachiral Auxetics Under Impact Loadings: Experimental Study

Xin Li [1], Chuanqing Chen [2]

[1] *Nanjing University of Science and Technology, Nanjing, China*

[2] *Nanjing University, Nanjing, China*

In this work, the dynamic response of gradient hexachiral auxetic metamaterials were experimentally investigated under dynamic and explosive loadings. Five gradient design strategies were employed in the test, including uniform, positive, negative, centre positive, and centre negative gradients. The effects of gradient distribution on deformation/failure modes under different loading conditions were analysed. Experimental results revealed that the gradient design can mitigate the shear deformation of hexachiral auxetics, which efficiently remain its negative Poisson's ratio effect under dynamic loading. Compare with the quasi-static loading, earlier failure of auxetics were observed under dynamic loads, which diluted their negative Poisson's ratio effect. Under explosive loads, hexachiral cores with larger radius nodes on the blast surface are more likely to undergo compression deformation. This work offers profound insights into enhanced performance mechanisms and provides avenues for optimizing structural design of auxetic metamaterials.

Keywords: Dynamic response, Impact Loadings, Gradient Hexachiral Auxetics.

1. Hexachiral Auxetics Under Quasi-Static and Dynamic Loadings

In this section, dynamic compression tests are conducted under constant compression velocities of 10 mm/min and 5 m/s for analysing the deformation modes of gradient hexachiral auxetics. To enhance the capture of detailed deformation characteristics during compression, the auxetics were designed with 5 node layers, as illustrated in Figure 1.

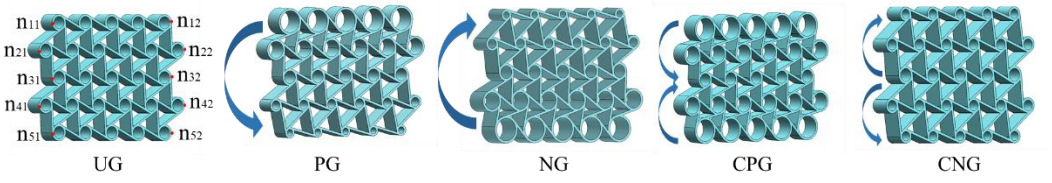

Figure 1 Specimen structures of hexachiral auxetic cell structure

Figure 2 (a) presents the deformation profiles of various gradient hexachiral auxetics at ε_y ranging from 0.1 to 0.6, subjected to an impact velocity of 5 m/s. At ε_y of 0.1, the deformation modes closely resemble those observed under quasi-static loading, as depicted in Figure 3, characterized by rotational deformation of the central layer nodes and flattening deformation of the large-radius nodes. However, dynamic loading introduces both inertial effects and stress wave propagation. The inertial effect imposes additional stress on the structure, while stress wave propagation causes localized stress concentration. Consequently, structural damage

occurs at lower strains compared to quasi-static loading, leading to significant deviations in the structure's deformation mode under both loading conditions. Particularly in the UG configuration, a distinct shear deformation along the diagonal becomes evident. This shear deformation arises from nodes being distributed in a quasi-parallelogram during auxetic deformation, facilitating the transmission of shear forces. In contrast, other gradient hexachiral auxetics do not display such shear deformation, despite experiencing local structural damage and intricate deformation patterns.

The Poisson's ratio-strain curves of different gradient hexachiral auxetics under dynamic compression are depicted in Figure 2(b). The NPR effect of the CNG configuration is comparable to that of the PG configuration, followed by the NG configuration, while the UG and CPG configurations exhibit the weakest NPR effect. In addition, through detailed numerical comparisons with quasi-static condition, the overall Poisson's ratio curves for UG, NG and CNG experience increases, signifying a weakening of the NPR effect under v = 5 m/s in these three configurations. It can be attributed to occurrence of the localized structure damage caused by inertial effects and wave propagation.

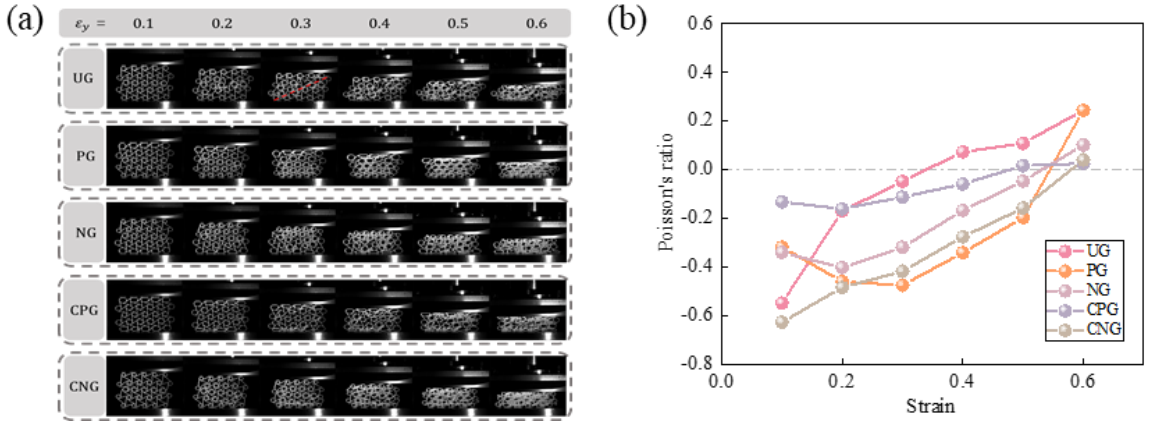

Figure 2 Deformation modes of diverse gradient hexachiral auxetics under dynamic: (a) profiles and (b) Poisson's ratio.

2. Sandwich Panels with Hexachiral Auxetic Cores Under Explosive Loading

Figure 3(a) displays the central cross-sections of five distinct gradient hexachiral core specimens with their respective enlargements shown in Figure3 (b). These specimens were exposed to impulses of 31.29, 36.90, 30.45, 28.02, and 37.80 Ns. Deformation was notably localized in three areas: the center (indicated by red dotted rectangles) and the clamped regions on both sides (defined by red solid lines). The experiments revealed that except for PG, all cores had deformation confined to the first ligament layer, limiting the NPR effect. The UG-3 and CPG-3 specimens showed similar compressive deformation patterns, with node flattening near the front face sheet and bending in the first ligament layer. espite a smaller impulse, CPG-3 exhibited more node flattening than UG-3. NG-3, subjected to a similar impulse as UG-3, demonstrated superior compression resistance with minimal node deformation, limited to slight

bending in the first ligament layer, much less than UG-3. PG-3 experienced the most significant deformation, with extensive flattening and bending across the first and second layers of nodes and ligaments, and multiple joint fractures, attributable to a higher impulse. Conversely, CNG-3, with a similar impulse to PG-3, showed less deformation, primarily in the first ligament layer's bending and fewer joint fractures. The findings indicate that node size significantly influences compression deformation. Configurations with larger nodes adjacent to the front face sheet, such as PG and CPG, were more prone to compression deformation.

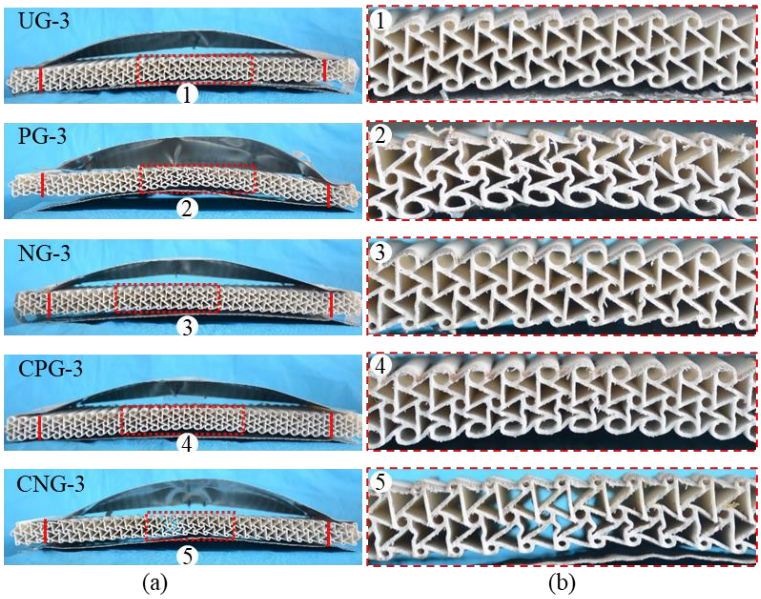

Figure 3 (a) Compress deformation of specimens with different gradient auxetic cores, and (b) enlargements of central parts of the auxetic cores.

3. CONCLUSION

Gradient strategies play significant roles in the deformation modes of hexachiral auxetics under different loading conditions. Dynamic loading introduces earlier and more structural damage than quasi-static conditions, reducing NPR effects. Gradient design can mitigate the shear deformation under dynamic loadings. In both quasi-static and dynamic loading conditions, the CNG configuration exhibits a substantial NPR effect, while the CPG configuration performs the least. Under explosive loads, configurations with larger nodes adjacent to the front face sheet are more prone to compression deformation.

REFERENCES

[1]. Prall, D., & Lakes, R. S. (1997). Properties of a chiral honeycomb with a poisson's ratio of—1. International Journal of Mechanical Sciences, 39(3), Article 3. https://doi.org/10.1016/S0020-7403(96)00025-2

[2]. Chen, C., He, Y., Xu, R., Gao, C., Li, X., & Lu, M. (2024). Dynamic behaviors of sandwich panels with 3D-printed gradient auxetic cores subjected to blast load. International Journal of Impact Engineering, 188, 104943. https://doi.org/10.1016/j.ijimpeng.2024.104943

Submission ID: 7387

CONTACT EXPLOSION RESISTANCE OF A STEEL SANDWICH PANEL CONTAINING AN ALUMINUM HONEYCOMB LAYER

N. Chikhradze,
Prof., G. Tsulukidze Mining Institute, 7 Mindeli Str., 0186 Tbilisi, Georgia, chikhradze@mining.org.ge

E. Mataradze
Dr., G. Tsulukidze, G. Tsulukidze Mining Institute, 7 Mindeli Str., 0186 Tbilisi, Georgia, emataradze@yahoo.com

I. Akhvlediani
Dr., G. Tsulukidze Mining Institute, 7 Mindeli Str, 0186 Tbilisi, Georgia, irakliakhvlediani@hotmail.com

ABSTRACT

Contact explosion occurs when an explosive device is detonated on the surface of an object, such as a building, tank, or a vehicle. It is used to maximize the effect of explosive on a specific target. Methods and means of protecting steel plates from contact explosions are the subject of many studies. In recent years, there has been increased interest in innovative composite structures that use new energy-absorbing materials as a damping layer. This paper presents the results of experimental studies of the explosion resistance of a sandwich panel containing two steel plates, one of which is 2mm thick and another – 3mm thick, and an aluminum honeycomb plate placed between them. At different stages of the experiments, sandwiches with a honeycomb plate the thickness of which was 10 mm and 30 mm, as well as steel plates without an energy-absorbing layer were tested. The processes of deformation and destruction of sandwiches during the contact explosion of hexogen charges weighing 5-75 grams were recorded by a video camera at a frequency of 16,000 frames per second. Explosion resistance was assessed by the minimum mass of the contact charge and the overpressure impulse causing a local rupture of all sandwich layers and the formation of a penetrating hole. Four modes of deformation and destruction of the tested sandwich panel under the impact of a contact explosion were identified: Mode I: residual bend of a steel plates, all three plates retain integrity. Mode II: the honeycomb layer is destroyed (burned), both steel plates retain integrity. Mode III: rupture of the steel plate on the side of the explosion, rupture of aluminum honeycomb plate. The steel plate on the side opposite to the explosion retains integrity. Mode IV: rupture of all three plates and formation of a through hole, the sandwich panel loses its operational properties. The comparative analysis of sandwiches with and without a protective layer showed that an aluminum honeycomb layer significantly increases the explosion resistance of a sandwich. More specifically, explosion resistance of a sandwich with a 10 mm thick aluminum honeycomb layer increases by 1.8 times, and with a 30 mm thick layer - by 3 times.

Keywords: Contact explosion, steel plate, aluminum honeycomb plate.

\

Figures

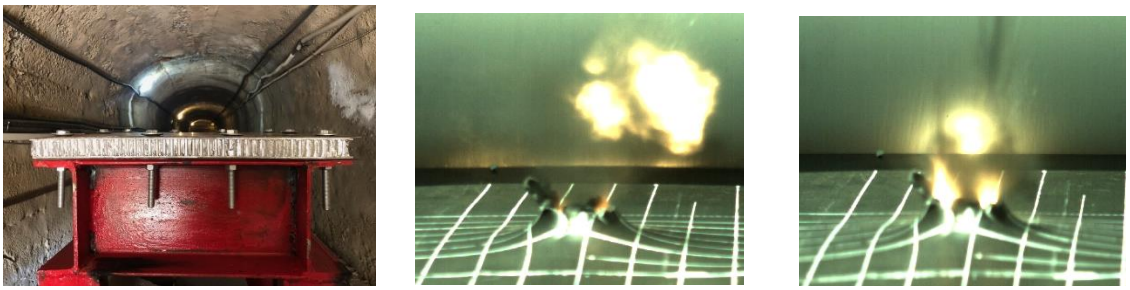

1 2 3

Figure 1. Video frames of the steel sandwich panel before the explosion and at different points in time after detonation. 1 - before the explosion, 2 - 468 μs after detonation (through hole formation), 3 - 1092 μs after detonation (ejection of fragments)

1 **2** **3**

Figure 2. Photo after the explosion. Charge weight 35 gram. 1- 3 mm thick steel plate (on the side opposite the explosion), 2- 10 mm thick aluminum honeycomb plate, 3- 2 mm thick steel plate (on the side of explosion)

Reference

1. M.D. Olson, G.N. Nurick, J.R. Fagnan. Deformation and rupture of blast loaded square plates—predictions and experiments. International Journal of Impact Engineering. Volume 13, Issue 2, 1993, Pages 279-291

2. G.S. Langdon, S.Chung Kim Yuen, G.N. Nurick. Experimental and numerical studies on the response of quadrangular stiffened plates. Part II: localised blast loading. International Journal of Impact Engineering. Volume 31, Issue 1, January 2005, Pages 85-111

3. McDonald B., Bornstein H., Langdon G., Curry R., Daliri A., Orifici A. Experimental response of high strength steels to localised blast loading. Int. J. Impact Eng. 2018;115:106–119.

4. M.-O. Sturtzer, S.Trélat, E. Schmitt. Effects of explosive charges in contact with steel plates: small-scale experimental investigation using high-speed imaging. International Journal of Protective Structures, 2023.

5. Alex Remennikov, Igor Mentus and Brian Uy. Explosive Breaching of Walls with Contact Charges: Theory and Applications. International Journal of Protective Structures, Volume 6, 2015

6. A. Razak and A. Alias. The Response of Steel Plates Subjected to Close-in Blast Loads. IOP Conf. Series: Earth and Environmental Science 682 (2021).

7. Björn Zakrisson, Bengt Wikman, Hans-Åke Häggblad. Numerical simulations of blast loads and structural deformation from near-field explosions in air. International Journal of Impact Engineering 38 (2011).

8. R. Rajendran, J.M. Lee. Blast loaded plates. Marine Structures. Volume 22, Issue 2, April 2009, Pages 99-12.

9. Carlos Jacinto, Ricardo Daniel Ambrosini, Rodolfo Francisco Danesi. Experimental and computational analysis of plates under air blast loading. International Journal of Impact Engineering. Volume 25, Issue 10, November 2001, Pages 927-947

10.Fu T., Zhang M., Zheng Q., Zhou D., Sun X., Wang X. Scaling the response of armor steel subjected to blast loading. Int. J. Impact Eng. 2021

11.Amika Moda (2020) Booking of modern domestic tanks. Tank armor Composite tank armor. (2020) Available at: https://amikamoda.ru/en/bronirovanie-sovremennyh-otechestvennyh-tankov-tankovaya-bronya-kompozitnaya.html.

12. Tarlochan F (2021) Sandwich Structures for Energy Absorption Applications: A Review. *Materials* 14(16): 4731. DOI: 10.3390/ma14164731.

13. Ma Q, Rejab M, Siregar JP et al. (2021) A review of the recent trends on core structures and impact response of sandwich panels. *Journal of Composite Materials* 55(18): 1–43. DOI: 10.1177/0021998321990734.

Impact of Reinforcement ratio and CFRP on the Blast Performance of Reinforced Concrete slabs: A Numerical Approach

Sai G R K O[1], Arumugam D [2], Tamilselvan K [3] and Dhanasekaran B[4]

[1]*Design engineer, L&T Construction, Chennai, India*

[2] *Lead Engineering Manager, L&T Construction, Chennai, India*

[3] *SR. Chief Engineering Manager, L&T Construction, Chennai, India*

[4] *JGM & Head - Engineering, L&T Construction, Chennai, India*

The increasing need to protect structures from threats like terrorism and potential war has made blast-resistant design essential. Blast shelters are typically constructed as fully reinforced concrete (RC) structures to withstand blast from a standoff distance. During a blast, most of the pressure is exerted on the walls, making it crucial to study their behavior and reinforce them appropriately. As blast tests are resource-intensive and risky, numerical simulations provide an alternative to study blast scenarios, aiding in the design of effective strengthening techniques to improve blast resistance. Several researchers studied the behavior of RC slabs under blast, and some compared the effects of varying levels of reinforcement or strengthening techniques, such as the use of Carbon Fiber Reinforced Polymer (CFRP). The current study offers a novel approach by comparing RC slabs of equal capacity but varying reinforcement or strengthening levels of CFRP. This contrasts with previous research, which typically compares slabs of different capacities (due to variations in reinforcement or strengthening despite having the same depth). By focusing on slabs with identical capacity, the current study aims to better isolate and understand the impact of reinforcement percentage and strengthening techniques on blast resistance. This approach could provide deeper insights into optimizing the balance between reinforcement levels and the use of advanced strengthening materials, ultimately leading to more efficient and cost-effective designs for enhancing blast performance.

Keywords: RC slabs, blast resistance, reinforcement ratio, CFRP.

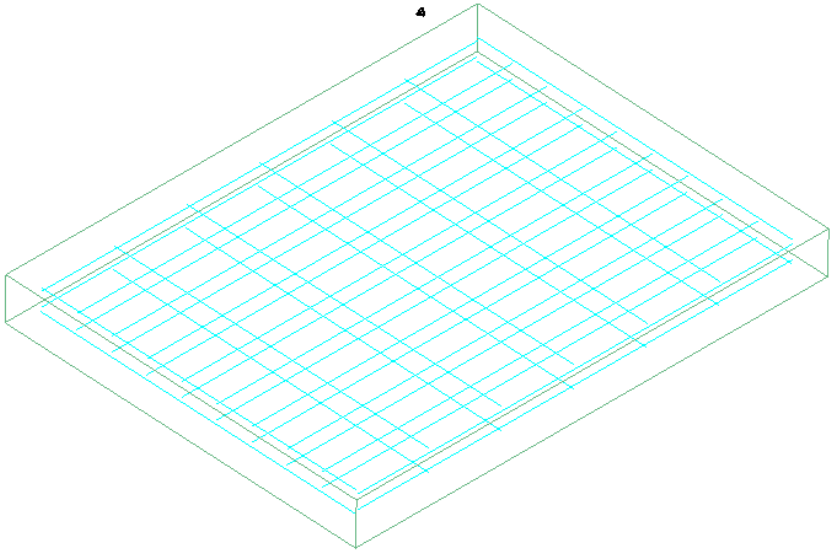

Figure 1: Numerical model of the slab before subjected to blast load.

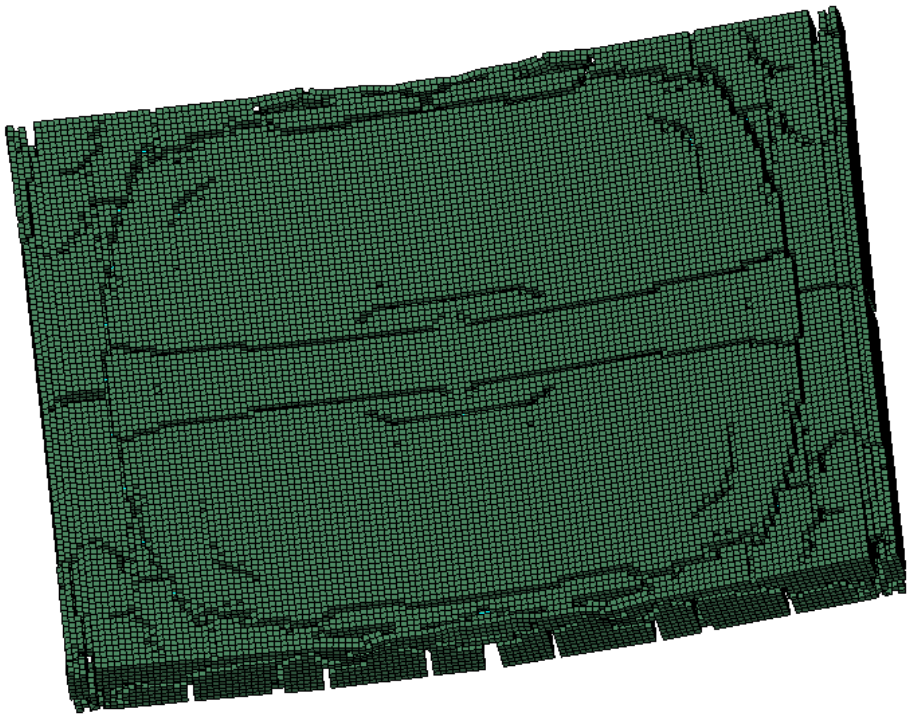

Figure 2: Numerical model of the slab after subjected to blast load.

BLAST LOADING OF CIRCULAR RC COLUMNS USING A SMALL-SCALE EXPLOSIVE-DRIVEN SHOCK TUBE

Ben Rhouma Mohamed[1,2], Maazoun Azer[3],Aminou Aldjabar[1,2], Belkassem Bachir[1], Tine Tysmans[2], and Lecompte David[1]

[1]*Royal Military Academy, Structures and Effects of Explosions Department, Avenue de la Renaissance 30, 1000 Brussels, Belgium*

[2]*Vrije Universiteit Brussels, Mechanics of Materials and Constructions Department Pleinlaan 2, 1050 Brussels, Belgium*

[3] *Military Academy of Fondouk Jedid, Civil Engineering Department, 8021 Nabeul, Tunisia*

Abstract

Public and critical infrastructures have been and continue to be potential targets for terrorist bombings. Reinforced Concrete (RC) columns, being axial bearing components in buildings, are susceptible to damage and failure when subjected to blast loading. Failure of these columns can trigger the progressive collapse in the targeted building. The primary objective of this study is to investigate the failure characteristics of laboratory-scaled RC columns subjected to localized blast loading. The columns, with a length of 1500 mm and an outer diameter of 100 mm, are reinforced with 6-mm-diameter longitudinal bars and 2-mm-diameter steel ties. The blast loading is generated using an Explosive-Driven Shock Tube (EDST) positioned at 4 mm from the mid-span of the RC columns. High-speed stereoscopic Digital Image Correlation (DIC) is used in addition to Linear Variable Displacement Transducers (LVDTs) to capture the global response of the RC columns, as indicated in Figures (1) and 2, respectively. Furthermore, a Finite Element (FE) model is developed in LS-DYNA and validated against experimental data. The concrete is modeled using Concrete Damage Release 3, which incorporates strain rate effects and the ability to predict damage, while Piecewise_Linear_Plasticity is used for the steel reinforcement. The experimental results show that The DIC technique can quantify the damage pattern of the blast-loaded RC columns. The proposed FE approach can reproduce the applied blast loading regarding reflected pressure and impulse. It can also replicate the deformation and failure characteristics of the blast-loaded columns.

Keywords: (Laboratory-scaled RC column, Numerical analysis, Blast response, stereoscopic high-speed DIC, EDST).

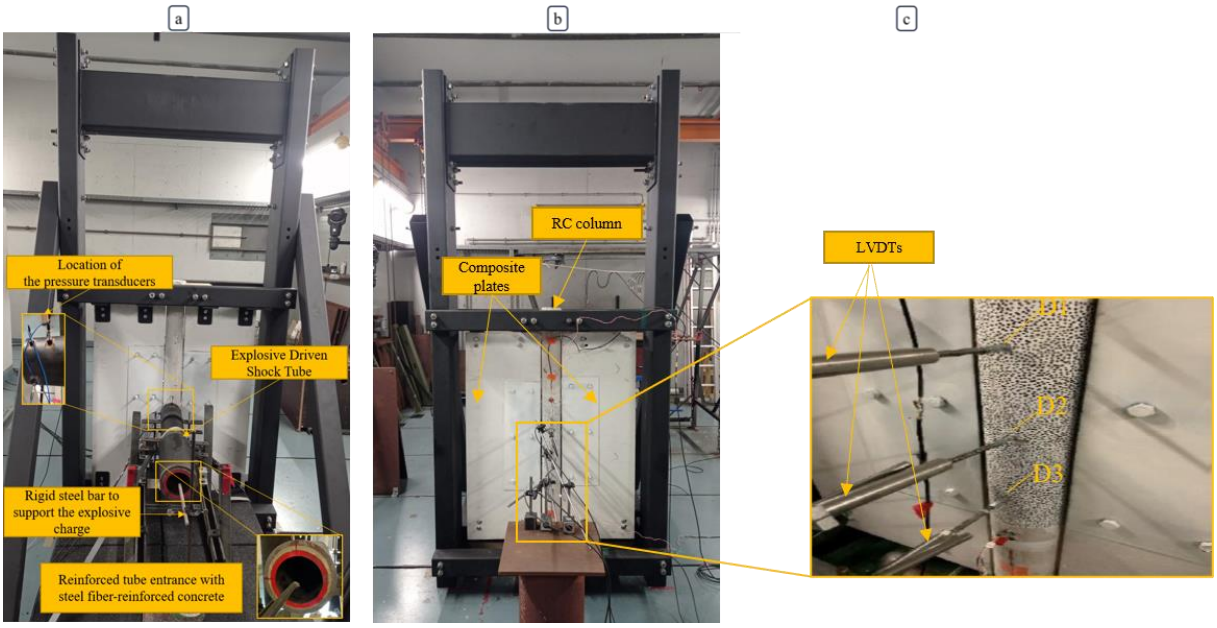

Figure 1: Experimental set-up showing: (a) the set-up with EDST (b)-(c) the LVDTs used to capture the out-of-plane displacement of the columns.

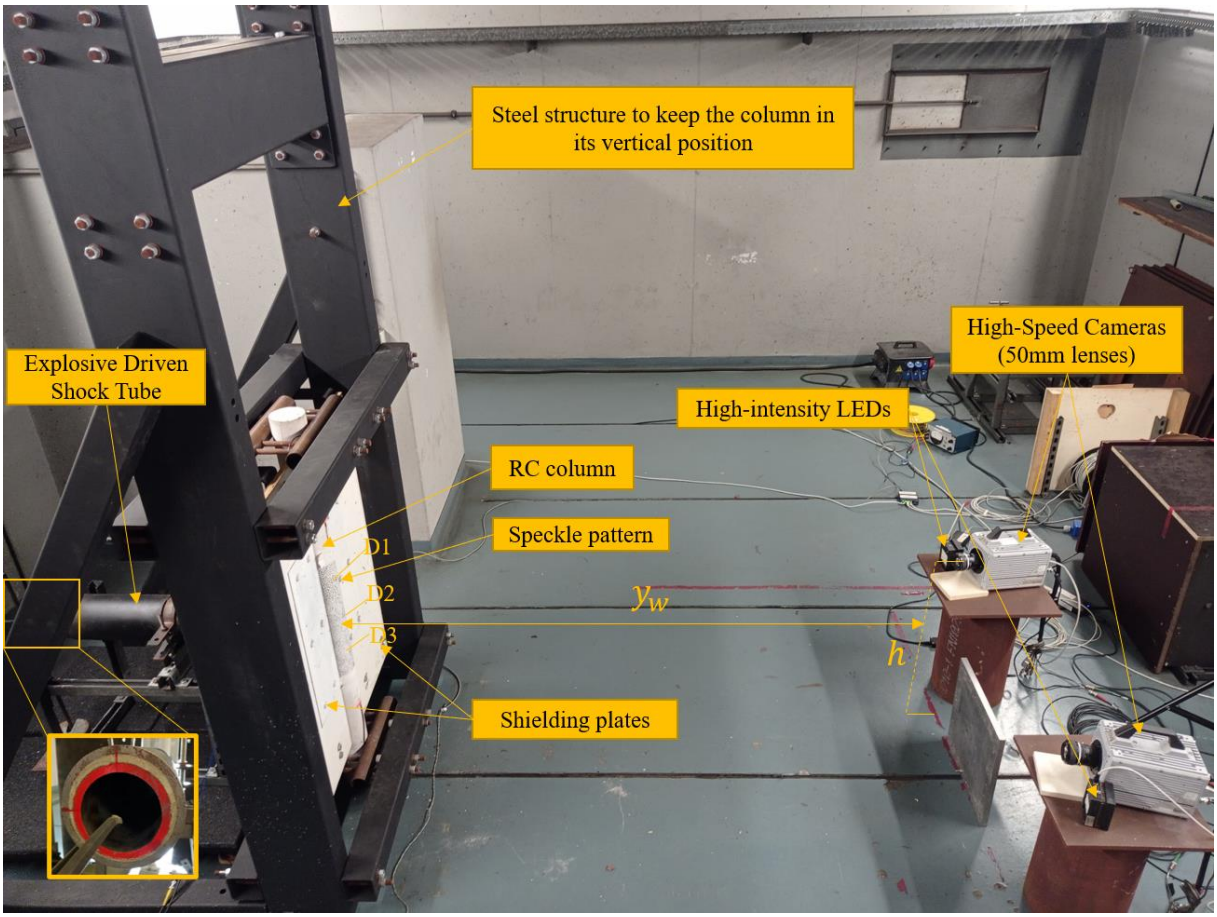

Figure 2: Experimental set-up for the out-of-plane displacement measurement of the columns using the digital image correlation technique.

Detonation chamber for end of life warheads disposal in fully confined conditions: from design to proof tests

Jérôme Mespoulet[1], Maëlle Peyratout[1], Sébastien Boussac[1] and Paul Deconinck[1]

[1]*Shock Physics Department, Thiot Ingenierie, 830 route Nationale, 46130 Puybun, France*

Warheads design is focused on defeating targets by mastering the various components such as natures of the materials (explosive, liner or ammunition body), geometries or location and number of ignition points. Besides their nominal use, they sometimes need to be dismantled because of aging (bad storage conditions), untriggered systems (fuse malfunction), or reduction of stockpile. Those operations, done in safe conditions, can either be done under unconfined or fully confined conditions.

Destruction in unconfined conditions are the historical way to remediate explosives, ammunitions and warheads in open air, buried in soil or undersea. They allow large amount quantities dismantling in a single raw but it implies large safety distances (overpressure and fragments projection) and human footprint on the environment is a huge drawback. Another destruction technic consists in setting up temporary structures around the threat such as to decrease safety distance and collect generated fragments in a restricted zone [1].

Destruction in full confined conditions using a detonation chamber annihilates pollution, especially when linked to a filtration and gas analysis system. The main drawback is the mandatory to master all hazards the warhead is designed for once initiated (overpressure and fragments impacts).

In this trend, a 60kg NEQ TNT detonation chamber has been designed to ensure dismantling of reformed and not transportable stockpile of missiles (warhead and propellant). This work illustrates the methodology used for the chamber design and results obtained. The first part reminds the various steps followed to sustain blast and multi-fragments impacts from threat analysis to initial destruction [2][3]. The second part details how the inner protection shielding was optimized by numerical simulations.

Keywords: warheads, detonation chamber, multi-fragments

References

[1] Mespoulet, J., Plassard, F., Rodier, R., (2023). Design methodology for UneXploded Ordnance (UXO) protection structures in pyrotechnical depollution: illustration with a 155mm round and a 1000lbs GP bomb, Europyro, Saint-Malo, France.

[2] Mespoulet, J., Boussac, S, (2019). Explosion chamber for confinement of ammunition destruction: design rules and application, 44th International Pyrotechnics Society Seminar, Tours, France.

[3] Mespoulet, J., Abdulhamid, H., Deconinck, P., (2022). Impact tests with single or multi impactors using a gas gun to reproduce IEDs' and uncommon threat, 32nd International Symposium on Ballistics, Reno Nevada.

A self-consistent modelling methodology for predicting the mechanical behavior of interleaved composites

Yanhong Chen[1], Ziwen Xu[1], Licheng Guo[1]

[1]*Harbin Institute of Technology, Harbin, People's Republic of China*

Thanks to their improved damage tolerance compared to conventional laminates, interleaved composites are increasingly favoured for critical load-bearing applications like turbine engine fan blades and casings. However, their pseudo-woven internal architecture often leads to the formation of large unit cells (LUCs), with the typical characteristic length reaching hundreds of millimetres. As a result, interleaved composites are macroscopic heterogeneous, posing significant challenges in both characterising their properties and modelling their structural response, thus limiting their engineering applications and potential. This research was aimed at developing a combined experimental and numerical methodology to evaluate the mechanical performance of interleaved composites (Figure 1) and thus address the aforementioned challenges. The experimental part included a series of characterisation tests conducted to obtain the material properties of the internal constituents of interleaved composites at various strain rates. Several macroscale tests were also performed to provide model validation data for the numerical work. In the numerical part, a modelling strategy was proposed to automatically and consistently map the mesoscale architecture onto the macroscopic finite element (FE) model, allowing the homogenisation of the behaviour of each macroscopic element uniquely based on the material constituents within the element (Figure 2). At the constituent level, both the nonlinearity and rate dependent of tapes were considered according to the results obtained from the characterisation tests. Also, the Puck and Pinho criteria were employed to describe the failure of tapes. The proposed modelling methodology was implemented into the commercial FE software LS-DYNA. Simulations of the validation experiment were performed, and the results suggest that the proposed model was effective in predicting the mechanical performance of interleaved composites. In sum, this research offers a practical approach for experimentally characterizing the behaviour of interleaved composites and numerically predicting their performance, thereby facilitating their engineering application.

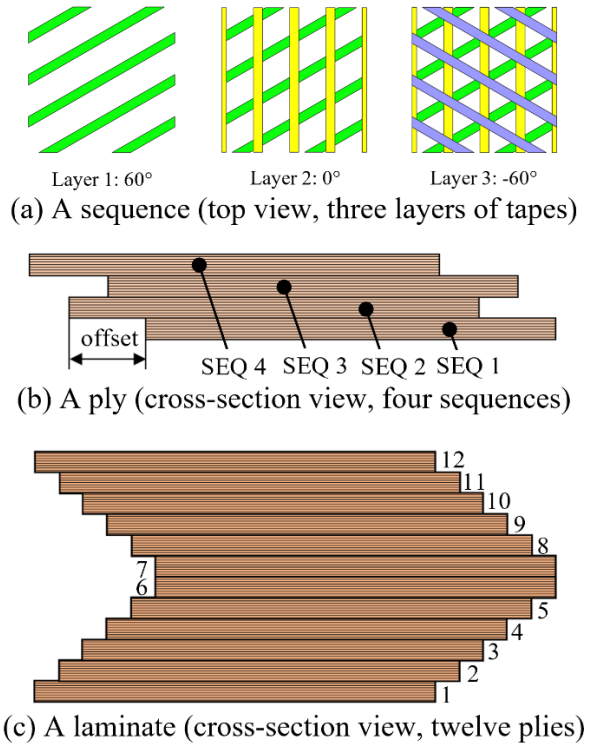

Figure 1: Layup detail of a typical interleaved composites

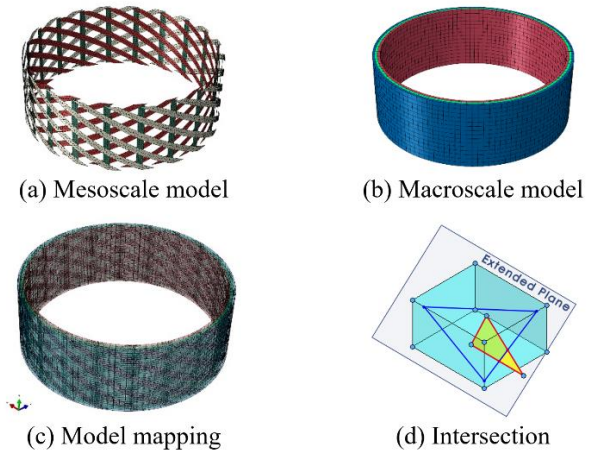

Figure 2: Illustration of the self-consistent modelling methodology

Keywords: Interleaved Composites, Strain Rate Effects, Unit Cell, Predictive Modelling

[1] Puck, A., Schürmann H. (2002). Failure analysis of FRP laminates by means of physically based phenomenological models. Composites Science and Technology, 62, 1633-1662.

[2] Pinho, S. T., Iannucci, L., Robinson, P. (2006). Physically-based failure models and criteria for laminated fibre-reinforced composites with emphasis on fibre kinking: Part I: Development. Composites Part A: Applied Science and Manufacturing, 37, 63-73.

Experimental study on structural behavior of GFRP-concrete-steel double-skin tubular column under near-field blast load

Jun Yu[1,2], Yunhao Geng[1,2] , and Xiaowei Feng[3]

[1] *Engineering Research Center of Safety and Protection of Explosion & Impact of Ministry of Education, Southeast University, Nanjing 211189, China*

[2] *School of Civil Engineering, Southeast University, Nanjing 211189, China*

[3]*Institute of Systems Engineering, China Academy of Engineering Physics, Mianyang 621999, China*

Abstracts: The newly developed hybrid FRP-concrete-steel double-skin tubular column (DSTC) integrates both high corrosion resistance and load-bearing capacity, enabling its potential for applications in high-temperature, high-humidity, and highly corrosive island environments, compared to traditional reinforced concrete or steel columns. From the perspective of multi-hazard mitigation, existing research on DSTC columns has predominantly focused on their static and seismic performance, while studies on the behavior of DSTC columns under near-field blast load are scarce. In this paper, four glass fiber reinforced polymer (GFRP)-concrete-steel double-skin tubular columns (GFRP-DSTC) were fabricated and tested under near-field explosion with same TNT equivalent but different scaled distances (ranging from 0.37 m/kg$^{1/3}$ to 0.24 m/kg$^{1/3}$). The GFRP tube was made through filament-wound technique and vinyl ester resins, and the glass fibers were oriented at ±80º with respect to the longitudinal axis of the column. The GFRP-DSTCs were installed in a field with bottom end fixed and top end simply supported. The results show that under near-field blast loading, the damage to GFRP-DSTC was concentrated in the region of the blast-facing side, where material failure and localized deformation were observed. Under identical TNT equivalent and scaled distance, the detonation height exerted a notable influence on the localized residual deformation of GFRP-DSTC. When the scaled distance exceeds 0.30 m/kg$^{1/3}$, the specimens showed only localized inward bending, with the surface of the GFRP tube on the blast-facing side subjected to the impact of detonation products, resulting in a roughened surface. Additionally, the surface turned black due to impinging of the explosion fireball. While the scaled distance was less than and equal to 0.30 m/kg$^{1/3}$, the specimens exhibited significant localized rupture of the GFRP tube at the blast-facing face, accompanied by lamination along the thickness direction of the GFRP tube. Numerous circumferential cracks developed on both sides of the rupture zone in the GFRP tube, and the concrete at the blast-facing face was extensively crushed. As the scaled

distance further decreased to 0.24 m/kg$^{1/3}$, the concrete crushing zone was extended from the blast-facing face to the entire side face, while the rear face of the column was bulged outward. The inner steel tube was exposed, displaying significant inward bulging.

Keywords: GFRP-concrete-steel double-skin tubular column, near-field explosion, blast resistance, failure mode, blast testing

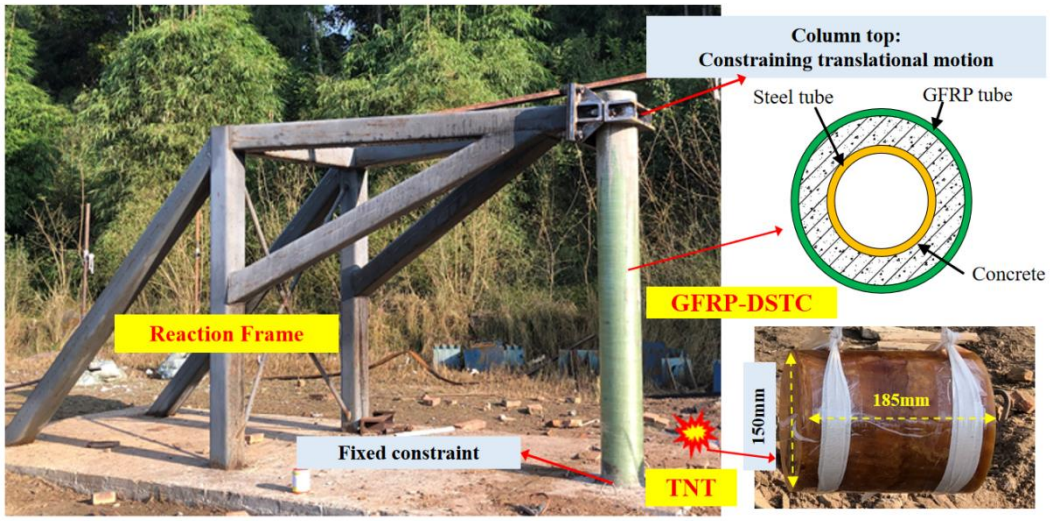

Figure 1. Experimental setup

Figure 2. Failure modes of GFRP-DSTC (scaled distance=0.30 m/kg$^{1/3}$)

Effect of Partial Composite Action on Performance of Precast Concrete Sandwich Wall Panels under Blast Load

Lekhani Gaur, Ph.D.[1], Bhavin Zaveri, P.E.[2] and Jagriti Mandal, Ph.D.[1]

[1]*Secure Design Practice Area, Walter P Moore Engineering India Pvt. Ltd, Pune, India*

[2] *Secure Design Practice Area, Walter P Moore and Associates, Inc., Austin, USA*

Abstract

The present study investigates the response of precast concrete sandwich wall panels under blast load incorporating varying degrees of composite action. The percentage of composite action quantifies a panel's composite behavior relative to a fully composite assumption, with 0% indicating a fully non-composite panel and 100% indicating a fully composite panel. For this study, the precast panel is modeled as an equivalent single degree of freedom (SDOF) system using the transformation factors. The panel is subjected to a range of blast load while the degree of composite action is varied from 0% to 100%. The response of the panels is evaluated in terms of support rotation, ductility, and support reactions. The effect of degree of composite action on the response of the panel is investigated for a range of blast impulses. The threshold blast impulse value is determined for each partial composite panel considering the moderate level of damage of the panel as per ASCE 59-11. Further, a range of optimum degree of composite action is identified while trading-off between support rotation and support reaction.

Keywords: Blast load, composite action, precast concrete sandwich wall panel, support rotation, support reactions

Introduction

The application of precast concrete sandwich wall panels as building envelope has increased significantly due to its strength, blast resistance, superior quality control during fabrication, and reduced carbon footprint. Shear ties or solid concrete zones are provided in the panels to ensure the integral behavior of the outer and inner wythes [1]. Generally, the ultimate flexural strength of these panels lies between the two extremes of non-composite and fully composite moment capacities shown as partially composite moment capacity in Figure 1, depending on the shear ties configurations [2]. During the design phase of a project, wall panel specifications are often established with conservative assumptions regarding wall panel thickness for given blast load. However, in production, achieving optimal design involves

balancing between the wall thickness and degree of composite action, to minimize support rotation while maintaining out-of-plane shear reactions within acceptable limits. This approach ultimately results in cost savings in panel material and panel connection designs. Hence, it is crucial to understand how the varying partial composite action affects the response of the panel and panel reactions under given blast load scenarios. The response of the panel is evaluated in terms of ductility, support rotation and support reactions. The present study delineates the effect of varying degree of composite action on the performance of precast sandwich panels through numerical single degree of freedom (SDOF) analyses.

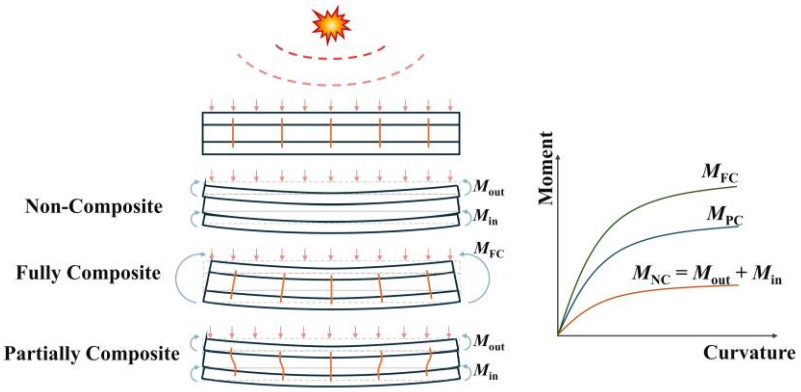

Fig 1. Behaviour of precast concrete sandwich panel under blast load

Methodology

In the present study, a 6 ft wide precast concrete sandwich panel with 20 ft long span is considered with outer and inner wythes sandwiched with an insulation layer. The thickness of outer wythe, insulation layer, and inner wythe are considered as 3, 3, and 5 inch, respectively, resulting in a total 11-inch-thick precast concrete sandwich panel. The outer and inner wythes are reinforced vertically with #3@12” and #4@12” OC spacing mild steel rebar, respectively. The moment capacity of fully composite section (M_{FC}) is evaluated by assuming the section as an 11-inch-thick monolithic concrete section with top and bottom reinforcement corresponding to the outer and inner wythes of sandwich panel, respectively. Further, the moment capacity of the non-composite panel (M_{NC}) is calculated as summation of moment capacity of the individual wythes as shown in Eq (1) [3].

$$M_{\mathrm{NC}} = M_{\mathrm{out}} + M_{\mathrm{in}} \tag{1}$$

where M_{out} and M_{in} are moment capacities of outer and inner wythes, respectively.

The moment capacity of partial composite panel (M_{PC}) is evaluated by adopting linear interpolation between M_{NC} and M_{FC} as mentioned in Eq (2). Herein, the degree of composite

action (*k*) is introduced as the fraction of the difference between the moment capacities of the fully composite panel and non-composite panel, varying from 0% to 100%.

$$M_{\mathrm{PC}} = M_{\mathrm{NC}} + k(M_{\mathrm{FC}} - M_{\mathrm{NC}}) \tag{2}$$

Further, the elastic perfectly plastic approach is used to model the precast panel as equivalent SDOF system using transformation factors [3]. The governing equation of motion of the equivalent SDOF system can be represented as

$$K_{\mathrm{LM}} M\ddot{y} + C\dot{y} + Ry = F(t) \tag{3}$$

where K_{LM} is load-mass factor, *M* is mass, *C* is damping coefficient, and *R* is resistance of the panel. *F*(*t*) represents the blast load time history. Herein, the blast load is idealized as triangular pressure-time history with impulse in the range from 28 psi-ms to 200 psi-ms. The above-mentioned equation of motion is solved using an in-house developed tool, *MooreDOF*. The response of the panel is evaluated in terms of support rotation, ductility, and support reactions. The effect of partial composite action on the performance of the precast panels is investigated. According to ASCE 59-11, the permitted element damage is considered as moderate level in the present study, which states the support rotation to be restricted to 2°.

Results

Herein, the performance of the panels is compared in terms of support rotation (θ). Figures 2(a) and 2(b) represent the variation of support rotation and support reaction with the degree of composite action (*k*) for different blast load impulse, respectively. It is observed that, at a smaller blast impulse of magnitude 28 psi-ms, there is not much variation in support rotation with degree of composite action. However, as the blast load increases, a significant reduction in θ can be observed with increasing *k* value. Further, the support reaction increases with the degree of composite action, which will influence the design of connection between the panels and the lateral framing structure. In other words, the robustness of the connection design increases with the degree of composite action, however it may also result in higher connection design costs. Figure 3 represents the approximate values of threshold blast impulse magnitude where the partial composite panel exceeds the limit of 2° support rotation. It can be stated that threshold blast impulse increases with the degree of composite action of the panel.

Figure 4 shows the variation of support rotation and scaled support reactions with respect to the degree of composite action on the same plot when panel experiences plastic deformation. It can be deduced that there is a trade-off between the degree of composite action to be provided to reduce the support rotation while keeping the out of plane shear reactions within a reasonable limit for optimized connection design. It is further observed that approximately

40% is the optimum degree of composite action in the present case that provides a good balance between the degree of composite action and support reactions. However, considering the inherent trade-off between minimizing support rotation and controlling support reactions, a range around 35-45% composite action may be identified as the zone of optimal solutions.

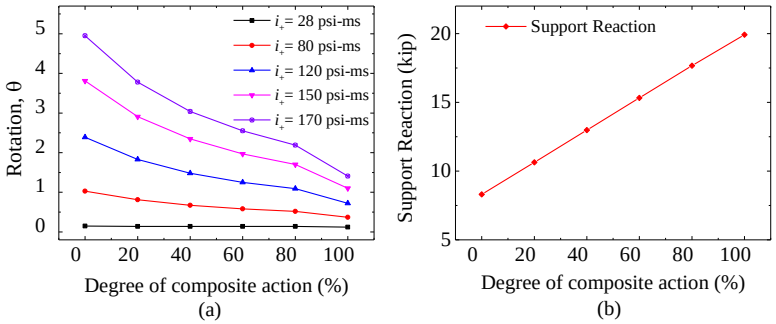

Fig 2. Variation of support rotation and support reaction with degree of composite action

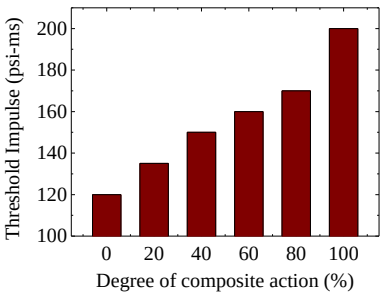

Fig 3. Threshold blast impulse

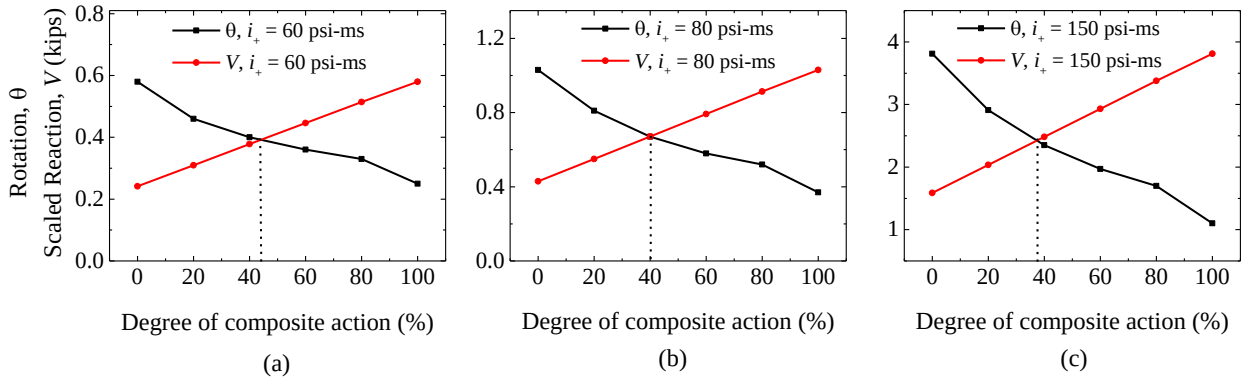

Fig 4. Variation of support rotation and scaled reactions with degree of composite action for blast impulse (a) i_+ = 60 psi-ms, (b) i_+ = 80 psi-ms, (c) i_+ = 150 psi-ms

Conclusions

The present study delineates the effect of degree of composite action on the performance of the precast concrete sandwich panels under blast load. It is observed that the support rotation of the precast concrete sandwich wall panels decreases whereas the support reaction increases with the degree of composite action. The findings of this study lays foundation for determination of an optimum degree of composite action that can ensure the optimized and cost-effective design of precast sandwich wall panel and its connection design.

References

[1] Losch, E. D., Hynes, P. W., Andrews Jr, R., Browning, R., Cardone, P., Devalapura, R., & Yan, L. (2011). State of the Art of Precast/Prestressed Concrete Sandwich Wall Panels. *PCI Journal*.
[2] Davidson, J. S., Dawson, H., Fisher, J., Gasulla, E., Ghosh, S. K., Hoemann, J., & Wan, D. (2014). PCI Design Handbook: Appendix A: Blast-resistant design of precast, prestressed concrete components. *PCI Journal*.
[3] Gombeda, M. J., Trasborg, P., Naito, C. J., & Quiel, S. E. (2017). Simplified model for partially-composite precast concrete insulated wall panels subjected to lateral loading. *Engineering Structures*, *138*, 367-380.
[4] Biggs, J. M. (1964). Introduction to Structural Dynamics, New York (NY): McGraw-Hill.

Experimental Analysis and Numerical Modeling of Energy Absorption Capability and High Deformation Response in 3D-Printed Multilayer Panels

Hour Alhefeiti[1], Amged Elhassan[1], Khalifa Harib[1], Waleed Ahmed[2,*], Farook K. Al-Jahwari[3], Kubilay Aslantas[4]

[1]*Mechanical and Aerospace Engineering Department, UAE University, UAE*
[2]*Engineering Requirements Unit, UAE University, UAE*
[3]*Department of Mechanical and Industrial Engineering, Sultan Qaboos University, Oman*
[4]*Department of Mechanical Engineering, Afyon Kocatepe University, Turkiye*

*Corresponding author email: w.ahmed@uaeu.ac.ae

Abstract

This study focuses on the experimental analysis and numerical modeling of the energy absorption capabilities and high deformation response of multilayer panels fabricated using 3D printing technology. With growing demands in aerospace, automotive, and civil engineering for lightweight materials that can withstand high-impact forces, 3D-printed composite panels offer significant design flexibility and material efficiency advantages. These panels are tailored to achieve enhanced energy dissipation and deformation control by integrating fiber-reinforced outer layers with optimized internal core structures. The research combines rigorous experimental testing using FEM to evaluate how these multilayer panels respond to high-impact and deformation scenarios. Mechanical tests were conducted to measure deflection, stress distribution, and failure patterns under different loads, revealing how variations in infill patterns, layer orientations, and print settings affect their ability to absorb energy and accommodate large deformations. FEM is used to simulate the experimental results by predicting deformation behaviors and stress concentrations observed in tests. The findings highlight the potential of 3D-printed multilayer composites for use in applications that require materials capable of absorbing energy and enduring high deformation without compromising structural integrity. This study demonstrates the effectiveness of optimizing print parameters to enhance the performance and reliability of 3D-printed components under demanding conditions through addressing key challenges such as anisotropy and layer adhesion in additive manufacturing,

Keywords: 3D Printing, energy absorption, FEM, impact resistance

Preliminary Study on Design, Manufacture and Finite Element Analysis of The Absorbing Liner for Motorcycle Helmet

Henry Lim Yi Zong[1], S Kanna Subramaniyan[2]

[1]*Department of Mechanical Engineering, Faculty of Mechanical and Manufacturing Engineering, Universiti Tun Hussein Onn Malaysia, 86400 Parit Raja, Johor, Malaysia*

[2]*Department of Mechanical Engineering, Faculty of Mechanical and Manufacturing Engineering, Universiti Tun Hussein Onn Malaysia, 86400 Parit Raja, Johor, Malaysia*

The existing impact absorbing liner for a commercialized helmet, mostly made by expanded polystyrene (EPS) foam, do not fully prevent head and neck injuries, due to unable to withstand high impact during collisions. This paper proposes an innovative structure that enhance the impact absorbing abilities without neglecting the scratch resistance of a helmet liner. A sandwich structure using pyramidal lattice core, with vertical strut member was designed using SolidWorks™ software. The sandwich structure was fabricated using fused deposition modelling (FDM) with Polyamide-12 (nylon) filament for its heat and scratch resistance, and lastly filled with EPS foam through an EPS spray. Through observation, the printing result showed that no cracking and deformation issues during printing process. Finite element analysis (FEA) is then carried out using Ansys Workbench Software to test the designed sandwich structure model under a impact loading. The same testing was also conducted on a full EPS model to compare the impact absorbing behavior and efficiency of both structures. Under a simple collision with 10ms-1 hard surface, the results demonstrate that the new liner design absorbed impact more effectively, which reduces the force transferred to the rider's head. Also, the sandwich structure model successfully dissipated the impact energy and spreaded to each lattice structure evenly, while the full EPS model only transmit the impact energy to the edge of model. However, further testing is needed to assess factors like weight, comfort, and cost before commercial implementation.

Keywords: helmet liner design, impact absorption, pyramidal lattice structure, fused deposition modelling, finite element analysis.

Experimental and numerical investigation on the attenuation of blast stress waves in concrete induced by dynamic explosion

Xin Zhou[1,2], Bin Feng[1,2], Li Chen[1,2]

1. School of Civil Engineering, Southeast University, Nanjing, 210096, China

2. Engineering Research Center of Safety and Protection of Explosion & Impact of Ministry of Education, Southeast University, Nanjing 211189, Jiangsu, China

Concrete materials are widely used in protective structures to resist the impact and blast loadings of traditional weapons, especially Earth Penetrating Weapons (EPWs). Current research predominantly assumes stationary charge explosions when assessing the stress wave effects on concrete induced by traditional weapons with moderate impact velocities. However, it is not uncommon that the charge in warhead is in motion at the instant of detonation (denoted as dynamic explosion) in actual combat scenarios. Besides, with the development of Hypersonic Weapons, which can attain velocities ranging from 5 to 20 Ma, the influence of moving charges can no longer be neglected. To reveal the characteristics of dynamic explosion loadings, the experimental and numerical investigation on the propagation and attenuation of stress waves in concrete induced by explosions of moving cylindrical charges is carried in this study. Firstly, four sets of static explosion tests were carried out, comprehensively considering influential factors including concrete strength, aspect ratio (l/d), depth of burial (DoB) and TNT mass. The data of blast stress waves was collected to provide fundamental data for further research. Then, based on the validated KCC model and multi-material ALE (MMALE) algorithm in LS-DYNA, a series of numerical simulations were conducted, with various cylindrical charge velocities, aspect ratios and DoBs, to investigate the attenuation of the blast stress waves in concrete induced by dynamic explosion. Finally, based on the numerical data, an empirical formula for peak stresses in concrete induced by dynamic explosion of cylindrical charges was established. It was found that the re-calibrated parameters of KCC model along with MMALE algorithm can accurately predict the propagation and attenuation of explosion stress waves in concrete. Additionally, the velocity effect of dynamic explosion significantly increases the speed and intensity of the shock wave in the direction of motion of the charge prior to detonation. The empirical formula is suitable for quick prediction of the peak stress from cylindrical charges in concrete with varied concrete strength, aspect ratio, charge velocity and DoB, which can provide a valuable reference for protective structures design.

Keywords: Concrete, Cylindrical charge, Dynamic explosion, Peak stress.

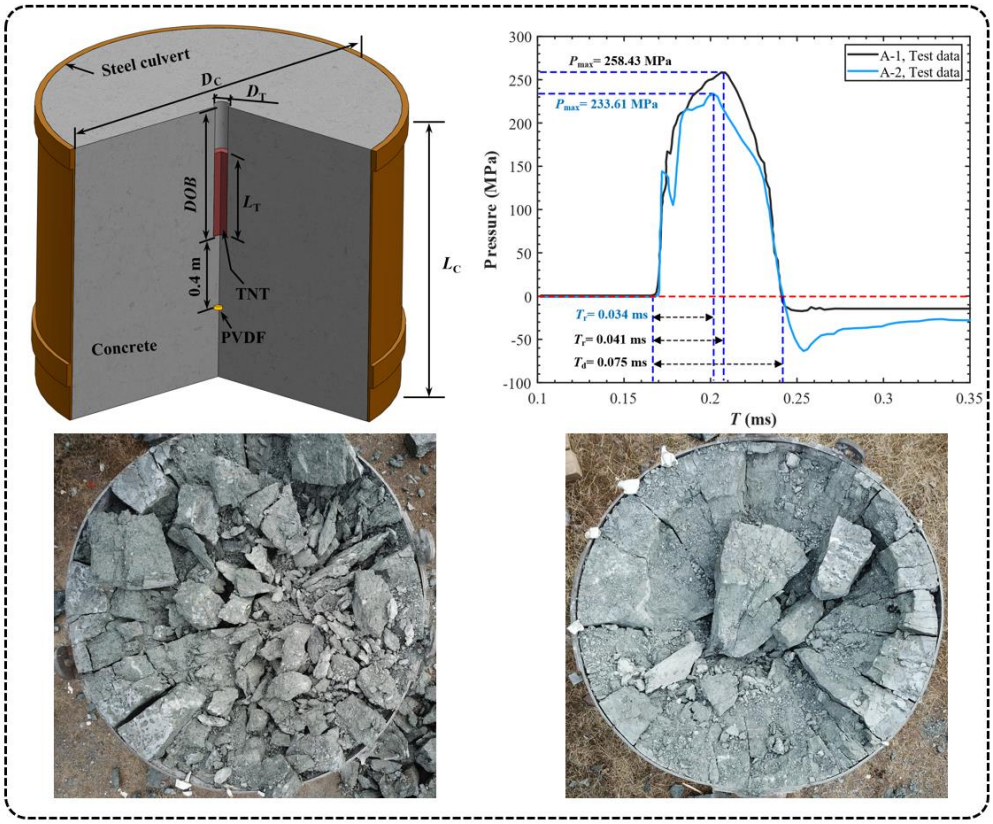

Fig 1. Damage of concrete targets and stress waves in concrete

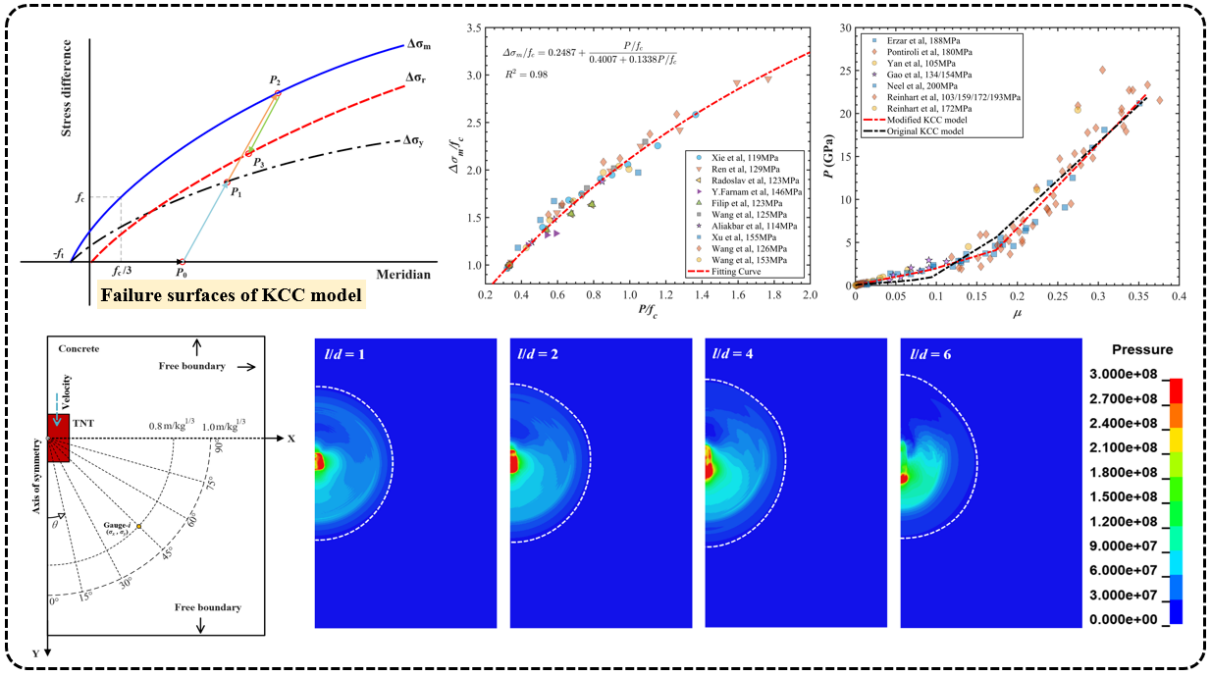

Fig 2. Calibration of parameters for the KCC model and pressure contours at 0.149 ms with different aspect ratios

Automated finite element modeling of multi-layer composite structures against projectile impact: from Abaqus plug-in to large language model-based applications

Fengbo Han, Kapil Krishnan, Jide Oyebanji, Changze Sun, Rafael Savioli, Naresh Kakur, Alia Ruzanna Aziz, Henrique Ramos, Nikolaos Nikos and Rafael Santiago

Advanced Materials Research Center, Technology Innovation Institute, Abu Dhabi, United Arab Emirates

Finite element (FE) modeling of multi-layer composite structures under projectile impact is a complex process, requiring meticulous tasks like material definition, geometry creation, meshing, and specifying contact and boundary conditions. To streamline these efforts, this study introduces two innovative automation solutions: an Abaqus plug-in with a parameterized graphical user interface (GUI) and a large language model (LLM)-based application featuring a natural language interface. The Abaqus plug-in, developed using the Abaqus GUI Toolkit, empowers users to configure multi-layer composite structures efficiently. Through the GUI, users can define the structure's configuration, select projectile types, assign materials to each layer, choose meshing strategies, and set other critical parameters with ease. In parallel, the LLM-based application leverages a fine-tuned large language model to translate natural language descriptions directly into fully defined FE models, complete with materials, mesh, and boundary conditions. Validation of the LLM-based application, conducted with two distinct prompt types, confirms its robustness, achieving 100% accuracy in generating accurate FE models. Together, these tools (the Abaqus plug-in and the LLM-based application) offer powerful automation for modeling composite structures against projectile impact. The LLM-based solution stands out for its intuitive human-AI interface, accessible across desktop, web, and mobile platforms, making it highly user-friendly. This work not only enhances automation in FE modeling but also advances the integration of large language models in finite element modeling practices.

Keywords: finite element modeling, multi-layer composites, projectile impact, Abaqus plug-in; large language model, artificial intelligence.

Computational simulations of blast loading of auxetic and TPMS-filled sandwich panels

Nejc Novak[1], Oraib Al-Ketan[2], Matej Vesenjak[1] and Zoran Ren[1]

[1] *Faculty of Mechanical Engineering, University of Maribor, Slovenia*

[2] *Core Technology Platform, New York University Abu Dhabi, United Arab Emirates*

Response of novel structures designed for impact, blast and ballistic protection can be enhanced using composite sandwich panels, which are able to extend the energy absorption capabilities. Cellular metals are used mainly as the core of such composite structures and consequently, offer very good energy absorption to weight ratio [1]. One of the most promising cellular cores for this kind of application are auxetic cellular structures and Triply Periodical Minimal Surface (TPMS), which are modern metamaterials with some unique and superior mechanical properties [2]. The effect of negative Poisson's ratio and sheet-based structures can be useful for many different applications to enhance properties in density, stiffness, fracture toughness, energy absorption and damping. Thus the auxetic material moves towards the impact zone and does not flow away from the impact area as in the case of conventional cellular materials with a positive Poisson's ratio. Such behaviour is of crucial importance in the case of blast loading and impact.

Three different methods for blast loading (ConWep, SPH, MMALE) were compared and validated based on the experimental data [3]. The Smooth Particle Hydrodynamic (SPH) method was chosen as the most appropriate, and used further for simulating the blast loading of the sandwich composite panels (Figure 1). The maximum displacement and SEA of the composite panel were evaluated to study the influence of the sandwich structure's core geometry to blast loading.

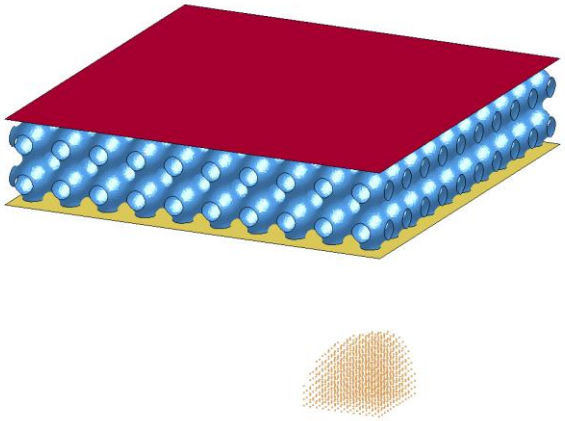

Figure 1: Geometry of the FE model

A Design Of Experiment study was performed to study the influence of the sandwich panel's geometry on the maximum displacement of the composite panels, where, in total, more than 150 finite element simulations were carried out (Figure 2). First, the influence of the cover plates` thickness was studied on the maximum displacement of the sandwich panel. As expected, larger thickness of the cover plate lowers the panel maximum displacement, while the SEA is larger when thinner cover plates are used. Next, the influence of the auxetic and TPMS core's geometry on the maximum displacement and SEA of the sandwich panel was studied, with varying the geometry of the unit cell. Overall, the specific energy absorption of TPMS filled sandwich panels is up to 25 % higher than in the sandwich panels filled with strut-based core with the same relative density [4]. The introduction of graded porosity using thickness and cell size variation shows that it is possible to tailor the mechanical and deformation response of the TPMS structures and TPMS filled sandwich panels while maintaining comparable energy absorption capabilities. The presented study illustrates great potential of using sandwich structures with designed auxetic cellular cores to improve the response of modern composite structures to blast loading.

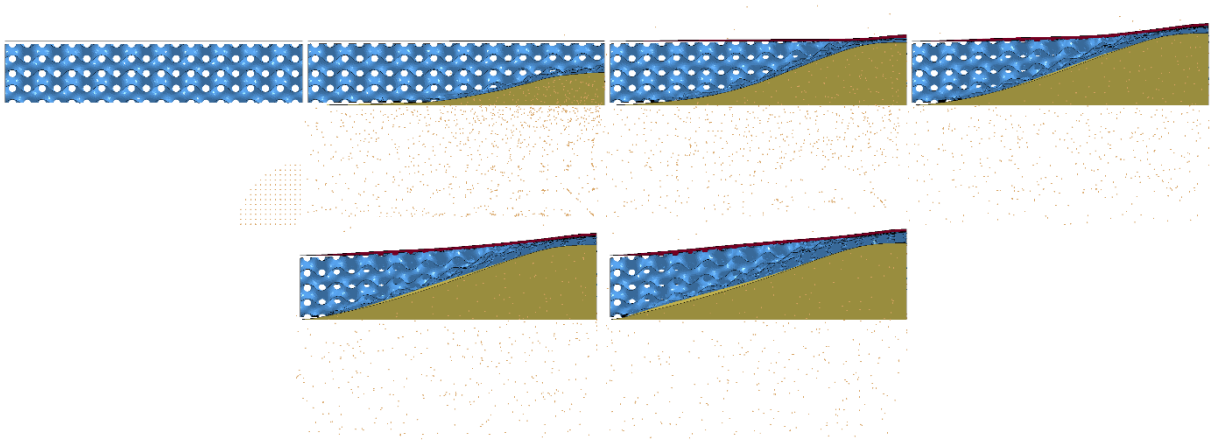

Figure 2: Deformation behaviour of TPMS filled sandwich panel (time step: 100 μs)

Keywords: sandwich panels, triply periodic minimal surface, auxetic, impact, graded structures, computational modelling, blast loading

[1] D. Lehmhus, M. Vesenjak, S. de Schampheleire, and T. Fiedler, "From stochastic foam to designed structure: Balancing cost and performance of cellular metals," *Materials (Basel).*, vol. 10, no. 922, pp. 1–32, 2017, doi: 10.3390/ma10080922.

[2] O. Al-Ketan, R. Rowshan, and R. K. Abu Al-Rub, "Topology-mechanical property relationship of 3D printed strut, skeletal, and sheet based periodic metallic cellular materials," *Addit. Manuf.*, vol. 19, 2018, doi: 10.1016/j.addma.2017.12.006.

[3] N. Novak, L. Starčevič, M. Vesenjak, and Z. Ren, "Blast response study of the sandwich composite panels with 3D chiral auxetic core," *Compos. Struct.*, vol. 210, no. November 2018, pp. 167–178, 2019, doi: https://doi.org/10.1016/j.compstruct.2018.11.050.

[4] N. Novak, M. Borovinšek, O. Al-ketan, Z. Ren, and M. Vesenjak, "Impact and blast resistance of uniform and graded sandwich panels with TPMS cellular structures," *Compos. Struct.*, vol. 300, no. April, 2022, doi: 10.1016/j.compstruct.2022.116174.

Crashworthiness of cellular protective structures: from positive to negative to zero Poisson's Ratio

Hasan Al-Rifaie [1], Nima Movahedi [2] and Teik-Cheng Lim [3]

[1] *Institute of Structural Analysis, Poznan University of Technology, 60-965, Poznan, Poland.*

[2] *College of Engineering, Science and Environment, The University of Newcastle, NSW, Australia.*

[3] *School of Science and Technology, Singapore University of Social Sciences, Singapore.*

With particular insight on Poisson's Ratio (PR), literature has extensively discussed cellular metamaterials with positive PR (non-auxetic) and negative PR (auxetic). Due to their energy absorption characteristics [1, 2], they are being used as protective sacrificial structures to absorb impact or blast energy through plastic deformation [3, 4]. However, to the best of the author's knowledge, topologies with zero PR are limited to a few studies, despite their higher impact energy absorption capacity. Therefore, this research aims to review previous studies [5, 6] and suggests a novel hybrid topology combining both auxetic and non-auxetic structures. To this end, the topologies of four cellular metamaterials (honeycomb, re-entrant, hybrid 1 and hybrid 2) are designed as shown in Figure 1. These four lattice structures are analyzed analytically in the first step. Then, a non-linear computational model is created to examine their behavior under dynamic impact using ABAQUS software. This study investigates their deformation patterns, energy absorption, reaction forces and Poisson's ratio values.

Both hybrid topologies show deformation patterns merging the X-shaped progressive collapse of the uniform non-auxetic honeycomb and the lateral shrinkage of the uniform auxetic re-entrant. In terms of normalized reaction forces, Hybrid 1 topology shows a lower reaction force per unit mass by 30% and 8.4% compared to the uniform honeycomb and re-entrant structures, respectively. Moreover, compared to the uniform honeycomb and re-entrant structures, the Hybrid 1 topology increases the Specific Energy Absorption (SEA) by 36.7% and 63.5%, respectively. Hybrid lattices in this study demonstrate near-zero PR values. The high SEA and low reaction forces confirm the superior performance of the suggested hybrid topology for use in applications requiring the mitigation of dynamic and impact loadings. The proposed hybrid cellular metamaterial is a promising solution for various civil and defense protective applications.

Keywords: Protective structures, cellular metamaterials, auxetic, honeycomb, impact, FEM, Poisson's ratio.

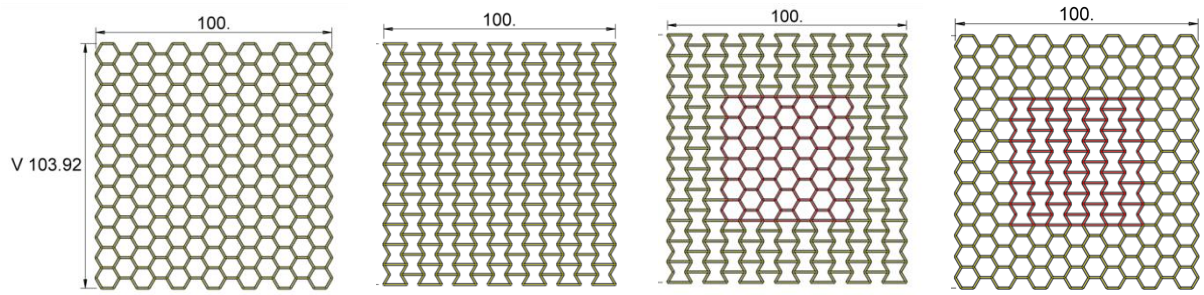

a. honeycomb b. re-entrant c. hybrid 1 d. hybrid 2

Figure 1. The geometries of the cellular metamaterials considered in this study.

References:

[1] Al-Rifaie, H., & Sumelka, W. (2019). The development of a new shock absorbing uniaxial graded auxetic damper (UGAD). *Materials*, *12*(16), 2573, https://doi.org/10.3390/ma12162573.

[2] Movahedi, N., Murch, G. E., Belova, I. V., & Fiedler, T. (2019). Functionally graded metal syntactic foam: Fabrication and mechanical properties. *Materials & Design*, *168*, 107652, https://doi.org/10.1016/j.matdes.2019.107652.

[3] Al-Rifaie, H., Studziński, R., Gajewski, T., Malendowski, M., Sumelka, W., & Sielicki, P. W. (2021). A new blast absorbing sandwich panel with unconnected corrugated layers-numerical study. *Energies*, *14*(1), 214, https://doi.org/10.3390/en14010214.

[4] Lim, T. C. (2020). *Mechanics of metamaterials with negative parameters*. Springer Nature, https://doi.org/10.1007/978-981-15-6446-8.

[5] Novak, N., Al-Rifaie, H., Airoldi, A., Krstulović-Opara, L., Łodygowski, T., Ren, Z., & Vesenjak, M. (2023). Quasi-static and impact behaviour of foam-filled graded auxetic panel. *International Journal of Impact Engineering*, *178*, 104606, https://doi.org/10.1016/j.ijimpeng.2023.104606.

[6] Al-Rifaie, H., & Hassan, A. (2024). Improving the Impact Resistance of Anti-Ram Bollards Using Auxetic and Honeycomb Cellular Cores. *Applied Sciences*, *14*(19), 8898, https://doi.org/10.3390/app14198898.

Hybrid metallic and composite armouring solution for blast protected vehicles

Ilyass Benmessaoud[1], Hugo Vanmaele[1], Paul Guillou-Keredan[1], Sebastien Lemercier[2], Francois Boussu[1]

[1]Univ. Lille, ENSAIT, ULR 2461 - GEMTEX - Génie et Matériaux Textiles, F-59000 Lille, France
[2]ARQUUS, 15 bis allée des marroniers, SAT TER 1 15, 78008 Versailles Cedex, France.

Armoured land transport vehicles are primarily protected against blast threats by reinforced metal structures. However, these solutions reduce the payload of the vehicle and for some lighter vehicles they cannot be used due to the low payload. To overcome this weight problem, the use of composite materials as additional armour for the vehicle can be an innovative and lightweight solution. To date, different configurations have been subjected to the blast effect and analysed to understand their dynamic behaviour. The first fibre reinforcements used, based on stacked layers of E-glass fabric, were able to withstand dynamic blast loads. However, these reinforcements tend to have the same performance as the all-steel solution for the same areal weight [1]. Therefore, an investigation has been carried out to introduce 3D woven fibre reinforcements based on E-glass yarn and use them in composite materials for better dynamic performance under blast effect.

Several authors have highlighted their various advantages as soft and hard protection solutions [2]. As pointed out by Tong et al [3], it is also confirmed that high performance fibres can be integrated into these multilayer woven structures without major degradation and more easily as weft and/or warp reinforcing yarns to increase the strength in both directions of the 3D warp interlock fabric. The same authors also point out the ease of implementation of a composite material with 3D fibre reinforcement [3], mainly due to its monolithic, compact and integrated architecture [4][5].

In 3D warp-interlock fabrics, the layers are bonded by warp yarns, providing greater cohesion, allowing a thick reinforcement to be produced directly [6], rather than a series of thin reinforcements that must be assembled subsequently [7], while retaining the ability to pass more resin than in 2D fabrics of equivalent thickness [8].

All of these targets were tested against the same blast threat in a free field configuration. The distance between the charge and the targets was kept constant (except for the 3D woven composite full thickness + steel 2). Dynamic deformation was measured using a metallic honeycomb cell placed on the back of the steel element. During the blast effect, the dynamic

deformation was recorded in the thickness direction and a comparison of the different targets is shown in Figure 1.

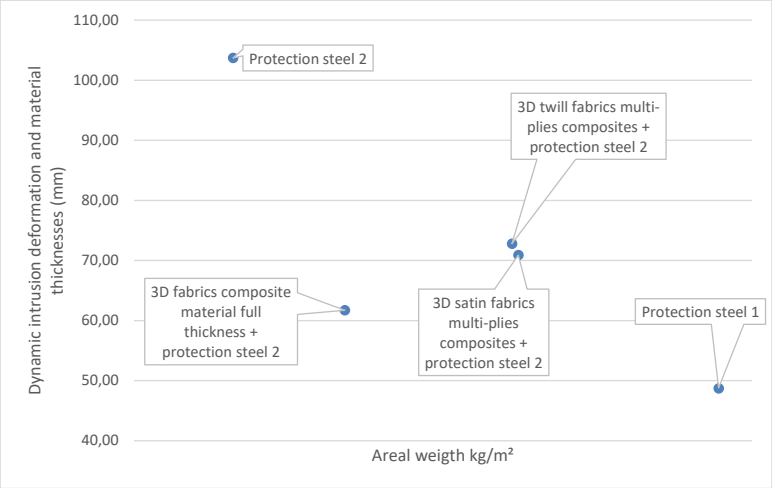

Figure 1. Comparison of different solutions submitted to explosion

According to the resulting dynamic deformation under the impact of the blast, a better performance of the full thickness 3D woven composite material matched with the protective steel plate was revealed.

Conclusion

This study shows that a hybrid composite/steel solution based on a 3D warp interlock fabric can significantly reduce the maximum dynamic deformation compared to the same mass solution made of protection steel. Further studies are required to confirm this trend.

Keywords: Armouring of vehicles, Composite material, 3D woven fabrics.

References

1. Voisin, A., Pariente, J., Lemercier, S., Soulat, D., Boussu, F.: Different composite behaviours under blast loading. (2019)
2. Kececi, A., Boussu, F., Soulat, D., Interesting Properties of 3D Warp Interlock Fabrics as Fibrous Reinforcement for Composite Material. In: American Society for Composites 2018. DEStech Publications, Inc., Lancaster, PA (2018)
3. Tong, L., Mouritz, A.P., Bannister, M.K.: Chapter 5 - 3D Woven Composites. In: Tong, L., Mouritz, A.P., and Bannister, M.K. (eds.) 3D Fibre Reinforced Polymer Composites. pp. 107–136. Elsevier Science, Oxford (2002)
4. Miravete, A.: Introduction: Why are 3-D textile technologies applied to composite materials? In: Miravete, A. (ed.) 3-D Textile Reinforcements in Composite Materials. pp. 1–8. Woodhead Publishing (1999)
5. Mouritz, A.P., Bannister, M.K., Falzon, P.J., Leong, K.H.: Review of applications for advanced three-dimensional fibre textile composites. Compos Part A Appl Sci Manuf. 30, 1445–1461 (1999). https://doi.org/https://doi.org/10.1016/S1359-835X(99)00034-2
6. Sheng, S.Z., van Hoa, S.: Modeling of 3D Angle Interlock Woven Fabric Composites. Journal of Thermoplastic Composite Materials. 16, 45–58 (2003). https://doi.org/10.1177/0892705703016001206

7. Ansar, M., Wang, X., Zhou, C.: Modeling strategies of 3D woven composites: A review, (2011)
8. Taylor, L.: Advances in the Manufacture of 3-D Preform Reinforcement for Advanced Structural Composites in Aerospace. In: DTI Global Watch Technology Mission Dissemination, HYBRIMAT 3 & 4 (2006)

Novel approaches to modeling debris loading after building structural collapse

Marcin Nowak[2], Piotr Nowak[1], Artur Szlachta[1], Franciszek Wołoch[1], Tomasz Gajewski[2], Piotr W. Sielicki[2]

[1]*Doctoral School, Institute of Structural Engineering, Faculty of Civil and Transport Engineering, Poznan University of Technology, 5 Piotrowo Street, 60-965 Poznan, Poland*

[2]*Institute of Structural Engineering, Faculty of Civil and Transport Engineering, Poznan University of Technology, 5 Piotrowo Street, 60-965 Poznan, Poland*

Keywords: military loading of structures; debris loading; structural collapse; design guidelines

The assessment of debris loading on underground shelters due to the collapse of aboveground structures impacted by military weaponry is crucial for evaluating design standards. This study focuses on modeling the loading conditions imposed by debris from in particular reinforced concrete multi-storey buildings. The research considers various structural configurations and failure mechanisms to provide an accurate representation of the debris distribution and loading on underground shelters based on the novelty finite element method approwach and using Abaqus Explocit scripting.

Advanced simulation techniques, including finite element modeling (FEM), were employed to capture the dynamic response of buildings subjected to external destructive forces which cause a random distribution of fragments. Key factors such as collapse patterns and interaction between debris and the underlying shelter were analyzed. The study reveals significant differences in debris load characteristics based on the construction type produce highly fragmented debris with non-uniform distribution, while reinforced concrete buildings result in larger debris pieces and more concentrated load impacts.

The findings contribute to improved predictive models for shelter design, ensuring enhanced safety and resilience in scenarios involving structural collapse. These insights are essential for civil and structural engineers tasked with developing protective underground facilities capable of withstanding complex debris loading conditions.

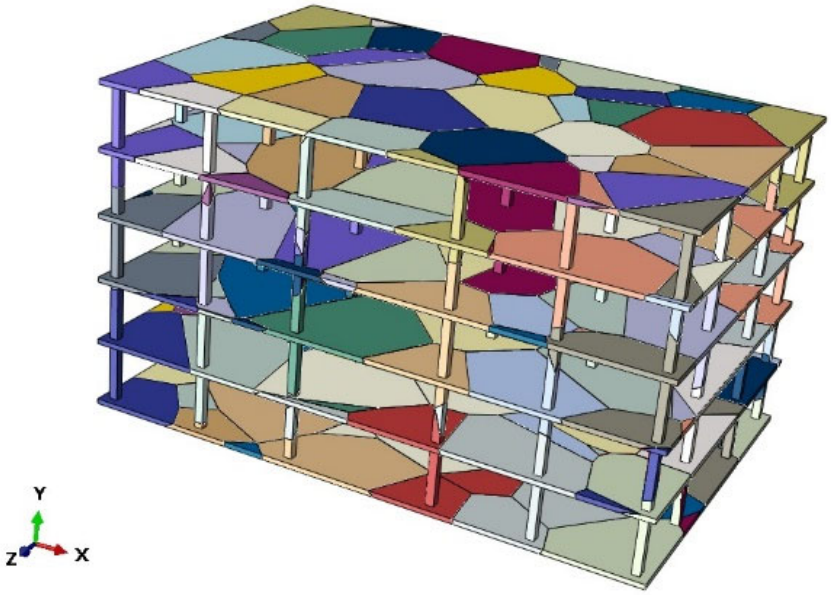

Fig. 1. Different projected debris variants using to assess ground loading

Results of actual debris loading were presented, developed based on the random discretization of an actual multi-story reinforced concrete building structure. This research underscores the importance of tailoring shelter designs based on the type of building above, enabling more efficient use of materials and construction techniques. The results support the development of standards that prioritize both cost-effectiveness and safety in protective construction. Future work should explore further variability in building materials and external impact types to refine predictive capabilities and broaden the applicability of the models developed.

A constitutive model considering hydrostatic damage for high dynamic properties of concrete

Jian Cui[1], Xianglong Guan [1], Yanchao Shi[1] and Zhong-Xian Li [1]

[1]*School of Civil Engineering, Tianjin University, Tianjin, China*

The concrete structure might be subjected to intensive dynamic loads such as close explosion and high speed impact during the service life, under which the material suffers the complicate stress state and the high hydrostatic pressure. However, the existing dynamic constitutive concrete model does not consider the hydrostatic pressure damage caused by material inhomogeneity, which will certainly affect the computational accuracy. In this paper, based on the theoretical framework of K&C concrete model, a dynamic constitutive concrete model considering the hydrostatic pressure damage is proposed. In this model, two hydrostatic damage equations are introduced respectively to quantify the strength and stiffness degradation caused by hydrostatic damage. Based on this, a shrinking failure surface method is proposed for the failure criterion to capture the strength degradation, and a novel unloading/reloading law is developed for the equation of state to describe the stiffness reduction non-linearly. Numerical hydrostatic tests using a single element are conducted to verify the accuracy of the model firstly, and the corresponding predictions are in good agreement with the experimental results. Numerical simulations of penetration tests are then performed, the comparisons between simulation and test results indicate that the presented model reflects the dynamic responses of concrete structures more accurately and reproduces the damage evolution of concrete more completely.

Keywords: Hydrostatic damage, Concrete material model, Strength criterion, Equation of state.

Experimental Analysis of Pre-cracked Sandstone Rock at High Strain-Rate Loading Conditions

Rabin Kumar Samal[1], Sunita Mishra[2]

[1]*Ph.D. Student, Department of Mining Engineering, IIT Kharagpur, India.*

[2]*Assistant Professor, Department of Mining Engineering, IIT Kharagpur, India.*

The planning and design of underground structures in rock domains are critical to ensuring their safety and stability. Rock masses are inherently heterogeneous, often characterized by discontinuities such as joints, faults, and fractures that significantly influence their mechanical behavior. These discontinuities tend to affect the structural integrity of the underground structures, particularly under high strain-rate loading conditions. While static loads pose a fundamental challenge, the presence of dynamic loads resulting from seismic events or blast loads further complicates the behavior of rock masses making the safety assessment of underground structures a complex yet crucial task. Thus, the aim of the present study is to experimentally investigate the mechanical response of some pre-cracked sandstone specimens under dynamic indirect tensile loading conditions. Moreover, the experiments are carried out with varying loading rates and pre-crack orientations depicting the scenarios of dynamic loading conditions and presence of various discontinuity planes with respect to the stress wave loading direction. The present study uses a fine-grained sandstone rock collected from a coal mining area from which cylindrical sandstone specimens of 48 mm diameter and slenderness ratio of 0.5 are prepared. Thereafter, a very thin pre-crack of 8 mm length and 1 mm width is fabricated at the center of the specimen with the help of a high-pressure water jet cutter. The dynamic tests are conducted using a split Hopkinson pressure bar (SHPB) device. The device uses a 300 mm long striker bar which is propelled with varying gas gun pressures of 0.15 MPa, 0.25 MPa, 0.35 MPa and 0.45 MPa. This particular combination of striker bar length and gas gun pressures produces a varying striker bar velocity of 12.74 m/s, 15.33 m/s, 18.92 m/s and 21.23 m/s. The pre-cracked specimen is placed in between the incident and transmission bars at varying orientations of 0°, 30°, 45°, 60°, 75°, and 90° with respect to the direction of loading of stress waves. Finally, a high-speed camera is synchronized with the SHPB device and placed in front of the specimen testing area to analyse the crack branching and complete deformation of the pre-cracked sandstone specimens. The results obtained in the present study provide a

comprehensive understanding of the dynamic behavior of pre-cracked sandstone specimens under varying loading rates and pre-crack orientations. The experimental findings, including the observed crack branching patterns and deformation characteristics, are crucial for validating, calibrating and refining numerical models that predict the dynamic response of fractured rock masses.

Keywords: Crack orientation, Dynamic tensile strength, Fine-grained sandstone, High-speed imaging, High strain-rate loading, Impact loading, Pre-crack, SHPB.

Behavior of structures fabricated of ice and thin steel plates impacted by high-speed striker

Maxim Yu. Orlov[1], Victor P. Glazyrin and Talgat V. Fazylov

[1]*National research Tomsk State University, Tomsk, Russian Federation*

At present, a relevance and complex scientific problem is the study of the behavior of ice under shock and explosive loads. The relevance is due to many practical applications, namely: the development of infrastructure in the Far North, the fight against ice jams on Siberian rivers, the extraction of natural resources in places where access to hydrocarbons is difficult due to the presence of rocks or permafrost, the need to protect structure of aircraft against high-speed impact of space debris and ice particles (hail, particles of micrometeorites), creation of impact-resistant of ice-composites to protect objects and equipment, etc. Currently, many researchers are joining together in scientific teams to solve this complex scientific problem [1-3]. However, in the authors' opinion, the basic concepts of ice failure are still being developed, and there is a need for adequate physical and mathematical models of ice behavior in a wide range of initial conditions. In the current study, the process of breaking through an ice block protected by a thin steel plates of high-speed ogive striker is simulated and studied in detailed. In all the designs considered, the ice block was protected on the front side by two thin metal plates made of mild steel. The number of layers located on the back side of the block reached six.

Material's response was described by macroscopic phenomenological theory of continuum mechanics. Governing equations were based on conservation laws of mass, energy and momentum impulse. Ice and ice sheet was modeled with isotropic, porous, elastic-plastic medium account to shock-wave phenomena and deterministic failure concept. Impact response of metal body was described by Walsch's equation-of-state. We used Prandtl–Reuss associated with von Mises equations as constitute ones.

A series of computational experiments were conducted using the numerical Lagrangian method modified for the numerical solution of modern dynamic problems of solids mechanics. We defined the problems are ones of penetration and perforation when targets was not-

monolithic (air-gapped, multilayered) and strikers has a complex shape (jacket, fill, shell). First, we compared the numerical results with the results of a ballistic test conducted in terms of depth of penetration. We then performed a limited we sensitivity analysis aimed at obtaining conservative results. Using the example of the problem of the collision of an ice cylinder with a rigid wall, we were able to compare our numerical results with the results of other researchers.

In all cases, the design was successfully perforated with striker via ductile hole growth. Its nose was slightly blunted and eroded. The time-dependencies of the residual striker velocity were typical. The average volume of damaged ice was almost 40%, and the perforation time was almost 120 μs. As expected, the dominant failure mechanism was brittle one. The ice crumbled into fragments of different sizes. Before the complete crushing of the ice block, a conical crater formed in it. Tunneling was also occurred in ice block in start of perforation process. The ballistic limit of each design and absorption energy were also calculated

Keywords: ice and ice sheet, model, FEM, perforation and penetration, failure, brittle fracture

The reported study was funded by RSF according to the research project https://rscf.ru/en/project/24-29-00187/

[1] Sherbun J.A., Horstemeyer M.F. (2010). Hydrodynamic modeling of impact craters in ice, International Journal of Impact Engineering 37, 27-36 doi.org/10.1016/j.ijimpeng.2009.07.001

[2] Banik A, Zhang C., Khan M.N., Wilson M., Tan K.T. (2022)Low-velocity ice impact response and damage phenomena on steel and CFRP sandwich composite. International Journal of Impact Engineering 162, 104-134. doi.org/10.1016/j.ijimpeng.2021.104134

[3] Glazova E.G., Krylov S.V., Chekmarev D.T. (2020) Numerical simulation of the ice sphere impact onto the barrier. Uchenye Zapiski Kazanskogo Universiteta. Seriya Fiziko-Matematicheskie Nauki, 162(2), 137–147. doi.org/10.26907/2541-7746.2020.2.137-147

Period-based anti-explosion protective wall. Design procedure and application manual

Alejandro Pérez Caldentey[1,2], María Chiquito[2], Anastasio P. Santos [2], Lina M. López[2], Ricardo Castedo[2]

[1]*FHECOR Consulting Engineers, Spain*

[2]*Universidad Politécnica de Madrid, Spain*

A new protection concept for key facilities was proposed by the first author at the PROTECT 2019 Colloquium in Whistler Canada [1]. The solution is based on changing the period of the structure by attaching to it a steel plate supported on rollers and connected to the protected structure by means of a series of linear elastic springs. As shown theoretically in the 2019 conference paper and as demonstrated by full-scale tests carried out in the framework of the MADEX project, partially financed by CDTI (Public Spanish Research Agency) and lead by FHECOR, RUESMA and INGE, the action on the structure is significantly reduced. The system was tested with decreasing scaled distances ranging from 1.392 m/kg$^{1/3}$ to 0.485 m/kg$^{1/3}$, using up to 70 kg of TNT equivalent, without any significant damage to the protected structure. The main advantage of the system is that it based mostly on linear elastic behaviour which means that the structure is protected against an attack consisting of more than one wave and does not require repair after an attack. In fact, the tested structure withstood a total of 12 different explosions.

This paper outlines a methodology for the design of the protection system, accounting for the geometry, the resistance of the protected structure, the complex distributions of overpressures and the characteristics of the protection system (spring stiffness, spring length, steel plate thickness [2]). The procedure accounts for the possible nonlinearities that can occur in the system when the capacity of the springs is reached, either in compression (when the minimum compressed length of the spring is reached) or in tension, which can lead to yielding of the spring's coils, as well as the possible nonlinear behaviour of the protected structure. The procedure is highlighted in a series of practical cases, and optimized design solutions are discussed. As an example of the analysis, two figures are shown below. Figure 1 shows the displacement of the bottom left and top right springs. The maximum compression displacement is limited by the available space between the protected wall and the protection plate, so that the

behaviour for this blast load is nonlinear at the beginning. Despite this fact, the top of the protected wall, which is a cantilever wall deforms only 2.5 mm as shown in Figure 2, which shows that the protection is efficient for this level of loading.

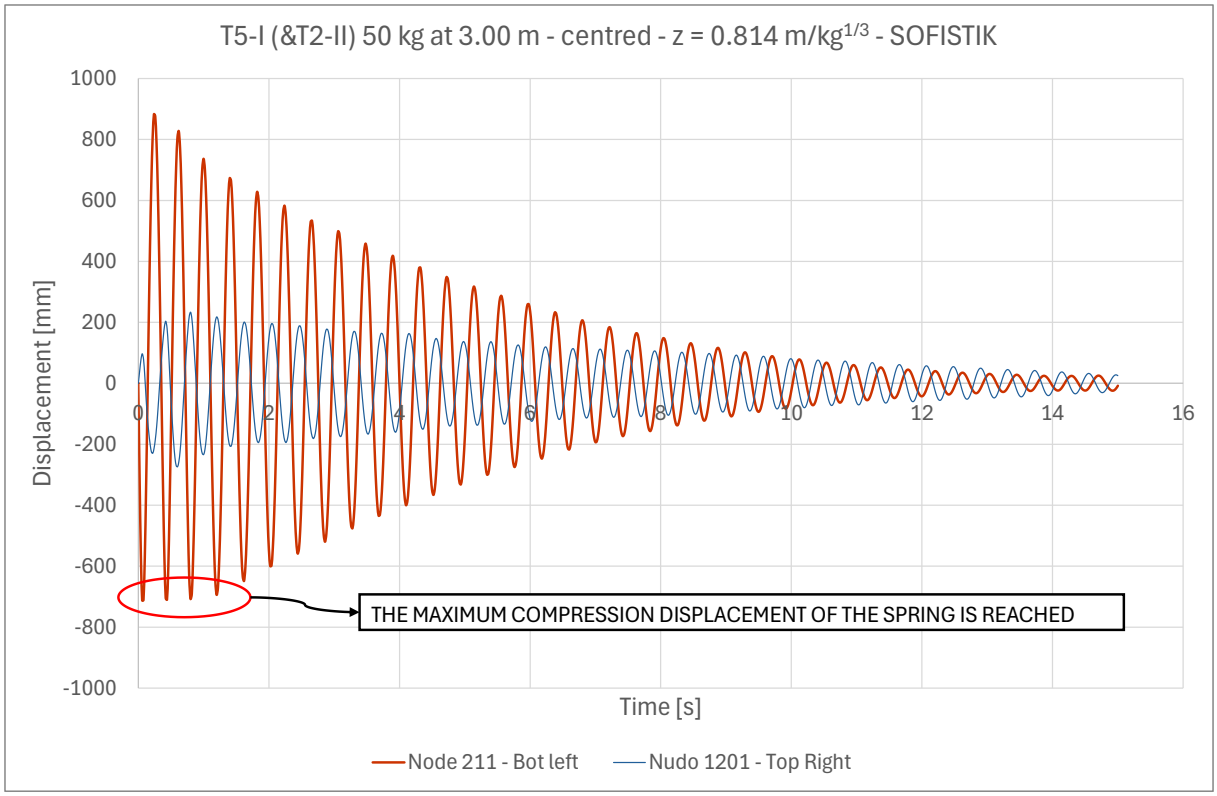

Figure 1 Displacement of bottom left and top right springs after blast

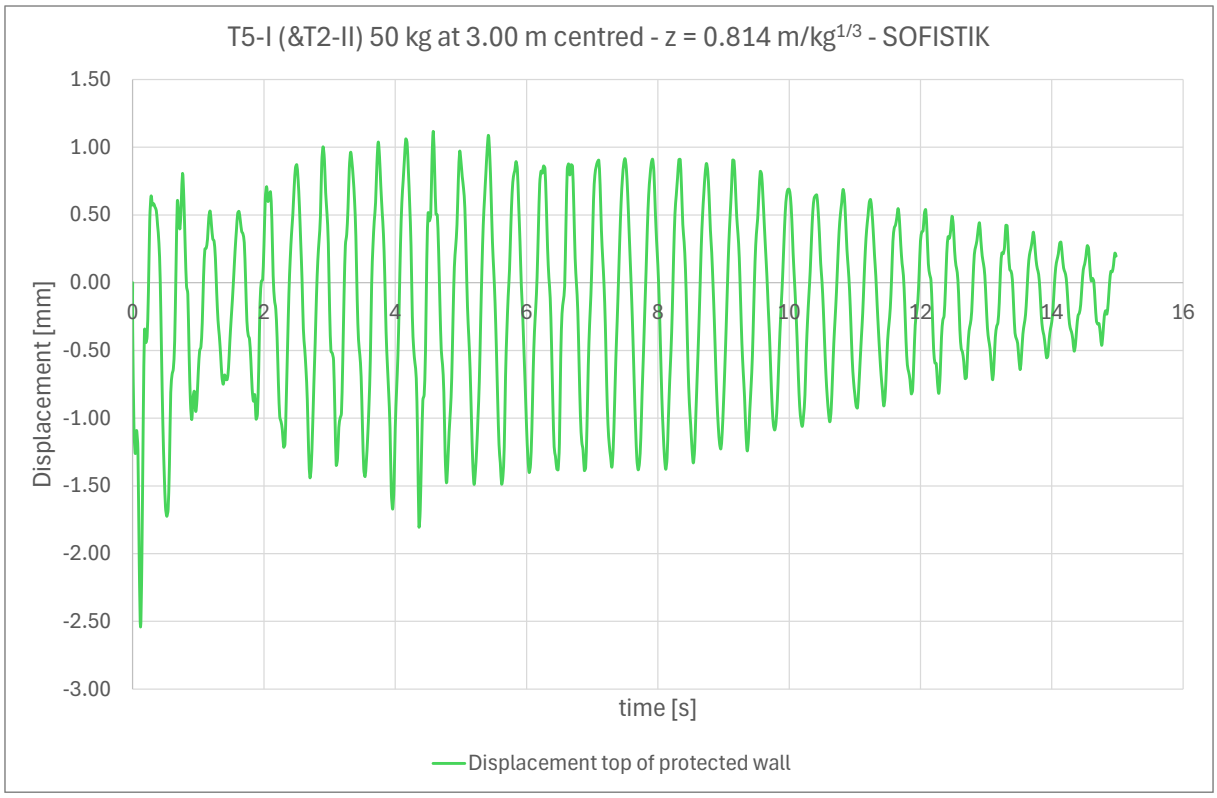

Figure 2 Displacement of top of protected wall

Keywords: blast loading, protective structure, nonlinear dynamic analysis, design, testing.

[1] Pérez Caldentey, A. (2019). New mass-based system for control room protection . *PROTECT 2019.* Whistler, Canada.

[2] Eytam, E., & Grisaro, H. (2024). Mitigating damage of structures under blast loads using linear protective layers. *9th International Colloquium on Performance, Protection & Strengthening of Structures Under Extreme Loading and Events.* Singapore.

Submission ID: 8328
(Full Paper)

Experimental Investigation of Energy Absorption in 3D-Printed Polymeric Axial Members Under High and Low-Speed Impact Using Various Infill Patterns

Raed R. SHWAISH[1,*], Hind H. Abdulridha[1], Adil Sh. Jaber[1], and Waleed AHMED[2*]

[1]Production Engineering and Metallurgy Department University of Technology, Baghdad, Iraq

[2]ERU, COE, UAE University, Al Ain, UAE

Corresponding authors: Raed.r.shwaish, W.ahmed@uaeu.ac.ae

Abstract

The response of structural elements to dynamic impact loads is crucial in protective design, particularly in applications where energy absorption is a primary concern. This study presents a comprehensive experimental investigation into the energy absorption capabilities of 3D-printed polymeric axial members subjected to both high-speed and low-speed impact tests. Using additive manufacturing techniques, axial members were fabricated with varying infill patterns, optimizing structural behavior under deformation. The study focuses on assessing the performance of different infill geometries to enhance energy dissipation during impact loading. Tests were conducted to evaluate the members' capacity to absorb impact energy, comparing response characteristics under varied strain rates. The findings indicate that specific infill patterns significantly improve energy absorption capabilities, highlighting their potential in applications requiring blast and impact-resistant designs. Furthermore, the results demonstrate that optimizing the internal structure of 3D-printed elements can effectively mitigate the effects of dynamic loads, making them a promising option for protective structures. The outcomes of this research contribute to the broader understanding of material behavior at high strain rates, offer insights into the design of lightweight, impact-resistant components, and provide new perspectives on utilizing innovative materials and manufacturing techniques to enhance structural resilience.

The Study on Interaction between Bubble and Double-layer Structure with Hole

Yuanxiang Sun

State Key Lab of Explosion Science and Safety Protection,

Beijing Institute of Technology, Beijing 100081, China

When warships and submarines are attacked by underwater weapons, they will be subjected to the shock wave and bubble load generated by explosive underwater explosions. The warship is mostly using double-deck grillage structure that are usually filled with ballast water. When it is under the impact of a near-field underwater explosion load produced by torpedoes and other underwater weapons, the outer structure is easy to break. The subsequent bubbles pulsation will be affected by the break. However, there is a lack of systematic studies on bubble pulsation and bubble jet in the double-layer structure with break. To study the interaction between the underwater explosion bubble and the ship's double-layer structure, the double-layer plate model with a circular hole was designed in this paper. The bubble pulsation and wall pressure caused by the bubble were obtained through experiments and numerical simulation. The variation patterns of bubble evolution and bubble loads under different conditions were compared and analyzed. The main conclusions are as follows:

(1) When the inter-plate water level is empty, the high-pressure gas inside the bubble is rapidly ejected into the double-layer plate, so that the inner plate is successively subjected to gas-liquid two-phase jet load, water jet load and surge load, of which the gas-liquid two-phase jet load (P_{b1}) is notable. When the inter-plate water level is full, the bubble is divided into the "outer bubble" and the "inner bubble", and both "inner bubbles" and "outer bubbles" form upward jets, and the "outer bubbles" collapse load (P_{b3}) and the water jet load (P_{b4}) is notable.

(2) When the inter-plate water level is between empty and full, the "outer bubble" forms a downward water jet, which can't load on the inner plate, while the water spike load of the "inner bubble" (P_{b2}) and the collapse load of "outer bubble" (P_{b3}) can load on the inner plate, which is the main load forms. The increase of Standoff distance R or Double-layer plate distance l makes the bubble collapse load and water spike load show a decreasing trend, while the increase of d makes the water spike load increase.

(3) For the protection of ship's double-layer structure, when the inter-plate water level is between empty and full, the formation of jets toward the structure is avoided, this situation provides optimal protection. When increasing the double-layer plate distance l, the water spike load (P_{b2}) and bubble collapse load (P_{b3}) would be attenuated.

(4) For the damage to ship's double-layer structure, reducing the standoff distance R can increase the water spike load (P_{b2}) and the bubble collapse load (P_{b3}) on the inner plate, and when the shock wave load makes the outer plate appear a larger hole, the water spike load on the inner plate (P_{b2}) increases significantly.

Keywords: underwater explosion, double-layer plate, bubble pulsation

[1] Zhang, Z, Wang, C, and Xu, W(2022). “Application of a new type of annular shaped charge in penetration into underwater double-hull structure”. Int. J. Impact Eng, 159, 104057.

[2]AKarri, B, Avila, SRG, and Loke, YC(2012). “High-speed jetting and spray formation from bubble collapse,” Phys. Rev. E -Stat. Nonlinear Soft Matter Phys, 85, 015303.

Experimental Investigation of Smart Composite Structural Insulated Panels with Integrated Piezoelectric Sensors for Damage Localization in Extreme Conditions

Anupoju Rajeev[1], Vishnu Vijay Kumar[2], Amit Shelke[3], Khaled Shahin[2], Prince Jeya Lal Lazar[4*]

[1]*Department of Civil and Environmental Engineering, National University of Singapore (NUS), Singapore*

[2]*Structural Engineering, Division of Engineering, New York University Abu Dhabi (NYUAD), Abu Dhabi, United Arab Emirates*

[3]*Department of Civil Engineering, Indian Institute of Technology Guwahati, India*

[4]*Department of Mechanical Engineering, Rajalakshmi Institute of Technology, Chennai, India*

*Corresponding author: princejeyalal@gmail.com

This study investigates the development and performance of smart composite structural insulated panels (CSIPs) integrated with piezoelectric sensors aimed at enhancing the resilience of structures in disaster-prone coastal communities. The primary objective is to evaluate the effectiveness of these smart panels in damage localization and structural health monitoring during extreme events such as hurricanes and tornadoes. The CSIPs consist of two Fibre Cement Board (FCB) face sheets enclosing an Expanded Polystyrene (EPS) core designed to provide superior insulation and structural integrity. A series of rigorous experimental tests, including four-point flexural tests and shock load simulations, were conducted to assess the mechanical properties and failure modes of the CSIPs. The flexural tests adhered to ASTM C393 standards, revealing critical insights into the panels' load-bearing capacity and deformation characteristics. The results indicated a peak load of 840 N and highlighted the brittle nature of the FCB face sheets, which contributed to specific failure mechanisms such as debonding and strain localization at the interface with the EPS core. To further understand the dynamic response of the CSIPs under shock loading, a shock and impact testing simulator was employed. This setup allowed for the generation of planar shock waves, with pressure profiles measured using dynamic pressure transducers. The data collected from these experiments were instrumental in validating finite element models, which simulated the structural behavior of the CSIPs under various loading conditions. The integration of piezoelectric sensors within the CSIPs provides real-time monitoring capabilities, enabling the detection of damage and strain

during extreme loading scenarios. This innovative approach not only enhances the safety and reliability of structures but also contributes to the development of smart infrastructure that can adapt to changing environmental conditions. Overall, the findings from this research underscore the potential of smart CSIPs as a viable solution for improving the resilience of buildings in vulnerable regions. By combining advanced materials with smart technology, this study paves the way for future innovations in structural engineering and disaster management, ultimately contributing to safer and more sustainable communities.

Keywords: Coastal resilience, Damage localization, FE Modeling, Piezoelectric Sensors, Shock Loading, Smart Composite Structural Insulated Panels (CSIPs), Structural Health Monitoring

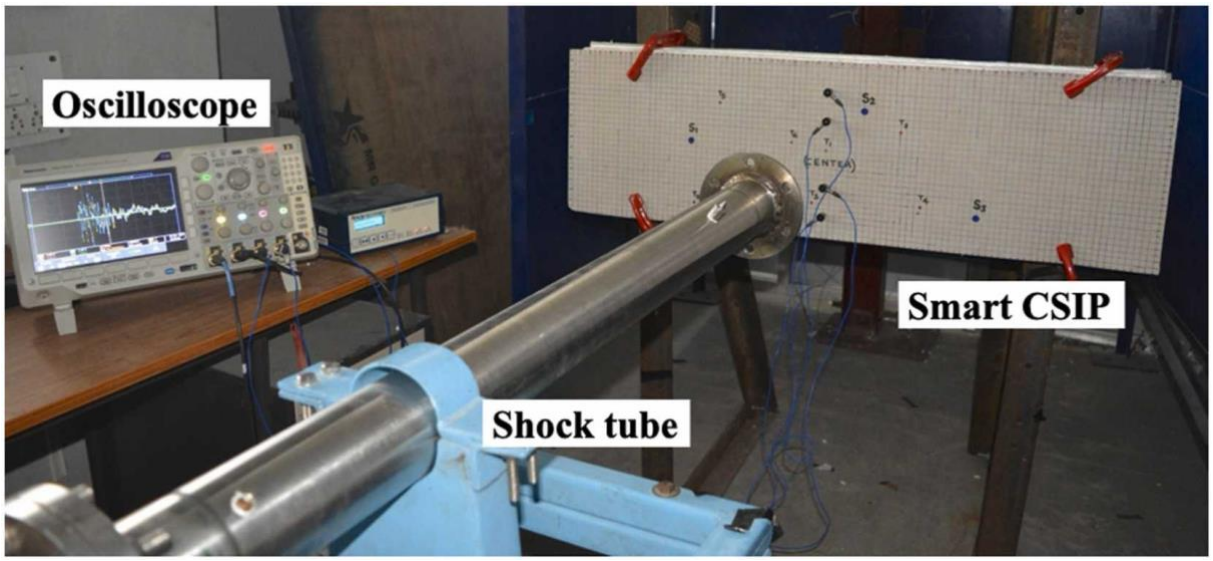

Fig 1. Experimental set up for shock tube with test specimen.

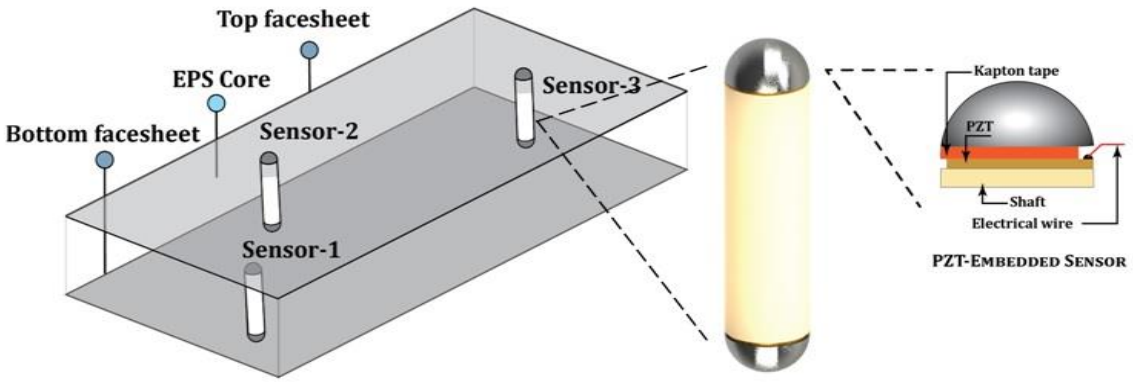

Fig 2. Detailed schematic of Smart-CSIP highlighting the sensor

EFFECTS OF RESIN COATING ON THE BLAST RESISTANT PERFORMANCE OF CONCRETE PLATES UNDER CONTACT EXPLOSION

Hiroyoshi Ichino[1], Yuto Nomura[1], Masuhiro Beppu[1], Toshiya Yamauchi[1]

[1] *Department of Civil and Environmental Engineering, National Defense Academy, Hashirimizu 1-10-20, Yokosuka, Kanagawa, 239-8686, Japan.*

Accidental explosive incidents bring near concrete structures, concrete walls are failed locally and concrete fragments cause damage behind the wall. Trying to prevent local failure and fragments by increasing the cross-section of reinforced concrete members often causes the extreme increase in self-weight and the limitation of interior volume due to the increase in wall thickness. Accordingly, methods to prevent local failure and fragments due to explosions without increasing the cross-section have been investigated. One option for protection from damage caused the local failure is to coat back side of concrete walls with resin. Although previous studies showed effectiveness of resin coating on fragments in concrete members subjected to a contact explosion, effects of mechanical properties of resin coating on the blast resistant performance of concrete under contact explosion are still in the process of being investigated. In this study, effects of mechanical properties of resin coating on the blast resistant performance of concrete plates under contact explosion have been investigated experimentally. In the experiment, concrete plate specimens were 500-mm by 500-mm and had a thickness 60-80 mm coated by 3 kinds of resin (polyurea, modified epoxy, modified urethane) with different mechanical properties. The tensile strength of these resins was ranging 3 N/mm^2 and 60 N/mm^2. The breaking elongation was ranging 10 % and 300 %. Damage of these specimens under contact explosion caused by between 15 g and 150 g of composition C-4 explosive were observed. From the results, mechanical properties of coating resin notably affected effectiveness of prevention from fragment caused by spalling as shown in **Figure 1**. Because fracture of resin coating leads to fragment scattering, the coating fracture is not permitted in the design of protective structures. The limit of whether the resin coating was fractured or not in each kind of resin was proposed as shown in **Figure 2**. It was found that in order to prevent the coating fracture, it is better to maintain the strength of the resin while improving its breaking

elongation, rather than simply increasing its strength. In the future, it is desired that methods of evaluation of fracture limit by mechanical properties and thickness of resin coating.

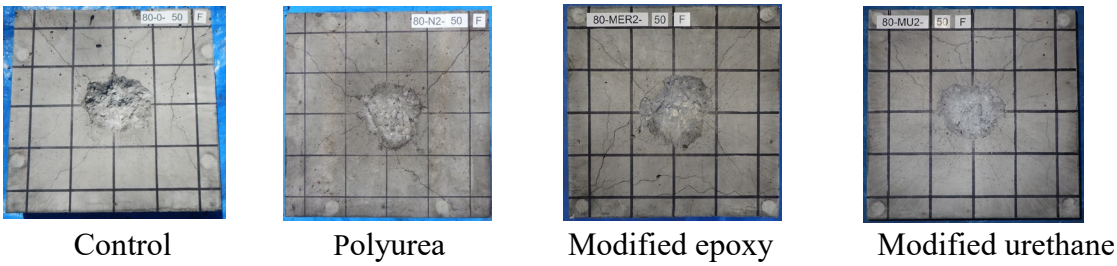

(a) Front surface

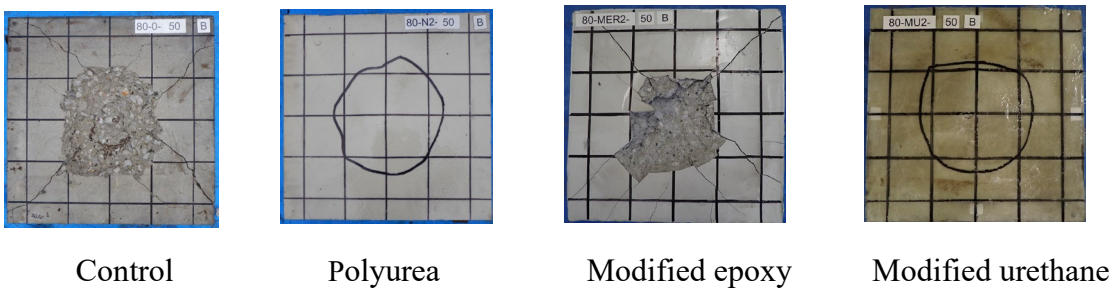

(b) Back surface

Figure 1. Typical examples of tested specimens (Concrete:80mm, Resin: 2mm, C-4: 50g)

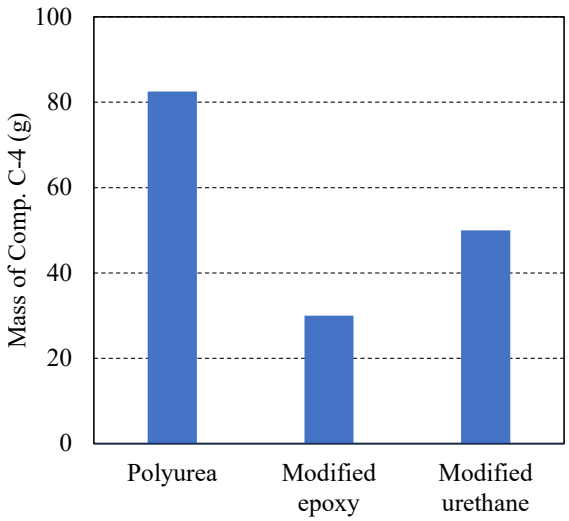

Figure 2. Fracture limit charge mass in a concrete plate 80 mm thick coated by 2 mm of resin

Keywords: contact explosion, concrete plate, resin coating, spalling, fragment

[1] Ichino, H., Beppu, M., Yamauchi T. and Fukui, S., (2023). Effects of polyurea coating on the blast resistant performance of concrete plates under contact explosion, Proceedings of The 11th International Symposium on Impact Engineering (ISIE2023).

EXPERIMENTAL STUDY ON FALLING DEBRIS IMPACT: A BASIS FOR PANCAKE-TYPE PROGRESSIVE COLLAPSE ASSESSMENT

Elahe Zeinali
Department of Structural, Geotechnical and Building Engineering (DISEG) - Politecnico di Torino, Torino, Italy, elahe.zeinali@polito.it (corresponding author)

Foad Kiakojouri
Department of Structural, Geotechnical and Building Engineering (DISEG) - Politecnico di Torino, Torino, Italy, foad.kiakojouri@polito.it

Valerio De Biagi
Department of Structural, Geotechnical and Building Engineering (DISEG) - Politecnico di Torino, Torino, Italy, valerio.debiagi@polito.it

ABSTRACT

Recent research on the progressive collapse of buildings has predominantly focused on the redistribution of loads following the failure of critical members, commonly referred to as "re-distributional progressive collapse". However, many notable structural failures have resulted from a different mechanism, known as "impact-type progressive collapse", which remains less understood. This type of collapse, often triggered by dynamic events such as falling debris or fire scenarios, introduces complex interactions between the impacting body and the structure. These interactions are difficult to capture using traditional static or quasi-static models, leaving a significant gap in our understanding of how impact-type progressive collapses occur. This study aims to bridge that gap by investigating the forces generated during impacts between concrete bodies. This experimental study examines the impact forces between concrete bodies of varying geometries. Spherical, semi-spherical, and cubic concrete samples dropped onto a reinforced concrete plate from various controlled heights. Additionally, a high-speed camera was utilized to capture the impact events, facilitating an in-depth analysis of the contact dynamics. Several key parameters were varied throughout the tests, including impactor weight and velocity, the contact radius, and concrete compressive strengths. Advanced data processing techniques, namely Variational Mode Decomposition (VMD), were employed to analyze the data. Results demonstrated that by increasing the impact velocity about 73%, the maximum contact force rose by 75%. Furthermore, the results underscore a significant influence of sample geometry, with spherical and semi-spherical specimens generating up to 64% higher maximum contact forces than equivalent cubes. The tests also revealed that compressive strength had a relatively minor effect, increasing the contact force by only 9% when raised by 50%. This observation is further confirmed by high-speed camera footage illustrating a much more concentrated impact scenario in spherical samples. No meaningful differences were observed between spherical and semi-spherical specimens of the same weight but with different contact radii.

Keywords: Falling Debris, Impact, Progressive Collapse

INTRODUCTION

The robustness of a building, defined as its capacity to resist collapse, is frequently evaluated using the alternate load path method [1, 2]. In this method, the building's ability to withstand a sudden column removal is analyzed. Irrespective of what triggers the column's failure, the progressive collapse process is typically broken down into two phases [3]. The initial phase focuses on how the load is redistributed and whether the surrounding structural members can carry the transferred load. If these elements are unable to bear the redistributed loads, the second phase of progressive collapse may occur. During this phase, falling debris is generated from damaged elements near the failed column. This debris impacts the floor beneath, which must withstand the dynamic impact to stop the progression of the collapse. Among the various forms of progressive collapse, pancake-type collapse is a notable example of impact-type collapse. In this scenario, the upper floors of a building collapse in succession, with each floor falling on top of the one below it, much like the layers of a pancake. While falling debris is commonly seen in these collapse events, it is important to emphasize that this debris is usually not the triggering event of the collapse; rather, it emerges as a consequence of the initial failure in the structure. While re-distributional collapse mechanisms have been extensively studied [4], the impact-type progressive collapse mechanism remains less understood [5]. Understanding and mitigating the dynamic effects of such impacts is critical for enhancing structural robustness and safety. Impacts can expose structures to severe risks of collapse, challenging their overall stability and resilience, especially when they occur on critical load bearing elements [6, 7, 8]. Impacts involve complex dynamic interactions between impacting bodies and structural elements. These interactions cannot be accurately captured by traditional static or quasi-static models [9]. Consequently, the lack of detailed research on impact dynamics creates a significant gap in the ability to design structures resilient to such events.

Studies of structural response to impact events typically adopt one of three approaches: experimental testing, numerical simulations, or analytical modeling. Experimental investigations are critical for replicating real-world impacts in controlled environments and validating theoretical models. However, such campaigns are constrained by their high costs, time requirements, and limited number of test scenarios [10].

An important gap in the literature is the lack of studies focusing on the behavior of contact forces during concrete-to-concrete impacts. Although numerous drop weight tests on reinforced concrete elements have been conducted, most studies involve a steel [11, 12] or other non-concrete drop weight [13] impacting the structure. Li et al. [6], emphasize that various material of impactor and the presence or absence of interlayers—significantly influence the impact behavior of RC beams. However, there are few studies [14] that systematically explore the effects of direct concrete-to-concrete contact during impacts. To the best of the author's knowledge, no research has specifically evaluated how factors such as geometry, velocity, and material properties influence the contact force during concrete-to-concrete impacts, which is critical for understanding and assessing structural response to falling debris in progressive collapse scenarios.

This study seeks to address the gap in knowledge by analyzing dynamic impact forces generated during debris impacts on a reinforced concrete plate. An experimental campaign was conducted, employing load cells, accelerometers, and a high-speed camera to capture detailed data on impacts between concrete specimens of varying geometries.

EXPERIMENTAL PROCEDURE

A schematic representation of the experimental setup is shown in Figure (1). The target plate used for impact tests measures 35 cm × 35 cm × 12 cm and weighs 33.1 kg. It is composed of fiber-reinforced concrete (C25/30 premixed concrete with 0.75 kg of hooked-end steel fibers), designed to avoid the need

for reinforcement bars. The plate is supported by three PCB Piezotronics Model M203B piezoelectric force rings [15]. These sensors are arranged at the vertices of an equilateral triangle with a 20 cm side length. The geometric center of this triangle aligns with the vertical projection of the plate's centroid, ensuring accurate force measurement during impact.

A high-frequency piezoelectric accelerometer is installed at the geometric center of the plate's bottom face to protect it from direct impact. Impact events are recorded using a Photron Fastcam Nova S12 monochrome high-speed camera [16] equipped with a Zeiss Milvus 85 mm f/1.4 lens [17]. A frame rate of 10,000 frames per second (fps) was chosen to ensure accurate capture of rapid impact phenomena.

The impact tests are conducted by releasing concrete specimens from a platform at predefined heights above the plate. Upon release, the specimens achieve a free-fall velocity of $v = \sqrt{2gh}$ at the moment of impact, where h is the height from the top surface of the plate to the bottommost point of the falling object (see Figure (1)). The impacting bodies included various concrete specimens: square cubes measuring 5 cm × 5 cm × 5 cm, rectangular cubes measuring 5 cm × 5 cm × 10 cm, and spherical and semi-spherical samples with diameters ranging from 6 cm to 10 cm. The samples had weights between 140 g and 561 g and two distinct compressive strengths: T1 = 50 N/mm² and T2 = 72 N/mm². The concrete mix design and specimen fabrication were carried out in accordance with Eurocode 2 (EN 1992-1-1) guidelines to ensure consistent material properties and reliable test conditions. To isolate the effect of shape, some specimens were prepared with identical weights but different geometries. For samples requiring weight adjustments, small metallic particles were added as needed. These specimens were released from heights of 70 cm, 140 cm, and 210 cm, corresponding to impact velocities of approximately 3.7 m/s, 5.2 m/s, and 6.4 m/s, respectively. Each test was conducted on three identical specimens, with each specimen being tested three times to ensure reproducibility and minimize experimental uncertainty.

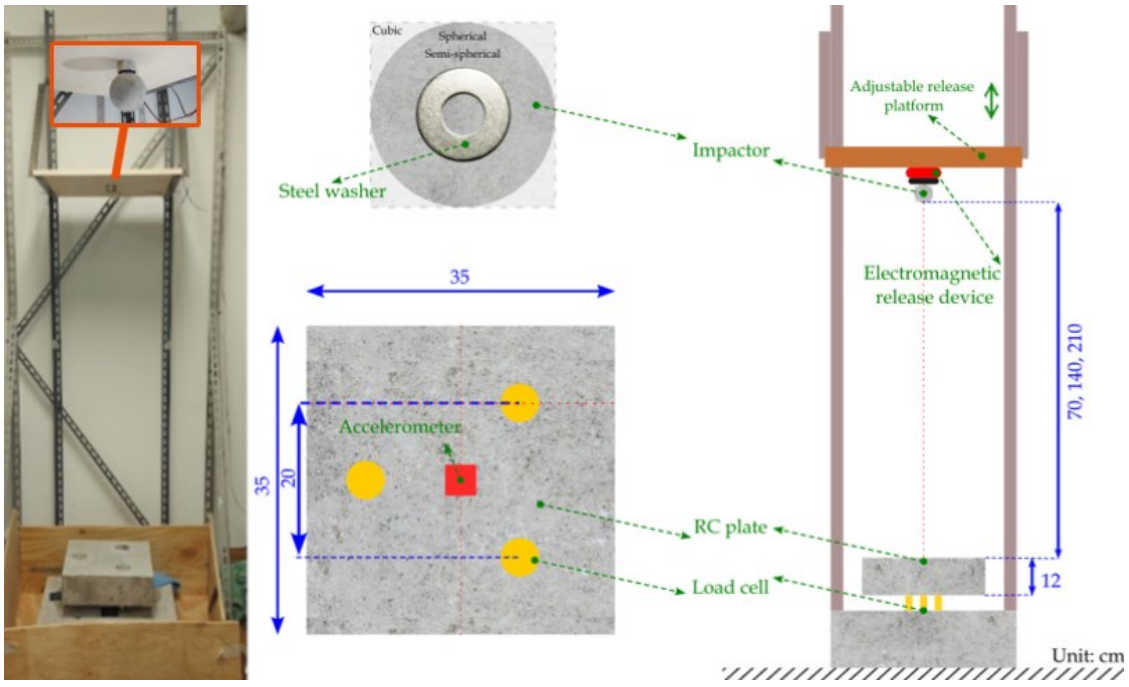

(a) **(b)**

Figure 1. Experimental setup: (a) front view, (b) schematic of the experimental setup.

The total force and the acceleration during the tests are recorded through the three PCB Piezotronics Model M203B piezoelectric force rings (measurement range 88.96 kN, sensitivity 56.2 mV/kN, upper frequency limit 60 kHz) and a uni-axial Wilcoxon 732 A high frequency piezoelectric accelerometer (500 g peak, sensitivity 10 mV/g, resonance frequency 60 kHz) mounted on the plate. Advanced data analysis techniques, including Fast Fourier Transforms (FFT) and Variational Mode Decomposition (VMD), are used to extract the contact force from the raw data. The interpretation of these measurements follows a method proposed by De Biagi and Marchelli [14], where the VMD algorithm is implemented in MATLAB to accurately derive the contact force during collision events. The influence of critical parameters, such as weight, shape, velocity, and compressive strength of the impacting bodies, as well as the contact radius, is examined to evaluate their effects on the dynamic response of the system.

RESULTS AND DISCUSSIONS

The effect of the contact radius on the maximum contact force was assessed by comparing the specimens SP-6cm-T2 (a spherical specimen with a diameter of 6 cm) and SS-8cm-T2 (a semi-spherical specimen with a diameter of 8 cm). Both specimens have the same weight (245 grams), identical impact velocities of 3.7 m/s, and the same material properties. As illustrated in Figure (2a) and Table (1), their maximum contact forces are around 2.5 kN (less than 1% difference), particularly at lower velocities. This indicates that the contact radius has minimal influence on the maximum contact force under these conditions.

Table 1. Experimental specimens and the relates results. Nomenclature of the specimens: SS denotes semi-spherical specimens, SP spherical specimens, SC square cubes, and RC rectangular cubes. The number following the shape indicates the diameter (for spheres and semi-spheres) or dimensions (for cubes), while T1 and T2 refer to compressive strengths of 50 N/mm² and 75 N/mm², respectively.

Specimens	Weight (gr)	Max Contact Force (kN) for Height=70 cm	Max Contact Force (kN) for Height=140 cm	Max Contact Force (kN) for Height=210 cm
SP-6cm-T1	212	2.36	3.21	4.23
SS-6cm-T1	140	1.45	1.75	1.99
SP-6cm-T2	245	2.54	3.81	4.83
SS-6cm-T2	140	1.58	1.91	2.08
SP-7cm-T2	392	4.52	6.54	7.67
SP-8cm-T2	561	6.35	9.08	11.25
SS-8cm-T2	245	2.48	3.52	4.31
SS-9cm-T2	392	4.18	6.37	7.01
SS-10cm-T2	561	5.63	7.98	9.24
SC1-5cm-T2	245	1.54	2.14	2.82
SC2-5cm-T2	392	1.82	2.81	3.78
RC-15×5×5-T2	561	4.36	5.41	6.41

However, when comparing these spherical and semi-spherical specimens to a cube of the same weight (SC1-5cm-T2), a notable difference in maximum contact force is observed. At a release height of 70 cm, the maximum contact force for the cubic specimen is around 1.54 kN, whereas the spherical specimen exhibits a contact force of approximately 2.48 kN, representing around 67% difference between spherical/semi-spherical and cubic specimens.

As the release height increases, this difference becomes more pronounced. For example, at a height of 210 cm, the maximum contact force reaches approximately 4.83 kN for the previous mentioned spherical specimen and 2.82 kN for the same cubic specimen. This suggests that a smaller contact surface area, as in the case of spheres and semi-spheres, acts as a concentrated load, resulting in higher maximum contact forces. These results emphasize the critical role of contact surface geometry in dynamic impact scenarios, where a reduced contact radius leads to increased stress concentrations and higher contact forces during impact. Figure (2b) further illustrates the effect of different geometries on the maximum contact force.

To evaluate the influence of material properties on the maximum contact force, semi-spherical specimens SS-6cm-T1 and SS-6cm-T2 were selected. These specimens share the same weight, velocity, and shape, but different compressive strengths. As illustrated in Figure (2c) and detailed in Table 1, increasing the compressive strength by 44% results in a slight increase in the maximum contact force, from 1.45 kN to 1.58 kN, which is approximately 9% higher. This suggests that while material strength has a measurable impact on the contact force, the effect is relatively minor.

The observed increase is attributed to the higher stiffness of the impacting specimen. A stiffer impactor experiences less internal deformation upon contact, concentrating the interaction force at the contact interface. Moreover, the inertia of the impactor maintains resistance to sudden deceleration, ensuring that more kinetic energy is transferred directly to the target plate instead of being absorbed through internal deformation. This phenomenon leads to a higher peak contact force despite minimal changes in overall contact duration or energy dissipation.

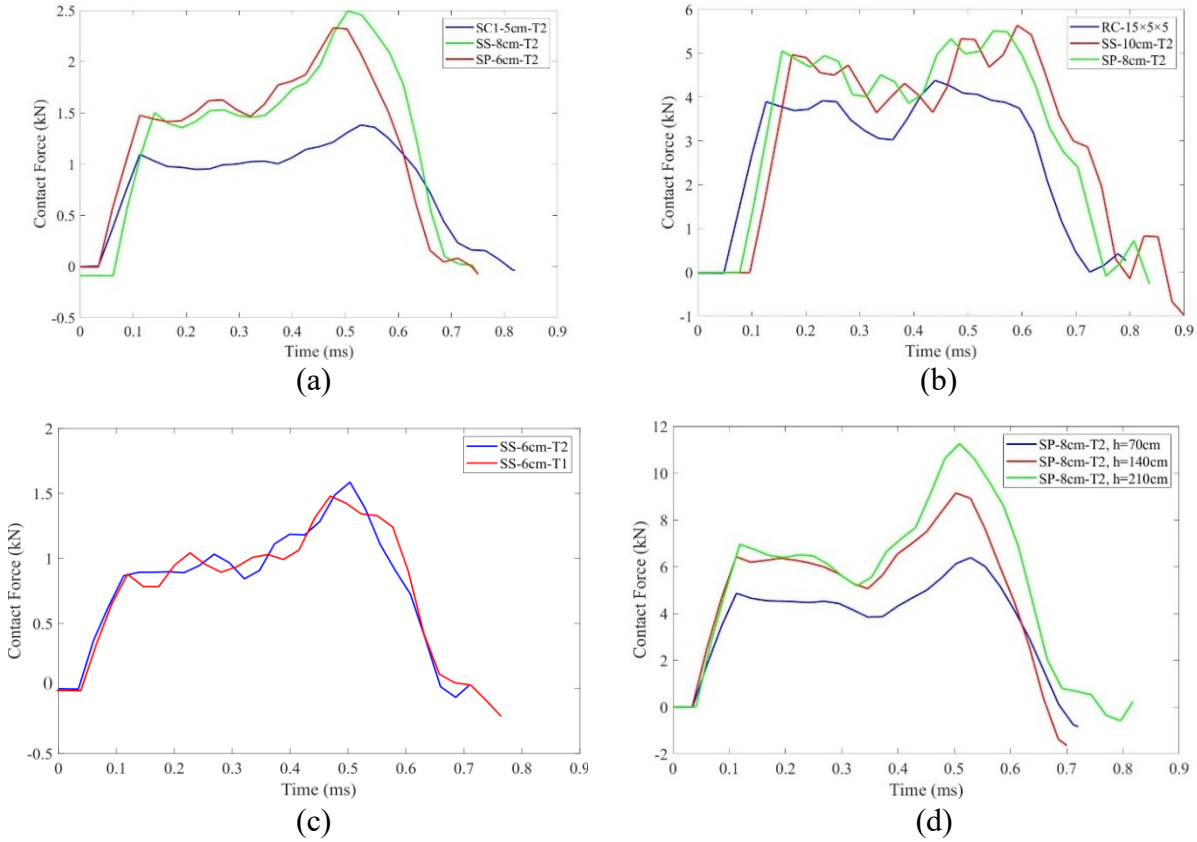

Figure 2. Time-history of contact force for samples with different: (a) contact radii, (b) shape, (c) compressive strength, and (d) impact velocity which is based on the falling height.

For specimen SP-8cm-T2 (weight 561 g), the maximum contact forces recorded at different heights are 6.40 kN, 9.08 kN, and 11.25 kN for falling heights of 70 cm, 140 cm, and 210 cm, respectively. The contact force increases by 40.6% from 70 cm to 140 cm and by 24.4% from 140 cm to 210 cm. These results highlight a significant rise in maximum contact force (Figure (2d)) with increasing impact velocity, though the rate of increase diminishes at higher velocities. This suggests a nonlinear relationship between velocity and contact force, indicating that velocity is one of the most influential parameters affecting contact force.

When the impacting mass has zero velocity, all its momentum has been transferred into collision force. The impulse theorem states [18] that the change in momentum equals the integral of the force that caused the deceleration over time. The impulse J is expressed as $J = \int_0^{t_c} F(t)dt$, where t_c is the total contact duration (Figure (3)). To evaluate when the impactor reaches zero velocity, the integral of the force over time was calculated from the initiation of contact to the midpoint of the contact duration. For specimen SP-8cm-T2, with an initial impact velocity of 5.24 m/s, the total contact duration was measured to be 0.63 milliseconds. Half of the total contact duration occurred at approximately 0.35 milliseconds, and the impulse up to this point was calculated to be 2.2 kN·s, approximately 51.8% of the total impulse of 4.31 kN·s. The slight discrepancy indicates that variations in force distribution affect the exact zero-velocity point.

The presence of multiple peaks in the contact force diagrams shown in Figure (2) is attributed to repeated impacts between the specimen and the plate. This behavior is confirmed by high-speed camera footage, as illustrated in Figure (4), which captures successive contact events. The images show that after the initial contact, the specimen bounces and makes additional contact with the plate, generating subsequent peaks in the force-time history. These repeated impacts lead to a dynamic force response, characterized by more than one peak in the diagrams.

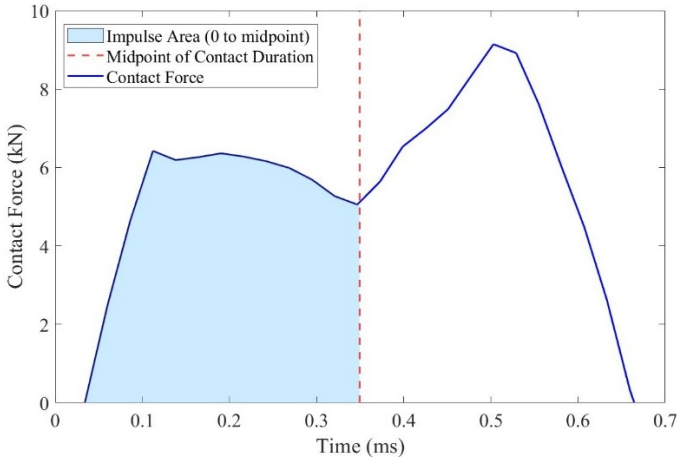

Figure 3. Force-time curve for SP-8cm-T2 (5.24 m/s), with midpoint and impulse area highlighted.

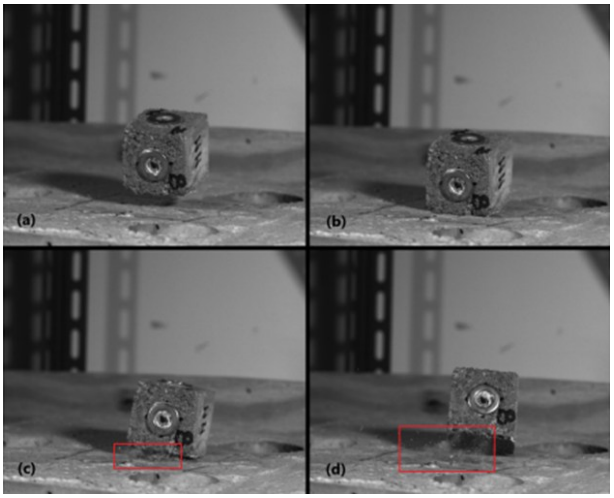

Figure 4. Frames captured with the high-speed camera for SC1-5cm-T2 cubic specimen: (a) instant before contact; (b) first contact between specimen and plate; (c) second contact between specimen and plate; (d) instant after contact.

CONCLUSIONS

This study has provided insights critical parameters influencing contact force. The experimental results demonstrated that sample geometry, material properties, and impact velocity significantly affect the maximum contact force. Notably, spherical and semi-spherical specimens, with their smaller contact areas, generated much higher peak forces than cubic specimens of the same weight, highlighting the role of stress concentration. However, the effect of material compressive strength on the contact force was found to be relatively minor, with only a 9% increase in force despite a 44% increase in strength, attributed to increased stiffness and energy transfer efficiency.

The experiments also confirmed that impact velocity is a dominant factor, with contact force rising by 40.6% between heights of 70 cm and 140 cm, and 24.4% between 140 cm and 210 cm. This nonlinear relationship underscores the importance of velocity in dynamic loading conditions. Furthermore, high-speed camera footage revealed that multiple peaks in the contact force-time history result from repeated impacts, as specimens bounce and recontact the plate. These findings are crucial for understanding and predicting pancake-type progressive collapse scenarios, emphasizing the need for design strategies that account for dynamic impact forces and stress concentration effects in critical structural elements. This research provides a foundation for future studies aimed at enhancing structural resilience to extreme events.

ACKNOWLEDGMENTS

The authors would like to express their sincere gratitude to Dr. Devid Falliano from the Department of Structural, Geotechnical and Building Engineering (DISEG) at Politecnico di Torino for his valuable assistance in the design, preparation and fabrication of the concrete samples used in this study.

REFERENCES

[1] General Services Administration, Disproportionate Collapse Analysis and Design Guidelines for New Federal Office Buildings and Major Modernization Projects, Technical Report, General Services Administration, Washington, DC, 2003.

[2] Department of Defense, UFC 4-023-03: Design of Buildings to Resist Disproportionate Collapse, Technical Report, United Facilities Criteria, Washington, DC, 2013.

[3] Jawdhari, A., Orton, S., Izzuddin, B., & Cormie, D. (2018, April). Dynamic debris loading in flat plate and steel framed buildings. In Structures Conference 2018 (pp. 299-310). Reston, VA: American Society of Civil Engineers.

[4] Kiakojouri, F., De Biagi, V., Chiaia, B., & Sheidaii, M. R. (2020). Progressive collapse of framed building structures: Current knowledge and future prospects. *Engineering Structures*, 206, 110061.

[5] Kiakojouri, F., Zeinali, E., Adam, J. M., & De Biagi, V. (2023). Experimental studies on the progressive collapse of building structures: A review and discussion on dynamic column removal techniques. *Structures,* 57, 105059.

[6] Li, H., Chen, W., & Hao, H. (2019). Influence of drop weight geometry and interlayer on impact behavior of RC beams. *International Journal of Impact Engineering*, 131, 222-237.

[7] Sielicki, P. W., Ślosarczyk, A., & Szulc, D. (2019). Concrete slab fragmentation after bullet impact: An experimental study. *International journal of protective structures*, 10(3), 380-389.

[8] Ning, J., Meng, F., Ma, T., & Xu, X. (2020). Failure analysis of reinforced concrete slab under impact loading using a novel numerical method. *International Journal of Impact Engineering*, 144, 103647.

[9] Zhang, C., Gholipour, G., & Mousavi, A. A. (2021). State-of-the-art review on responses of RC structures subjected to lateral impact loads. *Archives of Computational Methods in Engineering*, 28(4), 2477-2507.

[10] Adam, J. M., Buitrago, M., Bertolesi, E., Sagaseta, J., & Moragues, J. J. (2020). Dynamic performance of a real-scale reinforced concrete building test under a corner-column failure scenario. *Engineering Structures*, 210, 110414.

[11] Zineddin, M., & Krauthammer, T. (2007). Dynamic response and behavior of reinforced concrete slabs under impact loading. *International Journal of Impact Engineering*, 34(9), 1517-1534.

[12] Senthil, K., Kubba, Z., Sharma, R., & Thakur, A. (2021, March). Experimental and numerical investigation on reinforced concrete slab under low velocity impact loading. *IOP conference series: materials science and engineering*, Vol. 1090, No. 1, p. 012090. IOP Publishing.

[13] Zhan, T., Wang, Z., & Ning, J. (2015). Failure behaviors of reinforced concrete beams subjected to high impact loading. *Engineering Failure Analysis*, 56, 233-243.

[14] De Biagi, V., & Marchelli, M. (2025). An experimental setup to study the collision force between brittle impacting bodies. *International Journal of Impact Engineering*, 196, 105160.

[15] PCB Piezotronics, "Model 203B ICP® Quartz Force Ring," [Online]. Available: https://www.pcb.com/products?m=203b.

[16] Photron. "FASTCAM Nova S12 High-Speed Camera." https://photron.com/fastcam-nova-s/.

[17] Zeiss. "Milvus 1.4/85." https://www.zeiss.com/consumer-products/us/photography/milvus/milvus-1485.html.

[18] Hibbeler, R. C. (2004). Engineering mechanics: dynamics. Pearson Educación.

Large-caliber Compressive Air Gun in Tongji University, China

Liangliang Ma*, De Chen, Hao Wu, Yuehua Cheng

College of Civil Engineering, Tongji University, Shanghai, China

Corresponding author: Liangliang Ma, E-mail: 24310004@tongji.edu.cn

Military facilities are exposed to the threat of high-velocity strikes from earth-penetration weapons, and civilian structures, e.g., bridges, nuclear power plants and rock shelters, are susceptible to low- and medium-velocity impact accidents. The existing test equipment in China is difficult to fully cover the abovementioned scenarios, and thus a large-caliber compressed air gun system was developed in Tongji University, as shown in Fig. 1. This air gun consists of 200 mm and 400 mm caliber barrels, with the maximum capacity to drive a 200 kg mass to a velocity of 200 m/s to impact a 3 m×3 m slab, or a 3-m-long beam/column, or a frame with dimensions of 6 m×6 m×4.5 m, and all parameters have reached the global leading level. Utilizing this air gun, the rockfall impact test on the flexible barrier and reinforced concrete (RC) slab (Fig. 2), the wind-borne missile impact test on both the RC and steel slab, the pipe whipping test on the nuclear power plant structure, and the penetration test on the ultra high performance concrete slab have been done. The corresponding missile-target interaction, the damage evolution, as well as the dynamic responses, i.e., strain-, displacement-, and force-time histories of the target were well recorded by the high-speed camera and the data acquisition system. The high-speed camera has a maximum resolution of 1024×1024 at the speed of 16000 FPS and the data acquisition system has 64 channels available for all kinds of dynamic data. To conclude, the air gun is applicable to projectile penetration (350 m/s), bird striking aircraft (70-200 m/s), pipe whipping (70-160 m/s), wind-borne missile impact (40-80 m/s), rockfall impact (10-50 m/s), vehicle/vessel impact (0.5-33 m/s), electric car battery pack collision (8-20 m/s) and mudslide impact (1-10 m/s) and other types of different qualities of high and low speed impact scenarios.

Keywords: large caliber, air gun, high/low-velocity impact, military and civilian structures

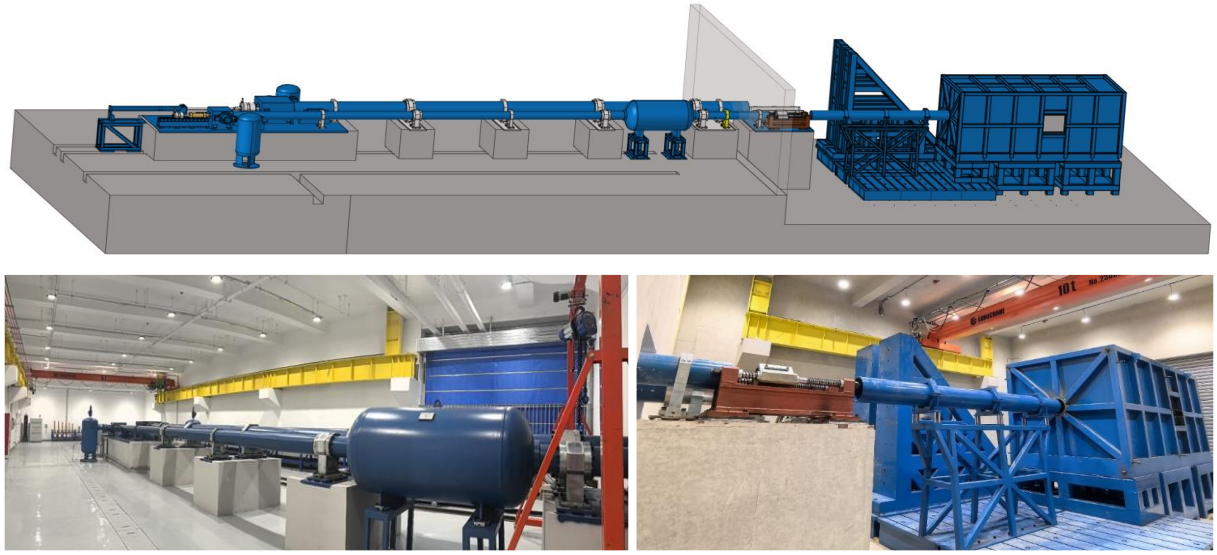

Fig. 1 Large-caliber compressive air gun in Tongji University, China

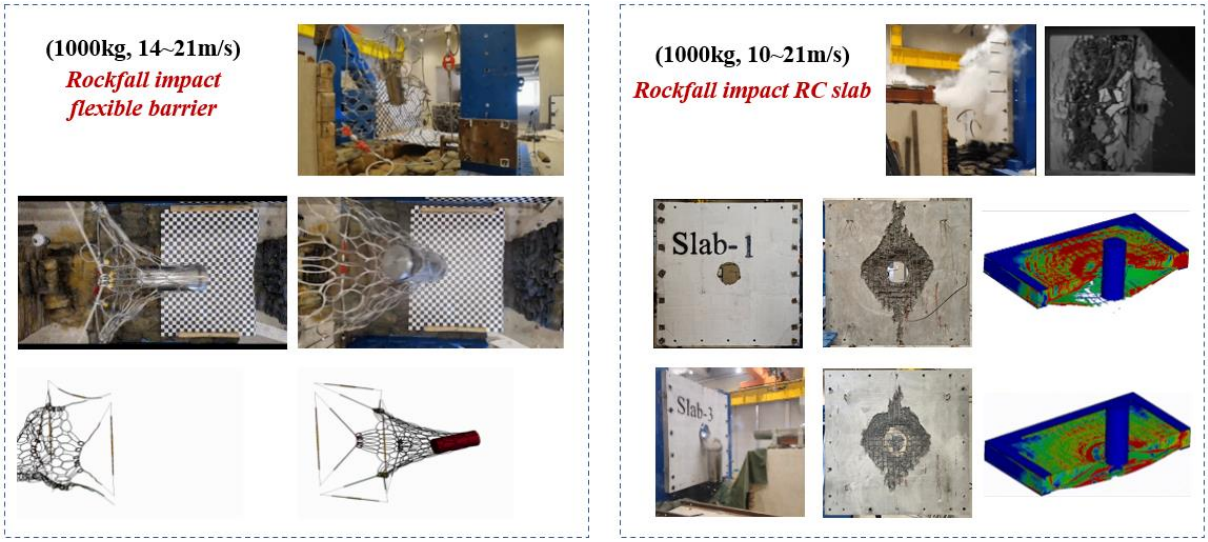

Fig. 2 Rockfall impact test

Accidental Explosions in Urban Environments: A Case Study of a 2024 Blast in Poznań

Peter G McDonald[1], Andrew Nicholson[1], Christopher G. Stirling[1] and Piotr Sielicki [2]

[1]*Viper Applied Science, Scotland, United Kingdom*

[2]*Poznań University of Technology, Poznań, Poland*

This study investigates the propagation of explosion effects in a 19th-century masonry building during a significant incident that occurred in Poznań, Poland, in 2024 (Figure *1*). Historical structures such as this are known for their unique material characteristics and structural vulnerabilities, which can influence blast dynamics and structural response in complex ways. Consequently, understanding how pressure waves from an internal explosion move through such a building—and then extend beyond it to impact neighbouring areas—is essential for accurate blast modelling and damage assessment. This study primarily focuses on solving the propagation of pressure waves within the building, tracking their progression as they exit the structure, and analysing their effects on nearby streets and surrounding buildings. Post-event data on structural damage, particularly to nearby windows and facades, has been incorporated to provide a benchmark for comparing simulated results with real-world impacts.

The simulation work was conducted using Viper::Blast, a specialized CFD code developed for modelling blast dynamics in intricate urban environments. This software allows for detailed analysis of blast wave propagation, structural interactions, and resultant damage patterns. In this study, different explosive mixtures were evaluated to approximate the explosion's potential sources accurately, each influencing the pressure wave dynamics and, in turn, impacting how the blast energy disperses both inside and outside the structure. A key aspect of this research involved modelling not only the internal blast wave effects but also the propagation of overpressures and impulses as they travelled down adjacent streets, interacting with nearby buildings in varying degrees.

To quantify the blast effects on neighbouring structures, the integrated Pressure-Impulse (P-I) curves within Viper::Blast were employed, which enabled the assessment of potential damage thresholds and provided a basis for understanding observed post-event damage (Figure *2*). Particular emphasis was placed on window damage in neighbouring buildings, as windows are often a critical indicator of blast pressure levels and wave effects. By comparing these

simulations against the actual damage observed after the event, we were able to refine our models and enhance the predictive capabilities of Viper::Blast.

The implications of this work are significant, especially for urban planning and the preservation of historic structures. This study provides insights into the damage mechanisms within masonry structures and offers a framework for future blast assessments in similar urban environments. Furthermore, this research highlights the importance of incorporating realistic geometry and explosive source compositions to develop more accurate, context-sensitive blast models. The findings can inform not only emergency response strategies but also policies and guidelines for mitigating damage to buildings in densely populated urban areas.

Figure 1; Post incident - Poznan August 2024

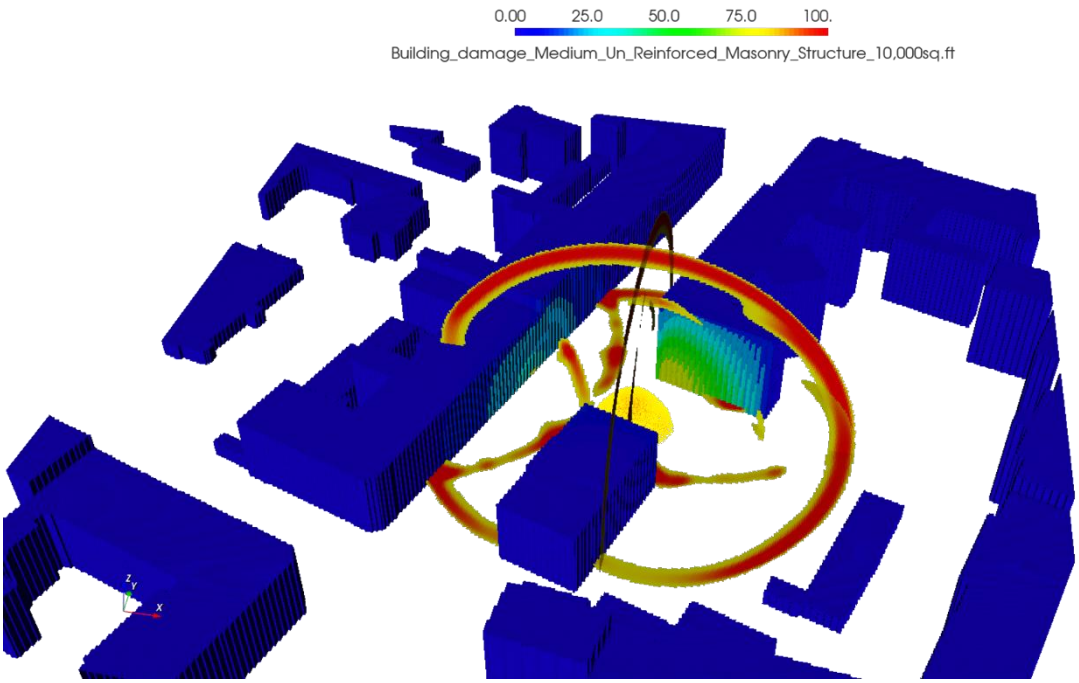

Figure 2; Example Viper::Blast analysis of surrounding Poznan city geometry.

Keywords: cfd, blast, propagation, comparison, hydrogen, urban

Fragmentation Analysis of Unexploded Underwater Ordnance

Piotr Nowak[1], Ross Waddoups[2,4], Dain Farrimond[2,4], Tomasz Gajewski[1], Tommy Lodge[2,4], Genievieve Langdon[2], Andy Tyas[2,4], Piotr Sielicki[1], Elliot Tam[3] and Mark Whittaker[3]

[1]*Country Poznan University of Technology, Poznan, Poland*

[2] *University of Sheffield, Sheffield, United Kingdom*

[3] *Defence Science and Technology Laboratory, Porton Down, United Kingdom*

[4] *Blastech Ltd., Sheffield, United Kingdom*

Unexploded ordnance (UXO) poses a threat to human life, local ecosystems and infrastructure. During the detonation of cased munitions, the rapid energy released from the chemical process is transferred to the surrounding media, resulting in fragmentation. This can cause damage in addition to that resulting from an air blast. National and international publications concerning explosive safety [1,2] recommend simple mathematical formulae and tables to estimate the physical effect of munition detonation in open-air scenarios.

Fragments are explosively driven projectiles resulting from the failure of casing materials, usually of irregular mass and shape [2]. The hazard level associated with fragmenting casings is governed by the probability of interaction at a given distance and the kinetic energy of the projectile at the target. The blast and fragmentation parameters on land for commonly used explosive ordnance are described by manufacturers [3], military regulations and procedures [1], explosive safety standards [2], and scientific research [4]. During land ordnance disposal, these two hazard mechanisms are considered to ensure safe working distances of operatives and infrastructure. The danger area is estimated using the total mass of explosive (or its TNT equivalent) and important safety factors.

Underwater ordnance clearance estimates usually omit or ignore the fragmentation risk. This may be justified when clearing ordnance in deep seas, as fragmentation can only propagate so far within water. However, most disposal operations occur in shallow waters (Fig.1), close to shorelines or near critical maritime infrastructure, meaning a higher likelihood of fragmentation damage. In some situations, an underwater mine or bomb must be lifted from the bottom and transported to a disposal site, with the maximum fragmentation distance on land is used as the evacuation distance.

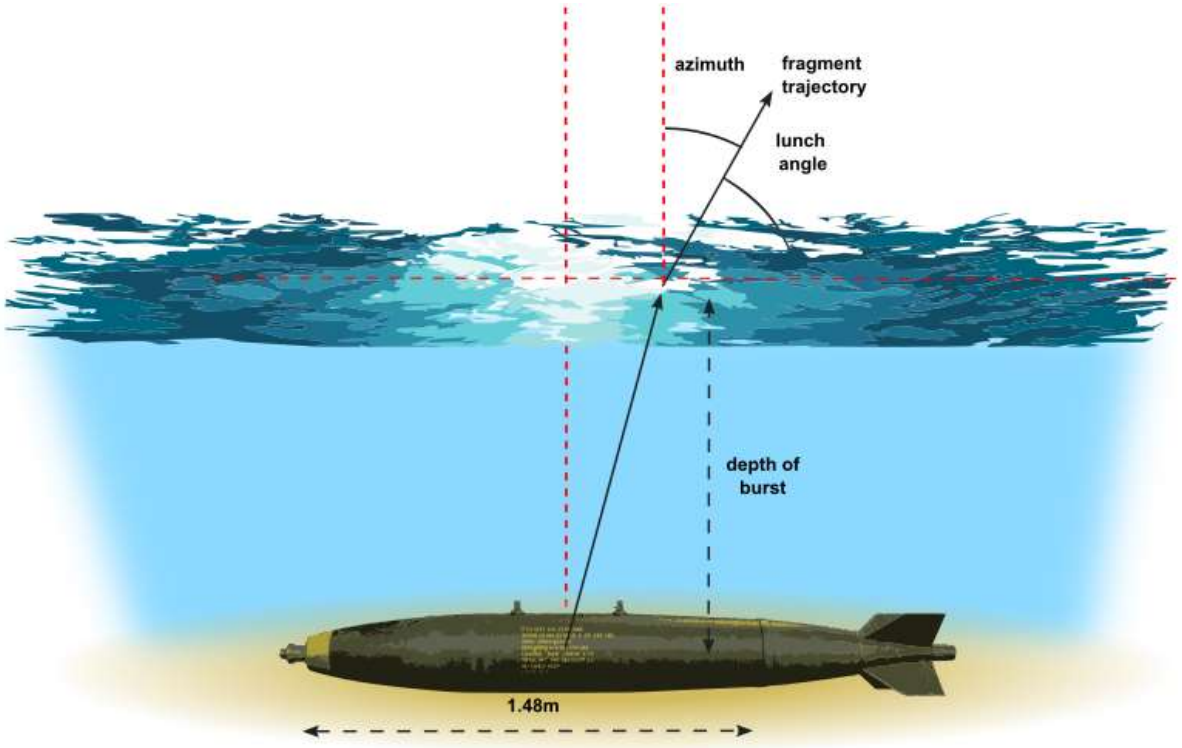

Fig. 1. Explosive ordnance at shallow waters.

For naval munition located below the water surface, the risk of fragmentation cannot be ignored, nevertheless there is no common method in military procedures for calculating safe distance as a function of depth.

This paper presents a series of experimental trials which compare both air and underwater cased explosive charges at various depths to investigate the characteristics and distribution of the associated fragmentation. Three types of steel casing were used to evaluate the fragmentation phenomena. The primary case design was a steel machined liner intended to replicate a typical munition body. The number and size of natural fragments vary from test to test due to the random division of the casing material. To obtain the behaviour of idealised fragmentation, two sizes of spherical steel orbs were selected and enclosed in a 3D-printed jacket. Both high-speed videography (Fig.2), and witness panels have been utilized to capture in-flight velocities and fragment distribution.

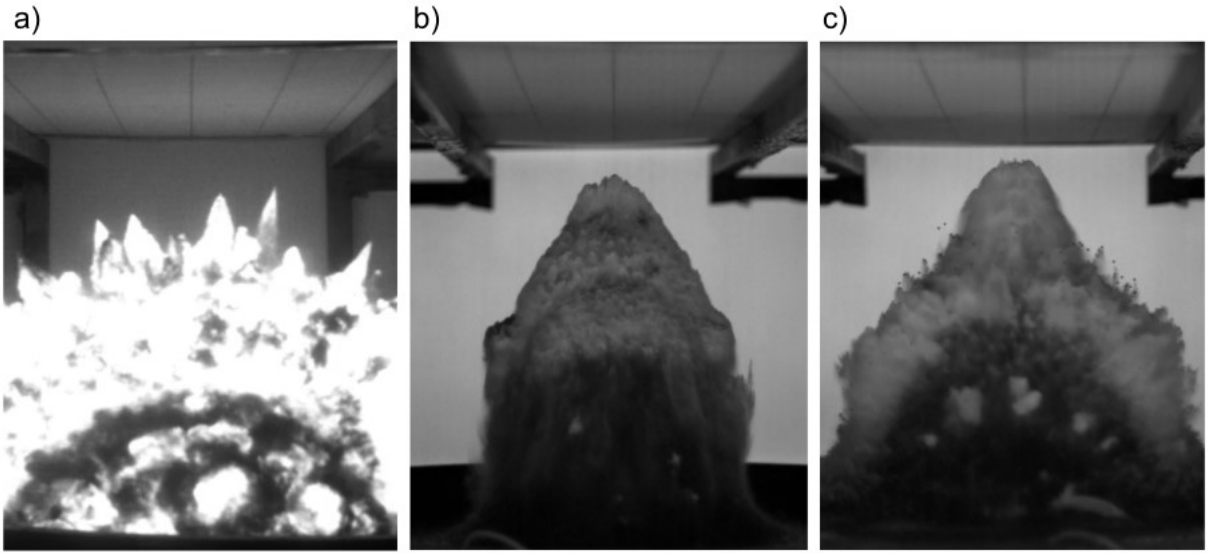

Fig. 2. High speed video (HSV) recording showing a range casing and depth combinations for illustrative purposes a) 1.7 mm balls in air, b) machined liner at 45 mm, c) 2.6 mm balls at 95 mm.

Based on small explosive tests the fragments parameters and the damping properties of water were demonstrated by direct comparisons between explosions in air and within varying depths of water. Despite limitations related to charge mass and case design, the presented results show a clear relationship between detonation depth and the fragmentation behaviour of the steel shell. Applying appropriate hazard mitigation measures during UXO removal, e.g. minimal towing depth, will increase safety during military operation.

Keywords: ordnance disposal, underwater explosion, fragmentation, blast.

[1]. Army TM 5-1300, (1990). Structures to Resist the Effects of Accidental Explosions, Départements of the Army, the Navy and the Air Force.

[2]. United Nations Office for Disarmament Affairs (UNODA), (2021). International Ammunition Technical Guidelines 01.80.

[3]. Australian Munitions, (2016). Hand grenades - Designed for operational effectiveness.

[4]. Absil, L.H., Kodde, H.H., & Weerheijm, J. (1996). Evaluation of Safety Distances for UXO Disposal Operations.

Deep Learning-based Framework to Predict Spatio-temporal Reflected Pressure on Structural Surfaces

Chamodi Widanage[1], Kasun Wijesooriya[1], Chi-King Lee[1] and Damith Mohotti[1]

[1]*School of Engineering and Technology, The University of New South Wales, Canberra, ACT, 2600, Australia*

In engineering practice, the prediction of blast loads in explosion events is typically conducted with numerical simulations. While these methods offer high accuracy and reliability, their significant computational demands, especially when modelling complex blast scenarios, can limit efficiency and productivity. Hence, there has been growing interest in developing fast-running surrogate models for blast analysis to overcome this challenge. Since 2006, deep learning (DL) has emerged as a promising technology, providing an effective alternative to traditional numerical simulations for blast analysis by significantly reducing computational time while preserving accuracy. Most existing research focuses on the spatial distribution of peak blast load values. Yet, blast-resistant design requires a full understanding of blast dynamics, including both spatial and temporal blast load variations. However, research in this area is limited, with no published studies focused on developing a generalised predictive model for the spatio-temporal reflected pressures on rigid structures induced by high-explosive blasts. To address this research gap, a novel DL framework was developed to predict spatio-temporal reflected pressures on rigid structures. The framework utilises multiple artificial neural networks (ANNs) working collaboratively to predict reflected pressure time histories at a given location. This staged approach streamlines the prediction process, reducing both training and computation times. The training datasets for the ANNs were generated using results from validated numerical models. Each ANN in the framework was evaluated individually based on statistical error metrics to ensure robust performance. To assess the predictability of the DL-based framework, a comparative analysis was conducted against numerical model predictions. This included predicting reflected pressure time histories for six random blast events. Five key parameters related to the reflected pressure time histories were then used to benchmark the DL framework's accuracy against the numerical model outputs. Additionally, the similarity between the DL framework's predictions and numerical model results was quantified using the cross-correlation coefficient, with results showing a 68–91% similarity across various blast

events. The computational time of the DL framework is 1% of that of the numerical model which highlights computational efficiency. These findings demonstrate the capability of the developed DL-based framework to deliver both time-efficient and accurate predictions, marking a promising advancement in blast load analysis.

Keywords: Reflected pressure, Blast load, Structural surface, Time history, Artificial neural networks, Computational time.

High-Strain Rate Characterization of Loblolly Pine Mechanical Properties under Extreme Temperature and Moisture Conditions

Ryan Holtzscher [1], James Davidson [1], David Roueche [1], and Kadir Sener [1]

[1]*Civil and Environmental Engineering, Auburn University, Auburn, Alabama, USA*

The utilization of wood as a viable construction material for protective structures, particularly those used in defense industry facilities, has gained significant traction in recent years. Protective structural designs intended for these applications demand materials capable of enduring high-strain rate loads that simulate blast-loading scenarios. These loads can be compounded by extreme environmental conditions, including severe temperature and moisture variations, which are atypical for commercial applications. Consequently, protective designs must incorporate accurate material-level models of the mechanical properties, validated through experimental testing under such unique conditions. To address these needs, this research undertakes a comprehensive experimental investigation into the high-strain rate mechanical behavior of Loblolly Pine, the most abundant subspecies of the Southern Pine group, across a wide range of temperature and moisture scenarios. The overarching objective of this study is to establish experimentally validated material models that are needed for advanced engineering applications.

The testing program was executed using a specialized high-rate universal testing machine (UTM), designed to achieve crosshead speeds of up to 20 m/s, coupled with an environmental chamber for precise condition control, as shown in Figure 1. Specimens were tested using special fixtures as shown in Figure 1, across a wide range of strain rates, spanning from 1 ε/s to 1000 ε/s, under extreme temperatures (ranging from -70°F to 150°F) and varying moisture contents (from 3% to the fiber saturation point). Evaluations were conducted for multiple loading scenarios, including compression and tension (both parallel and perpendicular to the grain), bending, shear, and impact loading, all in adherence to ASTM standards. Data collection was enhanced using advanced force and displacement measurement systems as well as digital image correlation (DIC) techniques, ensuring a high degree of accuracy in capturing the mechanical behavior.

Quasi-static baseline tests, as a tension test illustrated in Figure 2, established fundamental mechanical property data, which were consistent with findings from prior studies. These tests

indicated a notable decrease in mechanical properties at higher moisture levels, while lower moisture content was correlated with enhanced mechanical performance. Temperature variations, particularly those at elevated levels, showed relatively marginal effects on the material properties. In contrast, high-strain rate testing revealed substantial deviations in stress-strain responses, dynamic increase factors, and failure mechanisms, emphasizing the critical influence of strain rate on material performance.

The experimental matrix was designed to include five distinct environmental conditioning states, combining three temperature settings (30°F, 70°F, and 150°F) with three moisture levels (4%, 12%, and 25%). This systematic approach ensured the isolation of specific environmental effects on key mechanical properties, including stiffness, strength, and ductility. Findings from this study demonstrate the impact of environmental factors on the high-strain rate performance of wood, offering critical insights necessary for developing accurate constitutive models tailored for protective design applications.

This investigation contributes significantly to the understanding of how environmental conditions interplay with high-strain rate mechanical behavior of wood, thereby reinforcing its potential as a sustainable and resilient material for protective structural applications.

Figure 1 – High-rate UTM Compression Testing

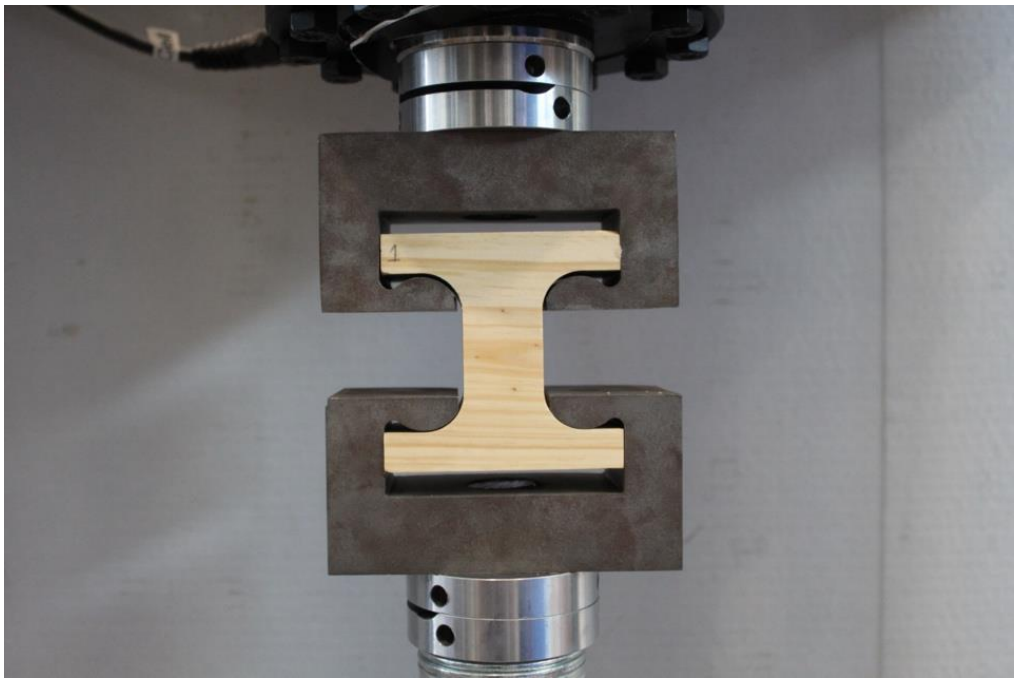

Figure 2 – Quasi-Static Tension Testing of Wood Samples Perpendicular to Grain

Numerical investigations on the dynamic response of near-field blast-loaded steel plates

Jiannan Ye[1], Weifang Xiao[1] and Xianzhong Zhao[1]

[1] *College of Civil Engineering, Tongji University, Shanghai, China*

Abstract: Terrorist activities and accidental explosions have occurred frequently in the past, resulting in structural damage and casualties and posing serious threats to the safety of civil buildings and critical infrastructures. To ensure the safety of buildings and the people's lives and property, the blast loads on the structure and the pertinent structural response should be better understood. The response of steel structures subjected to the blast loading has long been a main concern in the blast-resistant design. Steel plates are widely used in various structures, e.g. buildings, ships, bridges, and vehicles. This study investigated numerically the dynamic response of steel plates subjected to near-field explosions. Two modelling approaches were utilised, i.e. fluid-structure interaction (FSI) models and two-stage uncoupled models. For two-stage uncoupled models, a multi-material Arbitrary-Lagrangian-Eulerian (MM-ALE) numerical simulation is carried out in the first stage to obtain the maximum impulses distributed over the steel plate. By converting the maximum impulses into the initial velocities at the nodes of the plate. A Lagrangian model is established in the second stage to predict the dynamic response of steel plates, which are subjected to the near-field explosions. The primary objective is to determine the applicable range of the two-stage uncoupled method. The FSI models are first validated against the experimental data, confirming their predictive accuracy. After that, the validated FSI models are employed as the baseline models to study the effect of several parameters, e.g. plate shape and dimensions, on the applicable range of the two-stage uncoupled models. It was indicated that the two-stage uncoupled models are invalid for plates with small lengths or diameters. Furthermore, circular plates possess a broader applicable range than square plates. It was demonstrated that the two-stage uncoupled models can be used for the rapid prediction of the dynamic response of steel plates subjected to near-field explosions. The findings enable a quick evaluation of the blast resistance of steel structures while maintaining the balance between the accuracy and the computational efficiency.

Keywords: Near-field explosion; Fluid-structure interaction (FSI); Two-stage uncoupled models; Dynamic response; Blast-loaded plate.

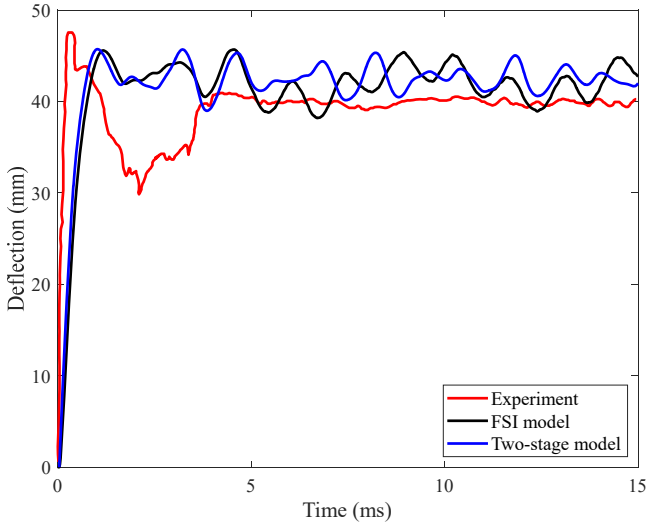

Fig. 1. Numerical and experiment results of deflection-time history at the center of the steel plate

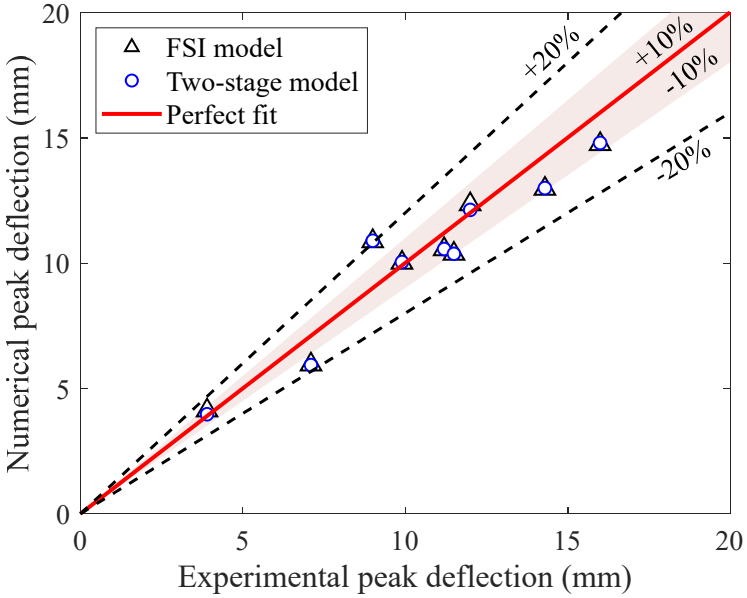

Fig. 2. Numerical and experimental values of peak deflections at the center of the steel plate

Influence of Layering on the Blast Performance of Laminated Glass

Sa-aadat Parker, Steeve Chung Kim Yuen and Gerald Nurick

Blast Impact and Survivability Research Unit, Department of Mechanical Engineering, University of Cape Town, Rondebosch, South Africa

A key trend in architecture is utilising glass in building design for aesthetic, sustainability and energy efficiency reasons. The use of double-glazing, consisting of two glass panes separated by a gap filled with air or other gas, has become the new standard in many European countries. The growing use of glass has driven the need for stronger and more durable types of glass to enhance safety and resilience against impact or any accidental or intentional explosion. The glass shards from blast loading can cause many injuries, as evident in Oklahoma City [1] and Beirut [2]. Laminated glass, consisting of two or more layers of glass bonded with a plastic interlayer that is typically made of polyvinyl butyral (PVB), is often used to mitigate the risk of flying shards. The interlayer retains the glass upon impact, preventing it from shattering into sharp fragments. Instead, the glass may crack but remains largely intact, providing enhanced security in buildings and reducing the risk of injury.

Experimental blast testing of glass has usually been performed in open air with solid explosives [3-6]. Failure at the glass pane attachment to the frame is an important consideration, and different materials have been used at the frame-glass interface, such as rubber [3], structural silicon [4] or other polymer strips [5], to prevent glass contact with a metal frame. Parametric studies have also been performed to investigate size effects (length, width and thickness) that influence laminated glass under blast loading [6, 7]

Most of these studies have, however, focused on the response of a single pane of glass to blast loading. In this paper, the results of an experimental study on the response of multi-layered glass pane, specifically related to double-glazing configurations, are presented. This study examines how different configurations of multi-layered glass panes (varying air gap) respond to “uniform” blast loading generated by the detonation of 4 g of PE4 at different stand-off distances (325 mm, 650 mm, and 1300 mm) within a square blast tube. The laminated glass panes comprised two 3 mm glass layers joined by a 0.76 mm PVB interlayer and had an area exposed to the blast of 300 mm by 300 mm with a 15 mm edge clamped inside a polymer frame.

The clamped multi-layered glass panes were mounted onto a suspended blast tube that acted as a ballistic pendulum to determine the impulse transferred to the glass panes.

Typical fracture behaviour of the glass panes (front-facing and back-facing panes) subjected to a charge detonated at a stand-off distance of 650 mm is shown in Figure 1(a) and (b), respectively. In this example, there was no air gap between the two glass panes. The damage percentages were determined using image analysis and were higher for the back plate at 66% compared to the blast-facing front plate at 55%.

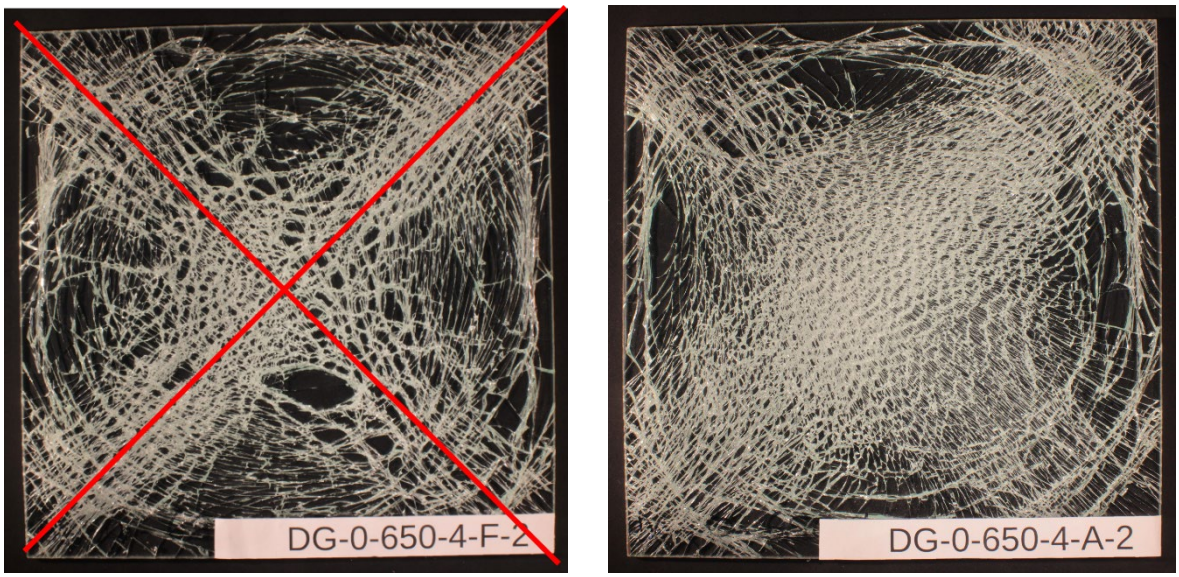

(a) Front facing pane (b) Back Pane

Figure 1: Photograph showing Damage of laminated glass pane

Keywords: double glazing, laminated glass, uniform blast load

References[1] Norville, H. S., Harvill, N., Conrath, E. J., Shariat, S., & Mallonee, S. (1999). Glass-related injuries in Oklahoma City bombing. Journal of Performance of Constructed Facilities, 13(2), 50–56. https://doi.org/10.1061/(asce)0887-3828(1999)13:2(50)

[2] Abu-Faraj, Z. O. (2020). Shattered glass is allegedly blamable for most of the victims of Beirut's blast. LinkedIn Pulse. August, 26.

[3] Chen, S., Zhu, C.-G., Li, G.-Q., & Lu, Y. (2016). Blast test and numerical simulation of point-supported glazing. Advances in Structural Engineering, 19(12), 1841–1854. https://doi.org/10.1177/1369433216649387

[4] Hooper, P. A., Sukhram, R. A., Blackman, B. R., & Dear, J. P. (2012). On the blast resistance of laminated glass. International Journal of Solids and Structures, 49, 899–918. https://doi.org/10.1016/j.ijsolstr.2011.12.008

[5] Zhang, X., Hao, H., & Wang, Z. (2015). Experimental study of laminated glass window responses under impulsive and blast loading. International Journal of Impact Engineering, 78, 1–19. https://doi.org/10.1016/j.ijimpeng.2014.11.020

[6] El-Sisi, A., Elbelbisi, A., Elemam, H., Elkilani, A., Newberry, M., & Salim, H. (2024). Effect of glass type and thickness on the static and blast response of LG panels. Journal of Building Engineering, 86, 108870. https://doi.org/https://doi.org/10.1016/j.jobe.2024.108870

[7] Wang, X., Zhong, B., Tang, J., Gao, C., & Li, M. (2023). Study on the Influence of Window Glass Size on Blast-Resistant Performance. Sustainability, 15(12). https://doi.org/10.3390/su15129325

Structural response and failure modes of armor steel plates under dynamic underwater explosions

Prince Jeya Lal Lazar[1], Vishnu Vijay Kumar[2], Khaled Shahin[2], Anupoju Rajeev[3*]

[1]*Department of Mechanical Engineering, Rajalakshmi Institute of Technology, Chennai, India*

[2]*Structural Engineering, Division of Engineering, New York University Abu Dhabi (NYUAD), Abu Dhabi, United Arab Emirates*

[3]*Department of Civil and Environmental Engineering, National University of Singapore (NUS), Singapore*

*Corresponding author: dranupojurajeev@gmail.com

This study investigates the structural resilience and failure modes of various armor-grade steel plates when subjected to underwater explosions. Using a validated computational fluid-structure interaction (FSI) approach, we examined the blast resistance of five steel grades: AL6XN, SS304, AISI 4340, Mild Steel, and Q235. The analysis focused on steel plates measuring 0.250 x 0.3 x 0.002 meters, exposed to air-backed underwater explosions with shock factors ranging from 0.42 to 0.73 at a standoff distance of 0.150 meters. The simulation methodology was employed to model the steel plates as elastic-plastic materials defined by Johnson-Cook (JC) parameters. An incident wave interaction module was utilized to simulate the fluid-structure interaction. Through these simulations, we evaluated key dynamic responses, including midpoint deflection and equivalent plastic strain under explosive stress. The results revealed diverse failure modes across the tested materials, ranging from plastic midpoint deflection to partial and complete tensile tearing, with some plates experiencing midpoint rupture. Remarkably, AISI 4340 steel emerged as the superior performer, demonstrating a 35.5% improvement in blast mitigation capability compared to other armor-grade steels tested. These findings establish AISI 4340 as a particularly suitable material for protective structures in underwater environments. The comprehensive analysis provides valuable insights for material selection in applications where underwater blast resistance is crucial, serving as a practical guide for designing protective structures in marine environments.

Keywords: Armor-grade steel, Blast mitigation, Fluid-structure interaction, Naval protection systems, Numerical simulation, Underwater explosion

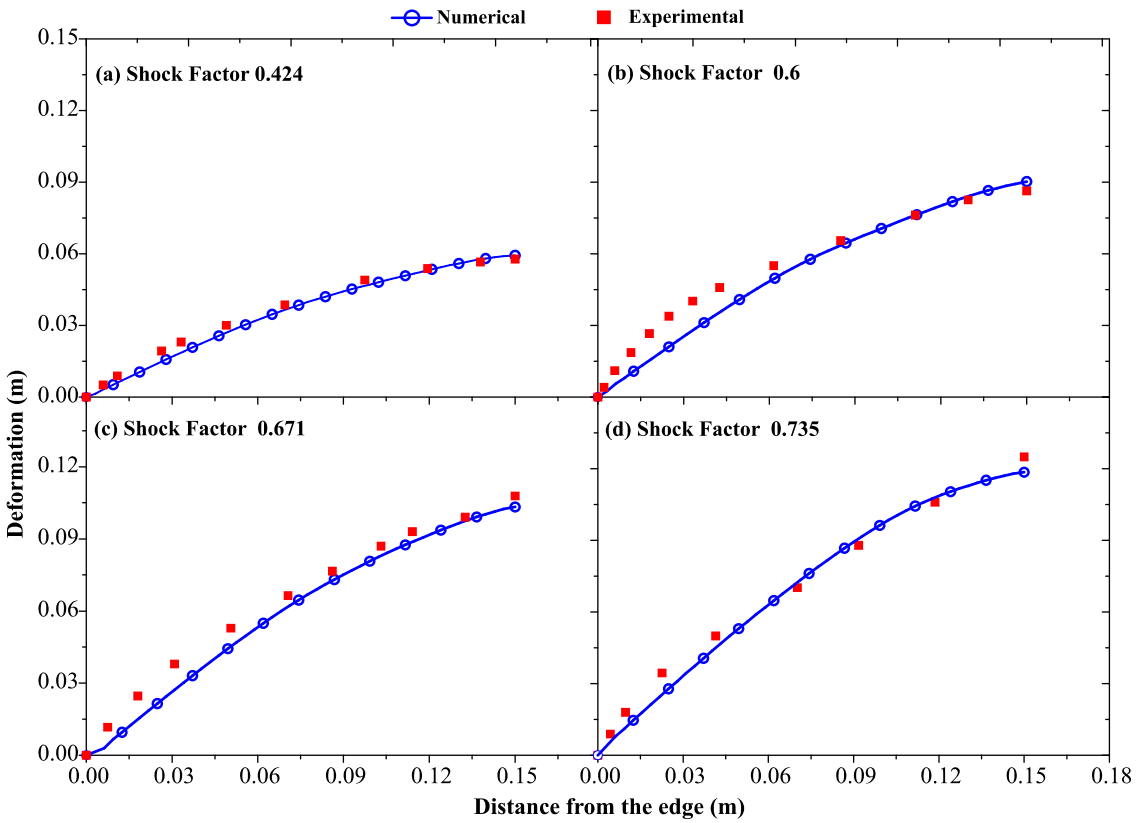

Figure 1. Validation of the present FSI model with experimental data [1] for varying SFs

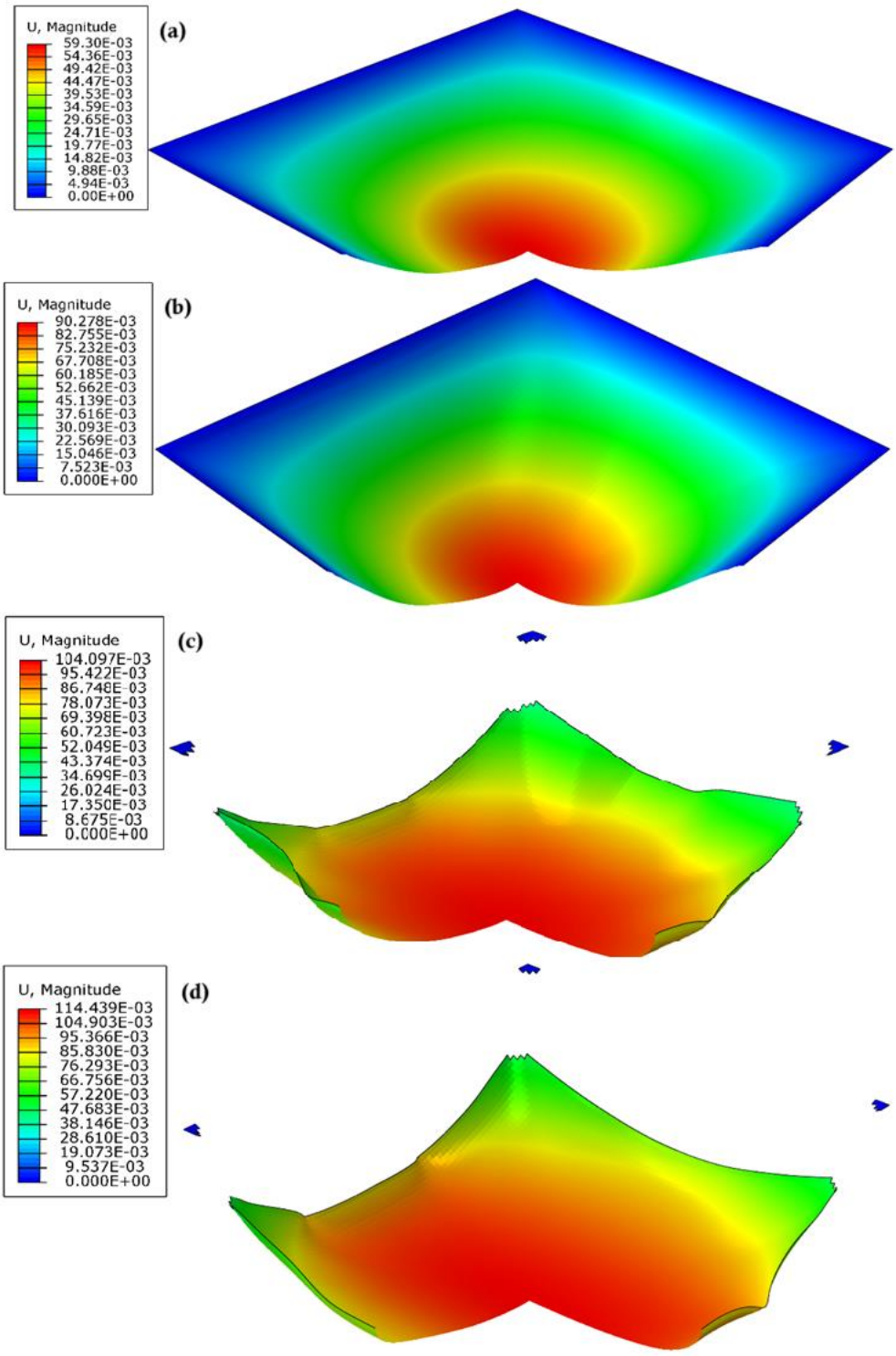

Figure 2. Deformation contours of mild steel plates subjected to underwater explosions

(a) SF 0.42 (b) SF 0.6 (c) SF 0.67 (d) SF 0.73

References

[1] K. Ramajeyathilagam, C.P. Vendhan, Deformation and rupture of thin rectangular plates subjected to underwater shock, International Journal of Impact Engineering, Volume 30, 2004, Pages 699-719, https://doi.org/10.1016/j.ijimpeng.2003.01.001

RC beams: full-scale tests and numerical modelling

Ricardo Castedo[1], Ángel Prado[2], Alejandro Alañón[2], Anastasio P. Santos[1], Lina M. López[1], María Chiquito[1]

[1]*Universidad Politécnica de Madrid, Madrid, Spain*

[2]*Escuela Politécnica Superior de Ávila – Universidad de Salamanca. Spain.*

The rising threat of terrorism and accidental explosions has increased focus on the blast resistance of buildings and structural elements. Reinforced concrete, valued for its affordability, durability, and strength, is central to these efforts, making it vital to understand its response to explosive loads to ensure structural and occupant safety. This paper presents a series of tests of concrete beams with a size equal to 4 × 0.25 × 0.20 m (length × width × height) against near blast. Three tests were conducted with 2 kg (Eq. TNT) at 1 m and one test with 4 kg at 1 m. This makes a total of four trials, all of which were instrumented with pressure and acceleration sensors. The numerical model has been carried out with LS-DYNA, using various combinations for the description of the blast load and for the concrete describing the behavior of the beam. For the explosive load, CONWEP has been used implicitly and SPH (Smooth Particle Hydrodynamic) implicitly. The implicit technique incorporates the well-known CONWEP (through the Load Blast Enhanced - LBE card) which applies empirical pressure-time curves (UFC 3-340-02) to a given surface. With the SPH it is necessary to know the equation of state of the explosive and some of its properties (TNT properties), and the result depends on the number of SPH elements used, so simulations have been carried out with 800,000; 1,600,000; and 3,200,000 particles. As for the concrete, three different models have been used: Continuous Surface Cap Model (CSCM), Riedel-Hiermaier-Thoma (RHT), and the Karagozian & Case model (K&C) with three meshing for the solid elements 10, 15 and 20 mm. Regarding the measured pressure, the LBE model shows very good results with errors of less than 10%, however, with the SPH model these values cannot be measured. But if the detonation pressure values are compared with the pressure values at the CJ point, with 800,000 particles the difference is 20%, with 1,600,000 the difference decreases to 17% and with 3,200,000 the difference decreases to 14%. If accelerations are compared, the simulations agree well with the experimental values. In some cases (10 mm mesh; models with RHT) there are discrepancies, with higher peak acceleration values compared to experimental records. This happens regardless of the model used for the description of the explosive (LBE or SPH). When the mesh

becomes thicker (20 mm), the acceleration in all models and SPH meshes tend to reduce coinciding with the ranges measured in the tests. From this work, the importance of the (complex) relationship between the SPH particle number and the mesh size of the solid elements is evident. Generally, a decrease in the number of SPH produces higher accelerations, as does a reduction in the size of the solid elements.

Keywords: LS-DYNA, concrete models, beams, field tests.

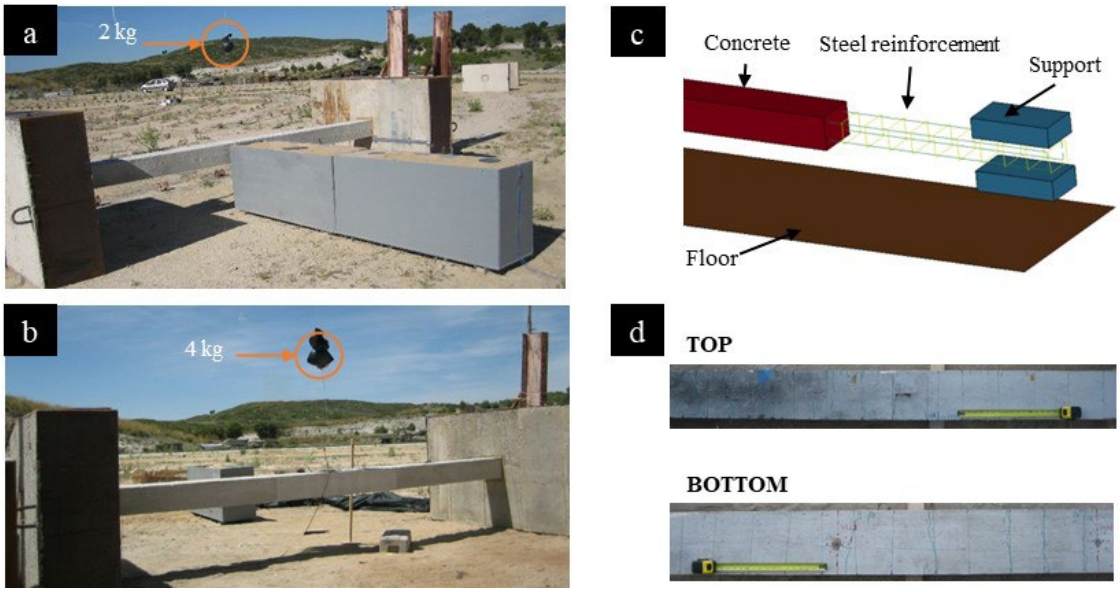

Figure 1. a) Tests with 2 TNT Eq. at 1 m distance. b) Test with 4 TNT Eq. at 1 m distance. c) Details of the numerical model. d) Results of the test b) after blast.

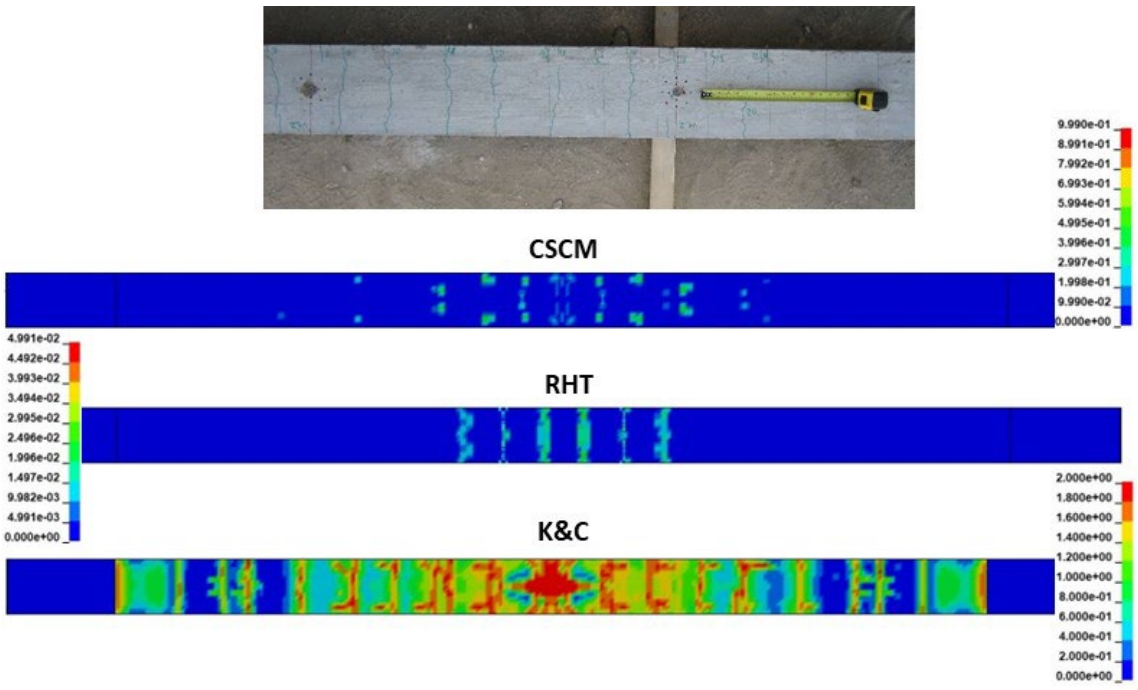

Figure 2. Field test and numerical results (LBE) of the 2 kg at 1 m distance test.

Numerical investigations on the effects of detonation products on blast load

Pu Huo[1,2], Jun Yu[1,2], Banruo Li[1,2]

[1] *Engineering Research Center of Safety and Protection of Explosion & Impact of Ministry of Education, Southeast University, Nanjing 211189, China*

[2] *School of Civil Engineering, Southeast University, Nanjing 211189, China*

Abstract: Near-field blast loads are composed of the action of both shock waves and detonation products. However, obtaining experimental data in the near field is typically challenging. To investigate the blast load distribution characteristics in the near field and the influence range of detonation products, a finite element (FE) model was developed using the open source software blastFoam. In the numerical model, the 3rd Birch-Murnaghan and Jones-Wilkins-Lee (JWL) equations of states were used to define the unreacted TNT and detonation products, while the air was defined using the ideal gas equation of state. The FE model was validated through comparing simulation results with experimental data obtained from a field test, which was conducted on a two-story RC frame structure. During the testing, a 2 kg cylindrical TNT charge was placed at the center of the second-floor ceiling. Validation included a comparison of the shock wave front obtained from the FE model with the one recorded by a high-speed camera. The time histories of reflected overpressure at key measurement points were also compared to confirm the validity and accuracy of the FE model. The analysis further examined the distribution characteristics of overpressure fields and detonation products in free air. Results revealed that for a cylindrical TNT charge, detonation products primarily propagate along the diameter and longitudinal directions, with maximum horizontal and vertical influence ranges reaching approximately 20 times the charge radius and 40 times the charge height, respectively. The detonation products further affect the time histories of overpressure in the near field, leading to two distinct overpressure peaks. Within a range of four times the charge radius, the effects of detonation products cause the first overpressure peak to occur prior to the arrival of the shock wave. In the range between four and fifteen times the charge radius, detonation products contribute to a second overpressure peak. As the distance increases, the overpressure peak generated by detonation products significantly decreases. A pronounced double-peak phenomenon of the overpressure time histories was observed within eight times the charge radius. Moreover, the impulse generated by detonation products within this range plays a critical role in the calculation of blast loads. The numerical results demonstrated the necessity

of considering both shock waves and detonation products in the calculation of blast loads under near-field explosions. Additionally, the study recommends that the influence range of detonation products be considered as extending up to 20 times the radius of the cylindrical TNT charge. This modeling method offers a robust framework for studying near-field explosion effects.

Keywords: Near-field explosion, blast load, detonation products, shock waves

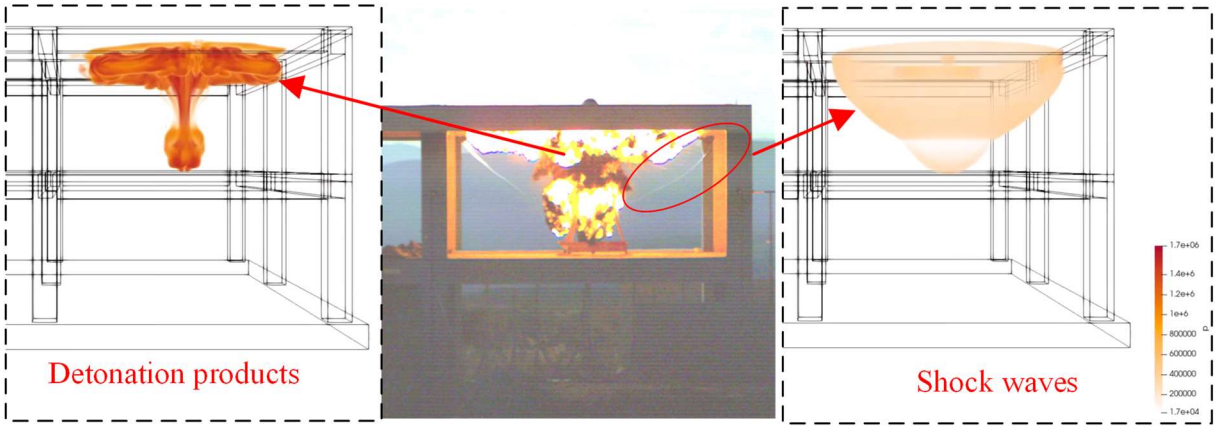

Figure 1. Comparison of the shock waves between experimental result and numerical simulation

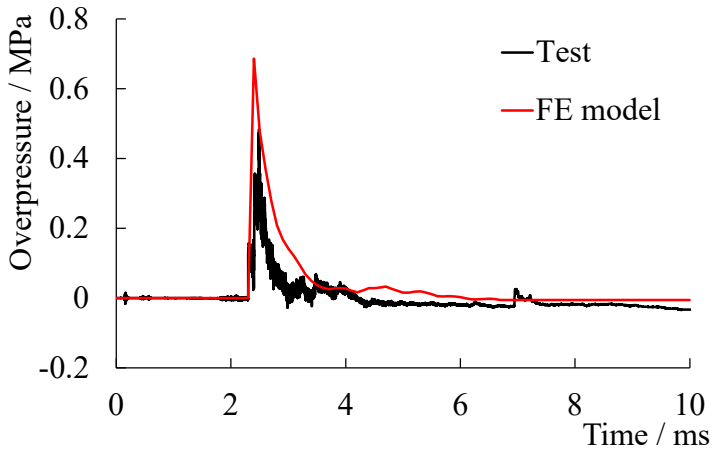

Figure 2. Comparison of the reflected overpressure time histories between experimental results and numerical simulation

Impact performance of RC beam-column joints with seismic-induced damage

Jixian Li[1], Hongyu Chen[1], Huawei Li[1, *], Wensu Chen[2], Hong Hao[1, 2]

[1] *Earthquake Engineering Research & Test Center, Guangzhou University, Guangzhou, China*

[2] *Centre for Infrastructural Monitoring and Protection, School of Civil and Mechanical Engineering, Curtin University, Perth, Australia*

*Corresponding authors: huawei.li@gzhu.edu.cn (Huawei Li)

Reinforced concrete (RC) frame structures are often exposed to extreme events such as earthquake, blast, and fire over their service life. Among their critical components, beam-column joints play a vital role in maintaining the structural integrity and safety of RC frames. The failure of these joints can lead to the progressive collapse of the entire structure, posing severe risks to its stability. Therefore, ensuring the safety of RC beam-column joints under various hazard scenarios is crucial to mitigating the potential for progressive collapse. In addition to withstanding the substantial internal forces generated during seismic events, RC joints are also subjected to impact loads, such as those caused by falling debris during earthquakes. Consequently, RC joints with seismic-induced damage often experience subsequent impact loads, as illustrated in Figure 1. Although previous studies have extensively investigated the seismic and impact resistance of RC joints independently, relatively little attention has been devoted to understanding their impact performance when pre-damaged by seismic events. This study focused on the behavior of exterior beam-column joints in RC frames under combined seismic and impact loading conditions. Experimental tests, including cyclic loading and drop-weight impact tests, were conducted to investigate the damage evolution mechanisms and mechanical behavior of RC joints with varying levels of initial seismic-induced damage. Failure modes and dynamic responses were analyzed to assess the influence of initial seismic-induced damage on the impact resistance of RC beam-column joints. The results revealed that for RC joints with slight to moderate seismic-induced damage, new concrete cracks formed in the beam ends near the joint area. In contrast, the RC joint with severe seismic damage subjected to impact loading exhibited complete concrete failure in the joint region, as shown in Figure 2. In the severely damaged RC joint, the impact energy was primarily dissipated through longitudinal reinforcement. As the level of initial seismic-induced damage increased, the RC joints experienced lower peak impact forces, longer impact durations, and greater deformations. Furthermore, the cumulative displacement and damage caused by

combined seismic and impact loading were significantly larger than those induced by seismic loading alone. Neglecting the complex interactions between seismic and impact loads on RC joints could lead to an underestimation of their vulnerability under multi-hazard scenarios.

Keywords: beam-column joint, seismic-induced damage, impact loads, damage evolution, dynamic response

Figure 1. Seismic-induced damage of beam-column joints

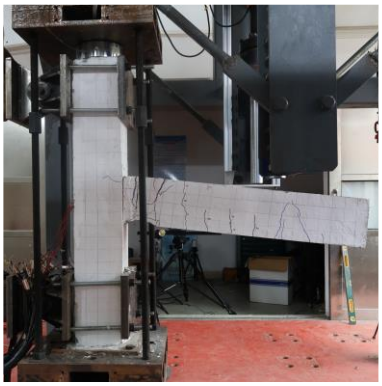

(a) RC joint with slight seismic-induced damage

(b) RC joint with moderate seismic-induced damage

(c) RC joint with severe seismic-induced damage

Figure 2. Impact damage mode of RC joint with various seismic-induced damage

Experimental and Numerical Investigation of Aluminum/Polyethylene Sandwich Structures under Varied Loading Rates and Temperatures for Protective Applications

Amine Bendarma [1,2], Tomasz Jankowiak [2], Alexis Rusinek [3], Christophe Czarnota [3] ,Tomasz Lodygowski [2], Richard Bernier [3]

[1]*Arts et Métiers Campus of Rabat*

Technopolis, Rocade de Rabat-Salé, 11100 Sala Al Jadida, Morocco

bendarma.amine@artsetmetiers.ma

[2] *Poznan University of Technology, Institute of Structural Analysis, Piotrowo 5, 60-965, Poznan, Poland*

[3] *University of Lorraine, Laboratory of Microstructure Studies and Mechanics of Materials LEM3, 7 Rue Félix Savart, 57070 Metz, France*

Abstract: Aluminum/polymer/aluminum sandwich composites, such as Alucobond, are increasingly favored in engineering applications requiring high strength-to-weight ratios and thermal insulation. This research examines the mechanical response of these structures under a range of loading rates and temperatures, providing insights essential for applications subject to dynamic environments. The study includes experimental analyses under dynamic and quasi-static compression and tensile loading, complemented by perforation tests. To capture strain rate and temperature dependencies, quasi-static tests were conducted across multiple strain rates, while dynamic tests spanned higher strain rates (up to 10^{-5} s^{-1}) and temperatures from room temperature up to 100°C. The low-density polyethylene (LDPE) core was characterized to establish a constitutive model, emphasizing the core's impact on the overall response of the composite. Furthermore, finite element (FE) simulations using ABAQUS offered additional insights into the behavior of impacted structures, considering variables such as projectile geometry, impact velocity, and thermomechanical properties of the composite. This comprehensive approach highlights the interplay of material composition and loading conditions in optimizing aluminum/polymer sandwich structures for protective applications.

Keywords: aluminum/Polyethylene Sandwich Structures, dynamic and Quasi-static Loading, constitutive Modeling.

The role of metamaterials in protecting ship equipment from underwater explosion shock

Jacopo Bardiani [1], Giada Kyaw Oo D'Amore [2], Giovanni Marchesi [1], Marco Biot [2], Claudio Sbarufatti [1] and Andrea Manes [1]

[1]*Polytechnic of Milan, Department of Mechanical Engineering, Milano, Italy*
[2]*University of Trieste, Department of Engineering and Architecture, Trieste, Italy*

Military ships subjected to underwater explosions (UNDEX) face significant challenges beyond the immediate structural damage caused by the primary shock wave. While ruptures or tears in the ship's compartments can often be managed by sealing off the affected areas, the shock wave poses a far more pervasive threat to onboard equipment and instrumentation [1], even at considerable distances from the explosion's point of impact. The energy from the shock wave propagates through the ship's hull, creating vibrations that can reverberate throughout the entire structure, severely affecting the functionality of critical systems, such as navigation controls, power supplies, and communication networks. Disruptions to these systems, especially during combat operations, can lead to significant operational risks, including losing control or communication failures in critical moments.

To address this, various shock protection devices, such as shock mounts, isolators, and dampers, are currently employed to shield equipment from the damaging effects of underwater explosions. These devices aim to absorb or redirect the shock wave's energy, thereby reducing the vibrations that reach sensitive systems. However, despite the availability of these technologies, they often need to be improved, particularly when exposed to more intense or repeated explosion events. The limitations of traditional shock protection measures highlight the need for enhanced strategies to safeguard onboard systems more effectively.

One emerging and promising approach that has yet to be extensively explored in the literature is the application of metamaterials in vibration confinement for UNDEX scenarios. Metamaterials, engineered to have properties not found in naturally occurring materials, offer the unique ability to control the propagation of mechanical waves, including shock-induced vibrations [2]. Through their carefully designed internal structures, metamaterials can be

tailored to confine vibrations to specific regions or redirect them, thereby reducing the impact on critical equipment. Metamaterials can be used to decouple the equipment from the ship structures or inserted in the mounting structures to dissipate vibrations. For the last purpose, Acoustic Black Holes (ABH) can represent a valid and innovative solution. Examples of decoupling metamaterials and ABH geometries are provided in Figure 1. This capability offers a new frontier for improving the resilience of military vessels, as metamaterials can be customized to address specific frequencies or intensities of shock waves, providing adaptable protection that conventional materials cannot achieve.

This study explores the potential of metamaterials in vibration confinement to mitigate the detrimental effects of underwater shock waves on naval vessels. By focusing on a real-world application, using a patrol ship model as a case study (Figure 2), the dynamic response of the ship structures subjected to UNDEX are evaluated and the vibrations are calculated in prescribed points where equipment should be mounted. A frequency response analysis is then used to evaluate the effectiveness of a designed metamaterial configuration in comparison with traditional mounting and protective systems. The findings could pave the way for developing new protective solutions that offer superior performance compared to traditional methods, contributing to more robust and resilient naval platforms capable of withstanding the growing threats of UNDEX.

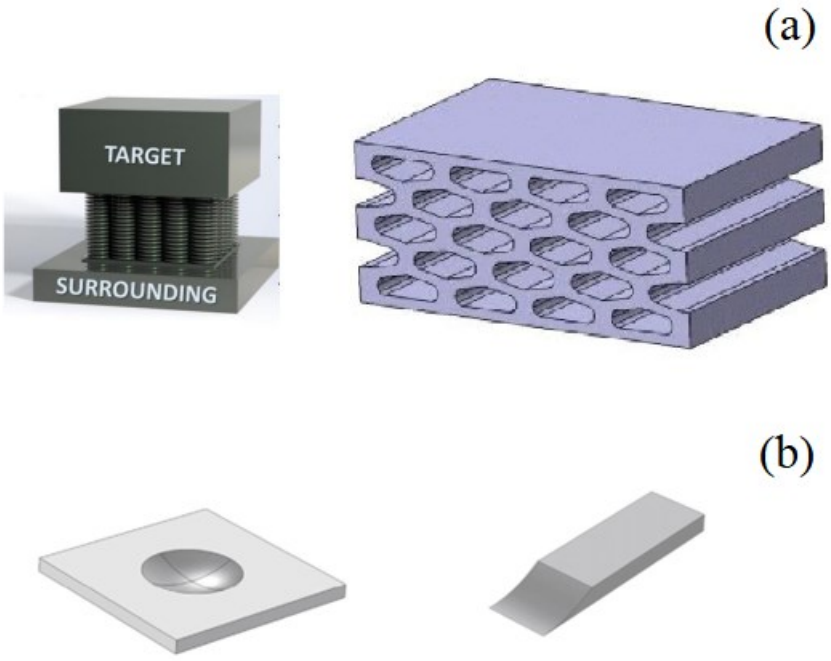

Figure 1. Examples of (a) metamaterials for vibration insulation; (b) ABH geometries.

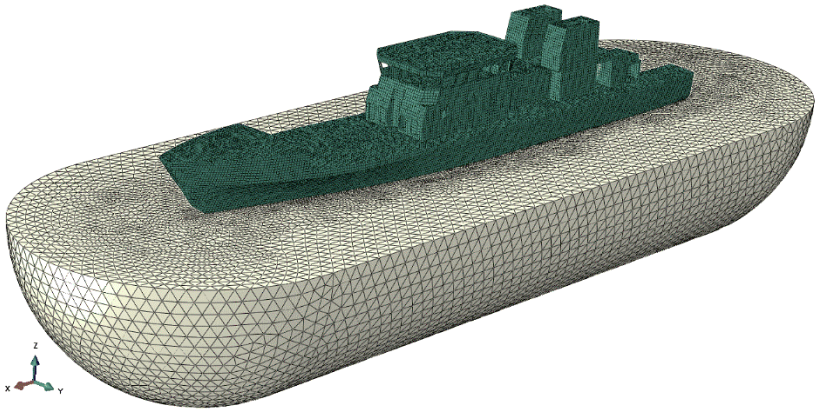

Figure 2. Example of an acoustic-structural model for UNDEX simulation in ABAQUS CAE.

Keywords: underwater explosion, hull vibrations, equipment safeguard, metamaterials, shock protection.

[1] Sigrist JF, Broc D. (2023). A versatile method to calculate the response of equipment mounted on ship hulls subjected to underwater shock waves. Finite Elements in Analysis and Design, https://doi.org/10.1016/j.finel.2023.103917.

[2] A. Pelat, F. Gautier, S.C. Conlon, F. Semperlotti (2020). The acoustic black hole: A review of theory and applications, J. Sound Vib., https://doi.org/10.1016/j.jsv.2020.115316.

Submission ID: 9483

7th International Conference on Protective Structures (ICPS7)
12th – 15th May 2025, Abu Dhabi, UAE

DEVELOPMENT OF GYROID LATTICE STRUCTURES FOR ENHANCING THE ENERGY ABSORPTION OF MOTORCYCLE HELMETS AT REALISTIC IMPACT CONDITIONS

Henrique Ramos[1,2], Rafael Santiago[2], Marcilio Alves[1]

[1]Department of Mechatronics and Mechanical Systems Engineering, Group of Solid Mechanics and Structural Impact, University of Sao Paulo, Brazil, henriqueramos@usp.br (corresponding author)

[2]Technology Innovation Institute, Advanced Materials Research Center, Abu Dhabi, United Arab Emirates

ABSTRACT

Motorcycle helmets are essential for reducing traumatic brain injuries (TBI) during accidents, especially in oblique impact conditions where rotational forces significantly contribute to such injuries. This study examines the impact response of gyroid lattice structures as energy-absorbing helmet liners, exploring their potential to replace commercially used expanded polystyrene (EPS) foams. A full-face commercial helmet was experimentally drop tested, followed by the development of a numerical model, that was compared with experimental data, showing strong agreement between acceleration histories. The helmet liner was then segmented into four impact regions and coupled with a biomechanical head model (THUMS) to assess brain injury risk at oblique impact conditions. A transversely anisotropic crushable foam was used for sensitivity analysis, identifying influential parameters affecting brain strain levels. Later, the design and incorporation of gyroid lattice configurations were developed into the helmet line. Numerical optimisation was conducted on the lattice structure at oblique impacts. The results demonstrated significant reductions in brain strain and peak accelerations, highlighting the effectiveness of gyroid lattice structures in improving helmet safety. This methodology provides a foundation for future developments in lightweight lattice structures for helmet liners, contributing to enhanced rider protection and a reduced risk of traumatic brain injuries.

Keywords: Brain Injury Prevention, Gyroid, Impact, Helmet, Optimisation

INTRODUCTION

Head injuries rank among the most severe consequences of motorcycle accidents, accounting for 67% of all powered two-wheeler (PTW) crashes [1,2]. Helmets remain the primary protective measure against traumatic brain injuries (TBI), particularly in oblique impact scenarios where rotational forces generate high shear strains in brain tissue, often leading to diffuse axonal injuries and increased concussion severity [3,4]. Conventional helmet liners, typically made from expanded polystyrene (EPS), are effective at attenuating normal impacts but fail to provide sufficient protection against oblique impacts, where rotational acceleration remains a critical factor in brain injury risk [5].

Expanded polystyrene (EPS) liners, despite being the industry standard for motorcycle helmets, have notable limitations in mitigating oblique impacts. EPS is designed to deform upon linear impact, reducing peak acceleration in direct collisions [6,7]. However, its inability to absorb and dissipate rotational energy makes it less effective in preventing brain injuries caused by shear forces [7,8]. Research has shown that traditional EPS liners do not adequately mitigate rotational accelerations, which are responsible for diffuse axonal injury (DAI) and concussions [7]. This limitation underscores the need for alternative impact-absorbing structures that effectively address both linear and rotational energy dissipation.

The advancement of additive manufacturing has allowed for the exploration of lattice structures as a more effective energy-absorbing mechanism [9,10]. Lattice structures, particularly those based on gyroid designs, provide tunable mechanical properties that enhance impact energy dissipation and allow improved control over force distribution [11,12]. Gyroid lattices facilitate progressive deformation, effectively distributing impact forces while providing higher structural stiffness and customisable density [13]. This makes them a promising alternative to replace EPS liners, particularly for addressing the shortcomings in oblique impact protection.

This study evaluates the use of gyroid lattice structures in motorcycle helmet liners through numerical simulations, optimising their configuration to enhance oblique impact protection. By addressing both linear and rotational impact mitigation, this research aims to develop an advanced helmet liner that enhances rider safety and reduces the severity of head injuries in real-world crash scenarios.

MATERIALS AND METHODS

Experimental Setup

The commercial full-face motorcycle helmet was experimentally evaluated through standardised drop tests (NBR-7471). The helmet was positioned on a rigid headform instrumented with a tri-axis accelerometer (Kistler 8763B) recording impact acceleration history. To qualitatively analyse helmet deformation, a high-speed camera (Photron SA5) captured the impact sequence at 3000 frames per second. A schematic representation of the drop tower experimental setup for testing the helmet is shown in Figure 1(a). Two primary impact locations, such as the Crown and Lateral regions of the helmet, were analysed experimentally. The helmet was dropped from 2.5 meters, and obtained an impact velocity of 7 m/s per the standardised test. Acceleration-time histories were recorded to compute.

Helmet Design and Finite Element Modeling

The full-face motorcycle helmet was designed using Fusion 360 (Autodesk, U.S.). The geometric dimensions of the helmet were based on the tested experimental commercial helmet, which served as a reference for developing the helmet model, as seen in Figure 1(b). The geometry was then pre-processed

in HyperMesh (Altair HyperWorks, U.S.) before being imported into the LS-DYNA (Ansys, U.S.) explicit simulation code and literature-based material properties. The finite element model (FEM) consists of five primary components:

- Outer shell (ABS material) - Modeled with MAT_24 (elastoplastic material)
- Absorbing liner (EPS foam) - Modeled with MAT_63 (crushable foam material)
- Comfort liner (soft padding for fitment)) - Modeled with MAT_63 (crushable foam material)
- Headform (rigid, mass = 5.7 kg) - Modeled with MAT_20 (rigid body material)
- Impact anvil (rigid surface for drop test validation) - Modeled with MAT_20 (rigid body material)

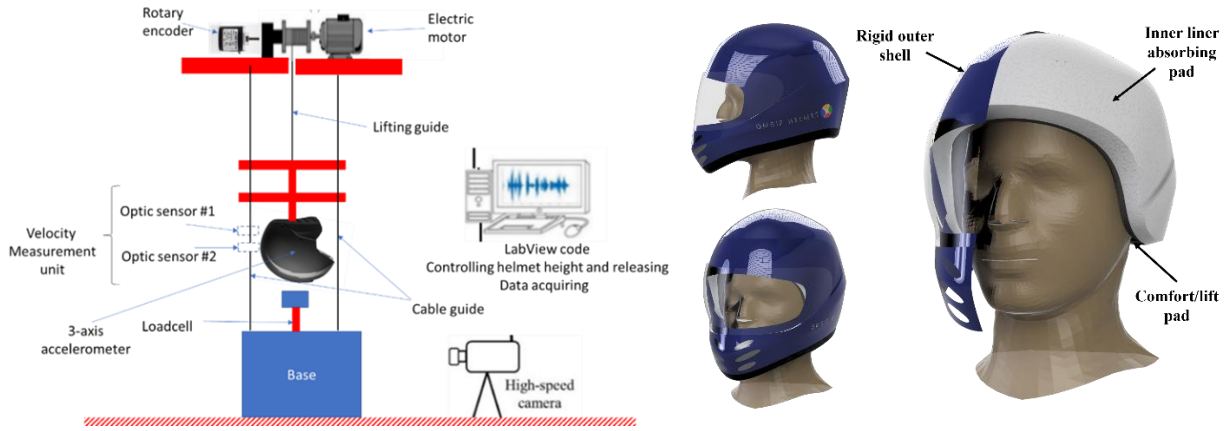

(a) **(b)**

Figure 1. (a) Helmet testing machine experimental setup and (b) representative design of full-face motorcycle helmet.

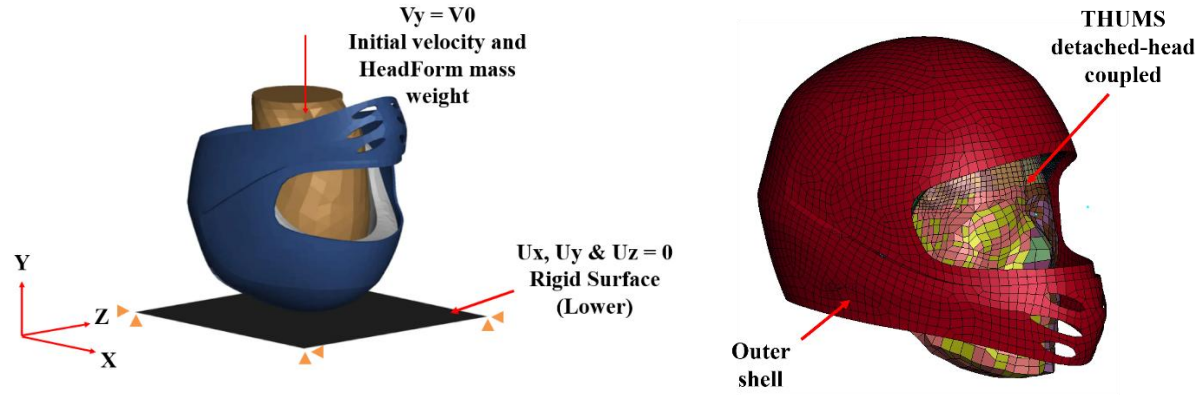

(a) **(b)**

Figure 2. (a) Details for the helmet model development of the commercial helmet and (b) Toyota-THUMS head model [14] **enclosed by the commercial helmet.**

The helmet shell was meshed using 4-node shell elements (3 mm thick), while the EPS liner was meshed using solid elements with variable thickness (13 mm to 46 mm). The Toyota-THUMS [14] male detached-head model was also used to evaluate brain strain and biomechanical responses under helmeted impact conditions. The THUMS model incorporates critical anatomical features such as the skull, cerebrum, cerebrospinal fluid, and soft tissues, allowing for an accurate prediction of brain deformation and injury risk during oblique impact.

Sensitivity Analysis

Sensitivity analysis was conducted using an idealised transversely anisotropic crushable foam model (MAT_142) to systematically evaluate the parameters influencing brain strain levels. The helmet liner was segmented into four impact regions (rear, frontal, superior, and lateral). At a testing velocity of 7.0 m/s, the optimisation process included assessments in oblique impact conditions at a 30 ° angle, a scenario associated with commonly real-impact conditions [2]. Each functional Impact-Liner section was analysed to determine the optimal mechanical response of the material to achieve a compressive and shear response capable of minimising brain damage, as depicted in, and the oblique impact was conducted in each of the impact regions, as shown in Figure 3(a). The transversely anisotropic crushable foam model parameters were analysed using the THUMS model to determine their impact on head injury reduction. The transversely anisotropic Tsai-Wu yield surface can be expressed as:

$$F_{11}\sigma_{xx}^2 + F_{22}\sigma_{yy}^2 + F_{22}\sigma_{zz}^2 + F_{44}\sigma_{xy}^2 + F_{55}\sigma_{yz}^2 + F_{44}\sigma_{zx}^2 + 2F_{12}\sigma_{xx}\sigma_{yy} + \cdots \\ \ldots + 2F_{23}\sigma_{zz}\sigma_{yy} + 2F_{12}\sigma_{xx}\sigma_{zz} \leq 1 \quad (1)$$

being longitudinal tension and compression (F_{11}), transverse tension and compression (F_{22}), strong shear (F_{44}), weak shear (F_{55}), off-axis tension and compression with strong/weak directions (F_{12}), and off-axis tension and compression with weak/weak directions (F_{23}).

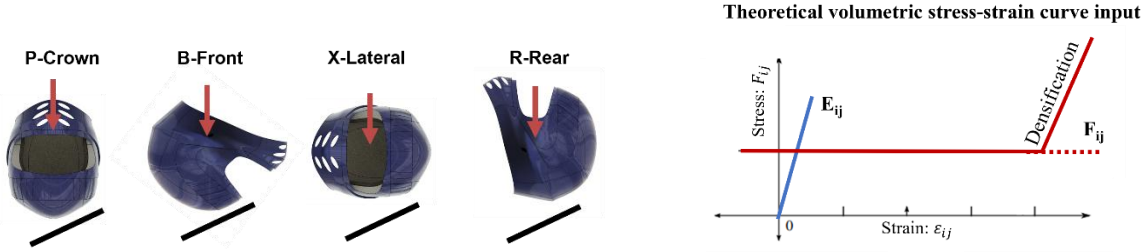

(a) **(b)**

Figure 3. (a) Schematic representation of the impacted region of helmet sections and (b) Representative loading curve input for anisotropic crushable foam (MAT_142).

Equation 1 outlines the determination of six coefficients by correlating subsequent load scenarios with variations in volumetric strain. The material model requires input curves for nominal axial stress-volumetric strain. The load curve input, as shown in Figure 3(b), presents values, F_{ij} as input values that represent the idealised helmet liner material and are aligned with the element's local material directions, ensuring an accurate representation of anisotropic behaviour under dynamic loading. For the parametric study, the optimisation problem is defined as:

$$\min_{\varepsilon_{Brain}} f(F_{ij}, E_{ij}) \\ 0.1 \leq F_{ij} \leq 10.0 \\ 0.1 \leq E_{ij} \leq 10.0 \quad (2)$$

where ε_{Brain} represents the plastic strain observed in the cerebrum (both white and gray matter), and F_{ij} and E_{ij} are the material compression level and elastic modulus values, respectively. To systematically assess the contribution of each parameter, Analysis of Variance (ANOVA) was applied to quantify the significance of all input variables. LS-OPT (Livermore Software Technology Corporation, U.S.) was used to structure the design process, explore the design space, and compute optimal parameter configurations based on the specified objectives to optimise the material parameters.

Design of Gyroid Lattice Structures in the Helmet

The gyroid lattice structure was integrated into the helmet liner in the sectioned regions using nTop (nTopology, U.S.) software. Figure 4(a) shows the gyroid samples presented with unit cell dimensions of 7.5 mm x 7.5 mm x 7.5 mm schematic, with shelled wall thickness (g_{th}) to be further optimised, determining the optimal thickness for minimising brain damage. The gyroid lattice was analysed by assigning thermoplastic elastomers (TPEs) powder (Luvosint X92A-1, Lehmann & Voss & Co; Hamburg, Germany), following material properties obtained by the authors [15]. This is the final model illustrated in Figure 4 (b), representing the oblique impact condition in the frontal section. The numerical optimisation framework was implemented in LS-OPT (Livermore Software Technology Corporation, U.S.). The Efficient Global Optimization (EGO) method was used to iteratively refine lattice geometry and minimise brain strain levels at oblique impact, later, performance was compared with commercial helmet EPS-absorbing foam.

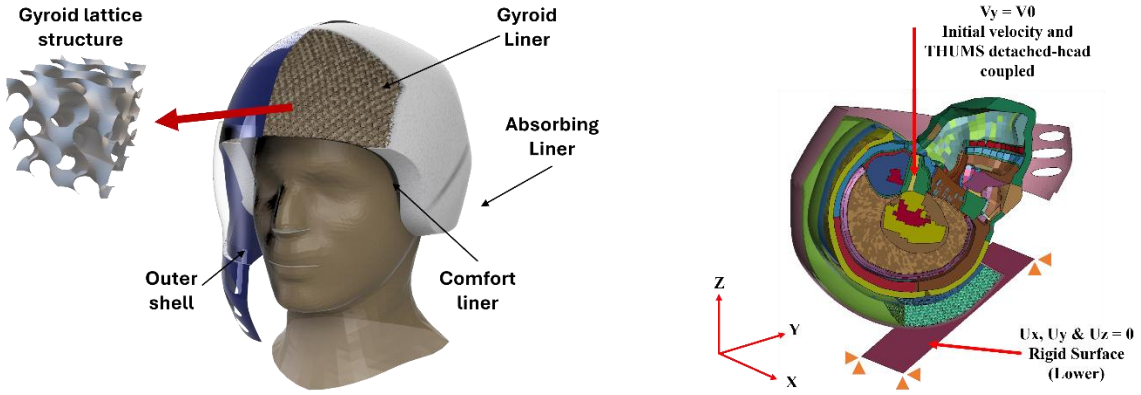

(a) **(b)**

Figure 4. (a) Helmet design with exemplification of gyroid lattice structure integrated into the frontal helmet liner section and (b) cross-section THUMS head model enclosed by the commercial helmet subjected to frontal oblique impact.

RESULTS AND DISCUSSION

Validation of the Helmet Model

The comparison of acceleration data histories between experimental and numerical simulations is illustrated in Figures 5(a) and (b), which show a good agreement between the helmet model and the experimental sample. The peak linear acceleration obtained from the numerical simulations closely corresponds to the experimental acceleration response measured during impact. However, in the left lateral impact (X-Lateral), it is possible to observe that the slope of the numerical simulation is steeper. This difference could be attributed to slight deviations in the design and dimensions between the simulated model and the experimentally tested helmet. Moreover, the modelled commercial helmet, which features inner liner configurations similar in thickness and density to the tested helmet, demonstrates a high correlation with the experimental data. F_{ij} and E_{ij}.

Sensitivity Analysis Results

The sensitivity analysis of the anisotropic crushable idealised foam (stress versus volumetric strain load curve level (F_{ij}) and Elastic Modulus (E_{ij})) parameters was conducted to identify the key factors influencing the response in an oblique crash impact. Figure 6 presents the ANOVA outcomes for each

helmet-impacted region. By comparing the ANOVA responses, it becomes possible to identify the most influential parameters for minimising brain damage during the compression of the inner liner material in the helmet at oblique impact. The results show that the transverse stress versus volumetric strain load curve (F_{22}) and shear stress 23 versus volumetric strain load curve (F_{23}) exert minimal influence across all impact directions. In contrast, parameters F_{11} and E_{12} significantly influence the response in all impacted regions, as observed from the expansion of strain levels measured in the brain. The sensitivity analysis determined that F_{11} and E_{12} were the most influential parameters for inner liner helmet optimisation. This finding effectively provides valuable information, as EPS foam exhibits excellent energy absorption capacity by density and becomes poorer after its first impact with limited elastic recovery [16]. Additionally, while EPS liners offer good protection against linear impacts, their performance in oblique impacts where rotational acceleration often exceeds safety thresholds remains challenging. Also, despite the continued usage of EPS foam in commercial helmets, its limited flexibility and inferior shear capacity restrict its ability to mitigate brain injuries [5,7,17,18]. An optimal helmet liner should absorb energy in axial and shear directions (F_{11} and E_{12}), making gyroid lattice structures a promising alternative. Gyroid lattice structures have demonstrated superior absorption of compressive and shear forces [19–21], making them ideal for helmet inner liners.

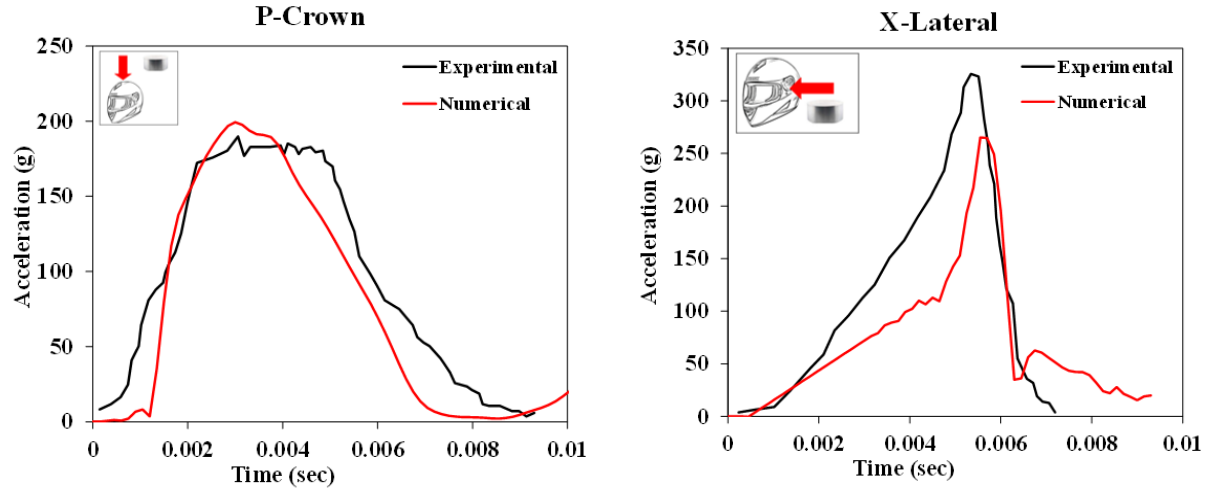

(a) **(b)**

Figure 5. Acceleration history comparison between experimental and numerical simulations for (a) crown and (b) lateral impact.

Performance of Gyroid Lattice Structures

Figure 7 illustrates the optimisation of gyroid thickness using the EGO optimisation process. The results highlight the minimisation of the objective function through the tailored thickness of the gyroid lattice, where the algorithm effectively identified the most promising regions in the domain, specifically, the region containing the current best thickness design for the different impact regions analysed. The findings indicated significant reductions in brain strain levels across all impact scenarios. For the B-Frontal impact, the optimisation reduced plastic strain levels to $\varepsilon_{Brain} = 0.44$, with an optimal gyroid thickness of 2.81 mm. In the crown impact scenario, the optimal thickness reached the upper boundary limit of 4 mm but effectively reduced strain. However, the X-lateral impact showed only minor strain changes, with variations in gyroid thickness resulting in minimal differences between the minimum and maximum values. In the R-Rear impact, the optimal thickness of 3.72 mm—near the boundary constraint—demonstrated noticeable differences in plastic strain across the evaluated domain.

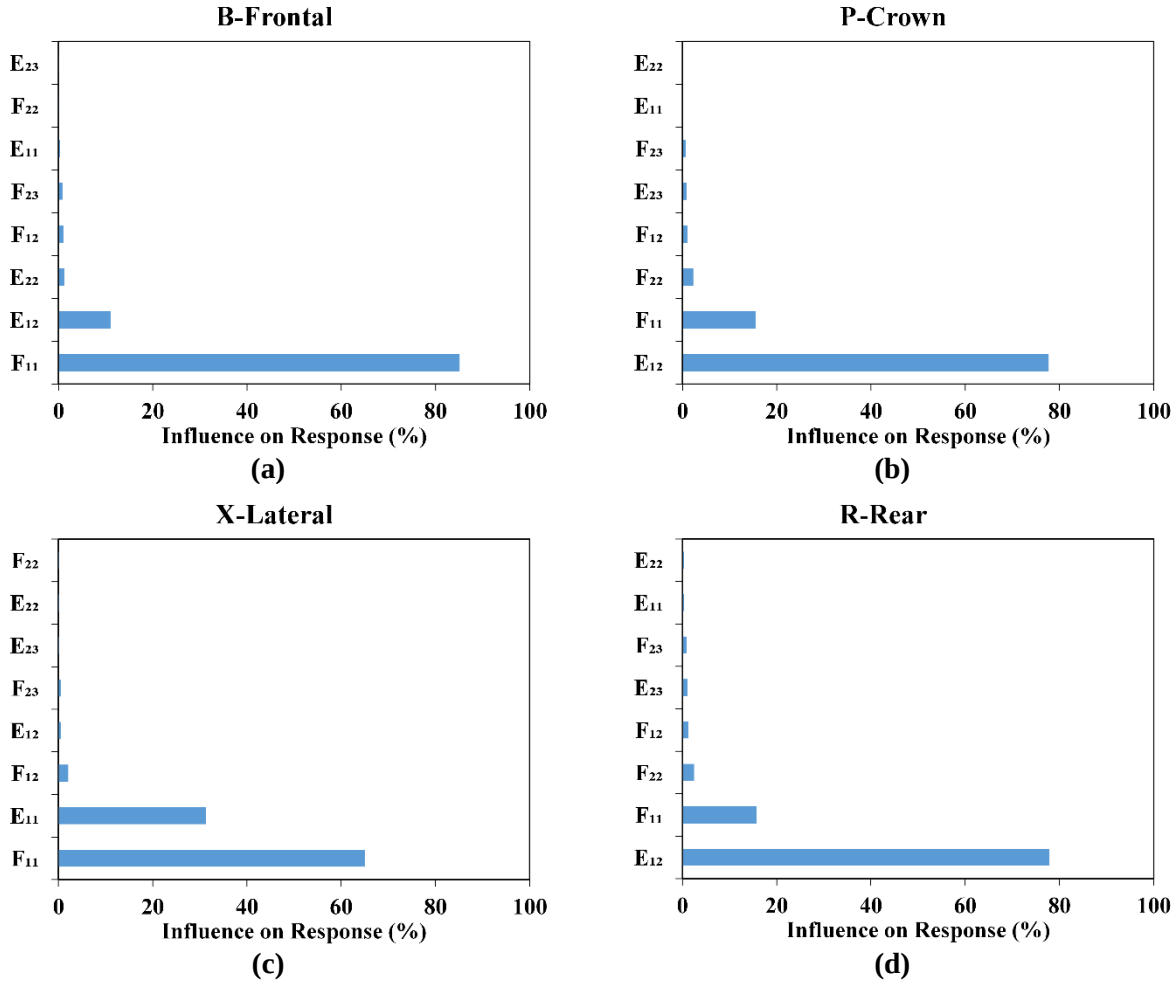

Figure 6. Analysis of variance (ANOVA) results illustrating the influence of variables on the linear approximation for different impacted regions: (a) B-Frontal, (b) P-Crown, (c) X-Lateral, and (d) R-Rear

The fringe response mapping, as presented in Figure 8(a)-(d), depicts the time sequence of plastic strain levels, highlighting brain damage in both the cerebrum's white and grey matter. By comparing the fringe levels between the commercial EPS liner and the optimal gyroid lattice liner thickness for each impact region, the results indicate that the complex geometry of the gyroid structure resulted in reductions in both translational and rotational acceleration under oblique impact conditions. An apparent decrease in plastic strain levels was observed between the commercial helmet and the gyroid lattice liner. Furthermore, the gyroid lattice structure's response reproduced the proposed idealised helmet liner, demonstrating its suitability for such impact applications. The optimised gyroid lattice liner exhibited significant improvements over traditional EPS liners. The gyroid design reduced peak acceleration by 8-29%, demonstrating superior impact energy absorption. The uniform distribution within the lattice structure minimised localised stress concentrations, thereby reducing the risk of severe brain injuries.

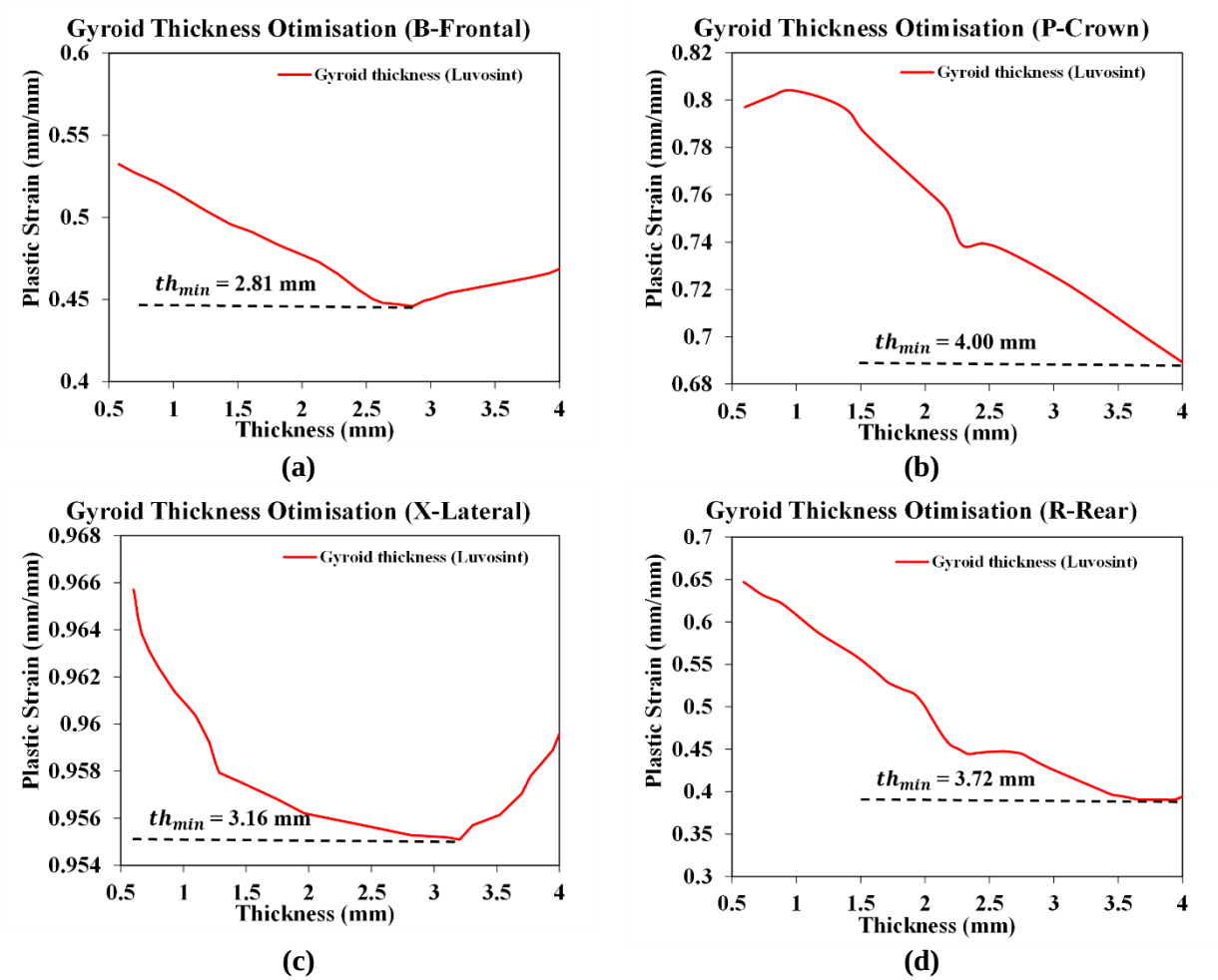

Figure 7. Gyroid thickness response plots evaluating the brain strain level mitigation for different impact regions (a) B-Frontal, (b) P-Crown, (c) X-Lateral, and (d) R-Rear.

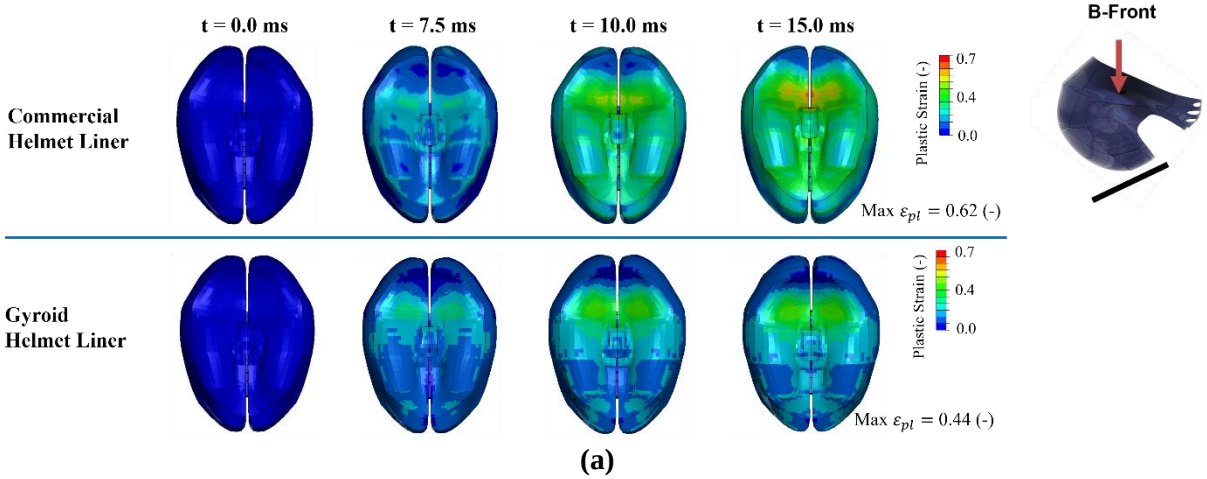

(a)

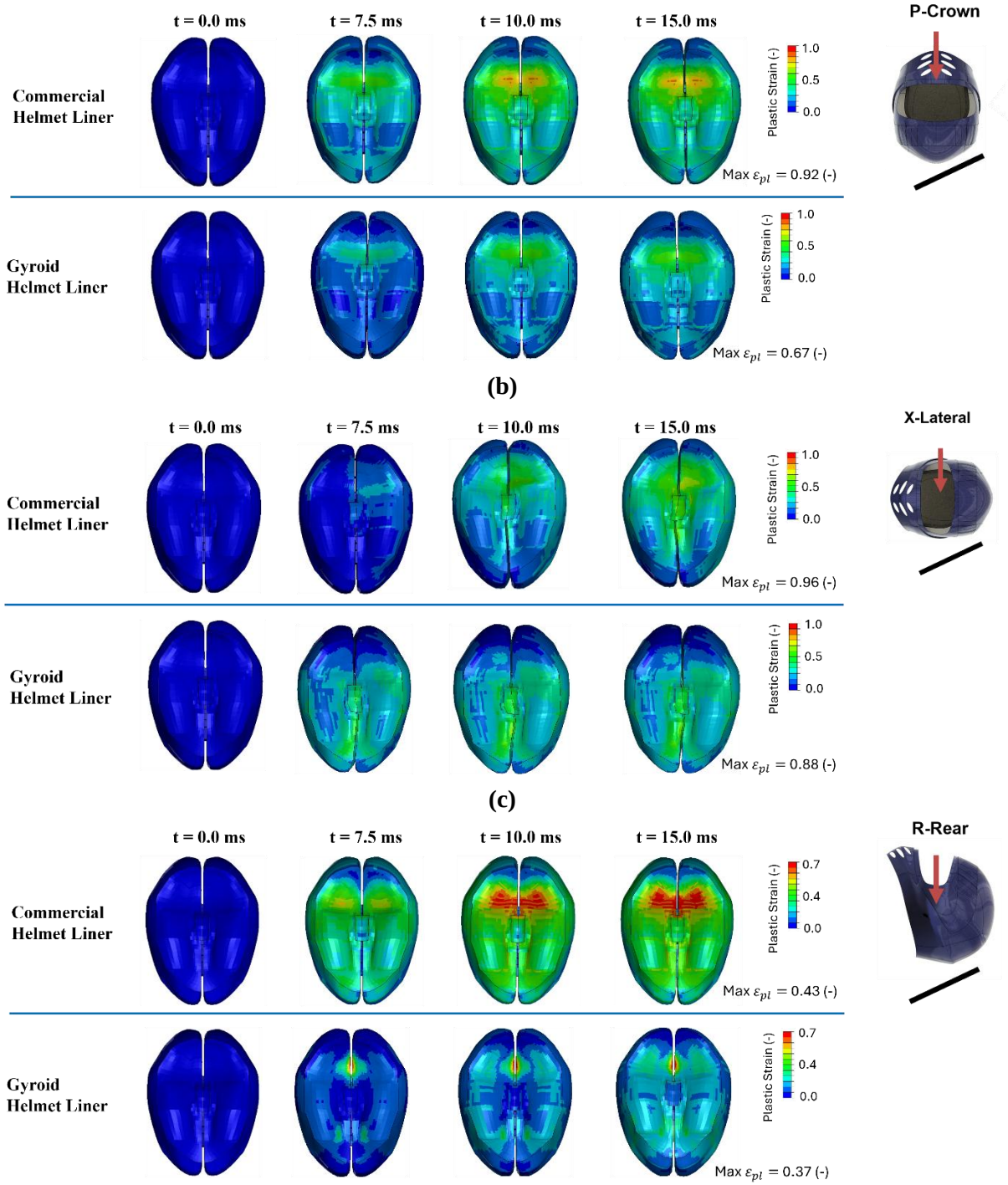

Figure 8. Fringe levels of plastic strain in the cerebrum's white and gray matter for different impact regions (a) B-Frontal, (b) P-Crown, (c) X-Lateral, and (d) R-Rear, by comparing the brain damage using the commercial EPS liner and optimised gyroid liner.

CONCLUSIONS

This study demonstrates the potential of gyroid lattice structures to enhance helmet safety by reducing peak acceleration and rotational forces during impact events. Numerical simulations confirmed that the optimised liner provided superior energy absorption, addressing the limitations of EPS liners in oblique impacts. The results show that for frontal impact, tailoring the gyroid lattice structure can reduce brain damage by up to 29%. Future work should focus on further experimental validation and large-scale manufacturability assessments to facilitate the real-world implementation of gyroid-based helmet liners.

ACKNOWLEDGMENTS

The authors acknowledge the FAPESP project 2019/05444-0 from Brazil for the financial support and the Advanced Materials Research Center from the Technology Innovation Institute of the United Arab Emirates.

REFERENCES

[1] H.H. Hurt, Motorcycle accident cause factors and identification of countermeasures, The Administration, 1981.

[2] B. Chinn, B. Canaple, S. Derler, D. Doyle, D. Otte, E. Schuller, R. Willinger, COST 327 Motorcycle safety helmets, European Commission, Directorate General for Energy and Transport (2001).

[3] T. Whyte, C.A. Stuart, A. Mallory, M. Ghajari, D.J. Plant, G.P. Siegmund, P.A. Cripton, A review of impact testing methods for headgear in sports: Considerations for improved prevention of head injury through research and standards, J Biomech Eng 141 (2019) 070803.

[4] F.A.O. Fernandes, R.J. Alves de Sousa, M. Ptak, J. Wilhelm, Certified motorcycle helmets: computational evaluation of the efficacy of standard requirements with finite element models, Mathematical and Computational Applications 25 (2020) 12.

[5] M. Aare, P. Halldin, A new laboratory rig for evaluating helmets subject to oblique impacts, Traffic Inj Prev 4 (2003) 240–248.

[6] L. Di Landro, G. Sala, D. Olivieri, Deformation mechanisms and energy absorption of polystyrene foams for protective helmets, Polym Test 21 (2002) 217–228.

[7] N.J. Mills, A. Gilchrist, Response of helmets in direct and oblique impacts, International Journal of Crashworthiness 2 (1996) 7–24.

[8] S. Kleiven, Why most traumatic brain injuries are not caused by linear acceleration but skull fractures are, Front Bioeng Biotechnol 1 (2013) 15.

[9] E. Bliven, A. Rouhier, S. Tsai, R. Willinger, N. Bourdet, C. Deck, S.M. Madey, M. Bottlang, Evaluation of a novel bicycle helmet concept in oblique impact testing, Accid Anal Prev 124 (2019) 58–65.

[10] S.F. Khosroshahi, S.A. Tsampas, U. Galvanetto, Feasibility study on using a hierarchical lattice architecture for helmet liners, Mater Today Commun 14 (2018) 312–323.

[11] I. Maskery, N.T. Aboulkhair, A.O. Aremu, C.J. Tuck, I.A. Ashcroft, Compressive failure modes and energy absorption in additively manufactured double gyroid lattices, Addit Manuf 16 (2017) 24–29. https://doi.org/10.1016/j.addma.2017.04.003.

[12] J.-H. Park, J.-C. Lee, Unusually high ratio of shear modulus to Young's modulus in a nano-structured gyroid metamaterial, Sci Rep 7 (2017) 10533.

[13] H. Ramos, R. Santiago, S. Soe, P. Theobald, M. Alves, Response of gyroid lattice structures to impact loads, Int J Impact Eng (2022) 104202. https://doi.org/10.1016/j.ijimpeng.2022.104202.
[14] M. Iwamoto, Y. Nakahira, A. Tamura, H. Kimpara, I. Watanabe, K. Miki, Development of advanced human models in THUMS, in: Proc. 6th European LS-DYNA Users' Conference, 2007: pp. 47–56.
[15] R. Adams, S.P. Soe, R. Santiago, M. Robinson, B. Hanna, G. McShane, M. Alves, R. Burek, P. Theobald, A novel pathway for efficient characterisation of additively manufactured thermoplastic elastomers, Mater Des (2019) 107917.
[16] F.A.O. Fernandes, R.J. Alves De Sousa, Motorcycle helmets - A state of the art review, Accid Anal Prev 56 (2013) 1–21. https://doi.org/10.1016/j.aap.2013.03.011.
[17] T.Y. Pang, K.T. Thai, A.S. McIntosh, R. Grzebieta, E. Schilter, R. Dal Nevo, G. Rechnitzer, Head and neck responses in oblique motorcycle helmet impacts: a novel laboratory test method, International Journal of Crashworthiness 16 (2011) 297–307.
[18] K. Hansen, N. Dau, F. Feist, C. Deck, R. Willinger, S.M. Madey, M. Bottlang, Angular Impact Mitigation system for bicycle helmets to reduce head acceleration and risk of traumatic brain injury, Accid Anal Prev 59 (2013) 109–117.

Analysis on the effect of crash-induced shock on representative electric vehicle battery modules and packs

Yuyang Xing [1], Q. M. Li [1]

[1] *School of Engineering, The University of Manchester, Manchester M13 9PL, UK*

With the global rise in electric vehicles (EV) adoption, ensuring the safety of Li-ion batteries (LIB) has become a major concern. However, it has been noted that EV's LIB may be malfunctioned or damaged due to the crash-induced shock in a survivable vehicle crash, even though the structural integrity of the vehicle is preserved. Therefore, the current shock standards and the crash-induced shock signals collected from National Highway Traffic Safety Administration (NHTSA) New Car Assessment Program (NCAP) tests are analysed via various shock analysis methods including signal characteristics in time domain, power spectral density (PSD) and shock response spectrum (SRS) in frequency domain, and the acceleration/velocity-change diagram. It is found that crash-induced shocks cannot be fully represented by the half-sine pulse adopted in shock testing standards. In both time and frequency domains, the existing shock testing standards generally underestimate the severities of the crash-induced shocks, and therefore, are non-conservative. It also shows that the correct selection of a filter for the processing of original crash-induced shock signal is crucial for the specification of EV battery shock environment and shock response analyses. An evaluation of the current shock standard and the crash-induced shock signals is performed using Finite Element Analysis (FEA) method in this study. Representative experiments are designed to validate FEA models for LIB module. Three different materials are used to represent the homogenous LIB cells. The results of the FEA models also indicate that severer shock response could be caused by the crash-induced shock signals. Not only the front-row battery cell in the module experience severe shock, but the transmission of shock also significantly affects the battery cells positioned in the rear of the module. The application of an inappropriate filter would reduce the shock response and lead to incorrect safety assessment of LIB. The results obtained in this research can support the development of more reliable shock testing standards for EV batteries.

Keywords: Mechanical shock, Battery safety, Test standards, Shock response spectrum (SRS)

Review of modern design methods for blast loaded floor slabs

Franciszek Wołoch[1], Piotr Nowak[1], Artur Szlachta[1],
Tomasz Gajewski[2], Piotr W. Sielicki[2]

[1]*Doctoral School, Institute of Structural Engineering, Faculty of Civil and Transport Engineering, Poznan University of Technology, 5 Piotrowo Street, 60-965 Poznan, Poland*
[2]*Institute of Structural Engineering, Faculty of Civil and Transport Engineering, Poznan University of Technology, 5 Piotrowo Street, 60-965 Poznan, Poland*

Keywords: blast loadings, protective structures, floor slabs, buried structures

The effect of explosive loads on protective structures is a fundamental design challenge for both above- and underground structures. In addition to the structural solutions themselves, such as floor thickness, concrete or steel grade or the increasingly used modern composite materials, the soil above the floor slab is an important protective layer [1].

The strength of the floor, which as a rule determines the resistance of the entire structure, is determined not only by its technical parameters such as thickness, materials used or reinforcement. The properties of the soil forming the backfill are also one of the factors determining the resistance of both the floor and the entire structure. As previous studies have shown, depending on the type of soil backfill, it can both dampen explosive waves and exhibit high impedance, thus transferring more energy to the floor of the protective structure [1]. Furthermore, additional reinforced concrete slabs on the ground surface, also known as detonation slabs, can provide an additional protection for the floor.

The main objective of this study is to compare analytical methods for the design of floor slabs for protective above-ground as well as underground structures with proposed numerical analyses. As a result of the numerical experiments and comparative calculations, parameters critical for the resistance of floor slabs were determined, including the thickness and parameters of the soil layer above the floor. The analytical calculations used standard provisions and experimental formulas [2]. The load induced by the detonation of a load of 25 kg TNT equivalent was assumed as the basic load. This value corresponds in an order of magnitude to the standard Shahed drone warheads currently in use, e.g. during the war in Ukraine. Potential developments in the technology of means of destruction were also taken into account in the calculations by analysing the impact of the use of heavier payloads and comparing the impact of the adopted warheads with payloads characteristic of 155 mm artillery shells.

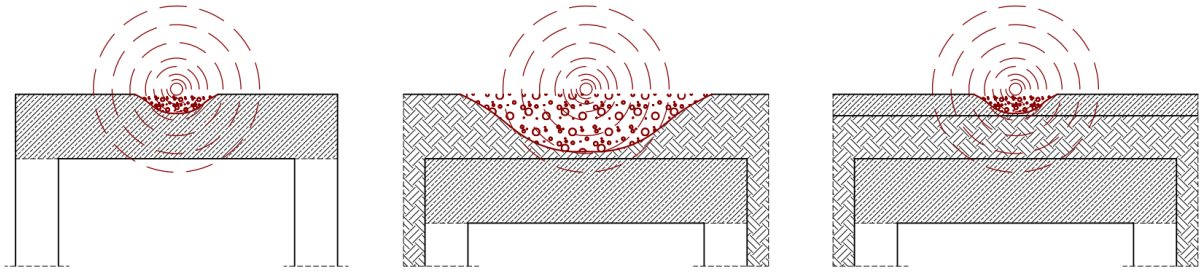

Fig. 1. Various forms of blast impact on the floor slab.

The numerical calculations were carried out using the finite element method with RFEM 6 and ABAQUS. In RFEM 6, the floor slabs were dimensioned using quasi-static forces and the procedures specified in Eurocode 2. On the other hand, a complete analysis of the propagation of stress waves travelling through the soil was carried out in ABAQUS. A pre-calibrated numerical concrete damage plasticity (CDP) model was used in the numerical tasks. During the calculations, the influence of the concrete strength was checked, among other things, by testing classes with strengths C20/25, C30/37, C40/50, among others. The influence of reinforcing steels with strength classes higher than those indicated in Eurocode 2was also checked. At this stage, the parameters of the selected soil types for the Coulomb-Mohr model were adopted for the calculations.

The results obtained in this study make it possible to determine the parameters that have a decisive influence on the load-bearing capacity of the floor slab of an underground facility subjected to explosive loading occurring on the surface. The research carried out is a starting point for a planned research trial in real-scale conditions on the military range.

[1] Mohammadi, P. K. M., Khalilpour, S. H., & Sareh, P. (2022). Simulating the response of buried structures to external blast loads: Methods, challenges, and advances. Engineering Reports, 5(6). https://doi.org/10.1002/eng2.12607

[2] Handbook for Blast-Resistant Design of Buildings. (2010). In Wiley eBooks. https://doi.org/10.1002/9780470549070

Penetration Resistance of Green Concrete and a Predictive Model Based on Macroscopic Effective Hardness

Jie Zhang, Leong Hien Poh

Department of Civil and Environmental Engineering, National University of Singapore, Singapore

Green concrete, which integrates waste materials as one of its components, offers a promising solution for mitigating the environmental footprint of the concrete industry. Considerable research has been dedicated to assessing its mechanical properties, workability, durability, and environmental aspects. However, as the application of green concrete extends to civil and military defensive construction, the investigation of its anti-penetration capabilities becomes crucial. In this study, the green concrete mixes were formulated utilizing Portland blast furnace cement (PBFC), where 70% wt.% of OPC was replaced by ground granulated blast furnace slag (GGBS), and carbon mineralization was conducted during the casting process. Various aggregate configurations were devised for these concrete mixes, including granite coarse aggregates, granite fines, recycled coarse aggregates (RCA), and lightweight aggregates (LWA). The mechanical properties of these concretes, along with those of ordinary Portland cement (OPC) concrete (mixed with granite coarse aggregates and fine sand), were investigated in terms of compressive stress-strain behavior, splitting tensile strength, and effective hardness index. Then non-deformable ogive-nosed projectiles, with 3 in caliber radius-head (CRH), 28 mm in diameter and 250g in mass, were used to impact the OPC concrete and green concrete targets at the velocities of ~400m/s and ~600m/s. The damage characteristics for all concrete targets were measured and compared in terms of depth of penetration (DOP) equivalent crater diameter, and crater volume. In addition, a pronounced correlation has been identified between DOP and the effective hardness index calculated based on the hardness and proportion of the coarse aggregate and mortar matrix. This finding suggests that many of these mixes possess the potential to substitute conventional concrete mixes without displaying significant differences in penetration resistance. And the proposed correlation can also extend to other types of concrete with compressive strengths up to 220 MPa, as supported by the existing impact tests.

Keywords: green concrete, penetration resistance, effective hardness.

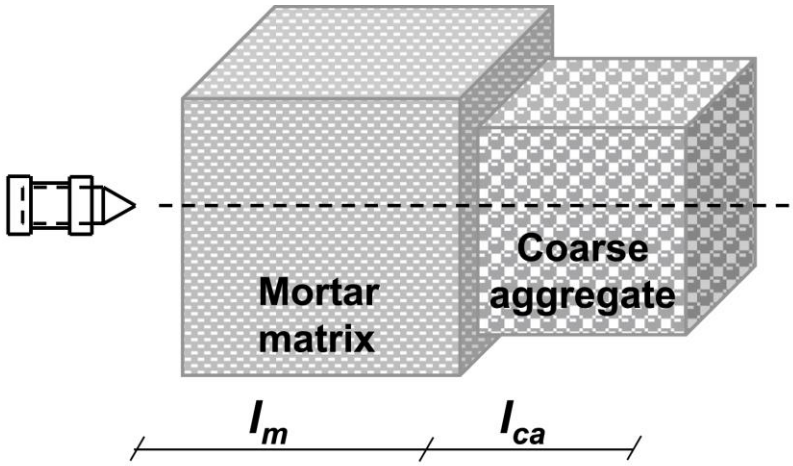

Figure 1. 1-D equivalent length assumption for the effective hardness of concrete.

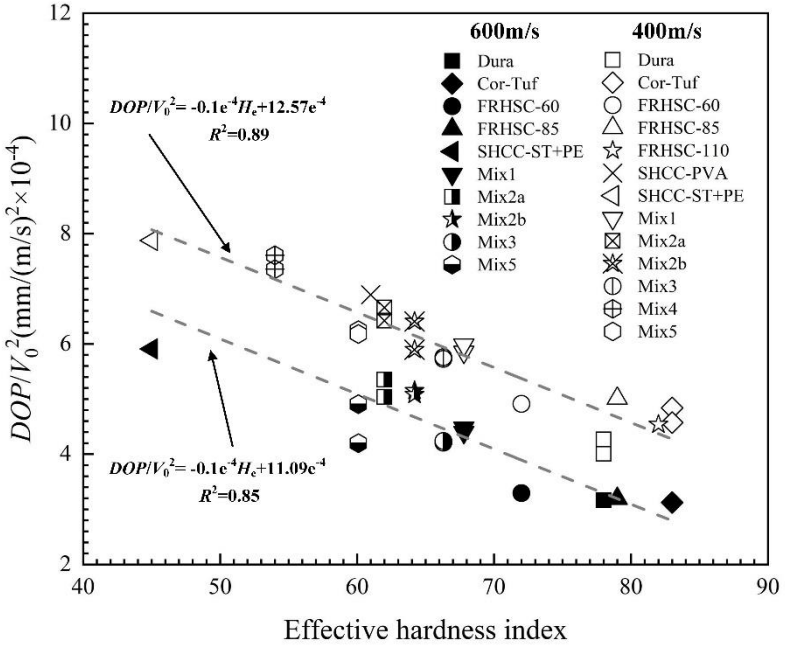

Figure 2. Normalized DOP with respect to the effective hardness index.

Modelling of the Retrofitting of Existing Structural Shielding in Radiology Facilities

Mustafa Majali[1], Ali Al Remeithi[2], Buthaina Al Ameri[3], Kaltham Al Hosani[4]

[1]Federal Authority for Nuclear Regulation, Ph.D. CHP, Abu Dhabi, UAE
[2]Federal Authority for Nuclear Regulation, MSc , Abu Dhabi, UAE
[3]Federal Authority for Nuclear Regulation, MSc, Abu Dhabi, UAE
[4]Federal Authority for Nuclear Regulation, MEM, Abu Dhabi, UAE

Structural radiation shielding is an important pillar in radiation protection as an engineering control deemed highly effective to provide adequate protection and safety for workers and the public and comply with the safety standards requirements. The assessment typically examines the safety measures instituted through design and engineered safety features aimed at hazard control. An integral part of this assessment involves the identification and evaluation of hazards from every source, collected and reviewed through detailed information about the potential or existing hazards within the facility or activity. This in turn aids in pinpointing a range of controls that provide protection against hazards and minimize the incident occurrence.

The challenge of designing suitable structural shielding is shared between designers and regulatory assessors due to the high level of knowledge and competency required in understanding shielding design concepts. To aid shielding designers in conducting this crucial aspect of safety assessment efficiently and accurately, the Federal Authority for Nuclear Regulation (FANR), the nuclear and radiological regulator in of the United Arab Emirates, has developed and modeled a comprehensive computer code to serve as a valuable tool for researchers and other radiation protection professionals with moderate expertise in planning and designing new X-ray facilities or remodeling existing ones.

Furthermore, post-construction corrections or additions to facilities often incur significant expenses especially when an institution may undertake substantial changes by entering into new businesses or services, purchase of new X-ray modality, or alteration in the use or occupancy of existing X-ray rooms or adjacent areas. However, accurate redesign of existing shielding, considering the cost of shielding and monetary cost-benefit, application of the ALARA principle, and the usage of alternative additional shielding materials, becomes inevitable and unavoidable.

In order to obtain as accurate as possible the equivalent and adequate shielding required for retrofitting and avoiding the extensive costs to achieve, FANR software for shielding calculations has been designed to include a large set of shielding thickness data for different shielding materials (concrete, lead, steel, Plate Glass, Gypsum and Wood) and for wide spectrum of x-ray modalities at diverse setting and assumption. In addition, a conservatively safe approach in specifying radiation barriers has been applied.

This innovative technical modeling code for shielding design and retrofitting of existing installation is publicly available on the FANR website. The code serves as a technical tool for

researchers in the field of radiation shielding designing and can be used by students and young professionals for educational purposes to deepen their understanding of radiation shielding principles. The code garnered attention internationally from regulatory bodies, medical professionals, shielding designers, construction engineers, universities, and researchers. Its growing user base, illustrated by the thousands of accesses and offers to translate the code into various languages, highlights its global relevance and utility in advancing safety practices within diagnostic radiology.

Keywords: shielding, radiation protection, modelling, retrofitting.

Exploring the role of detailing in earth-covered magazines: review of current design solutions

Fabio Brantschen[1], Andrea Peruzzi[2], Duarte Miguel Viula Faria[2] and Miguel Fernández Ruiz[3]

[1]*armasuisse Real Estate, Bern, Switzerland*

[2]*MFIC ingénieurs civils SA, Morges, Switzerland*

[3]*Professor, Universidad Politécnica de Madrid, Spain*

The structural performance of reinforced concrete Earth-Covered Magazines (ECMs) under explosive loads has been investigated in the past, but the critical influence of detailing remains unclear with respect to a number of aspects. Yet, detailing –encompassing the design and arrangement of reinforcement, joints, and connections– is known to play a central role in the flexural, shear, membrane, and catenary responses of RC elements. Such load-transfer mechanisms are essential for redistribution of internal forces and the overall resilience of protective structures. This paper emphasizes the decisive impact of detailing on the blast resistance and energy absorption capacity of ECMs, particularly in scenarios where these structures are subjected to inner explosions –a condition for which they are not specifically designed.

While ECMs are primarily designed to resist external threats (blasts from weapon detonation), assessing their ability to absorb energy from internal accidental explosions can indicate potentially-critical weak points in existing structures potentially affecting the security in direct proximity. Such knowledge can inform on targeted retrofitting strategies to enhance resilience or to optimize designs for sustainability without overdesign. Through a comparative exploration of current international design solutions, the paper illustrates how variations in structural detailing can influence key behaviours, such as bending or catenary action. To that aim, the paper introduces a comprehensive database compiled on standardised ECM structural designs, focusing on the detailing of 50 frame corners. On that basis, and by using analytical models from the literature, it is identified a number of potentially-critical details.

This contribution aims at a dialogue within the community, challenging conventional practices that often regard detailing as a secondary design consideration, but whose role is instrumental to ensure structural robustness for low and medium loading densities. By asserting that detailing

is instrumental for the structural behaviour under explosive loads, this study paves the way for enhanced safety, targeted retrofitting, and more sustainable ECM and protective structure new designs.

Keywords: earth-cover magazines (ECMs), performance, reinforcement detailing, structural toughness, internal explosion

An overview of building protection and an experimental design of bunker buster slab under projectile impact in UAE

Abdulla Al-Dhaheri [1]

[1]*Montana State University, Montana, United States*

Building hardened underground facilities is key asset for protecting man, weapons, equipment and other capabilities. In the past, these underground facilities are designed to resist different shockwaves of blasts and can be an alternative protection for leaders in wars and even an emergency plan alternative in case of surface bust nuclear weapons. With technological evolution in recent years, several different weapons have been designed to attack these underground facilities known as bunker busters, which penetrate deep into the earth or through dozens of reinforced concrete before exploding; this study explores an overview of analyzing protection structures across the UAE industries. These topics are studied through the UAE industrial vision of protection, creating various of designs, examining small-medium scale experiments, and analyzing results using statistical analysis

Keywords: Bunker, concrete, slab, blast.


TII
Technology
Innovation
Institute